



N OVA
NOVA SCHOOL OF
SCIENCE & TECHNOLOGY

U. PORTO



universidade
de aveiro

DEPARTAMENT OF CHEMISTRY

THE DIFFERENT FACES OF IBUPROFEN-BASED IONIC LIQUIDS AND EUTECTIC SYSTEMS: PROMISING INNOVATIVE IONIC-LIQUID-BASED FORMULATIONS OF AN OVER-THE-COUNTER ANTI-INFLAMMATORY DRUG

JOANA CAMPAINHAS BASTOS
Master in Biochemistry for Health

DOCTORATE IN SUSTAINABLE CHEMISTRY
NOVA University Lisbon
March 2023



THE DIFFERENT FACES OF IBUPROFEN-BASED IONIC LIQUIDS AND EUTECTIC SYSTEMS: PROMISING INNOVATIVE IONIC-LIQUID-BASED FORMULATIONS OF AN OVER-THE-COUNTER ANTI-INFLAMMATORY DRUG

JOANA CAMPAINHAS BASTOS

Master in Biochemistry for Health

Adviser: Doutor João Miguel Mendes de Araújo
NOVA School of Science and Technology, NOVA University Lisbon

Co-adviser: Doutora Ana Belén Pereiro Estévez
NOVA School of Science and Technology, NOVA University Lisbon

Examination Committee:

Chair: Doutora Ana Isabel Nobre Martins Aguiar Oliveira
Ricardo
Professora Catedrática da Faculdade de Ciências e Tecnologia da
Universidade NOVA de Lisboa

Rapporteurs: Doutor Carlos Alberto Mateus Afonso
Professor Catedrático da Faculdade de Farmácia da Universidade de
Lisboa
Doutora Maria Eugénia Rebello de Almeida
Macedo
Professora Associada com Agregação da Faculdade de Engenharia
da Universidade do Porto

Adviser: Doutor João Miguel Mendes de Araújo
Investigador Auxiliar da Faculdade de Ciências e Tecnologia da
Universidade NOVA de Lisboa

Members: Doutora Ana Isabel Nobre Martins Aguiar Oliveira
Ricardo
Professora Catedrática da Faculdade de Ciências e Tecnologia da
Universidade NOVA de Lisboa

The Different Faces of Ibuprofen-Based Ionic Liquids and Eutectic Systems: Promising Innovative Ionic-Liquid-Based Formulations of an Over-the-Counter Anti-Inflammatory Drug

Copyright © Joana Campaignhas Bastos, NOVA School of Science and Technology, NOVA University Lisbon.

The NOVA School of Science and Technology and the NOVA University Lisbon have the right, perpetual and without geographical boundaries, to file and publish this dissertation through printed copies reproduced on paper or on digital form, or by any other means known or that may be invented, and to disseminate through scientific repositories and admit its copying and distribution for non-commercial, educational or research purposes, as long as credit is given to the author and editor.

À minha família e amigos,

ACKNOWLEDGMENTS

A realização desta dissertação contou com importantes apoios e incentivos sem os quais não se teria tornado uma realidade e aos quais estarei eternamente grata. Gostaria desde já reconhecer o apoio financeiro dado pela Fundação para a Ciência e Tecnologia através das bolsas PD/BD/135078/2017 e COVID/BD/151824/2021 e à NOVA School of Science and Associated Laboratory for Green Chemistry (LAQV - REQUIMTE) por providenciar os equipamentos e serviços necessários para a realização deste projeto.

Ao Doutor João Araújo, pela sua orientação, total apoio, disponibilidade, pelo saber que transmitiu, total colaboração no solucionar de dúvidas e problemas que foram surgindo ao longo da realização deste trabalho. Durante estes anos reconheço que consegui ganhar mais autonomia no laboratório e um sentido mais crítico perante os meus resultados tendo em conta todas as observações, opiniões e críticas dadas.

À Doutora Ana Pereiro, que orientou a minha dissertação de mestrado e que aceitou também co-orientar a minha dissertação de doutoramento, revelando uma especial delicadeza e atenção, o meu obrigado pela paciência e dedicação. Os seus conselhos e sugestões bem como a permanente valorização do trabalho desenvolvido foram determinantes para o resultado alcançado.

Aos meus colegas de trabalho e amigos, Eduardo e Sara, por todas as pausas de café para ganhar coragem para mais umas horas seguidas de ensaios sem descanso. Obrigada pelos desabafos e apoio. À Margarida e à Nicole, que trabalham comigo mas são das melhores amigas que alguém pode ter e tive a sorte de conviver com elas no meu local de trabalho. Obrigada por acreditarem em mim e por me fazerem ser uma pessoa melhor dentro e fora do laboratório.

Aos meus pais o meu eterno obrigado por todos os sacrifícios que fizeram para eu conseguir realizar os meus sonhos e chegar onde estou hoje. Prometo levar como exemplo o vosso e fazer pelo Matheus o que vocês fizeram e ainda fazem por mim. À minha avó Lurdes e à minha tia Paula que sempre acreditam que eu conseguia chegar longe e sempre me apoiaram.

Ao David pelo seu amor e amizade. Obrigada por me fazeres ser uma pessoa melhor e por não me deixares desistir dos meus sonhos. Obrigada por me ajudares a passar os piores momentos desta caminhada e seguires comigo rumo à conquista.

Por último, mas não menos importante, ao meu filho Matheus. Apesar das lutas contra o sono e não deixar a mãe muito tempo concentrada ao computador, o seu sorriso e carinho deu-me força e animo para conseguir terminar esta etapa.

“Live as if you were to die tomorrow. Learn as if you were to live forever.”

Mahatma Gandhi

ABSTRACT

The global goal of the current thesis is to demonstrate the feasibility of the ionic liquids (ILs) platform to boost “old” drugs efficiency. With this ground, cholinium- and imidazolium-based ILs were used to formulate pharmaceutically active ILs (API-ILs) and eutectic systems with ibuprofen (Ibu) as parent active pharmaceutical ingredient (API). The aqueous solubility, water and simulated biological fluids, of the IBU-based ILs and eutectics relatively to Ibu neutral and salt form (sodium ibuprofen) were assessed. Jointly, insights into task-specific fluorinated ILs that reduce the impact of the addition of water upon the IL’s H-bond acceptance ability, a key factor to obtain functionalized materials to be used in the dissolution of drugs or biomolecules, were attained. The cytotoxic profiles were characterized for both IBU-based ILs and eutectics, as well as for the parent API (Ibu), using two human cells lines, colon carcinoma cells (Caco-2) and hepatocellular carcinoma cells (HepG-2). The biocompatibility of all Ibu formulations was also evaluated through a hemolytic activity assay. Moreover, the anti-inflammatory properties of all Ibu formulations, ILs, eutectics, and parent API, were assessed through the inhibition of bovine serum albumin (BSA) denaturation and inhibition of cyclooxygenases (COX-1 and COX-2). The assessment of ionicity, through measurements of density, viscosity, and ionic conductivity, was carried out to evaluate the formation of ion-pairs or clusters that enhance membrane permeation. In the end, an in vitro skin permeation assay was attained through Skin Parallel Artificial Membrane Permeability Assays (Skin-PAMPA) to evaluate the Ibu-based ILs and eutectics skin permeability. The evaluation of the permeation potential allows to guide the design of transdermal drug delivery systems. The results of this thesis comprise a proof of concept for the feasibility of task-specific ILs and IL-based eutectics, namely API-ILs and API-based eutectics, in the development of novel drug delivery systems, and more broadly for biological, biochemical, and pharmaceutical applications.

Keywords: Ionic Liquids, Eutectic Systems, Ibuprofen, Solubility, Cytotoxicity, Haemolytic Activity, Anti-inflammatory Activity, BSA denaturation, COX-1 , COX-2, Ionicity, Skin Permeation.

RESUMO

O objetivo global da presente tese é demonstrar a viabilidade do uso da plataforma de líquidos iônicos (LIs) para aumentar a eficiência de fármacos “antigos”. Desta forma, LIs à base de colínio e imidazólio foram usados para formular LIs farmacologicamente ativos (API-ILs) e sistemas eutéticos com ibuprofeno (Ibu) como princípio ativo (API) de origem. A solubilidade aquosa, em água e em fluidos biológicos simulados, dos LIs à base de Ibu e eutéticos em relação ao Ibu neutro e na forma de sal (ibuprofeno sódico) foi avaliada. Foram também obtidas informações sobre LIs fluorados que reduzem o impacto da adição de água devido à sua capacidade de aceitação de ligações de hidrogénio, um fator chave para se obter materiais funcionalizados para serem usados na dissolução de fármacos ou biomoléculas. Os perfis citotóxicos foram caracterizados tanto para ILs baseados em Ibu como para os sistemas eutéticos e o API de origem (Ibu), usando duas linhagens de células humanas, células de carcinoma de cólon (Caco-2) e células de carcinoma hepatocelular (HepG-2). A biocompatibilidade de todas as formulações de Ibu também foi avaliada através de um ensaio de atividade hemolítica. As propriedades anti-inflamatórias de todas as formulações de Ibu, ILs, eutéticos e API de origem, foram avaliadas através da inibição da desnaturação da albumina sérica bovina (BSA) e inibição das ciclooxigenases (COX-1 e COX-2). A avaliação da ionicidade através da medição de densidade, viscosidade e condutividade iônica, foi realizada para avaliar a formação de pares iônicos ou aglomerados que poderão aumentar a permeação nas membranas. Por fim, foi realizado um ensaio de permeação cutânea *in vitro* através do sistema *Skin Parallel Artificial Membrane Permeability Assay* (Skin-PAMPA) para avaliar a permeabilidade cutânea dos Lis e eutéticos à base de Ibu. A avaliação do potencial de permeação permite orientar a correta formulação de um novo sistema de entrega transdérmica de fármacos. Os resultados desta tese compreendem uma prova de conceito para a viabilidade do uso de LIs e eutéticos baseados em IL, nomeadamente API-ILs e eutéticos baseados em API, no desenvolvimento de novos sistemas de administração de fármacos e, mais amplamente, para aplicações biológicas, bioquímicas e aplicações farmacêuticas.

Palavras-Chave: Líquidos Iônicos, Sistemas Eutéticos, Ibuprofeno, Solubilidade, Citotoxicidade, Atividade Hemolítica, Atividade Anti-inflamatória, Desnaturação de BSA, COX-1, COX-2, Ionicidade, Permeação cutânea.

PREFACE

The present thesis is composed of articles which were published as results of my work during my PhD project. Therefore, the reader may encounter some variations in the style of writing which are due to the different journal guidelines. The chapters of the present thesis are based on the following manuscripts:

Chapter 2: Joana C. Bastos, Sara F. Carvalho, Tom Welton, José N. Canongia Lopes, Luis Paulo N. Rebelo, Karina Shimizu, João M. M. Araújo, Ana B. Pereira. Design of task-specific fluorinated ionic liquids: nanosegregation versus hydrogen-bonding ability in aqueous solutions. *Chem. Commun.*, 2018, 54, 3524. DOI: 10.1039/c8cc00361k

Chapter 3: Joana C. Bastos, Nicole S. M. Vieira, Maria Manuela Gaspar, Ana B. Pereira, João M. M. Araújo. Human Cytotoxicity, Hemolytic Activity, Anti-Inflammatory Activity and Aqueous Solubility of Ibuprofen-Based Ionic Liquids. *Sustain. Chem.* 2022, 3, 358–375. DOI:10.3390/suschem3030023

Chapter 4: Joana C. Bastos, Maria Manuela Gaspar, Ana B. Pereira, João M. M. Araújo. Role of Ionic Liquids in Ibuprofen-based Eutectic Systems: Aqueous Solubility, Permeability, Human Cytotoxicity, Hemolytic Activity and Anti-Inflammatory Activity. *Pharmaceuticals* 2023. (*in press*); Joana C. Bastos, Ana B. Pereira, João M. M. Araújo. Liquid Ibuprofen Formulations by Eutectic Formation Between Ibuprofen-based Ionic Liquids and Ibuprofen: Human Cytotoxicity, Hemolytic Activity and Anti-Inflammatory Activity. *Pharmaceutics* 2023 (*Submitted*)

Chapter 5: Joana C. Bastos, Ana B. Pereira, João M. M. Araújo. Enhanced Membrane Permeability of Ibuprofen: Interplay of Ionic Liquids and Eutectics on Ionicity and Skin-PAMPA Permeability. *Journal Molecular Liquids* 2023 (*Submitted*)

CONTENTS

1. GENERAL INTRODUCTION.....	1
1.1 Non-steroidal anti-inflammatory drugs (NSAIDs).....	4
1.2 Ionic liquids and their role in the pharmaceutical field.....	6
1.3 Eutectic systems: fundamental aspects and current understanding in the pharmaceutical applications.....	9
1.4 Objectives and thesis outline.....	11
1.5 References.....	12
2. THE HYDROGEN-BONDING IN AQUEOUS SOLUTIONS OF IONIC LIQUIDS.....	18
2.1 Abstract.....	20
2.2 Introduction.....	21
2.3 Results and Discussion.....	22
2.4 References.....	28
2.5 Supporting Information.....	29
3. HUMAN CYTOTOXICITY, HEMOLYTIC ACTIVITY, ANTI-INFLAMMATORY ACTIVITY AND AQUEOUS SOLUBILITY OF IBUPROFEN-BASED IONIC LIQUIDS.....	44
3.1 Abstract.....	46
3.2 Introduction.....	48
3.3 Materials and Methods.....	52
3.3.1 Materials.....	52
3.3.2 Nuclear Magnetic Resonance (NMR).....	54
3.3.3 Differential Scanning Calorimetry (DSC).....	54
3.3.4 Solubility Studies.....	54
3.3.5 Cytotoxicity Assays.....	55
3.3.6 Hemolytic Activity.....	56
3.3.7 Protein Albumin Denaturation Assay.....	57
3.3.8 Cyclooxygenases (COX-1 and COX-2) Imhibition Assays.....	57

3.4 Results and Discussion.....	58
3.4.1 Characterization of the Ibuprofen-Based Ionic Liquids.....	58
3.4.2 Equilibrium Solubility in Water and Simulated Biological Fluids.....	60
3.4.3 Cytotoxicity Profile in Human Cell Lines.....	63
3.4.4 Hemolytic Activity.....	66
3.4.5 Protein Albumin Denaturation Assay.....	67
3.4.6 Cyclooxygenases (COX-1 and COX-2) Inhibition Assay.....	68
3.5 Conclusions.....	70
3.6 References.....	71
3.7 Supporting Information.....	77
4. IBUPROFEN-BASED EUTECTIC SYSTEMS.....	86
4.1 Role of Ionic Liquids in Ibuprofen-based Eutectic Systems: Aqueous Solubility, Permeability, Human Cytotoxicity, Hemolytic Activity and Anti-Inflammatory Activity.....	88
4.1.1 Abstract.....	88
4.1.2 Introduction.....	90
4.1.3 Materials and Methods.....	93
4.1.3.1 Materials.....	93
4.1.3.2 Preparation of Ibuprofen-based eutectic systems.....	94
4.1.3.3 Nuclear magnetic resonance (NMR).....	95
4.1.3.4 Differential Scanning Calorimetry (DSC).....	95
4.1.3.5 Solubility in water and simulated biological fluids.....	96
4.1.3.6 Density, Viscosity and Conductivity.....	96
4.1.3.7 Kamlet-Taft solvatochromic parameter: Hydrogen-bond acceptor ability (β).....	97
4.1.3.8 Cytotoxicity assays.....	98
4.1.3.9 Hemolytic Activity.....	100
4.1.3.10 Protein albumin denaturation assay.....	100
4.1.3.11 Cyclooxygenases (COX-1, COX-2) inhibition assay.....	101

4.1.4	Results.....	101
4.1.4.1	Characterization of ibuprofen-based eutectic systems.....	101
4.1.4.2	Hydrogen-bond acceptor ability (β) and dipolarity/polarizability (π^*) of Ibuprofen-based eutectics.....	106
4.1.4.3	Solubility of ibuprofen-based eutectics in water and biological simulated.....	110
4.1.4.4	Ionicity versus permeation potential of ibuprofen-based eutectic systems.....	116
4.1.4.5	Hemolytic activity and cytotoxic profile of ibuprofen-based eutectic systems.....	120
4.1.4.6	Anti-inflammatory activity of ibuprofen-based eutectic systems.....	122
4.1.5	Conclusions.....	126
4.1.6	References.....	127
4.1.7	Supplementary Materials.....	139
4.2	Liquid Ibuprofen Formulations by Eutectic Formation Between Ibuprofen-based Ionic Liquids and Ibuprofen: Human Cytotoxicity, Hemolytic Activity and Anti-inflammatory Activity.....	155
4.2.1	Abstract.....	155
4.2.2	Introduction.....	157
4.2.3	Materials and Methods.....	160
4.2.3.1	Materials.....	160
4.2.3.2	Preparation of pharmaceutically active eutectic systems.....	160
4.2.3.3	Nuclear Magnetic Resonance (NMR).....	161
4.2.3.4	Differential Scanning Calorimetry (DSC).....	161
4.2.3.5	Cytotoxicity profiles.....	162
4.2.3.6	Haemolytic activity.....	163
4.2.3.7	Protein albumin denaturation assay.....	164
4.2.3.8	Anti-inflammatory activity.....	164
4.2.4	Results and Discussion.....	165

4.2.4.1	Thermal and structural characterization of the eutectic systems...	165
4.2.4.2	Cytotoxic profile and hemolytic activity of ibuprofen-based eutectic systems.....	169
4.2.4.3	Anti-inflammatory activity: COXs and BSA inhibition.....	172
4.2.5	Conclusions.....	176
4.2.6	References.....	177
4.2.7	Supporting Information.....	183
5.	ENHANCED MEMBRANE PERMEABILITY OF IBUPROFEN: INTERPLAY OF IONIC LIQUIDS AND EUTECTICS ON IONICITY AND SKIN-PAMPA PERMEABILITY.....	190
5.1	Abstract.....	192
5.2	Introduction.....	194
5.3	Materials and Methods.....	201
5.3.1	Materials.....	201
5.3.2	Preparation of Ibuprofen-based eutectic systems.....	202
5.3.3	Density, Viscosity and Conductivity measurements.....	204
5.3.4	Skin Parallel Artificial Membrane Permeability Assay (Skin-PAMPA).....	204
5.4	Results and Discussion.....	206
5.4.1	Ionicity of ibuprofen-based eutectic systems and their membrane transport potential.....	206
5.4.2	Skin permeation prediction (Skin PAMPA).....	214
5.5	Conclusions.....	219
5.6	References.....	220
5.7	Supporting Information.....	226
6.	GENERAL CONCLUSIONS.....	234

LIST OF FIGURES

Figure 1.1 General mode of action of NSAIDs.....	5
Figure 2.1. Structures of ILs used in this work (complete designation in SI).....	22
Figure 2.2. Kamlet–Taft parameters (dye set Reichardt’s dye, N,N-diethyl-4-nitroaniline and 4-nitroaniline; cf. SI) for the binary systems $[C_2C_1Im][RSO_3] + H_2O$ at 298 K.....	23
Figure 2.3. Discrete probability distribution functions of water aggregate sizes, $P(na)$, for four IL + H ₂ O systems, each represented by 90, 50 and 30 wt _{IL} % composition mixtures (in green, cyan and blue, respectively). The snapshots (IL colour code in SI) represent the simulation boxes for the 30 wt _{IL} % mixtures.....	25
Figure 2.4 Discrete probability distribution functions of water aggregate sizes, $P(na)$, for four IL + H ₂ O systems, each represented by 90, 50 and 30 wt _{IL} % composition mixtures (in green, cyan and blue, respectively). The snapshots (IL colour code in SI) represent the simulation boxes for the 30 wt _{IL} % mixtures.....	26
Figure 2.S1. Comparison between experimental and literature data [S3] of Kamlet-Taft parameters for traditional ionic liquids at 298.15 K: a) 1-butyl-3-methylimidazolium bis(trifluoromethylsulfonyl)imide, $[C_4C_1Im][NTf_2]$; b) 1-butyl-3-methylimidazolium perfluoromethanesulfonate, $[C_4C_1Im][C_1F_3SO_3]$	33
Figure 2.S2. Kamlet-Taft parameters (dye set Reichardt’s dye, N,N-diethyl-4-nitroaniline and 4-nitroaniline) for the binary systems $[C_2C_1Im][RCO_2] + H_2O$ at 298.15 K.....	33
Figure 2.S3 Kamlet-Taft parameters (dye set Reichardt’s dye, N,N-diethyl-4-nitroaniline and 4-nitroaniline) for the binary systems $[C_2C_1Im][RSO_3] + H_2O$ (a–e) and $[C_2C_1Im][RCO_2] + H_2O$ (f, g) at 298.15 K, expressed in mol _{IL} %.....	35
Figure 2.S4 Electrical conductivity profile of $[C_2C_1Im][C_4F_9SO_3] + H_2O$ system at 298.15 K. The three critical aggregation concentrations (solid red lines) and the herein studied FIL	

concentrations in wt% (dashed blue lines) are also depicted. a) full concentration range and b) inset. Data adapted from reference S4.....36

Figure 2.S5 Electrical conductivity profile of [C₂C₁Im][C₄F₉SO₃] + H₂O system at 298.15 K. The three critical aggregation concentrations (solid red lines) and the herein studied FIL concentrations in mol% (dashed blue lines) are also depicted. a) full concentration range and b, c) inset. Data adapted from reference S4.....36

Figure 2.S6 Discrete probability distribution functions of water aggregate sizes, $P(n_a)$, for different compositions of water-IL mixtures.....40

Figure 2.S7 Discrete probability distribution functions of water aggregate sizes, $P(n_a)$, for different compositions of water-IL mixtures.....40

Figure 2.S8 Pair radial distribution functions, $g(r)$, between oxygen atoms in water (left column), and between sulphur atoms in the anion and oxygen atoms in water (right column) for different compositions of water-IL mixtures (green, cyan and blue represent 90, 50 and 30 wt_{IL}% compositions, respectively). To have a fair comparison between the first peaks in the different water-IL mixtures, the RDFs were multiplied by the corresponding numerical density (inset). The average size of contact neighbours, N_i , in the water aggregates and anion-water aggregates are also presented in the figure and were calculated from the integration of the first peaks of the corresponding $g(r)$ functions.....41

Figure 3.1. Solubility of ibuprofen, ibuprofen sodium salt and ibuprofen-based ILs in water (A). Solubility of ibuprofen, ibuprofen sodium salt and cholinium-based API-ILs in isotonic ionic strength aqueous solution (0.15 M NaCl), simulated gastric fluid (pH 1.0) and simulated intestinal fluid (pH 6.8) (B). All experiments were performed at 25 °C. * $p < 0.05$, ** $p < 0.01$63

Figure 3.2. Cytotoxicity profiles of ibuprofen in the neutral and sodium salt forms compared with [C₂C₁Im][Ibu] in Caco-2 (A) and HepG2 (B) with [C_{2(OH)}C₁Im][Ibu] in Caco-2 (C) and HepG2 (D) and with [N_{1112(OH)}][Ibu] in Caco-2 (E) and HepG2 (F). Both Caco-2 and HepG2 cells were exposed for 24 h to the respective API-ILs and parent API at the concentrations shown.....65

Figure 3.3. Inhibition profile of BSA denaturation by ibuprofen, ibuprofen sodium salt, [C ₂ C ₁ Im][Ibu], [C ₂ (OH)C ₁ Im][Ibu] and [N ₁₁₁₂ (OH)][Ibu].....	67
Figure 3.4. Selective inhibition of COX-1 and COX-2 enzymes for ibuprofen and ibuprofen-based ILs at 3 mM. The YY axis guideline corresponds to 50% COX inhibition.....	69
Figure 3.S1. DSC profile and analysis with TA Instruments Universal Analysis V4.5A software at 1°C/min of ibuprofen.....	81
Figure 3.S2. DSC profile and analysis with TA Instruments Universal Analysis V4.5A software at 1°C/min of [C ₂ C ₁ Im][Ibu].....	81
Figure 3.S3. DSC profile and analysis with TA Instruments Universal Analysis V4.5A software at 1°C/min of [C ₂ (OH)C ₁ Im][Ibu].....	82
Figure 3.S4. DSC profile and analysis with TA Instruments Universal Analysis V4.5A software at 1°C/min of [N ₁₁₁₂ (OH)][Ibu].....	82
Figure 3.S5. Non-linear regression fitting curves, calculated Log EC ₅₀ ± standard deviation and respective R-squared and p-value for ibuprofen (A), [C ₂ C ₁ Im][Ibu] (B), [C ₂ (OH)C ₁ Im][Ibu] (C), [N ₁₁₁₂ (OH)][Ibu] (D), [C ₂ C ₁ Im]Cl (E), [C ₂ (OH)C ₁ Im]Cl (F) and [N ₁₁₁₂ (OH)]Cl (G) in Caco-2 cell line.....	84
Figure 3.S6. EC ₅₀ values of ibuprofen, ibuprofen-based ILs and IL/salt cation “suppliers” for the API-ILs ([C ₂ C ₁ Im]Cl, [C ₂ (OH)C ₁ Im]Cl, [N ₁₁₁₂ (OH)]Cl) in Caco-2 cell line exposed to the compounds for 24h. The R-squared was greater than 0.9540 an P < 0.0001 for all fitted curves.....	85
Figure 4.1. DSC curves at 1° C/min for [N ₁₁₁₂ (OH)]Cl : Ibu systems, ibuprofen (HBD) and [N ₁₁₁₂ (OH)]Cl (HBA). Exo up in all thermograms.....	105
Figure 4.2. Hydrogen-bond acceptance ability (β) of ibuprofen-based eutectic systems. All β values are the average of three independent measurements.....	109
Figure 4.3. Dipolarity/polarizability (π^*) of ibuprofen-based eutectic systems at 25°C. All π^* values are the average of three independent measurements.....	110
Figure 4.4. Solubility of the ibuprofen-based eutectics, non-eutetics and neat ibuprofen in (A) water and buffer solutions suitable for dissolution testing, (B) isotonic ionic strength aqueous	

solution (0.15 M NaCl), simulated intestinal fluid (pH 6.8), and (D) simulated gastric fluid (pH 1.0), at 25°C. The * represents the non-eutectic systems.....115

Figure 4.5. Walden plot of ibuprofen-based eutectic systems.....119

Figure 4.6. Cytotoxicity profile of ibuprofen [18] compared with [C₂C₁Im]Cl-based eutectics in HEPG2 (A), HBA:Ibu 1:5 molar ratio eutectics in HEPG2 (B), [C₂C₁Im]Cl-based eutectics in Caco-2 (C) and HBA:Ibu 1:5 molar ratio eutectics in Caco-2 (D). Both cell lines were exposed for 24 h to the eutectic formulations prior to the cytotoxicity assessment. The XX axis guideline corresponds to the pharmacokinetic parameter maximum plasma concentration of ibuprofen (C_{max}, 0.175 mM).....122

Figure 4.7. Inhibition profile of BSA denaturation by the ibuprofen-based eutectic systems with the HBD [C₂C₁Im]Cl (A), the HBD [C_{2(OH)}C₁Im]Cl (B), and the HBD [N_{1112(OH)}]Cl (C). The profile of ibuprofen (parent-API) is also displayed123

Figure 4.8. Selective inhibition of COX-1 (ovine) and COX-2 (human) and COX-1/COX-2 selectivity for 3 mM ibuprofen and ibuprofen-based eutectics.....125

Figure 4.S1. DSC curves at 1° C/min for [C₂C₁Im]Cl: Ibu systems, ibuprofen (HBD) and [C₂C₁Im]Cl (HBA). Exo up in all thermograms.....142

Figure 4.S2. DSC curves at 1° C/min for [C_{2(OH)}C₁Im]Cl: Ibu systems, ibuprofen (HBD) and [C_{2(OH)}C₁Im]Cl (HBA). Exo up in all thermograms.....143

Figure 4.S3. DSC curves at 1° C/min for [C₂C₁Im][C₁CO₂]: Ibu systems, ibuprofen (HBD) and [C₂C₁Im][C₁CO₂] (HBA). Exo up in all thermograms.....143

Figure 4.S4. Density, viscosity and conductivity of the Ibuprofen-based eutectic systems based with [C₂C₁Im]Cl as hydrogen bond acceptor.....151

Figure 4.S5. Density, viscosity and conductivity of the Ibuprofen-based eutectic systems based with [C_{2(OH)}C₁Im]Cl as hydrogen bond acceptor.....151

Figure 4.S6. Density, viscosity and conductivity of the Ibuprofen-based eutectic systems based with [C₂C₁Im][C₁CO₂] as hydrogen bond acceptor.....151

Figure 4.S7. Density, viscosity and conductivity of the Ibuprofen-based eutectic systems based with [N _{1112(OH)}]Cl as hydrogen bond acceptor.....	152
Figure 4.S8. Selective inhibition of of COX-1 (ovine) and COX-2 (human) and COX-1/COX-2 selectivity for 3 mM ibuprofen, ibuprofen-based ionic liquids and ibuprofen-based eutectics.....	154
Figure 4.9. DSC profile with TA Instruments Universal Analysis V4.5A software at 1°C/min of (A) ibuprofen and N _{1112(OH)} [Ibu] and [N _{1112(OH)}][Ibu]-based systems, (B) [C ₂ C ₁ Im][Ibu] and [C ₂ C ₁ Im][Ibu]-based systems and (C) [C _{2(OH)} C ₁ Im][Ibu] and [C _{2(OH)} C ₁ Im][Ibu]-based systems.....	168
Figure 4.10. Cytotoxicity profiles for the eutectic systems containing pharmaceutically active ionic liquids in Caco-2 (A,C,E) and in HepG2 (B,D,F). Both cell lines were exposed for 24 h prior to the cytotoxicity assessment. Ibuprofen data were acquired from previous work. The vertical line represents the C _{max} of ibuprofen at 0.175 mM.....	171
Figure 4.11. Inhibition profile of BSA denaturation in [C ₂ C ₁ Im][Ibu]:Ibu (A), [C _{2(OH)} C ₁ Im][Ibu]:Ibu (B) [N _{1112(OH)}][Ibu]:Ibu (C) systems and compered to neat ibuprofen from previous work	173
Figure 4.12. Selective inhibition of COX-1 (ovine) and COX-2 (human) and COX-1/COX-2 selectivity at 3mM for the eutectic systems and their neat hydrogen-bond donor (ibuprofen) and hydrogen-bond acceptors([C ₂ C ₁ Im][Ibu], [C _{2(OH)} C ₁ Im][Ibu] and [N _{1112(OH)}][Ibu]).....	175
Figure 4.S9. Selective inhibition of COX-1 (ovine) and COX-2 (human) and COX-1/COX-2 selectivity at 3mM for the eutectic systems based on ILs ([C ₂ C ₁ Im]Cl, [C _{2(OH)} C ₁ Im]Cl and [N _{1112(OH)}]Cl) [S1] and for the eutectic systems based on API-ILs ([C ₂ C ₁ Im][Ibu], [C _{2(OH)} C ₁ Im][Ibu] and [N _{1112(OH)}][Ibu]).....	189
Figure 5.1. Parallel Artificial Membrane Permeability Assay (PAMPA) 96-well setup (left); a single well of PAMPA (right).....	199

Figure 5.2. Viscosity activation energies (E_η) for the eutectic systems calculated from Arrhenius equation (i.e., Eq. 5.1) for the IL-based eutectic systems and API-ILs-based eutectic systems.....	210
Figure 5.3. Conductivity activation energies (E_A) for the eutectic systems calculated from Arrhenius equation (i.e., Eq. 5.2) for the IL-based eutectic systems and API-ILs-based eutectic systems.....	212
Figure 5.4. Walden plot representation for the eutectic systems $[C_2C_1Im][Ibu]:Ibu$, $[C_{2(OH)}C_1Im][Ibu]$ and $[N_{1112(OH)}][Ibu]$ at the different molar ratios. The straight black line symbolizes the ideal electrode composed of a solution of KCL.....	214
Figure 5.5. Effective permeability (LogPe) obtained from Skin PAMPA of ibuprofen, ibuprofen-based API-ILs and ibuprofen-based eutectics at 250 mM for pH 6.5 (A) and pH 7.4 (B), at 25°C	218
Figure 5.S1 Density (A), Viscosity (B) and Conductivity (C) measurements for the formulations $[C_2C_1Im][Ibu]:Ibu$ 2:1, $[C_2C_1Im][Ibu]:Ibu$ 1:1, $[C_2C_1Im][Ibu]:Ibu$ 1:2 and $[C_2C_1Im][Ibu]:Ibu$ 1:5.....	229
Figure 5.S2. Density (A), Viscosity (B) and Conductivity (C) measurements for the formulations $[C_{2(OH)}C_1Im][Ibu]:Ibu$ 1:1, $[C_{2(OH)}C_1Im][Ibu]:Ibu$ 1:2 and $[C_{2(OH)}C_1Im][Ibu]:Ibu$ 1:5.....	229
Figure 5.S3 Density (A), Viscosity (B) and Conductivity (C) measurements for the eutectic formulations $[N_{1112(OH)}][Ibu]:Ibu$ 2:1, $[N_{1112(OH)}][Ibu]:Ibu$ 1:1, $[N_{1112(OH)}][Ibu]:Ibu$ 1:2 and $[N_{1112(OH)}][Ibu]:Ibu$ 1:5.....	229
Figure 5.S4 Density of the Ibuprofen-based eutectic systems at different molar ratio, namely 2:1, 1:1, 1:2 and 1:5.....	230
Figure 5.S5 Plot of the natural logarithm of the viscosity $\ln \eta$ versus the reciprocal temperature for the IL-based eutectic formulations ($[C_2C_1Im]Cl:Ibu$, $[C_{2(OH)}C_1Im]Cl:Ibu$, $[C_2C_1Im][C_1CO_2]:Ibu$ and $[N_{1112(OH)}]Cl:Ibu$ at the molar ratios 2:1, 1:1, 1:2 and 1:5[2]) and for the API-IL-based eutectic formulations ($[C_2C_1Im][Ibu]:Ibu$, $[C_{2(OH)}C_1Im][Ibu]:Ibu$ and $[N_{1112(OH)}][Ibu]:Ibu$ at the molar ratios 2:1, 1:1, 1:2 and 1:5).....	232

Figure 5.S6 Plot of the natural logarithm of the viscosity $\ln \eta$ versus the reciprocal temperature for the IL-based eutectic formulations ($[\text{C}_2\text{C}_1\text{Im}]\text{Cl}:\text{Ibu}$, $[\text{C}_{2(\text{OH})}\text{C}_1\text{Im}]\text{Cl}:\text{Ibu}$, $[\text{C}_2\text{C}_1\text{Im}][\text{C}_1\text{CO}_2]:\text{Ibu}$ and $[\text{N}_{1112(\text{OH})}]\text{Cl}:\text{Ibu}$ at the molar ratios 2:1, 1:1, 1:2 and 1:5 [2]) and for the API-IL-based eutectic formulations ($[\text{C}_2\text{C}_1\text{Im}][\text{Ibu}]:\text{Ibu}$, $[\text{C}_{2(\text{OH})}\text{C}_1\text{Im}][\text{Ibu}]:\text{Ibu}$ and $[\text{N}_{1112(\text{OH})}][\text{Ibu}]:\text{Ibu}$ at the molar ratios 2:1, 1:1, 1:2 and 1:5).....233

LIST OF TABLES

Table 2.S1. Description of the ionic liquids and inorganic salts used in this work.....	31
Table 2.S2 Kamlet-Taft parameters, hydrogen-bond donor (α), hydrogen-bond acceptor (β), and dipolarity/polarizability (π^*), with their corresponding standards deviations (σ), determined for the neat ILs and aqueous solutions studied in this work.....	34
Table 2.S3. Simulation conditions, size of the equilibrated boxes and concentrations.....	39
Table 3.1. Chemical structures and respective acronyms and molecular weights of ibuprofen, sodium ibuprofen and the ibuprofen-based API-ILs.....	53
Table 3.2. Chemical shifts for the hydrogens in positions 2 and 3 (as depicted in the chemical structure of ibuprofen on the bottom) for ibuprofen, sodium ibuprofen and API-ILs in DMSO.....	60
Table 3.3. Glass transition temperatures (T_g) and melting temperatures (T_m) of ibuprofen and ibuprofen-based ILs determined by DSC at a heating rate of 1 °C/min.....	60
Table 3.4. Solubility of ibuprofen, sodium ibuprofen and ibuprofen-based ILs in water and the solubility of ibuprofen, ibuprofen sodium and cholinium-based API-IL in buffer solutions suitable for dissolution testing, isotonic ionic strength aqueous solution (0.15 M NaCl), simulated gastric fluid (pH 1.0) and simulated intestinal fluid (pH 6.8). All experiments were performed at 25 °C \pm 0.1 °C. The solubility was the overall mean of at least two independent experiments \pm standard deviation.....	61
Table 3.5. EC ₅₀ values of ibuprofen, ibuprofen-based ILs and IL/salt cation “suppliers” for the API-ILs (i.e., [C ₂ C ₁ Im]Cl, [C ₂ (OH)C ₁ Im]Cl and [N ₁₁₁₂ (OH)]Cl) in the Caco-2 cell line exposed to the compounds for 24 h. The R-squared was greater than 0.9540 and $p < 0.0001$ for all fitted curves.....	65
Table 3.6. Inhibition of COX-1 (ovine) and COX-2 (human) and COX-1/COX-2 selectivity for 3 mM ibuprofen and ibuprofen-based ILs.....	70

Table 3.S1. Chemical shifts for the hydrogens in the position 2 and 3 (as depicted chemical structure of ibuprofen on the right) for ibuprofen, sodium ibuprofen and API-ILs in D ₂ O.....	83
Table 3.S2. Inhibition of BSA denaturation in PBS pH 7.4 at different concentrations for the neutral and salt form of ibuprofen and API-ILs. The presented value is the mean of at least two independent measures \pm standard deviation.....	85
Table 4.1. Designation, chemical structure, and molecular weight (Mw) of ibuprofen, cholinium salt and imidazolium-based ILs used along this work.....	94
Table 4.2. ¹ H NMR chemical shifts for the position 2 and 3 according to the chemical structure of ibuprofen (right) for all the eutectic systems in DMSO.....	104
Table 4.3. Thermal properties (<i>T_g</i> and <i>T_m</i>) of the ibuprofen-based eutectic systems, ibuprofen (HBD) and hydrogen-bond acceptors, determined by DSC at a heating rate of 1°C/min. A solid-solid transition is reported for [N _{1112(OH)}]Cl for eutectics validation in the range of temperatures tested by DSC.....	106
Table 4.4. Solubility of ibuprofen-based eutectic and non-eutectic systems in water, isotonic ionic strength aqueous solution (0.15 M NaCl), simulated intestinal fluid (pH 6.8) and simulated gastric fluid (pH 1.0) at 25°C. The solubility is the overall mean of three independent experiments \pm standard deviation.....	113
Table 4.5. Inhibition of COX-1 (ovine) and COX-2 (human) and COX-1/COX-2 selectivity for 3 mM ibuprofen and ibuprofen-based eutectics.....	126
Table 4.S1. Validation of the prepared ibuprofen-based mixtures as eutectic mixtures based on the Lab benchtop procedure (dynamic visual method) used to determine the liquid-solid transition of the prepared mixtures. All mixtures validated as eutectic systems were liquid at room temperature (RT).....	142
Table 4.S2. ¹ H NMR chemical shifts for the position 2' and 3' according to the chemical structure of [C ₂ C ₁ Im][C ₁ CO ₂] (right) for all the eutectic systems.....	142
Table 4.S3. Kamlet-Taft parameters, hydrogen-bond acceptor (β) and dipolarity/polarizability (π^*) with their corresponding standards deviations determined for the eutectic systems studied in this work.....	144

Table 4.S4. The effect of the different HBA's in ibuprofen solubility, eutectic and non-eutectic formulations, in water and simulated fluids (pH 1.0, pH 6.8 and 0.15M NaCl).....	145
Table 4.S5. The effect of the molar ratio in ibuprofen solubility, eutectic and non-eutectic formulations, in water and simulated fluids (pH 1.0, pH 6.8 and 0.15M NaCl).....	146
Table 4.S6. Density, ρ , dynamic viscosity, η , and ionic conductivity, k , as a function of temperature of ibuprofen-based systems with [C ₂ C ₁ Im]Cl as hydrogen bond acceptor.....	147
Table 4.S7. Density, ρ , dynamic viscosity, η , and ionic conductivity, k , as a function of temperature of ibuprofen-based systems with [C _{2(OH)} C ₁ Im]Cl as hydrogen bond acceptor.....	148
Table 4.S8. Density, ρ , dynamic viscosity, η , and ionic conductivity, k , as a function of temperature of ibuprofen-based systems with [C ₂ C ₁ Im][C ₁ CO ₂] as hydrogen bond acceptor.....	149
Table 4.S9. Density, ρ , dynamic viscosity, η , and ionic conductivity, k , as a function of temperature of [N _{1112(OH)}]Cl:Ibu 1:5.....	150
Table 4.S10. Inhibition of BSA denaturation in PBS pH 7.4 at different concentrations for ibuprofen-based eutectic systems. The presented value is the mean of at least two independent measures \pm standard deviation.....	153
Table 4.S11. Inhibition of COX-1 (ovine) and COX-2 (human) and COX-1/COX-2 selectivity for 3 mM ibuprofen, ibuprofen-based ionic liquids and ibuprofen-based eutectics.....	153
Table 4.6. Designation, chemical structure, and molecular weight (M_w) of ibuprofen and cholinium- and imidazolium-based API-ILs used along this work.....	160
Table 4.7. Glass transition temperatures (T_g) and melting temperatures (T_m) of the neat hydrogen-bond donor (ibuprofen), hydrogen-bond acceptors ([C ₂ C ₁ Im][Ibu], [C _{2(OH)} C ₁ Im][Ibu] and [N _{1112(OH)}][Ibu]) and the resulted binary combinations (API-IL:Ibu) acquired at 1°C/min.....	167
Table 4.8. ¹ H NMR chemical shifts (δ) for position 2 and 3 according to the chemical structure of ibuprofen (right) for all the eutectic systems in DMSO.....	169

Table 4.9. Inhibition of COX-1 (ovine) and COX-2 (human) and COX-1/COX-2 selectivity for 1mM of eutectic systems containing pharmacologically active ionic liquids and near ibuprofen at the molar ratios 1:1 and 1:5 at 37°C±1.....	176
Table 4.S9. ¹ H NMR chemical shifts for the position C2' according to the chemical structure of [C ₂ C ₁ Im][Ibu] and [C _{2(OH)} C ₁ Im][Ibu] (right) for the neat ionic liquid and its eutectic systems in DMSO.....	187
Table 4.S10. Inhibition of BSA denaturation in PBS pH 7.4 at different concentrations for ibuprofen-based eutectic systems. The presented value is the average of at least two independent measures ± standard deviation.....	188
Table 5.1. Designation, chemical structure, and molecular weight (Mw) of ibuprofen, cholinium salt and all the ionic liquids used along in this work.....	203
Table 5.2. Activation energy of density (E_{η}) and its constant (η_0) and activation energy of conductivity (E_A) and its constant (s_0) according to the Arrhenius equation for the IL-based eutectic formulations ([C ₂ C ₁ Im]Cl:Ibu, [C _{2(OH)} C ₁ Im]Cl:Ibu, [C ₂ C ₁ Im][C ₁ CO ₂]:Ibu) and [N _{1112(OH)}]Cl:Ibu and for the API-IL-based eutectic formulations [C ₂ C ₁ Im][Ibu]:Ibu, [C _{2(OH)} C ₁ Im][Ibu]:Ibu and [N _{1112(OH)}][Ibu]:Ibu at different molar ratios (2:1, 1:1, 1:2 and 1:5)....	209
Table 5.3. Effective permeability coefficient (Pe) and LogPe values from the Skin-PAMPA at pH 6.5 and pH 7.4 for ibuprofen at 250mM and 125 mM and ibuprofen-based API-ILs and ibuprofen-based eutectics at 250mM, at 25°C.....	216
Table 5.S1. Thermal properties (T_g and T_m) of the ibuprofen and ibuprofen-based formulations determined by DSC at a heating rate of 1°C/min.....	226
Table 5.S2. Density, ρ , dynamic viscosity, η , and ionic conductivity, k , as a function of temperature of ibuprofen-based systems with [C ₂ C ₁ Im][Ibu], [C _{2(OH)} C ₁ Im][Ibu] and [N _{1112(OH)}][Ibu] as hydrogen bond acceptor at the molecular ratios 2:1, 1:1, 1:2 and 1:5.....	227

Table 5.S3. Activation energy of density (E_η) and its constant (η_0) and activation energy of conductivity (E_A) and its constant (s_0) according to the Arrhenius equation for the IL-based eutectic formulations ([C₂C₁Im]Cl:Ibu, [C_{2(OH)}C₁Im]Cl:Ibu, [C₂C₁Im][C₁CO₂]:Ibu) and [N_{1112(OH)}]Cl:Ibu [2] and for the API-IL-based eutectic formulations [C₂C₁Im][Ibu]:Ibu, [C_{2(OH)}C₁Im][Ibu]:Ibu and [N_{1112(OH)}][Ibu]:Ibu at different molar ratios (2:1, 1:1, 1:2 and 1:5)...231

CHEMICAL FORMULAE

[Ran][Doc]	Ranitidine Docusate
[C_{2(OH)}C_{1Im}][Ibu]	1-(2-Hydroxyethyl)-3-methylimidazolium Ibuprofenate
[P₆₆₆₍₁₄₎][Amp]	Trihexyltetradecylphosphonium Ampicillin
[C_{2(OH)}C_{1Im}][Amp]	1-(2-Hydroxyethyl)-3-methylimidazolium Ampicillin
[N_{112(OH)}][Amp]	Cholinium Ampicillin
[Lid][Eto]	Lidocainium Etodolac
HCl	Hydrochloric acid
H	Hydrogen
[C₂C_{1Im}][C₁CO₂]	1-Ethyl-3-methylimidazolium Acetate
[C₂C_{1Im}]⁺	1-Ethyl-3-methylimidazolium
[RSO₃]⁻	Sulfonate-based anions
[RCO₂]⁻	Carboxylate-based anions
H₂O	Water
[C₁CO₂]⁻	Acetate
[C₁F₃CO₂]⁻	Trifluoroacetate
[C₁SO₃]⁻	Methanesulfonate
[C₁F₃SO₃]⁻	Trifluoromethanesulfonate
[C₂F₄SO₃]⁻	1,1,2,2-Tetrafluoro-ethanesulfonate
[C₂C_{1Im}][C₄F₉SO₃]	1-Ethyl-3-methylimidazolium Perfluorobutanesulfonate
[C₂C_{1Im}][C₈F₁₇SO₃]	1-Ethyl-3-methylimidazolium Perfluorooctanesulfonate
[C₄F₉SO₃]⁻	Perfluorobutanesulfonate
[C₈F₁₇SO₃]⁻	Perfluorooctanesulfonate
[C₄H₉SO₃]⁻	Butane Sulfonate

[C₂C₁Im][C₁F₃SO₃]	1-Ethyl-3-methylimidazolium Trifluoroacetate
[C₂C₁Im][C₂F₄SO₃]	1-Ethyl-3-methylimidazolium 1,1,2,2-Tetrafluoroethanesulfonate
[C₂C₁Im][C₁SO₃]	1-Ethyl-3-methylimidazolium Methanesulfonate
[C₂C₁Im][C₁F₃CO₂]	1-Ethyl-3-methylimidazolium Trifluoroacetate
[C₄C₁Im][CF₃SO₃]	1-Butyl-3-methylimidazolium Trifluoromethanesulfonate
[C₄C₁Im][NTf₂]	1-Butyl-3-methylimidazolium Bis(trifluoromethylsulfonyl)imide
[C₂C₁Im][Ibu]	1-Ethyl-3-methylimidazolium Ibuprofenate
[N_{1112(OH)}][Ibu]	Cholinium Ibuprofenate
[N_{1112(OH)}][Nal]	Cholinium Nalidixic
[N_{1112(OH)}][Nif]	Cholinium Niflumic
[C₂C₁Im][Amp]	1-Ethyl-3-methylimidazolium Ampicillin
[N_{1112(OH)}][Amp]	Cholinium Ampicillin
Na[Ibu]	Sodium Ibuprofen Salt
NaCl	Sodium Chloride
CO₂	Carbon dioxide
XTT	2,3-bis-(2-methoxy-4-nitro-5-sulfophenyl)-2H-tetrazolium-5-carboxanilide
[C₂C₁Im]Cl	1-Ethyl-3-methylimidazolium Chloride
[C_{2(OH)}C₁Im]Cl	1-(2-Hydroxyethyl)-3-methylimidazolium Chloride
[N_{1112(OH)}]Cl	Cholinium Chloride
TMPD	N, N, N' and N'-tetramethyl-phenylenediamine
-COOH	Hydroxyl group
DMSO	Dimethyl sulfoxide
D₂O	Deuterium oxide
[C₄C₁Im][Ibu]	1-Butyl-3-methylimidazolium Ibuprofenate

$[\text{N}_{1112}(\text{OH})]^+$	Cholinium
$[\text{C}_{2(\text{OH})}\text{C}_{1\text{Im}}]^+$	1-(2-Hydroxyethyl)-3-methylimidazolium
CDCl_3	Deuterated Chloroform

ACRONYMS AND ABBREVIATIONS

API	Active Pharmaceutical Ingredient
R&D	Research and Development
NSAID	Non-steroidal Anti-inflammatory Drug
COX-1	Cyclooxygenase 1
COX-2	Cyclooxygenase 2
PG	Prostaglandin
AA	Arachidonic Acid
Ibu	Ibuprofen
IL	Ionic Liquid
API-IL	Ionic Liquid with an Active Pharmaceutical Ingredient
HIV	Human Immunodeficiency Virus
HBA	Hydrogen-bonded Acceptor
HBD	Hydrogen-bonded Donor
EMLA	System Lidocaine and Prilocaine at 1:1 molar ratio
Caco-2	Human Colon Adenocarcinoma Cells
HepG2	Liver Carcinoma Cells
BSA	Bovine Serum Albumin
PAMPA	Parallel Artificial Membrane Permeability Assay
FIL	Fluorinated Ionic Liquid
DNA	Deoxyribonucleic Acid
MD	Molecular Dynamics Simulations
NMR	Nuclear Magnetic Resonance
Milli-Q	Ultrapure water

DCM	Dichloromethane
UV-vis	Ultraviolet-visible spectroscopy
DSC	Differential Scanning Calorimetry
PBS	Phosphate-Buffered Saline Solution
FBS	Fetal Bovine Serum
MEM	Minimum Essential Medium
MEM-NEAA	Minimum Essential Medium with Non-Essential Amino Acids
EDTA	Ethylene Diamine Tetraacetic Acid
Abs	Absorbance
EtOH	Ethanol
EMA	European Medicines Agency
PGG ₂	Prostaglandin G ₂
PGH ₂	Prostaglandin H ₂
GI	Gastrointestinal
BSC	Biopharmaceutics Classification System
POC	Poly Octanediol-co-citrate
Mw	Molecular Weight
RT	Room Temperature
PAMPA	Parallel Artificial Membrane Permeability Assay

SYMBOLS

pH	Potential of Hydrogen
pKa	Dissociation Constant
α	Kamlet-Taft parameter for hydrogen-bond donor capacity (acidity)
β	Kamlet-Taft parameter for hydrogen-bond acceptor capacity (basicity)
π^*	Dipolarity/Polarizability
K	Kelvin
P(n_a)	Size Distribution Probability
wt%	Weight Fraction
ρ	Density
k	Ionic conductivity
η	Dynamic viscosity
T	Temperatyre
η_{β}	Size binary parameter
l_{box}	Box Length
V_{box}	Box Volume
IC₅₀	Half Maximal Inhibitory Concentration
C_{max}	Maximum Plasma Concentration
°C	Celsius
T_m	Melting Temperature
rpm	Revolutions Per Minute
EC₅₀	Half Maximal Effective Concentration
C	Absorbance of the 100% initial activity
T	Subtraction of each inhibitor from the 100% initial activity

T_g	Glass Transition Temperature
δ	Chemical shift
LogP	Logarithmic partition coefficient
Eη	Activation energy of density
η_0	Constant of the activation energy of density
Eλ	Activation energy of viscosity
s_0	Constant of the activation energy of viscosity
Pe	Effective permeability coefficient
LogPe	Logarithmic effective permeability

GENERAL INTRODUCTION

The emerging trends in drug design and combinational chemistry have leading to the development of drugs candidates with greater lipophilicity, high molecular weight and poor water-solubility. Further, the major failure in the drug development process have been attributed to poor water-solubility where around 40% of drugs with market approval and nearly 90% of molecules in the discovery pipeline are poorly water-soluble, which compromise bioavailability and therapeutic efficacy and consequent failure in the later stages of development [1].

Active pharmaceutical ingredients (APIs) are the active components in drugs that are responsible for producing the required effect to treat a condition. APIs can be commercialized in several dosage forms but the solid form in the shape of a tablet have been the first choice of manufacturers over the years due to their comparatively low cost of manufacturing, packaging, shipping, and ease of administration [2]. However, the downsides of solid forms grasp from the irregular gastrointestinal absorption along with the low therapeutic efficiency to a possible toxicity and side-effects of polymorphs [3,4]. For instance, the differences in bioavailability among the different API's polymorphs as required different drug dosages to achieve the therapeutic effect and the therapeutic dosage of a certain API can correspond to a toxic or potential lethal dose of its polymorph. Thus, the polymorphism issues result in significant economic losses in sales and in R&D to enable novel formulations back into the market [4].

The oral ingestion is the most convenient and commonly employed route of drug delivery, however the major challenge with the design of oral dosage forms lies with the drug poor bioavailability. The oral bioavailability depends on several factors, but the most frequent causes are attributed to poor solubility and low permeability [5]. Solubility also plays a major role for other dosage forms like parental formulations where poorly water soluble drugs often required high doses in order to reach therapeutic plasma concentrations. Any drug to be absorbed must be present in the form of an aqueous solution at the site of absorption [5]. Examples of strategies for improving and maximizing the drugs solubilities include the use of salt forms with enhanced dissolution profiles, solubilisation of drugs in co-solvents and micellar solutions and the use of lipidic systems for the delivery of lipophilic drugs [1,6].

In the above context, liquid forms of APIs, such as pharmaceutically active ionic liquids (API-ILs) and eutectics systems [7–9], are appealing solutions to avoid both polymorphism and improve low-water solubility constraints, while allowing to reduce organic solvents use.

1.1 Non-steroidal anti-inflammatory drugs (NSAIDs)

In the 1830s the salicylate was isolated from willow bark, followed by the discovery of the acetyl salicylate (aspirin) by Felix Hoffman of Bayer industry, Germany, in 1897. Since the first discovery, non-steroidal anti-inflammatory drugs (NSAIDs) have been enjoying a blockbuster status in the pharmaceutical industry [10]. NSAIDs constitute 5% of all the prescribed medicines worldwide being the most popular over-the-counter drugs [11]. They are mainly use for the treatment of patients suffering from pain and inflammatory conditions such as chronic pain, osteoarthritis, rheumatoid arthritis, postoperative surgical conditions and menstrual cramps [12].

In addition to the common use of NSAIDs, a recent study on amyloid beta-induced experimental Alzheimer's disease in mice has shown that mefenamic acid, a fenamate NSAID used to relieve period pain, could offer protection by suppressing neuroinflammation and memory loss [13]. Despite this extensive therapeutic utility, the NSAIDs are infamous for multiple severe side effects including gastrointestinal toxicities, cardiovascular risks, renal injuries, and hepatotoxicity as well as hypertension and other minor disorders [12].

The general mode of action of NSAIDs involves the inhibition of cyclooxygenases (COXs) implicated in the biosynthesis of prostaglandin (PG) which is strongly implicated in inflammation as shown in **Figure 1.1**. The bioconversion of arachidonic acid (AA) into inflammatory prostanoids (prostaglandins and prostacyclins) is mediated by COX enzymes (COX-1 and COX-2) which can be inhibited by NSAIDs. COX-1 is referred to as a “constitutive isoform” and is considered to be expressed in most tissues under basal conditions being responsible for vital functions such as the maintenance of gastrointestinal tract and vascular homeostasis. In contrast, COX-2 is referred to as an “inducible isoform”, which is believed to be undetectable in most normal tissues, but

can be up-regulated during various conditions, many of them pathological [14]. Almost all the NSAIDs on the market inhibit both the COX isoforms at their therapeutic doses but the desired formulation is one NSAID that selectively inhibit only the COX-2 present in pathological conditions to prevent the common side effects associated to COX-1 selectivity [12]. Thus, newer approaches or alternative strategies were taken for a chemical modification to tame down the toxic side effects without compromising their beneficial health effects.

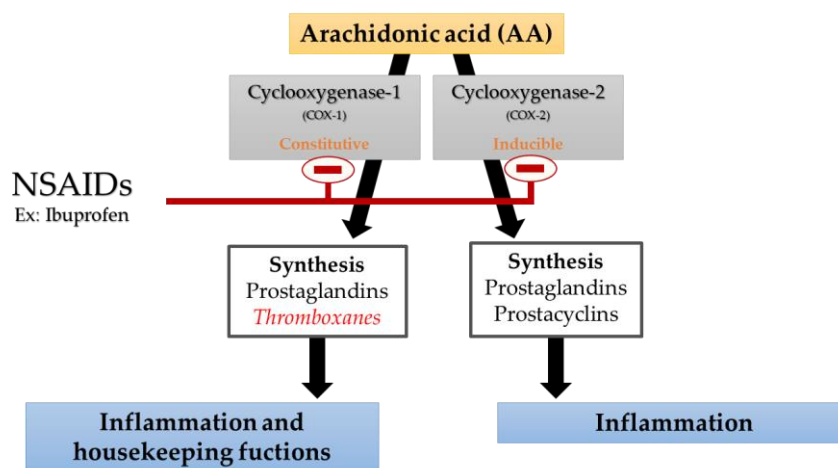


Figure 1.1 General mode of action of NSAIDs [15,16]

Ibuprofen (Ibu), chemically known as 2-(4-isobutylphenyl)-propionic acid, is a representative NSAID and it was the first member of propionic acid derivatives to be introduced in 1969 as a better alternative to aspirin [17]. Besides, ibuprofen is the most commonly used and most frequently prescribed NSAID [12]. It is considered a non-selective inhibitor of COX-1 and COX-2 enzymes used to treat rheumatoid arthritis and osteoarthritis, pain, and fever [17].

The most used delivery route of ibuprofen is the oral route, however, to treat pain and fever it is necessary to achieve quick relief which is directly related to the ibuprofen absorption rate into the blood ultimately depending on the drug dissolution rate and solubility [18]. Ibuprofen shows poor solubility in water and presents a relatively high lipophilicity. Its solubility mainly depends on the pH where solutions at a pH above the ibuprofen pKa (pKa = 4.44) the solubility is greatly increased resulting from ionisation [19]. Potthast et al. [18] showed that solubility of ibuprofen at 37°C was 0.038 mg/mL at pH 1 and it increased 2-fold (0.084 mg/mL) and almost 20-fold (0.685 mg/mL) when the

pH was changed to 4.5 and 5.5, respectively. When the authors increased the pH to 6.8 the solubility was increased by 100-times higher (3.37 mg/mL)[13]. The dosage of ibuprofen in common commercial formulas is generally 200 mg to be administered every 6h, however the quantity required for therapeutic purposes in adult is only 20 mg. The commercialized forms possess more than 10-fold this amount due to the ibuprofen poor absorption and first pass metabolism but also due to their poor aqueous solubility. This limited solubility and rate of solution demand that commercial formulas need to use higher doses to reach it therapeutic effect when administered contributing to the increase in some of the unwanted adverse effects [20].

The commercially used ibuprofen salt (NaIbu) is an example of the simplest modification required to increase ibuprofen solubility properties. The acid proton is replaced by the the sodium cation and solubility in polar solvents, including water, is significantly increased compared to parent acid, with a faster action leading to an earlier pain relief [21]. The ibuprofen anion was also paired with other organic cations such as arginine or lysine salts and, similar to sodium salt more commonly used, an increase in solubility is achieved and a higher mean maximum plasma or serum ibuprofen concentration in a shorter time was found [22–24]. Formation of ibuprofen ion-pairs using organic bases was also implemented to be an effective approach in topical ibuprofen administration. Dermal delivery overcomes several side effects of systemic use. It contends the therapeutic effects to the affected site and limits systematic absorption to the vascular system, thereby avoiding first-pass hepatic metabolism and ibuprofen gastrointestinal toxicity [17,25].

1.2 Ionic liquids and their role in the pharmaceutical field

The pharmaceutical industry has relied on the use of ionic forms to improve drugs solubility problems [22]. In this context, ionic liquids (ILs) disclose high potential in the pharmaceutical field mainly due to their high versatility in terms of chemical structure design towards a target application [26,27]. ILs are salts that are composed of a organic cation and an organic/inorganic anion where the large dimensions of their ions lead to charge dispersion making difficult the formation of a regular crystalline structure. Thus,

they can be solid at room temperature, however by definition the salts are considered ILs when their melting temperature is lower than 100°C [27]. ILs display a set of unique features, from which is possible to highlight, if properly designed, their high thermal and chemical stability and a strong solvation ability for a wide variety of compounds [28–30]. The proper selection of cation-anion combinations in ILs enables the use of drugs as ion components, allowing the conversion of solid active pharmaceutical ingredients in novel ionic liquid forms (API-ILs). Thus, this strategy solves the problem of polymorphism, provides improved bioavailability by enhancing solubility [3] and may display specific biological activities with promising results already disclosed, namely antioxidant, anti-tumoral, and antimicrobial activity, covering some of the main types of cation-based ILs studied so far [31].

The first API-IL was reported in 2007 by Rogers et al. [32] with the synthesis of ranitidine docusate ([Ran][Doc])[27]. Ranitidine is an anti-ulcer drug in current use and one of the 20 most frequently prescribed drugs. Crystalline ranitidine is polymorphic and exists in two crystalline forms known as Form 1 and Form 2, and in several pseudo-polymorphic forms [33]. Rogers and co-workers have demonstrated that by converting ranitidine into an IL, combining with docusate anion, the polymorphism problem is settled, and the API absorption is upgraded. After this pioneering work several different API-ILs with different pharmacological classes have been reported mainly using the API as the anion combined with a conventional cation such as cholinium or imidazolium since they are extensively studied in the literature and, especially the cholinium is known as a safe and low-cost cation source[34–37].

In general, the salt formation provided by the API-IL platform can exhibit improved solubility and bioavailability when compared with the original API. In fact, botulinic acid, a low-water soluble natural product with anti-cancer, anti-inflammatory and anti-HIV properties, has been converted into API-IL using cholinium as counterion. This combination significantly improved the aqueous solubility by 100-fold and its half maximal inhibitory concentration (IC₅₀) was upgraded from 60 to 22 µg mL⁻¹. This strategy resulted in a higher ability of liberating its latent biological activity for inhibition of HIV-1 protease [38]. Other poorly water-soluble APIs with anti-inflammatory

activities (diclofenac, ibuprofen, ketoprofen, naproxen) and antibiotic properties (sulfadiazine, sulfamethoxazole) and a first-generation potassium channel blocker (tolbutamide) were converted into tetrabutylphosphonium-based API-ILs, and their solubility in water was compared to their free acids versions [39]. The tetrabutylphosphonium-based ILs enhance the solubility of the corresponding API in aqueous media up to 80-fold, 60-fold and 70-fold for ibuprofen, ketoprofen and naproxen respectively. The higher upgrade in solubility was observed for the sulfadiazine API-IL with an increase up to 130-fold [39]. Regarding the conversion of ibuprofen into 1-ethanol-3-methylimidazolium ibuprofenate ($[\text{C}_{2(\text{OH})}\text{C}_1\text{Im}][\text{Ibu}]$), an increase in the API's solubility in water was achieved by 155-fold in comparison to the original API [40]. In another study, the authors prepared a set of ibuprofen-based ILs with different organic cations (e.g., cholinium, imidazolium and acetylpyridine) with increased solubility in aqueous media and negligible cytotoxicity towards human dermal fibroblasts and ovarian carcinoma cells [41].

Other example of API-ILs, among many that can be found in the open literature, is the conversion of ampicillin into imidazolium-based API-ILs, that has been described by several authors to enhance aqueous solubility, improve the API hydrophilicity and improve biological activities. Ferraz and co-workers [42] converted ampicillin into trihexyltetradecylphosphonium ampicillin ($[\text{P}_{666(14)}][\text{Amp}]$), 1-hydroxy-ethyl-3-methylimidazolium ampicillin ($[\text{C}_{2(\text{OH})}\text{C}_1\text{Im}][\text{Amp}]$) and cholinium ampicillin ($[\text{N}_{1112(\text{OH})}][\text{Amp}]$) and later determined the aqueous solubility and the respective hydrophilic/lipophilic balance of these API-ILs. The water solubility for $[\text{N}_{1112(\text{OH})}][\text{Amp}]$ and $[\text{C}_{2(\text{OH})}\text{C}_1\text{Im}][\text{Amp}]$ was found to be comparable to the water solubility of the respective ampicillin sodium salts and it increased by 9-fold at body's temperature in comparison with the pure salt. Additionally, an enhancement in the octanol–water partition coefficient by 11- and 7-fold for the cholinium and imidazolium-based API, respectively, was verified [26]. The antibacterial activity assay showed increased growth inhibition for some Gram-negative resistant bacteria, achieving MIC values 10–1000 higher than the ampicillin salt, including the action against resistant bacterial strains [43]. Additionally, the anti-tumoral activity of these ampicillin-based-ILs was assessed in human cancer cell lines and the $[\text{C}_{2(\text{OH})}\text{C}_1\text{Im}][\text{Amp}]$ shown to be the most relevant

ampicillin-based IL, with a higher antiproliferative activity and lower cytotoxicity being associated towards healthy cells[44].

The possibility of having an API in both the cation and the anion may lead to dual therapeutic functionalized ILs. An example of that is the API-IL composed of lidocaine and etodolac in the form of lidocainium etodolac ([Lid][Eto]). These dual function API-IL can exhibit superior water solubility than both APIs alone, with an increase of >90-fold for etodolac and two-fold for lidocaine [45]. The [Lid][Eto] is to date the first API-IL going under clinical trials. In 2013 the Japanese company MEDRx published the phase I trial data for the MRX-7EAT lidocaine etodolac topical patch, which resulted in a faster absorption through skin with mild to moderate adverse effects. The phase II and III trials have been conducted to evaluate the efficacy and safety of the patch in several types of pain treatment. However, at the end of November 2016 MEDRx decided to terminate the development of the MRX-7EAT topical patch due to unsatisfactory trial results [46]. In the future, the diversity of the API-IL toolbox, with multiple possibilities to provide new biologically active combinations, still must be more extensively investigated.

1.3 Eutectic systems: fundamental aspects and current understanding in the pharmaceutical applications

In recent years, eutectic systems have emerged as a valuable alternative to incorporate APIs in addition to the ILs platform, being also able to produce new liquid forms of pharmaceuticals and to ultimately enhance their bioavailability. They are characterized as mixtures constituted with a certain proportion of hydrogen-bonded acceptors (HBA) and hydrogen bonded donors (HBD) with strong nonbonding interactions, such as dipole, hydrogen bond, alkyl-alkyl interactions, halogen bonds, and Van der Waals forces, which lead to a significant depression of the melting point and inhibit the crystallization process [9,47]. Unlike ILs, eutectic systems are not considered pure compounds since they are a mixture, however their preparation is more unexpensive and greener since their synthesis usually involves the simple mixing of the components generally under stirring and moderate heating[9].

The first evidence of a eutectic system with therapeutic functions was observed in 1964 by Sekiguchi and Obi [48] with a eutectic system that distinctly improved the solubility and oral absorption rate of sulfathiazole [48]. The explanation for the enhancement of sulfathiazole solubility was found after dissolution of urea, used as high-water soluble carrier, when a fine suspension of drug particles was exposed to the dissolution medium. The smaller particle size and the better wettability of the drug particles in this suspension contributed to a faster dissolution rate. Later in 1998, Stott et al. [49] prepared a mixture comprised of menthol and ibuprofen with the purpose of increasing skin permeation and development of a transdermal delivery system for ibuprofen[50]. Nowadays, the eutectic formed by lidocaine and prilocaine in a molar ratio 1:1, known as EMLA, was the first eutectic to be commercialized and is one of the most widely used as a topical anesthetic. The combination analgesic effect of EMLA was observed to be higher than lidocaine and prilocaine alone [51].

The exponential interest in eutectics for pharmaceutical formulations can be associated to the simple and cost-effective preparation, easy to scale-up and highly stable compounds when compared to amorphous materials commonly used [52]. A eutectic system based on L-arginine and ethambutol bioactives combined with citric acid and water was developed focusing the tuberculosis therapy to reduce the dose needed for effective tuberculosis treatment. The authors produced a system with improved solubility and permeability in comparison to its isolated components [53]. In other work, felodipine which is used to treat high blood pressure to control hypertension was combine with nicotinamide or malonic acid. The solubility of the eutectics systems was evaluated in 0.1 N HCl (pH 1.2) and revealed that the systems exhibited higher solubility and release rate than the parent drug [54]. Dugar et al. [55] also used the eutectics platform to successfully increase the dissolution rate in different media of ibuprofen by combining the NSAID with poloxamer in a molar ratio 1:0.75. In an acidic medium the cumulative ibuprofen:poloxamer released 58.27%, where the ibuprofen alone only presented 3.67%.

More recently, Alshaiikh and co-workers [56] combined caffeine with three anti-inflammatory drugs (meloxicam, aceclofenac and flurbiprofen). The dissolution profiles

obtained in a phosphate buffer demonstrated a efficiency of 3.3, 1.4 and 1.7-fold increased for meloxicam, aceclofenac and flurbiprofen eutectic mixtures, respectively. Additionally, Duarte et al. [57] also reported a 12.7-fold enhancement in the solubility of ibuprofen when it was in the form of the ibuprofen:thymol eutectic system (26.8 ± 2.62 mg/mL) compared to ibuprofen powder (2.1 ± 0.23 mg/mL) in a phosphate buffer saline solution[52].

It is recognized that the eutectics platform can increase the solubility of poorly-water soluble drugs, and further the blending of therapeutically suitable active pharmacological ingredients (drug-drug) with higher stability and improved properties [52,58]. However, the difficulty in characterizing the eutectic systems is one of the reasons that keep researchers away from this simpler approach. The use of tools capable of better understanding the microstructure of eutectic systems, evaluate their toxicity and long-term use in the pharmaceutical sciences is still a challenge and an area that needs to be further explored and understood.

1.4 Objectives and thesis outline

The main goal of the present thesis is to study the use of ionic liquids and eutectics platforms to improve the solubility and bioavailability of NSAIDs, with ibuprofen as drug model, without impairing (or even improving) their pharmacological action. The thermophysical and chemical properties, namely melting and decomposition temperatures, density, viscosity, fluidity, conductivity and hydrogen bonding capacity and dipolarity/polarizability were accessed in order to characterize this pharmaceutically active ILs and eutectics. Further, the potential to enhance solubility of the prepared API-IL and eutectics was evaluated in water and simulated biological fluids (simulated gastric fluid, simulated intestinal fluid and isotonic ionic strength aqueous solution) and compared with the performance of conventional excipients, such as sodium ibuprofen, and the parent API. Since, the use of the proposed IL and eutectic platforms always raise the question of biocompatibility and toxicity because these compounds tend to interact with biological membranes, proteins and enzymes, the safety assessment and cytotoxicity evaluation is quite relevant. The cytotoxicity assays

were performed for the API-ILs and eutectics by using two different human cell cultures types, human colon adenocarcinoma cells (Caco-2) and liver carcinoma cells (HepG2), suitable and useful in vitro models for the intestinal barrier and hepatic metabolism studies, respectively. Another important evaluation is the anti-inflammatory effectiveness of the novel pharmaceutically active ILs and eutectics since the main purpose of the API used is to decrease the inflammatory response. In this context, the anti-inflammatory activity of the API-ILs and eutectics were assessed by the inhibition of bovine serum albumin (BSA) denaturation and the inhibition of cyclooxygenases (COX-1 and COX-2) enzymes using a colorimetric COX (COX-2, human; COX-1, ovine) inhibition assay, to evaluate the potential to maintain/upgrade the pharmacological activity of the parent API and to improve selectivity towards COX-2.

Finally, tuning and controlling membrane transport is the key to a variety of novel delivery methods, thus the determination of ionicity (via Walden plot) was attained, to look for the formation of large charged or non-charged aggregates (or the existence of ionic networks) that increase the potential of membrane permeation relatively to the parent API, and in vitro release studies using a Parallel Artificial Membrane Permeability Assay (PAMPA) with a specific membrane who mimic human skin (Skin-PAMPA) was used to evaluate the skin permeability of both eutectic systems and API-ILs (as well as parent API). Thus, this thesis constitutes an immeasurable contribution to the future application of ILs and eutectics platforms (alone or together) in the biomedical and pharmacological fields.

1.5 References

1. Kalepu, S.; Nekkanti, V. Insoluble Drug Delivery Strategies: Review of Recent Advances and Business Prospects. *Acta Pharm Sin B* 2015, 5, 442–453.
2. Shamshina, J.L.; Rogers, R.D. Overcoming the Problems of Solid State Drug Formulations with Ionic Liquids. *Ther Deliv* 2014, 5, 489–491.
3. Pedro, S.N.; Freire, C.S.R.; Silvestre, A.J.D.; Freire, M.G. The Role of Ionic Liquids in the Pharmaceutical Field: An Overview of Relevant Applications. *Int J Mol Sci* 2020, 21, 1–50.

4. Bauer, J.; Spanton, S.; Henry, R.; Quick, J.; Dziki, W.; Porter, W.; Morris, J. *Ritonavir: An Extraordinary Example of Conformational Polymorphism*; 2001;
5. Savjani, K.T.; Gajjar, A.K.; Savjani, J.K. Drug Solubility: Importance and Enhancement Techniques. *ISRN Pharm* **2012**, *2012*, 1–10, doi:10.5402/2012/195727.
6. Blagden, N.; de Matas, M.; Gavan, P.T.; York, P. Crystal Engineering of Active Pharmaceutical Ingredients to Improve Solubility and Dissolution Rates. *Adv Drug Deliv Rev* 2007, *59*, 617–630.
7. Abbott, A.P.; Ahmed, E.I.; Prasad, K.; Qader, I.B.; Ryder, K.S. Liquid Pharmaceuticals Formulation by Eutectic Formation. *Fluid Phase Equilib* **2017**, *448*, 2–8, doi:10.1016/j.fluid.2017.05.009.
8. Zhang, Q.; De Oliveira Vigier, K.; Royer, S.; Jérôme, F. Deep Eutectic Solvents: Syntheses, Properties and Applications. *Chem Soc Rev* **2012**, *41*, 7108, doi:10.1039/c2cs35178a.
9. Smith, E.L.; Abbott, A.P.; Ryder, K.S. Deep Eutectic Solvents (DESs) and Their Applications. *Chem Rev* 2014, *114*, 11060–11082.
10. Montinari, M.R.; Minelli, S.; De Caterina, R. The First 3500 years of Aspirin History from Its Roots – A Concise Summary. *Vascul Pharmacol* 2019, *113*, 1–8.
11. Tsutsumi, S.; Gotoh, T.; Tomisato, W.; Mima, S.; Hoshino, T.; Hwang, H.J.; Takenaka, H.; Tsuchiya, T.; Mori, M.; Mizushima, T. Endoplasmic Reticulum Stress Response Is Involved in Nonsteroidal Anti-Inflammatory Drug-Induced Apoptosis. *Cell Death Differ* **2004**, *11*, 1009–1016, doi:10.1038/sj.cdd.4401436.
12. Bindu, S.; Mazumder, S.; Bandyopadhyay, U. Non-Steroidal Anti-Inflammatory Drugs (NSAIDs) and Organ Damage: A Current Perspective. *Biochem Pharmacol* 2020, *180*.
13. Daniels, M.J.D.; Rivers-Auty, J.; Schilling, T.; Spencer, N.G.; Watremez, W.; Fasolino, V.; Booth, S.J.; White, C.S.; Baldwin, A.G.; Freeman, S.; et al. Fenamate NSAIDs Inhibit the NLRP3 Inflammasome and Protect against Alzheimer's Disease in Rodent Models. *Nat Commun* **2016**, *7*, doi:10.1038/ncomms12504.
14. Zidar, N.; Odar, K.; Glavac, D.; Jerse, M.; Zupanc, T.; Stajer, D. Cyclooxygenase in Normal Human Tissues - Is COX-1 Really a Constitutive Isoform, and COX-2 an Inducible Isoform? *J Cell Mol Med* **2009**, *13*, 3753–3763, doi:10.1111/j.1582-4934.2008.00430.x.
15. Rainsford, K.D. Ibuprofen: Pharmacology, Efficacy and Safety. *Inflammopharmacology* 2009, *17*, 275–342.
16. Mazaleuskaya, L.L.; Theken, K.N.; Gong, L.; Thorn, C.F.; Fitzgerald, G.A.; Altman, R.B.; Klein, T.E. PharmGKB Summary: Ibuprofen Pathways. *Pharmacogenet Genomics* **2015**, *25*, 96–106, doi:10.1097/FPC.000000000000113.

17. Janus, E.; Ossowicz, P.; Klebeko, J.; Nowak, A.; Duchnik, W.; Kucharski, Ł.; Klimowicz, A. Enhancement of Ibuprofen Solubility and Skin Permeation by Conjugation with L-Valine Alkyl Esters. *RSC Adv* **2020**, *10*, 7570–7584, doi:10.1039/d0ra00100g.
18. Potthast, H.; Dressman, J.B.; Junginger, H.E.; Midha, K.K.; Oeser, H.; Shah, V.P.; Vogelpoel, H.; Barends, D.M. Biowaiver Monographs for Immediate Release Solid Oral Dosage Forms: Ibuprofen. *J Pharm Sci* **2005**, *94*, 2121–2131.
19. Shaw, L.R.; Irwin, W.J.; Grattan, T.J.; Conway, B.R. The Effect of Selected Water-Soluble Excipients on the Dissolution of Paracetamol and Ibuprofen. *Drug Dev Ind Pharm* **2005**, *31*, 515–525, doi:10.1080/03639040500215784.
20. Pedro, S.N.; Mendes, M.S.M.; Neves, B.M.; Almeida, I.F.; Costa, P.; Correia-Sá, I.; Vilela, C.; Freire, M.G.; Silvestre, A.J.D.; Freire, C.S.R. Deep Eutectic Solvent Formulations and Alginate-Based Hydrogels as a New Partnership for the Transdermal Administration of Anti-Inflammatory Drugs. *Pharmaceutics* **2022**, *14*, doi:10.3390/pharmaceutics14040827.
21. Dewland, P.M.; Reader, S.; Berry, P. Bioavailability of Ibuprofen Following Oral Administration of Standard Ibuprofen, Sodium Ibuprofen or Ibuprofen Acid Incorporating Poloxamer in Healthy Volunteers. *BMC Clin Pharmacol* **2009**, *9*, 19, doi:10.1186/1472-6904-9-19.
22. Legg, T.J.; Laurent, A.L.; Leyva, R.; Kellstein, D. Ibuprofen Sodium Is Absorbed Faster than Standard Ibuprofen Tablets: Results of Two Open-Label, Randomized, Crossover Pharmacokinetic Studies. *Drugs R D* **2014**, *14*, 283–290, doi:10.1007/s40268-014-0070-8.
23. Moore, A.R.; Derry, S.; Straube, S.; Ireson-Paine, J.; Wiffen, P.J. Faster, Higher, Stronger? Evidence for Formulation and Efficacy for Ibuprofen in Acute Pain. *Pain* **2014**, *155*, 14–21, doi:10.1016/j.pain.2013.08.013.
24. Cristofolletti, R.; Dressman, J.B. Dissolution Methods to Increasing Discriminatory Power of In Vitro Dissolution Testing for Ibuprofen Free Acid and Its Salts. *J Pharm Sci* **2017**, *106*, 92–99, doi:10.1016/j.xphs.2016.06.001.
25. Irvine, J.; Afrose, A.; Islam, N. Formulation and Delivery Strategies of Ibuprofen: Challenges and Opportunities. *Drug Dev Ind Pharm* **2018**, *44*, 173–183, doi:10.1080/03639045.2017.1391838.
26. Florindo, C.; Araújo, J.M.M.; Alves, F.; Matos, C.; Ferraz, R.; Prudêncio, C.; Noronha, J.P.; Petrovski, Ž.; Branco, L.; Rebelo, L.P.N.; et al. Evaluation of Solubility and Partition Properties of Ampicillin-Based Ionic Liquids. *Int J Pharm* **2013**, *456*, 553–559, doi:10.1016/j.ijpharm.2013.08.010.
27. Araújo, J.M.M.; Florindo, C.; Pereira, A.B.; Vieira, N.S.M.; Matias, A.A.; Duarte, C.M.M.; Rebelo, L.P.N.; Marrucho, I.M. Cholinium-Based Ionic Liquids with

- Pharmaceutically Active Anions. *RSC Adv* **2014**, *4*, 28126–28132, doi:10.1039/c3ra47615d.
28. Vieira, N.S.M.; Luís, A.; Reis, P.M.; Carvalho, P.J.; Lopes-Da-Silva, J.A.; Esperança, J.M.S.S.; Araújo, J.M.M.; Rebelo, L.P.N.; Freire, M.G.; Pereira, A.B. Fluorination Effects on the Thermodynamic, Thermophysical and Surface Properties of Ionic Liquids. *Journal of Chemical Thermodynamics* **2016**, *97*, 354–361, doi:10.1016/j.jct.2016.02.013.
 29. Pereira, A.B.; Araújo, J.M.M.; Teixeira, F.S.; Marrucho, I.M.; Piñeiro, M.M.; Rebelo, L.P.N. Aggregation Behavior and Total Miscibility of Fluorinated Ionic Liquids in Water. *Langmuir* **2015**, *31*, 1283–1295, doi:10.1021/la503961h.
 30. Pereira, A.B.; Araújo, J.M.M.; Martinho, S.; Alves, F.; Nunes, S.; Matias, A.; Duarte, C.M.M.; Rebelo, L.P.N.; Marrucho, I.M. Fluorinated Ionic Liquids: Properties and Applications. *ACS Sustain Chem Eng* **2013**, *1*, 427–439, doi:10.1021/sc300163n.
 31. Zhuang, W.; Hachem, K.; Bokov, D.; Javed Ansari, M.; Taghvaie Nakhjiri, A. Ionic Liquids in Pharmaceutical Industry: A Systematic Review on Applications and Future Perspectives. *J Mol Liq* **2022**, *349*.
 32. Hough, W.L.; Smiglak, M.; Rodríguez, H.; Swatloski, R.P.; Spear, S.K.; Daly, D.T.; Pernak, J.; Grisel, J.E.; Carliss, R.D.; Soutullo, M.D.; et al. The Third Evolution of Ionic Liquids: Active Pharmaceutical Ingredients. *New Journal of Chemistry* **2007**, *31*, 1429, doi:10.1039/b706677p.
 33. Agatonovic-Kustrin, S.; Rades, T.; Wu, V.; Saville, D.; Tucker, I.G. *Determination of Polymorphic Forms of Ranitidine-HCl by DRIFTS and XRPD*; 2001; Vol. 25;.
 34. Fernandez-Stefanuto, V.; Tojo, E. New Active Pharmaceutical Ingredient-Ionic Liquids (API-ILs) Derived from Indomethacin and Mebendazole.; MDPI AG, November 15 2018; p. 48.
 35. Frizzo, C.P.; Wust, K.; Tier, A.Z.; Beck, T.S.; Rodrigues, L. V.; Vaucher, R.A.; Bolzan, L.P.; Terra, S.; Soares, F.; Martins, M.A.P. Novel Ibuprofenate- and Docusate-Based Ionic Liquids: Emergence of Antimicrobial Activity. *RSC Adv* **2016**, *6*, 100476–100486, doi:10.1039/C6RA22237D.
 36. Bica, K.; Rijksen, C.; Nieuwenhuyzen, M.; Rogers, R.D. In Search of Pure Liquid Salt Forms of Aspirin: Ionic Liquid Approaches with Acetylsalicylic Acid and Salicylic Acid. *Physical Chemistry Chemical Physics* **2010**, *12*, 2011–2017, doi:10.1039/c001176m.
 37. Hough, W.L.; Rogers, R.D. Ionic Liquids Then and Now: From Solvents to Materials to Active Pharmaceutical Ingredients. *Bull Chem Soc Jpn* **2007**, *80*, 2262–2269, doi:10.1246/bcsj.80.2262.

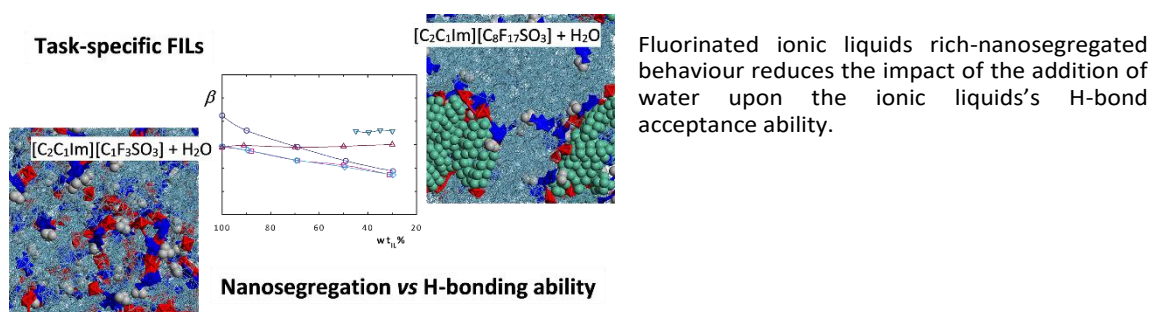
38. Zhao, H.; Holmes, S.S.; Baker, G.A.; Challa, S.; Bose, H.S.; Song, Z. Ionic Derivatives of Betulinic Acid as Novel HIV-1 Protease Inhibitors. *J Enzyme Inhib Med Chem* **2012**, *27*, 715–721, doi:10.3109/14756366.2011.611134.
39. Balk, A.; Wiest, J.; Widmer, T.; Galli, B.; Holzgrabe, U.; Meinel, L. Transformation of Acidic Poorly Water Soluble Drugs into Ionic Liquids. *European Journal of Pharmaceutics and Biopharmaceutics* **2015**, *94*, 73–82, doi:10.1016/j.ejpb.2015.04.034.
40. Viciosa, M.T.; Santos, G.; Costa, A.; Danède, F.; Branco, L.C.; Jordão, N.; Correia, N.T.; Dionísio, M. Dipolar Motions and Ionic Conduction in an Ibuprofen Derived Ionic Liquid. *Physical Chemistry Chemical Physics* **2015**, *17*, 24108–24120, doi:10.1039/c5cp03715h.
41. Santos, M.M.; Raposo, L.R.; Carrera, G.V.S.M.; Costa, A.; Dionísio, M.; Baptista, P. V.; Fernandes, A.R.; Branco, L.C. Ionic Liquids and Salts from Ibuprofen as Promising Innovative Formulations of an Old Drug. *ChemMedChem* **2019**, *14*, 907–911, doi:10.1002/cmdc.201900040.
42. Ferraz, R.; Branco, L.C.; Marrucho, I.M.; Araújo, J.M.M.; Rebelo, L.P.N.; da Ponte, M.N.; Prudêncio, C.; Noronha, J.P.; Petrovski, Ž. Development of Novel Ionic Liquids Based on Ampicillin. *Med. Chem. Commun.* **2012**, *3*, 494–497, doi:10.1039/C2MD00269H.
43. Ferraz, R.; Teixeira, V.; Rodrigues, D.; Fernandes, R.; Prudêncio, C.; Noronha, J.P.; Petrovski, Ž.; Branco, L.C. Antibacterial Activity of Ionic Liquids Based on Ampicillin against Resistant Bacteria. *RSC Adv* **2014**, *4*, 4301–4307, doi:10.1039/c3ra44286a.
44. Ferraz, R.; Costa-Rodrigues, J.; Fernandes, M.H.; Santos, M.M.; Marrucho, I.M.; Rebelo, L.P.N.; Prudêncio, C.; Noronha, J.P.; Petrovski, Ž.; Branco, L.C. Antitumor Activity of Ionic Liquids Based on Ampicillin. *ChemMedChem* **2015**, *10*, 1480–1483, doi:10.1002/cmdc.201500142.
45. Miwa, Y.; Hamamoto, H.; Ishida, T. Lidocaine Self-Sacrificially Improves the Skin Permeation of the Acidic and Poorly Water-Soluble Drug Etodolac via Its Transformation into an Ionic Liquid. *European Journal of Pharmaceutics and Biopharmaceutics* **2016**, *102*, 92–100, doi:10.1016/j.ejpb.2016.03.003.
46. Moshikur, R.M.; Goto, M. Ionic Liquids as Active Pharmaceutical Ingredients (APIs). In *Application of Ionic Liquids in Drug Delivery*; Springer Singapore: Singapore, 2021; pp. 13–33.
47. Hammond, O.S.; Mudring, A.V. Ionic Liquids and Deep Eutectics as a Transformative Platform for the Synthesis of Nanomaterials. *Chemical Communications* **2022**, *58*, 3865–3892, doi:10.1039/d1cc06543b.
48. Sekiguchi, K.; Obi, N.; Ueda, Yoshio Studies on Absorption of Eutectic Mixture. II. Absorption of Fused Conglomerates of Chloramphenicol and Urea in Rabbits. *Chem. Pharm. Bull.* **1964**, *12*, 134–144.

49. Stott, P.W.; Williams, A.C.; Barry, B.W. *Transdermal Delivery from Eutectic Systems: Enhanced Permeation of a Model Drug, Ibuprofen*; 1998; Vol. 50;.
50. Stott, P. Transdermal Delivery from Eutectic Systems: Enhanced Permeation of a Model Drug, Ibuprofen. *Journal of Controlled Release* **1998**, *50*, 297–308, doi:10.1016/S0168-3659(97)00153-3.
51. Nyqvist-Mayer, A.A.; Brodin, A.F.; Frank, S.G. Drug Release Studies on an Oil–Water Emulsion Based on a Eutectic Mixture of Lidocaine and Prilocaine as the Dispersed Phase. *J Pharm Sci* **1986**, *75*, 365–373, doi:10.1002/jps.2600750409.
52. Bazzo, G.C.; Pezzini, B.R.; Stulzer, H.K. Eutectic Mixtures as an Approach to Enhance Solubility, Dissolution Rate and Oral Bioavailability of Poorly Water-Soluble Drugs. *Int J Pharm* **2020**, *588*.
53. Santos, F.; Leitão, M.I.P.S.; Duarte, A.R.C. Properties of Therapeutic Deep Eutectic Solvents of L-Arginine and Ethambutol for Tuberculosis Treatment. *Molecules* **2019**, *24*, doi:10.3390/molecules24010055.
54. Chadha, K.; Karan, M.; Chadha, R.; Bhalla, Y.; Vasisht, K. Is Failure of Cocrystallization Actually a Failure? Eutectic Formation in Cocrystal Screening of Hesperetin. *J Pharm Sci* **2017**, *106*, 2026–2036, doi:10.1016/j.xphs.2017.04.038.
55. Dugar, R.P.; Gajera, B.Y.; Dave, R.H. Fusion Method for Solubility and Dissolution Rate Enhancement of Ibuprofen Using Block Copolymer Poloxamer 407. *AAPS PharmSciTech* **2016**, *17*, 1428–1440, doi:10.1208/s12249-016-0482-6.
56. Alshaikh, R.A.; Essa, E.A.; El Maghraby, G.M. Eutectia for Enhanced Dissolution Rate and Anti-Inflammatory Activity of Nonsteroidal Anti-Inflammatory Agents: Caffeine as a Melting Point Modulator. *Int J Pharm* **2019**, *563*, 395–405, doi:10.1016/j.ijpharm.2019.04.024.
57. Duarte, A.R.C.; Ferreira, A.S.D.; Barreiros, S.; Cabrita, E.; Reis, R.L.; Paiva, A. A Comparison between Pure Active Pharmaceutical Ingredients and Therapeutic Deep Eutectic Solvents: Solubility and Permeability Studies. *European Journal of Pharmaceutics and Biopharmaceutics* **2017**, *114*, 296–304, doi:10.1016/j.ejpb.2017.02.003.
58. neamah, A. jaber; Rashid, A.M.; Ghareeb, M.M. Eutectic Mixtures: A Promising Solvent in Drug Delivery System. *Maaen Journal for Medical Sciences* **2022**, *1*, doi:10.55810/2789-9128.1010.

**THE HYDROGEN-BONDING IN AQUEOUS
SOLUTIONS OF IONIC LIQUIDS**

2.1 Abstract

We demonstrate that fluorinated ionic liquids reduce the impact of the addition of water upon the ionic liquid's H-bond acceptance ability. This is a key factor to obtain functionalized materials to be used e.g. in the dissolution of biomolecules, extraction processes or material engineering.



Published in: [Joana C. Bastos](#), Sara F. Carvalho, Tom Welton, José N. Canongia Lopes, Luís Paulo N. Rebelo, Karina Shimizu, João M. M. Araújo, Ana B. Pereira. Design of task-specific fluorinated ionic liquids: nanosegregation versus hydrogen-bonding ability in aqueous solutions. *Chem. Commun.*, **2018**,54, 3524-3527.

Own experimental contribution: Kamlet-Taft parameters determination and analysis, mainly conventional ILs (including mere fluoro-containing ILs).

Own written contribution: Kamlet-Taft analysis, mainly, mainly conventional ILs (including mere fluoro-containing ILs).

Other contributions: Design Kamlet-Taft experiments, mainly conventional ILs (including mere fluoro-containing ILs)

2.2 Introduction

Ionic liquids (ILs) have been demonstrated to be excellent solvents, co-solvents and supported materials for the dissolution, extraction and purification of bioactive compounds from biomass [1]. This biomass has a great aptitude for the formation of hydrogen-bonding due to the presence of several hydrogen-bond donor and acceptor groups. The exceptional properties of ILs are related to their ionic nature and their ability to form distinct types of interactions (dipolar, dispersion or hydrogen-bonding) [2].

Fluorinated ionic liquids (FILs) are great candidates to be investigated as a type of tuneable materials due to their capacity to form three nanosegregated domains (polar, hydrogenated apolar and fluorinated apolar) [3]. This fact enhances their solvent quality and tuneability capacities compared to conventional ILs, offering a highly solvating medium for biomolecules. Accordingly, one can fine-tune the ideal “3 in 1” FIL through the selection of the size of each one of the three nanosegregated domains, and the contribution of each type of interaction (coulombic, van der Waals and hydrogen bonding). One of the major interests in FILs is that they combine the best properties of inert perfluorocarbon compounds with those of ILs. Previous works demonstrated that FILs can be non-toxic to different human cell lines [4], showing improved surface activity [5] and high surfactant power [6]. Also, FILs can be totally miscible with water, forming distinct self-assembled structures in aqueous solutions [6].

The hydrogen-bonding ability has been widely studied to address the performance of task-specific ILs used in the purification, extraction and dissolution of biomaterials. The Kamlet-Taft parameters are related to solvent polarity scales which characterize the H-bond donor and H-bond acceptor capacities of a solvent, denoted as α and β respectively [7]. Most of the relevant properties of ILs regarding biomass derived solute-solvent interactions are usually determined by the nature of the anion rather than the cation [8]. Accordingly, the hydrogen-bond basicity (β value) is one of the most important parameters, reflecting the hydrogen bond accepting ability of the IL anion [9]. ILs characterized by a high β parameter, indicate anions that can strongly interact with the H-bond donor groups of a biomaterial, promoting its dissolution [10]. 1-Ethyl-3-methylimidazolium acetate ($[\text{C}_2\text{C}_1\text{Im}][\text{C}_1\text{CO}_2]$, with $\beta = 0.95-1.09$), [11] has been

identified as a good solvent for biomacromolecules such as cellulose and suberin, [12] DNA, proteins, carbohydrates, and nucleic acid bases [13]. Doherty et al. [14] reported that the addition of water into ILs has a great impact on the β parameter, mainly due to water's relatively poor hydrogen bond basicity ($\beta = 0.14\text{--}0.18$) [14]. The control of the hydrogen-bond basicity, β value, in IL aqueous solutions is crucial to control the dissolution capacity towards biomaterials, because almost all-natural biomass matrices contain water, and most biological applications involve aqueous solutions (water and biological fluids).

The investigation carried out in this work is based on the monitoring and controlling of the hydrogen bonding capacity in aqueous media of novel materials based on FILs, using a combined experimental and theoretical approach. This work studies the behaviour of FILs (ILs with fluorinated alkyl chains with four or more carbon atoms) [4] versus conventional ILs (including mere fluoro-containing ILs). The structures of ILs used in this work are depicted in **Figure 2.1**.

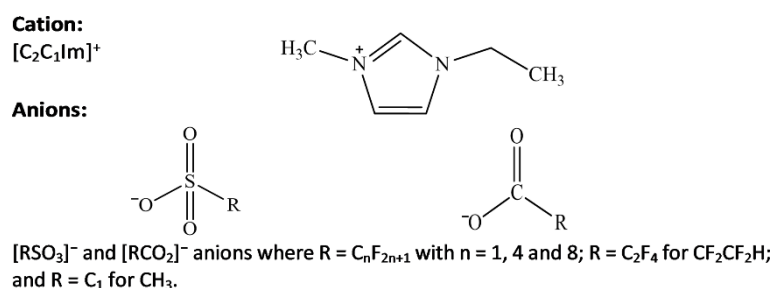


Figure 2.1 Structures of ILs used in this work (complete designation in SI)

2.3 Results and Discussion

The Kamlet-Taft approach is based on the analysis of UV-vis spectra of a set of dyes (*cf.* SI) [7]. This methodology provides three Kamlet-Taft parameters: π^* (dipolarity/polarizability effects); α (the H-bond acidity or the H-bond donation ability); and β (the H-bond basicity or the H-bond acceptance ability). The experimental Kamlet-Taft parameters, at 298.15 K, for the seven neat ILs sharing a common cation (1-ethyl-3-methylimidazolium, $[\text{C}_2\text{C}_1\text{Im}]^+$) and their aqueous solutions (100 to 30 wt.%; 100 to 1.4 mol.%) are plotted in **Figure 2.2** ($[\text{RSO}_3]^-$ -based ILs) and **Figure 2.S2** ($[\text{RCO}_2]^-$ -based ILs), and reported in **Table 2.S2** of SI. Additionally, the Kamlet-Taft parameters

for all the studied binary systems IL + H₂O expressed in mol_{IL}% are depicted in **Figure 2.S3** of SI. The water parameters have also been determined, agreeing with reported values [14] (*cf.* **Table 2.S2**). **Figure 2.2** and **Figures 2.S2 and 2.S3** (*cf.* SI) depict the impact of the addition of water upon the ILs' hydrogen-bonding ability (α and β) and dipolarity/polarizability (π^*). It gives us comparisons between: i) hydrogenated ILs and FILs; ii) acetate-based and sulfonate-based ILs; and iii) mere fluoro-containing ILs and FILs.

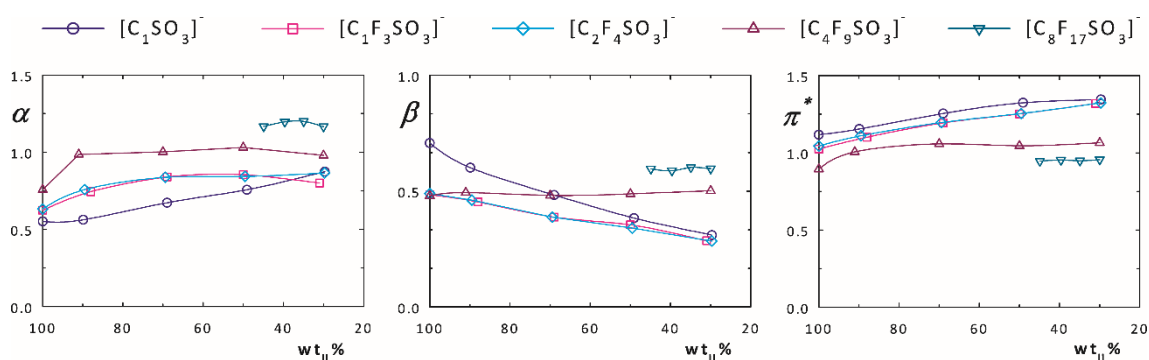


Figure 2.2 Kamlet–Taft parameters (dye set Reichardt's dye, N,N-diethyl-4-nitroaniline and 4-nitroaniline; *cf.* SI) for the binary systems [C₂C1Im][RSO₃] + H₂O at 298 K.

Sulfonate-based FILs, markedly structured liquid [3] with a very high surface organization [5], have demonstrated an unexpected total water solubility and improved surfactant capacity [6]. In this work, this family was selected to design a material with an invariant H-bond acceptor capacity in aqueous solution (water-content independent). Acetate-based ILs have also been studied for comparison purposes because they are excellent solubilizers of biomolecules [13].

Largely, both the hydrogenated ILs and mere fluoro-containing ILs become more acidic (increasing α) and less basic (β decreases) with the addition of water (*cf.* **Figures 2.2, 2.S2 and 2.S3**), as expected based on previous studies [15]. Concerning the π^* values, all ILs studied in this work presented an excellent polarizability, higher than that of water ($\pi^*=1.09$ - 1.33).¹⁴ The H-bond acceptor ability of [C₂C1Im][C₁CO₂] is much higher than that of the other compounds, as expected. The incorporation of a few fluorine atoms ([C₁CO₂]⁻ versus [C₁F₃CO₂]⁻) clearly decreases the β value. This trend is also verified for the sulfonate-based ILs. The greatest divergence, when water is added to the system, is observed for the β parameter: while (i) the incorporation of a few fluorine atoms

(hydrogenated vs. mere fluoro-containing ILs) only slightly reduces the water effect on the β value (*viz.* water addition trend of the β value for $[\text{C}_1\text{CO}_2]^-$ vs. $[\text{C}_1\text{F}_3\text{CO}_2]^-$, and $[\text{C}_1\text{SO}_3]^-$ vs. $[\text{C}_1\text{F}_3\text{SO}_3]^-$ and $[\text{C}_2\text{F}_4\text{SO}_3]^-$); (ii) the most interesting result is that the β parameter remains unchanged, upon water addition, for a fluorinated alkyl chain of four (or more) carbon atoms. The H-bond acceptor capacity of these FILs ($[\text{C}_2\text{C}_1\text{Im}][\text{C}_4\text{F}_9\text{SO}_3]$ and $[\text{C}_2\text{C}_1\text{Im}][\text{C}_8\text{F}_{17}\text{SO}_3]$) is maintained constant up to 70 wt_{H₂O}% (98.2 and 98.6 mol_{H₂O}% for $[\text{C}_4\text{F}_9\text{SO}_3]^-$ and $[\text{C}_8\text{F}_{17}\text{SO}_3]^-$, respectively; *cf.* **Figure 2.2** and **Figure 2.S3** of SI. $[\text{C}_8\text{F}_{17}\text{SO}_3]^-$, a solid in its neat state, was only measured from 45 to 30 wt_{IL}% due to turbidity issues, related to its high surfactant power [6]. The influence of the water content on the α and π^* parameters for these two FILs is only seen for the first 10 wt% of added water. **Figures 2.S4 and 2.S5** of SI (electrical conductivity profile and critical aggregation concentrations of $[\text{C}_2\text{C}_1\text{Im}][\text{C}_4\text{F}_9\text{SO}_3]$) [6] ascertain that in the studied composition range, the H-bond acceptance ability of these FILs depends on the nanosegregation of the IL, not on the micelles formation in aqueous solution.

As discussed above, the $[\text{C}_2\text{C}_1\text{Im}][\text{C}_1\text{CO}_2]$ has the highest β value up to nearly 70 wt_{IL}%. However, between 70 and 30 wt_{IL}%, the basicity trend changes to: $[\text{C}_8\text{F}_{17}\text{SO}_3]^- > [\text{C}_4\text{F}_9\text{SO}_3]^- > [\text{C}_1\text{CO}_2]^- > [\text{C}_2\text{F}_4\text{SO}_3]^- \approx [\text{C}_1\text{F}_3\text{SO}_3]^-$. These observations show the potential for fine-tuning the solutions' characteristics by choice of the fluorinated alkyl chain length of the anion, featuring the underlying, rich nanosegregation behaviour of these FILs [3,5].

Molecular dynamics simulations were carried out to probe the structure of the ionic liquids aqueous solution. Eight ILs with a common cation ($[\text{C}_2\text{C}_1\text{Im}]^+$) were studied in three different aqueous mixtures (30, 50 and 90 wt_{IL}%) for: (i) trifluoromethanesulfonate, $[\text{C}_1\text{F}_3\text{SO}_3]^-$; (ii) 1,1,2,2-tetrafluoro-ethanesulfonate, $[\text{C}_2\text{F}_4\text{SO}_3]^-$; (iii) perfluorobutanesulfonate, $[\text{C}_4\text{F}_9\text{SO}_3]^-$; (iv) perfluorooctanesulfonate, $[\text{C}_8\text{F}_{17}\text{SO}_3]^-$; (v) methanesulfonate, $[\text{C}_1\text{SO}_3]^-$; (vi) acetate, $[\text{C}_1\text{CO}_2]^-$; (vii) butane sulfonate, $[\text{C}_4\text{H}_9\text{SO}_3]^-$; and (viii) trifluoroacetate, $[\text{C}_1\text{F}_3\text{CO}_2]^-$. All ionic liquids were modelled according to a well-known force field [16] commonly used for ionic liquids aqueous solution at 300 K (*cf.* SI).

Figure 2.3 depicts four snapshots of equilibrated boxes for a 30 wt_{IL}%. The simulation boxes of these diluted solutions show that for the two ionic liquids with small fluorinated chains (*viz.* mere fluoro-containing ILs), $[\text{C}_2\text{C}_1\text{Im}][\text{C}_1\text{F}_3\text{SO}_3]$ and $[\text{C}_2\text{C}_1\text{Im}][\text{C}_2\text{F}_4\text{SO}_3]$, the

IL is not solely a set of isolated ions solvated by water molecules, but rather a series of small filamentous ionic strands integrated within the liquid water matrix. On the other hand, the increase of the fluorinated alkyl chain length (*viz.* FILs), $[\text{C}_2\text{C}_1\text{Im}][\text{C}_4\text{F}_9\text{SO}_3]$ and $[\text{C}_2\text{C}_1\text{Im}][\text{C}_8\text{F}_{17}\text{SO}_3]$, leads to larger IL aggregates. The size distribution probability functions [17], $P(n_a)$, of the water network are represented in green for 90 wtIL%, turquoise for 50 wtIL% and blue for 30 wtIL%. In the cases of 30 and 50 wtIL%, the water aggregates percolate the entire box. For the ILs $[\text{C}_2\text{C}_1\text{Im}][\text{C}_1\text{F}_3\text{SO}_3]$ and $[\text{C}_2\text{C}_1\text{Im}][\text{C}_2\text{F}_4\text{SO}_3]$ at 90 wtIL%, the water network is broken into smaller aggregates. The isolated water molecules represent 20% and 14 % for the first IL and the latter IL, respectively. The water aggregates grow with the increase of the fluorinated chain since the nonpolar region drives the water molecules to the polar domain of the IL.

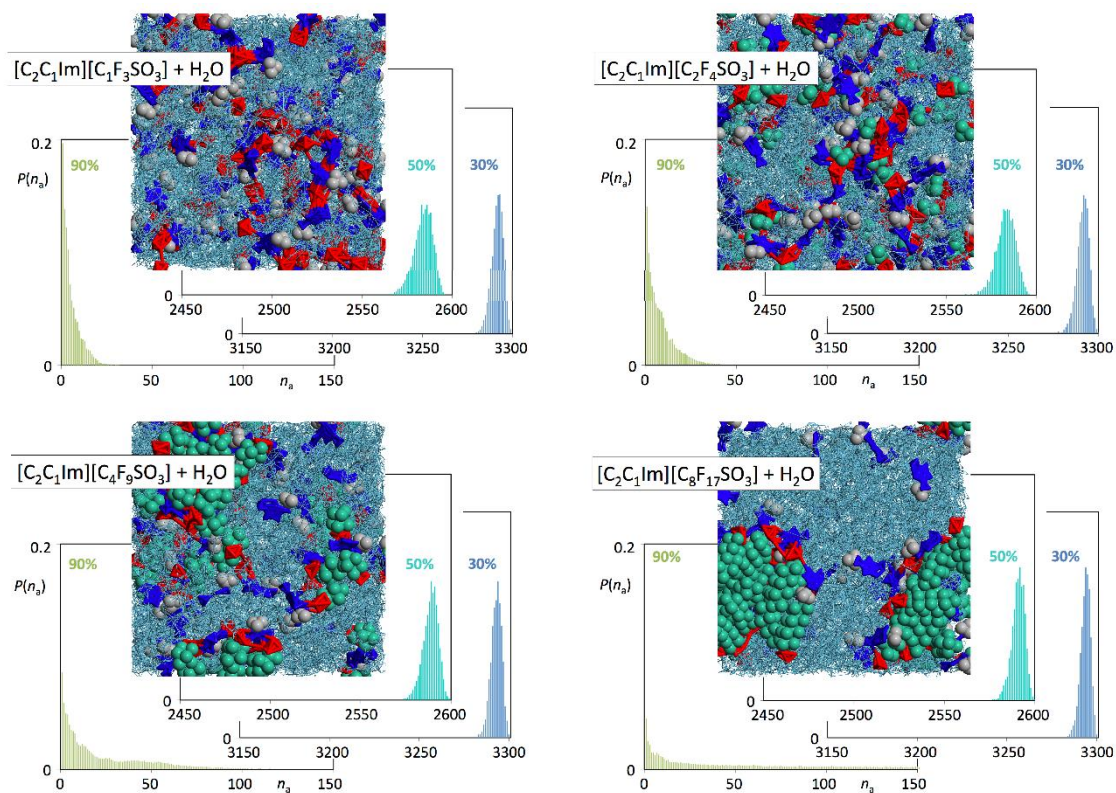


Figure 2.3 Discrete probability distribution functions of water aggregate sizes, $P(n_a)$, for four IL + H_2O systems, each represented by 90, 50 and 30 wtIL% composition mixtures (in green, cyan and blue, respectively). The snapshots (IL colour code in SI) represent the simulation boxes for the 30 wtIL% mixtures.

Figure 2.4 shows four snapshots of the simulation boxes for the other four ionic liquids at the same IL weight percentage of 30%. The equilibrated simulation boxes highlight that the diluted ILs are also a series of small filamentous ionic strands incorporated

within the water. The comparison between **Figure 2.3** and **Figure 2.4** shows that the hydrogenated and acetate systems lead to smaller water aggregates in the entire range of the IL composition. Note that for $[\text{C}_2\text{C}_1\text{Im}][\text{C}_1\text{CO}_2]$ at $\text{wtIL}\% = 90\%$, around 75 % of the water molecules remain isolated from each other.

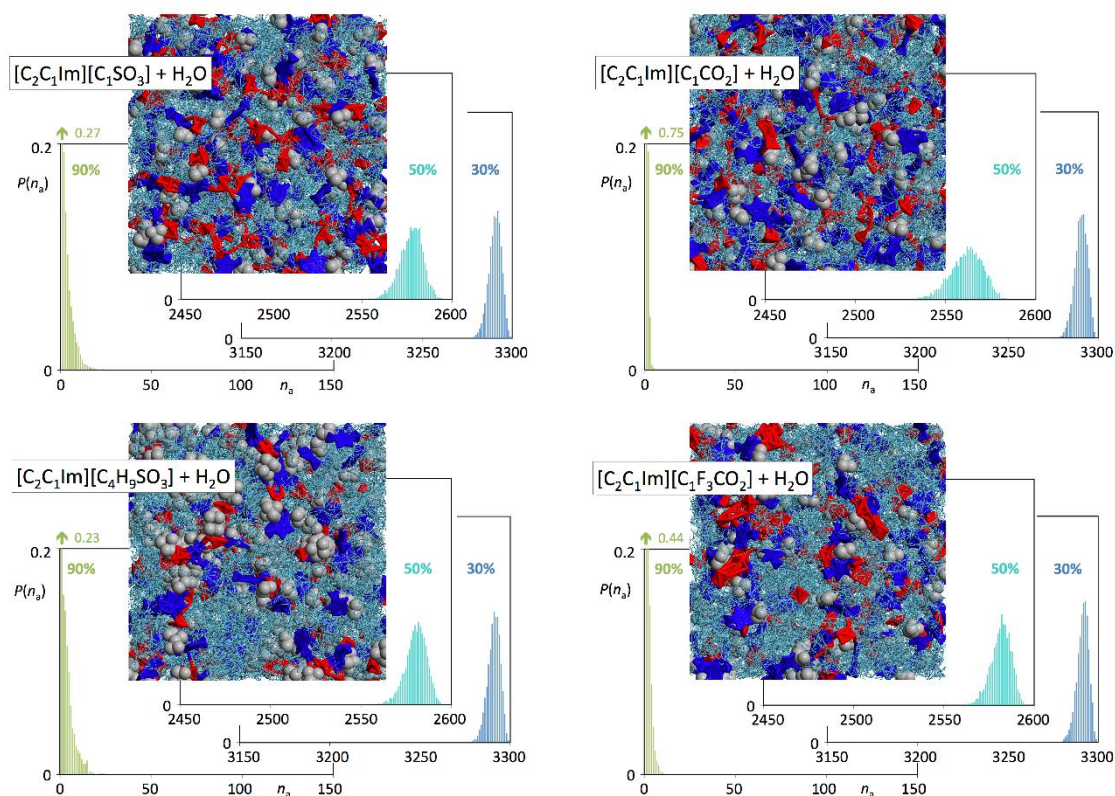


Figure 2.4 Discrete probability distribution functions of water aggregate sizes, $P(n_a)$, for four IL + H_2O systems, each represented by 90, 50 and 30 $\text{wtIL}\%$ composition mixtures (in green, cyan and blue, respectively). The snapshots (IL colour code in SI) represent the simulation boxes for the 30 $\text{wtIL}\%$ mixtures.

The specific H-bond-type interactions between the interactive centres of the anions (the sulphur atom of the sulfonate and the carbon atom of the acetate) and the hydrogen atoms of the water molecules help to create small networks of alternating water molecules and anions that can contain a few tens of species (*cf.* SI, **Figures 2.S6, 2.S7 and 2.S8**). Therefore, those interactions are responsible for the incorporation of the ionic liquids strands in the aqueous solution.

For the ILs with $[\text{C}_1\text{F}_3\text{SO}_3]^-$ and $[\text{C}_2\text{F}_4\text{SO}_3]^-$ anions, in the 90 $\text{wtIL}\%$, the smaller water aggregates, compared to $[\text{C}_4\text{F}_9\text{SO}_3]^-$ and $[\text{C}_8\text{F}_{17}\text{SO}_3]^-$ (**Figure 2.3**), suggest that the water molecules are in the vicinity of the anion, leading to the decrease in the β value observed experimentally (**Figure 2.2**). This is also corroborated by the water-IL aggregation

distributions in the same mixtures (*cf.* SI, **Figures 2.S6 and 2.S8**). For the FILs based on $[\text{C}_4\text{F}_9\text{SO}_3]^-$ and $[\text{C}_8\text{F}_{17}\text{SO}_3]^-$ anions, the water molecules tend to interact more with themselves than with the polar part of the anion, not affecting the basicity and consequently not inducing significant changes in the β value.

The comparison between the aqueous solutions of $[\text{C}_2\text{C}_1\text{Im}][\text{C}_1\text{SO}_3]$ and $[\text{C}_2\text{C}_1\text{Im}][\text{C}_1\text{CO}_2]$ pointed out that the $[\text{C}_1\text{CO}_2]^-$ anion has the ability to strongly interact with water. The abrupt decrease in β value for the $[\text{C}_2\text{C}_1\text{Im}][\text{C}_1\text{CO}_2]$ system as a function of water content is related to the presence of small water clusters in all compositions studied. The high hydrophobic character of the fluorinated chain is also observed in the behaviour of the β values for aqueous solutions of $[\text{C}_2\text{C}_1\text{Im}][\text{C}_1\text{F}_3\text{CO}_2]$. For instance, in the 90 wt_{IL}% the fraction of isolated water molecules represents 75% in the $[\text{C}_2\text{C}_1\text{Im}][\text{C}_1\text{CO}_2]$ mixture and 44% in the $[\text{C}_2\text{C}_1\text{Im}][\text{C}_1\text{F}_3\text{CO}_2]$ mixture.

In summary, the hydrogen-bonding ability and dipolarity/polarizability were evaluated using Kamlet-Taft parameters for neat and aqueous solutions of FILs and conventional ILs (including mere fluoro-containing ILs). Comparing the hydrogen bond acceptance and the hydrogen bond donation abilities, it is clear that the fluorination of the anion restricts the impact of the addition of water to the ILs. Moreover, we have demonstrated that by choice of a fluorinated alkyl chain with four (or more) carbon atoms in the IL anion one can make constant the hydrogen bond acceptance ability (β value equal to that of the neat FIL up to 70 wt_{H₂O}% (98.6 mol_{H₂O}%) of these novel FILs. Probing the structure of these FILs aqueous solutions with MD simulations, details that the rich-aggregation behaviour of these FILs stimulates the networking of water aggregates. The water aggregates grow with the increase of the fluorinated chain since the nonpolar part drives the water molecules to the polar domain of the IL. The design of the hydrogen-bonding ability of the proposed FILs aqueous solutions will provide novel task-specific ILs to be tested in fields as diverse as synthesis and catalysis, biochemistry and dissolution of biomaterials, extraction/purification processes, or material engineering.

Conflicts of interest

There are no conflicts to declare.

Funding Sources

Fundação para a Ciência e Tecnologia through Projects: PTDC/QEQ-EPR/5841/2014, PTDC/QEQ-FTT/3289/2014, IF/00210/2014/CP1244/CT0003 and UID/QUI/00100/2013. This work was also supported by the Associate Laboratory for Green Chemistry LAQV (financed by national funds from FCT/MCTES (UID/QUI/50006/ 2013) and co-financed by the ERDF under the PT2020 Partnership Agreement (POCI-01-0145-FEDER - 007265). Financial support was also obtained through the STSM-CM1206-061014-049092 COST Action.

Acknowledgement

The authors wish to thank FCT/MCTES (Portugal) for financial support through grant SFRH/BPD/94291/2013 (K.S.), contracts under Investigator FCT 2014, IF/00190/2014 (A.B.P.) and IF/00210/2014 (J.M.M.A.).

2.4 References

1. S. P. M. Ventura, F. A. e Silva, M. V. Quental, D. Mondal, M. G. Freire and J. A. P. Coutinho, *Chem. Rev.*, 2017, **117**, 6984; D. A. Fort, R. C. Remsing, R. P. Swatloski, P. Moyna, G. Moyna and R. D. Rogers, *Green Chem.*, 2007, **9**, 63.
2. N. V. Plechkova and K. R. Seddon, *Chem. Soc. Rev.*, 2008, **37**, 123; T. Welton, *Chem. Rev.*, 1999, **99**, 2071.
3. A. B. Pereira, M. J. Pastoriza-Gallego, K. Shimizu, I. M. Marrucho, J. N. C. Lopes, M. M. Piñeiro and L. P. N. Rebelo, *J. Phys. Chem. B*, 2013, **117**, 10826; M. L. Ferreira, M. J. Pastoriza-Gallego, J. M. M. Araújo, J. N. C. Lopes, L. P. N. Rebelo, M. M. Piñeiro, K. Shimizu and A. B. Pereira. *J. Phys. Chem. C*, 2017, **121**, 5415.
4. A. B. Pereira, J. M. M. Araújo, S. Martinho, F. Alves, S. Nunes, A. Matias, C. M. M. Duarte, L. P. N. Rebelo and I. M. Marrucho, *ACS Sustainable Chem. Eng.*, 2013, **1**, 427.
5. A. Luís, K. Shimizu, J. M. M. Araújo, P. J. Carvalho, J. A. Lopes-da-Silva, J. N. C. Lopes, L. P. N. Rebelo, J. A. P. Coutinho, M. G. Freire and A. B. Pereira, *Langmuir*, 2016, **32**, 6130.
6. A. B. Pereira, J. M. M. Araújo, F. S. Teixeira, I. M. Marrucho, M. M. Piñeiro and L. P. N. Rebelo, *Langmuir*, 2015, **31**, 1283.

7. M. J. Kamlet and R. W. Taft, *J. Amer. Chem. Soc.*, 1975, **99**, 377.
8. A. F. M. Cláudio, L. Swift, J. P. Hallett, T. Welton, J. A. P. Coutinho and M. G. Freire, *Phys. Chem. Chem. Phys.*, 2014, **16**, 6593.
9. K. A. Kurnia, F. Lima, A. F. M. Claudio, J. A. P. Coutinho and M. G. Freire, *Phys. Chem. Chem. Phys.*, 2015, **17**, 18980.
10. J. Zhang, H. Zhang, J. Wu, J. Zhang, J. He, J. Xiang, *Phys. Chem. Chem. Phys.*, 2010, **12**, 14829; S. Zhang, X. Qi, X. Ma, L. Lu, Y. Deng, *J. Phys. Chem. B*, 2010, **114**, 3912.
11. J. M. M. Araújo, R. Ferreira, I. M. Marrucho and L. P. N. Rebelo, *J. Phys. Chem. B*, 2011, **115**, 10739.
12. H. Garcia, R. Ferreira, M. Petkovic, J. L. Ferguson, M. C. Leitao, H. Q. N. Gunaratne, K. R. Seddon, L. P. N. Rebelo and C. S. Pereira, *Green Chem.*, 2010, **12**, 367; H. Ohno and Y. Fukaya, *Chem. Lett.*, 2009, **38**, 2.
13. J.M.M. Araújo, A.B. Pereiro, J.N.C. Lopes, L.P.N. Rebelo and I.M. Marrucho, *J. Phys. Chem. B*, 2013, **117**, 4109.
14. T. V. Doherty, M. Mora-Pale, S. E. Foley, R. J. Linhardt, J. S. Dordick, *Green Chem.*, 2010, **12**, 1967; W. Jin, Q. Yang, B. Huang, Z. Bao, B. Su, Q. Ren, Y. Yang and H. Xing, *Green Chem.*, 2016, **18**, 3549; C. Zhong, F. Cheng, Y. Zhu, Z. Gao, H. Jia and P. Wei, *Carbohydrate Polymers*, 2017, **174**, 400; D. L. Minnick, R. A. Flores, M. R. DeStefano and A. M. Scurto, *J. Phys. Chem. B*, 2016, **120**, 7906.
15. L. Crowhurst, P. R. Mawdsley, J. M. Perez-arlandis, P. A. Salter and T. Welton, *Phys. Chem. Chem. Phys.*, 2003, **5**, 2790.
16. J. N. Canongia Lopes, A. A. H. Pádua and K. Shimizu, *J. Phys. Chem. B*, 2008, **112**, 5039; N.S.M. Vieira, P.M. Reis, K. Shimizu, O.A. Cortes, I.M. Marrucho, J.M.M. Araújo, J.M.S.S. Esperança, J. N. Canongia Lopes, A.B. Pereiro and L.P.N. Rebelo, *RSC Adv.*, 2015, **5**, 65337.
17. A. F. M. Claudio, M. C. Neves, K. Shimizu, J. N. Canongia Lopes, M. G. Freire and J. A. P. Coutinho, *Green Chem.*, 2015, **17**, 3948.

2.5 Supporting Information

Experimental Section

Materials

1-Ethyl-3-methylimidazolium acetate, [C₂C₁Im][C₁CO₂], > 95 % mass fraction purity; 1-ethyl-3-methylimidazolium methanesulfonate, [C₂C₁Im][C₁SO₃], ≥ 99% mass fraction

purity; 1-ethyl-3-methylimidazolium trifluoroacetate, [C₂C₁Im][CF₃CO₂], ≥ 97% mass fraction purity; 1-ethyl-3-methylimidazolium trifluoromethanesulfonate, [C₂C₁Im][CF₃SO₃], ≥ 99% mass fraction purity; 1-ethyl-3-methylimidazolium 1,1,2,2-tetrafluoroethanesulfonate, [C₂C₁Im][C₂F₄SO₃], ≥ 98% mass fraction purity; 1-ethyl-3-methylimidazolium perfluorobutanesulfonate, [C₂C₁Im][C₄F₉SO₃], >97% mass fraction purity; 1-ethyl-3-methylimidazolium perfluorooctanesulfonate, [C₂C₁Im][C₈F₁₇SO₃], > 98% mass fraction purity; 1-butyl-3-methylimidazolium trifluoromethanesulfonate, [C₄C₁Im][CF₃SO₃], ≥ 99% mass fraction purity and 1-butyl-3-methylimidazolium bis(trifluoromethylsulfonyl)imide, [C₄C₁Im][NTf₂], ≥ 99% mass fraction purity, were acquired at IoLiTec. The purity of all ionic liquids was verified by ¹H and ¹⁹F NMR. Previously to any use, all samples were dried under a 3·10⁻² Torr vacuum and vigorous stirring for at least 48 hours to avoid volatile impurities. Acetate-based ILs were maintained at 313.15 K and the remaining ILs at 323.15 K. Then, water content was determined using Karl Fischer coulometric titration method (Metrohm 831 KF Coulometer) and it was less than 100 ppm. The structures and acronyms of the ionic liquids are listed in **Table 2.S1**.

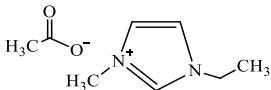
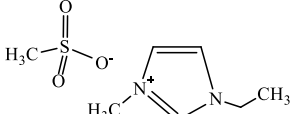
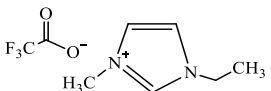
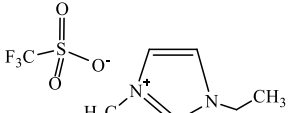
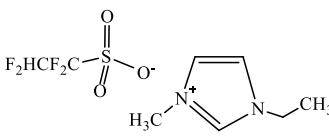
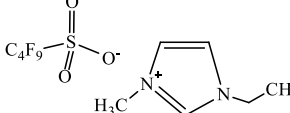
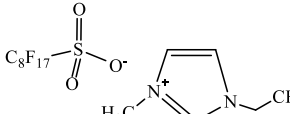
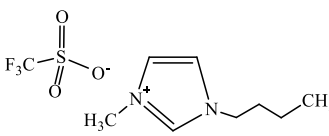
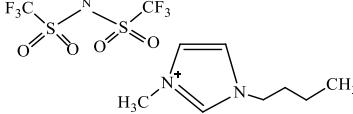
In order to characterize the polarity by the Kamlet-Taft method, three dyes were used: 4-Nitroaniline, ≥99% mass fraction purity acquired at Fluka; N,N-diethyl-4-nitroaniline, ≥97% mass fraction purity acquired at Fluorochem Ltd.; and 2,6-Diphenyl-4-(2,4,6-triphenyl-1-pyridinio)phenolate, also known as Reichardt's dye, with 90% mass fraction purity acquired at Sigma-Aldrich. Dichloromethane, ≥ 99.9% mass fraction purity acquired at Sigma-Aldrich, was used to dilute the dyes and Milli-Q ultrapure water (Milli-Q Integral Water Purification System) to dilute the samples.

Dye Solutions and Samples Preparation

The stock solutions of 4-nitroaniline, N,N-diethyl-4-nitroaniline and Reichardt's dye were prepared using ± 0.010 g of dye in a glass vial and mixed with 10 mL of dichloromethane (DCM). An additional 1:10 dilution with DCM was made in the case of 4-nitroaniline and N,N-diethyl-4-nitroaniline to ensure an absorbance less than 1.2. All

the stock solutions were previously maintained at 277 K after their preparation to avoid DCM evaporation.

Table 2.S1 Description of the ionic liquids and inorganic salts used in this work.

Formal Name	Structure	Abbreviation
1-Ethyl-3-methylimidazolium acetate		[C ₂ C ₁ Im][C ₁ CO ₂]
1-Ethyl-3-methylimidazolium methanesulfonate		[C ₂ C ₁ Im][C ₁ SO ₃]
1-Ethyl-3-methylimidazolium trifluoroacetate		[C ₂ C ₁ Im][C ₁ F ₃ CO ₂]
1-Ethyl-3-methylimidazolium trifluoromethanesulfonate		[C ₂ C ₁ Im][C ₁ F ₃ SO ₃]
1-Ethyl-3-methylimidazolium 1,1,2,2-tetrafluoroethanesulfonate		[C ₂ C ₁ Im][C ₂ F ₄ SO ₃]
1-Ethyl-3-methylimidazolium perfluorobutanesulfonate		[C ₂ C ₁ Im][C ₄ F ₉ SO ₃]
1-Ethyl-3-methylimidazolium perfluorooctanesulfonate		[C ₂ C ₁ Im][C ₈ F ₁₇ SO ₃]
1-Butyl-3-methylimidazolium trifluoromethanesulfonate		[C ₄ C ₁ Im][C ₁ F ₃ SO ₃]
1-Butyl-3-methylimidazolium bis(trifluoromethylsulfonyl)imide		[C ₄ C ₁ Im][NTf ₂]

Roughly 0.34 mL of 4-nitroaniline and N-N-diethyl-4-nitroaniline and 1.3 mL of Reichardt's dye were added to a glass vial with an open top screw-capped sealed with a silicone septum. To remove the DCM from dye solutions, samples were submitted to a $3 \cdot 10^{-2}$ Torr vacuum at room-temperature for at least 30 minutes. In order to prevent leakages in such extreme vacuum conditions, a 0.8 x 30 mm regular needle was slightly

skewered in to the silicone septum. Thus, 0.4 mg of sample is added to the vial and vigorously stirred in a vortex until all blended.

For neat ionic liquids measurements, samples were directly added to the dyes. To evaluate the water effect, 1.6 mL of ionic liquid aqueous solution was prepared in a clear glass vial using Milli-Q water. The different IL concentrations were prepared by weighting the ionic liquid and the Milli-Q water at fixed weight fractions. The range of concentrations varied from 100 wt% to 30 wt%, except for $[\text{C}_2\text{C}_1\text{Im}][\text{C}_8\text{F}_{17}\text{SO}_3]$ where the range concentration varied from 45 wt% to 30 wt%. This FIL is solid at room temperature (melting point = 367.72 K) [S1] and the Kamlet-Taft parameters at high concentrations was impossible to determine (turbidity problems) due to their high surfactant power and viscosity [S2].

Kamlet-Taft solvatochromic parameters were obtained using an UV-Vis VWR® spectrophotometer, model UV-6300PC. Each sample was loaded into a dry cuvette and measured in a scan range of 250 to 800 nm at 100.00 nm/min. In order to obtain a high spectra resolution, a 0.1 nm interval was chosen. The spectrum for each sample was recorded three times and the wavelengths in which the absorbance was maximum were acquired. All spectra were analysed using the UV-Vis Analyst Software.

Validation of Experimental Procedure

The experimental procedure used in this work was validated using conventional ionic liquids (1-butyl-3-methylimidazolium bis(trifluoromethylsulfonyl)imide, $[\text{C}_4\text{C}_1\text{Im}][\text{NTf}_2]$, and 1-butyl-3-methylimidazolium perfluoromethanesulfonate, $[\text{C}_4\text{C}_1\text{Im}][\text{C}_1\text{F}_3\text{SO}_3]$) [S3] as you can see in **Figure 2.S1**.

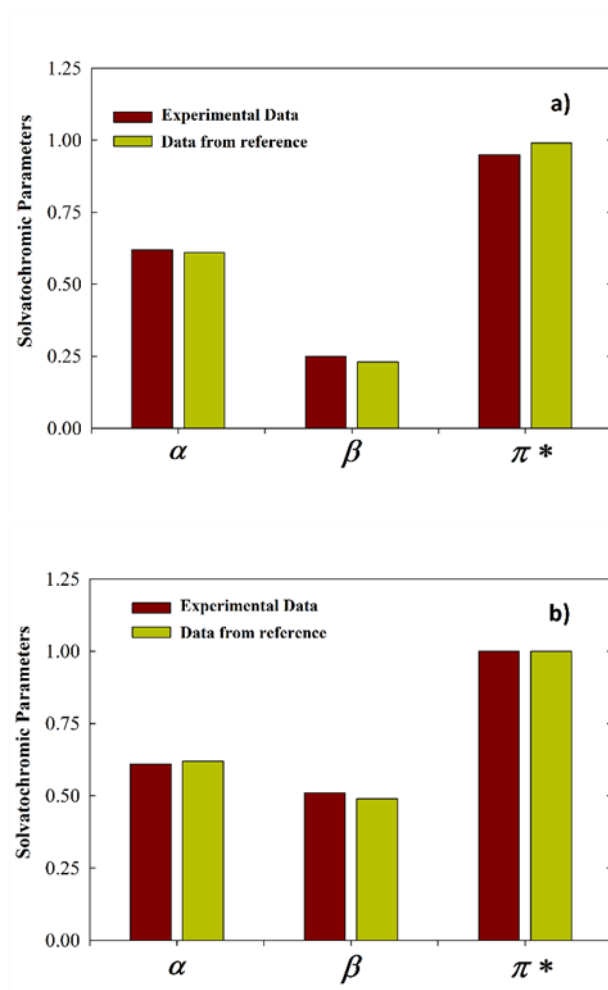


Figure 2.S1 Comparison between experimental and literature data (green) [S3] of Kamlet-Taft parameters for traditional ionic liquids at 298.15 K: a) 1-butyl-3-methylimidazolium bis(trifluoromethylsulfonyl)imide, [C₄C₁Im][NTf₂]; b) 1-butyl-3-methylimidazolium perfluoromethanesulfonate, [C₄C₁Im][C₁F₃SO₃] (red).

Kamlet-Taft Parameters of IL + H₂O Systems

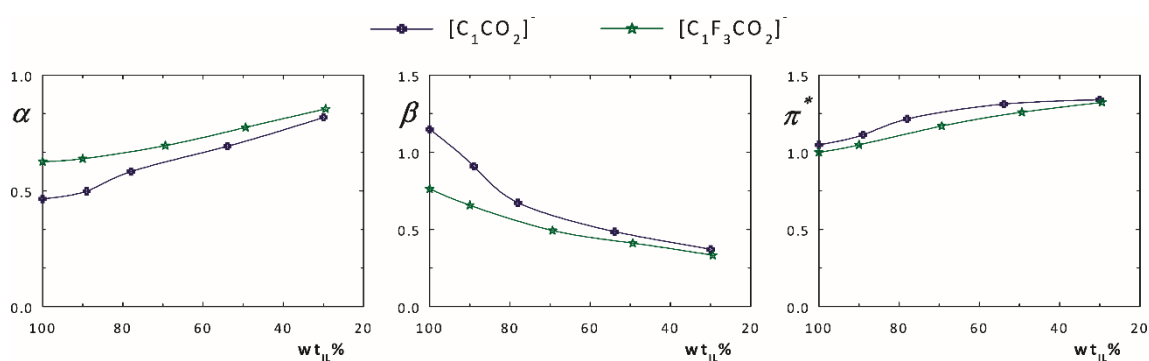


Figure 2.S2 Kamlet-Taft parameters (dye set Reichardt's dye, N,N-diethyl-4-nitroaniline and 4-nitroaniline) for the binary systems [C₂C₁Im][RCo₂] + H₂O at 298.15 K.

Table 2.S2 Kamlet-Taft parameters, hydrogen-bond donor (α), hydrogen-bond acceptor (β), and dipolarity/polarizability (π^*), with their corresponding standards deviations (σ), determined for the neat ILs and aqueous solutions studied in this work.

IL wt%	$\alpha \pm \sigma$	$\beta \pm \sigma$	$\pi^* \pm \sigma$	IL wt%	$\alpha \pm \sigma$	$\beta \pm \sigma$	$\pi^* \pm \sigma$	IL wt%	$\alpha \pm \sigma$	$\beta \pm \sigma$	$\pi^* \pm \sigma$
[C ₂ C ₁ Im][C ₁ CO ₂]				[C ₂ C ₁ Im][C ₁ SO ₃]				C ₂ C ₁ Im][C ₁ F ₃ CO ₂]			
100	0.465 ±0.001	1.15 ±0.040	1.05 ±0.002	100	0.552 ±0.004	0.708±0.012	1.12 ±0.005	100	0.627 ±0.002	0.762 ±0.001	1.00 ±0.002
89	0.499 ±0.002	0.909 ±0.001	1.11 ±0.001	90	0.562 ±0.001	0.601 ±0.002	1.15 ±0.002	90	0.639 ±0.001	0.656 ±0.002	1.05 ±0.002
78	0.583 ±0.002	0.672 ±0.004	1.22 ±0.002	69	0.672 ±0.004	0.483 ±0.001	1.25 ±0.001	69	0.695 ±0.001	0.492 ±0.005	1.17 ±0.001
56	0.692 ±0.001	0.485 ±0.007	1.31 ±0.001	49	0.756 ±0.001	0.383 ±0.007	1.32 ±0.001	49	0.774 ±0.008	0.411 ±0.003	1.26 ±0.001
30	0.817 ±0.001	0.370 ±0.016	1.34 ±0.001	30	0.874 ±0.001	0.310 ±0.014	1.35 ±0.012	29	0.854 ±0.004	0.332 ±0.001	1.32 ±0.001
[C ₂ C ₁ Im][C ₁ F ₃ SO ₃]				[C ₂ C ₁ Im][C ₂ F ₄ SO ₃]				[C ₂ C ₁ Im][C ₄ F ₉ SO ₃]			
100	0.465 ±0.001	1.15 ±0.040	1.05 ±0.002	100	0.632 ±0.002	0.489 ±0.001	1.04 ±0.002	100	0.757 ±0.001	0.479 ±0.006	0.894 ±0.001
89	0.499 ±0.002	0.909 ±0.001	1.11 ±0.001	90	0.758 ±0.001	0.461 ±0.006	1.11 ±0.003	91	0.986 ±0.001	0.494 ±0.007	1.01 ±0.001
78	0.583 ±0.002	0.672 ±0.004	1.22 ±0.002	69	0.837 ±0.013	0.387 ±0.006	1.20 ±0.003	70	1.00 ±0.011	0.482 ±0.022	1.06 ±0.002
56	0.692 ±0.001	0.485 ±0.007	1.31 ±0.001	50	0.843 ±0.002	0.340 ±0.001	1.25 ±0.001	50	1.03 ±0.004	0.488 ±0.006	1.05 ±0.006
30	0.817 ±0.001	0.370 ±0.016	1.34 ±0.001	30	0.865 ±0.001	0.284 ±0.001	1.32 ±0.001	30	0.979 ±0.017	0.502 ±0.038	1.06 ±0.019
[C ₂ C ₁ Im][C ₈ F ₁₇ SO ₃]				Water							
45	1.17 ±0.006	0.596 ±0.009	0.947 ±0.001	0 ^a	1.11 ±0.002	0.130 ±0.014	1.34 ±0.001				
40	1.20 ±0.002	0.588 ±0.007	0.954 ±0.003		(1.12) ^b	(0.14) ^b	(1.33) ^b				
35	1.20 ±0.001	0.602 ±0.002	0.949 ±0.002		(1.02-1.17) ^c	(0.14-0.18) ^c	(1.09) ^c				
30	1.17 ±0.003	0.597 ±0.006	0.956 ±0.003		(1.17) ^d	(0.17) ^d	(1.09) ^d				

^a Milli-Q ultrapure water; ^b data from reference S5; ^c data from reference S6; ^d data from reference S7

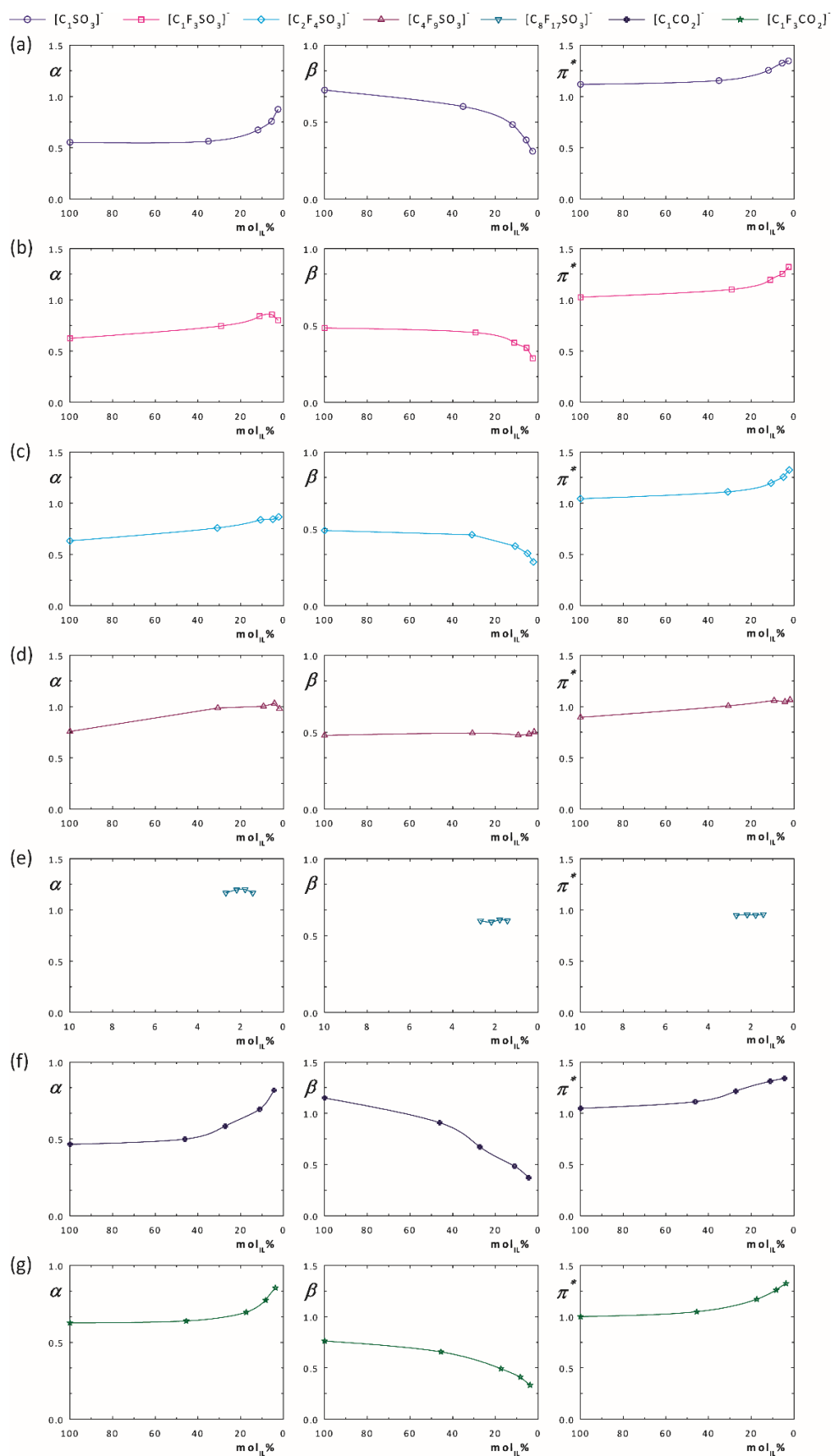


Figure 2.S3 Kamlet-Taft parameters (dye set Reichardt's dye, *N,N*-diethyl-4-nitroaniline and 4-nitroaniline) for the binary systems $[C_2C_1Im][RSO_3] + H_2O$ (a–e) and $[C_2C_1Im][RCO_2] + H_2O$ (f, g) at 298.15 K, expressed in mol.%.

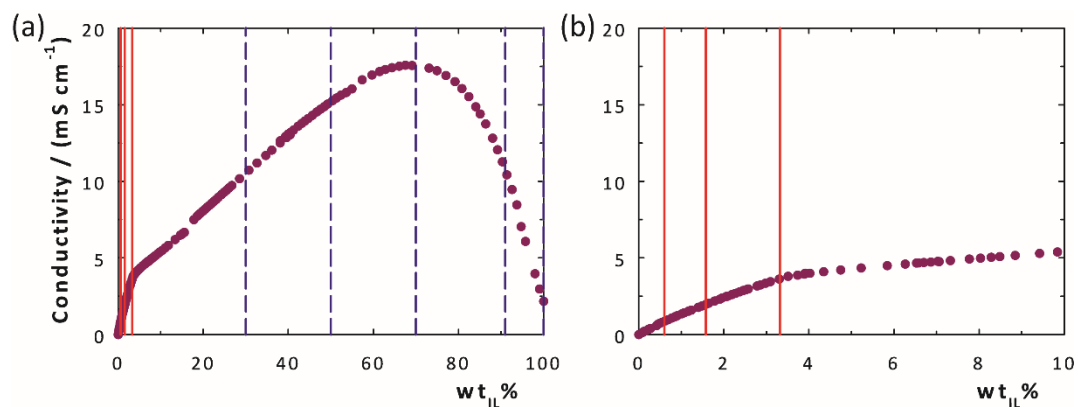


Figure 2.S4 Electrical conductivity profile of $[C_2C_1Im][C_4F_9SO_3] + H_2O$ system at 298.15 K. The three critical aggregation concentrations (solid red lines) and the herein studied FIL concentrations in wt% (dashed blue lines) are also depicted. a) full concentration range and b) inset. Data adapted from reference S4.

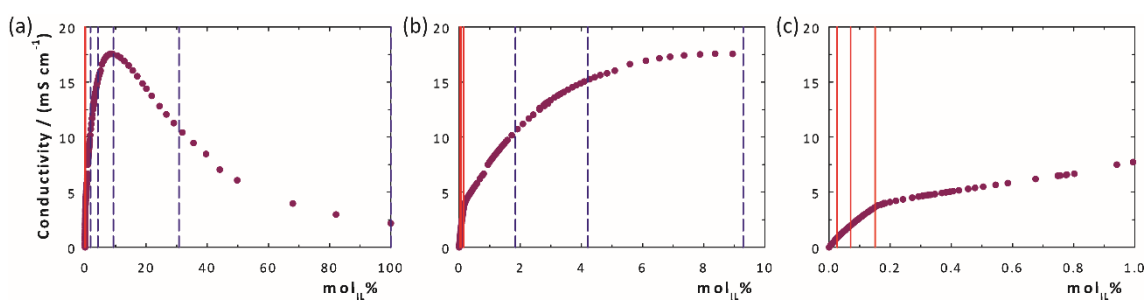


Figure 2.S5 Electrical conductivity profile of $[C_2C_1Im][C_4F_9SO_3] + H_2O$ system at 298.15 K. The three critical aggregation concentrations (solid red lines) and the herein studied FIL concentrations in mol% (dashed blue lines) are also depicted. a) full concentration range and b, c) inset. Data adapted from reference S4.

Molecular Dynamics Simulations.

The atomistic description of water, and the [C₂C₁Im][C₁F₃SO₃], [C₂C₁Im][C₂F₄SO₃], [C₂C₁Im][C₄F₉SO₃], [C₂C₁Im][C₈F₁₇SO₃], [C₂C₁Im][C₁SO₃], [C₂C₁Im][C₄H₉SO₃], [C₂C₁Im][C₁CO₂] and [C₂C₁Im][C₁F₃CO₂] ionic liquids was implemented using the SPC,[S8] and CL&P [S9-S11] force-fields, respectively. The MD simulations were carried out using the DL_POLY 2.20 [S12] and Gromacs [S13-S15] packages.

The runs in DL_POLY (systems 1 to 24 in **Table 2.S3**) started from low-density configurations built with the PACKMOL package [S16] and were performed using 2 fs timesteps and 2 nm cutoff distances. All simulations were subjected to equilibration runs under isobaric isothermal ensemble conditions ($p = 0.1$ MPa and $T = 300$ K with Nosé–Hoover thermostats and barostats with relaxation time constants of 1 and 4 ps, respectively) for 200 ps. Therefore, Gromacs simulations were performed using 2 fs timesteps and 2 nm cutoff distances, with Ewald summation corrections performed beyond the cutoffs. The isothermal-isobaric ensemble conditions used during equilibration were $p = 0.1$ MPa and $T = 300$ K with V-rescale thermostats and Berendsen barostats with relaxation time constants of 1 and 4 ps, respectively. After 10 ns, the density of each system reached constant and consistent values, indicating that equilibrium had been attained and possible ergodicity problems had been overcome. Finally, at least six consecutive production stages of 1.0 ns each were performed using 1 fs timestep, the isothermal-isobaric ensemble conditions used during equilibration were $p = 0.1$ MPa and $T = 300$ K with Nosé–Hoover thermostats and Parrinello-Rahman barostats with relaxation time constants of 1 and 4 ps, respectively. The combined results were used for the aggregation analyses of all studied ionic liquids (see below).

The aggregation analyses of the [C₂C₁Im][C₁F₃SO₃], [C₂C₁Im][C₂F₄SO₃], [C₂C₁Im][C₄F₉SO₃], [C₂C₁Im][C₈F₁₇SO₃], [C₂C₁Im][C₁SO₃], [C₂C₁Im][C₄H₉SO₃], [C₂C₁Im][C₁CO₂] and [C₂C₁Im][C₁F₃CO₂] ionic liquids and their mixtures with water focused on three types of issues: (i) the evaluation of the connectivity

between the charged moieties of the molecular ions that compose the so-called polar network; (ii) the evaluation of the connectivity within the water and an estimation of the corresponding aggregate size; and (iii) the evaluation of the connectivity between the anion of the ionic liquids and water. The connectivity analyses are based on algorithms [S17-S19] previously described based on neighbour lists and interaction distance criteria, adapted to take into account the interaction centres of the different species.

The ILs colour code in **Figure 2.3 and 2.4** of the manuscript is: red (negative charges) and blue (positive charges) segments represent the interactions from the polar network of the two ions; grey space-filled areas represent the domains caused by the hydrogenated side chains; while the groups of green spheres illustrate the perfluoroalkyl apolar domains. Please note that the polar part includes the first methylene/methyl or fluorinated methylene groups directly connected to the imidazolium ring or the sulfonate/carboxylate moiety. This means that $[C_1C_1Im]^+$ would be all blue and $[C_1F_3SO_3]^-$ is all red. In other words, the gray/green colour code only applies to alkyl/perfluorinated alkyl chains from the β carbon onwards.

Table 2.S3. Simulation conditions, size of the equilibrated boxes and concentrations.

	System	wt _{IL} %	n _{IL}	n _w	l _{box} nm	V _{box} nm ³
1	[C ₂ C ₁ Im][C ₁ F ₃ SO ₃] + water	30	100	3300	5.568	127.7
2	[C ₂ C ₁ Im][C ₁ F ₃ SO ₃] + water	50	180	2600	5.080	131.1
3	[C ₂ C ₁ Im][C ₁ F ₃ SO ₃] + water	90	390	620	5.158	137.2
4	[C ₂ C ₁ Im][C ₂ F ₄ SO ₃] + water	30	88	3300	5.035	127.6
5	[C ₂ C ₁ Im][C ₂ F ₄ SO ₃] + water	50	165	2600	5.109	133.4
6	[C ₂ C ₁ Im][C ₂ F ₄ SO ₃] + water	90	350	620	5.179	138.9
7	[C ₂ C ₁ Im][C ₄ F ₉ SO ₃] + water	30	62	3300	4.983	123.7
8	[C ₂ C ₁ Im][C ₄ F ₉ SO ₃] + water	50	115	2600	5.009	125.7
9	[C ₂ C ₁ Im][C ₄ F ₉ SO ₃] + water	90	250	620	4.999	124.9
10	[C ₂ C ₁ Im][C ₈ F ₁₇ SO ₃] + water	30	43	3300	4.969	122.7
11	[C ₂ C ₁ Im][C ₈ F ₁₇ SO ₃] + water	50	78	2600	4.967	122.6
12	[C ₂ C ₁ Im][C ₈ F ₁₇ SO ₃] + water	90	180	620	4.988	124.1
13	[C ₂ C ₁ Im][C ₁ SO ₃] + water	30	125	3300	5.106	133.1
14	[C ₂ C ₁ Im][C ₁ SO ₃] + water	50	230	2600	5.218	142.1
15	[C ₂ C ₁ Im][C ₁ SO ₃] + water	90	490	620	5.422	159.4
16	[C ₂ C ₁ Im][C ₄ H ₉ SO ₃] + water	30	105	3300	5.135	135.4
17	[C ₂ C ₁ Im][C ₄ H ₉ SO ₃] + water	50	190	2600	5.261	145.6
18	[C ₂ C ₁ Im][C ₄ H ₉ SO ₃] + water	90	420	620	5.573	173.1
19	[C ₂ C ₁ Im][C ₁ CO ₂] + water	30	150	3300	5.112	133.6
20	[C ₂ C ₁ Im][C ₁ CO ₂] + water	50	280	2600	5.249	144.6
21	[C ₂ C ₁ Im][C ₁ CO ₂] + water	90	600	620	5.560	171.8
22	[C ₂ C ₁ Im][C ₁ F ₃ CO ₂] + water	30	115	3300	5.054	129.1
23	[C ₂ C ₁ Im][C ₁ F ₃ CO ₂] + water	50	210	2600	5.127	134.8
24	[C ₂ C ₁ Im][C ₁ F ₃ CO ₂] + water	90	450	620	5.267	146.1

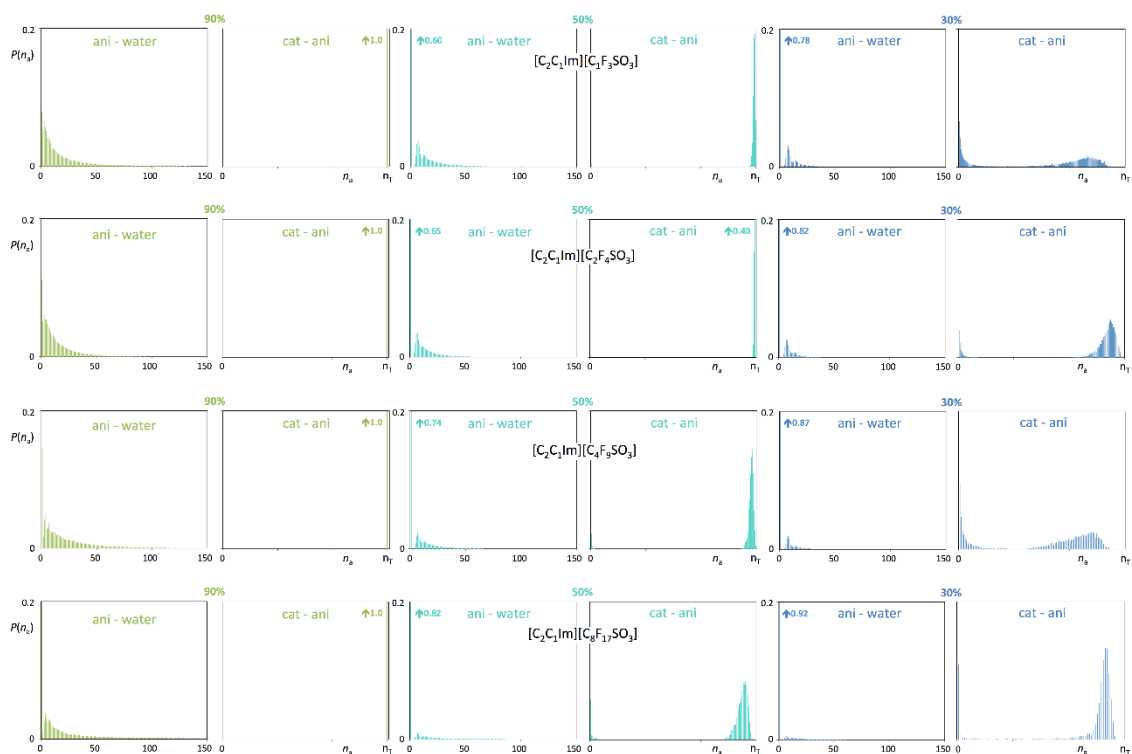


Figure 2.S6 Discrete probability distribution functions of water aggregate sizes, $P(n_a)$, for different compositions of water-IL mixtures.

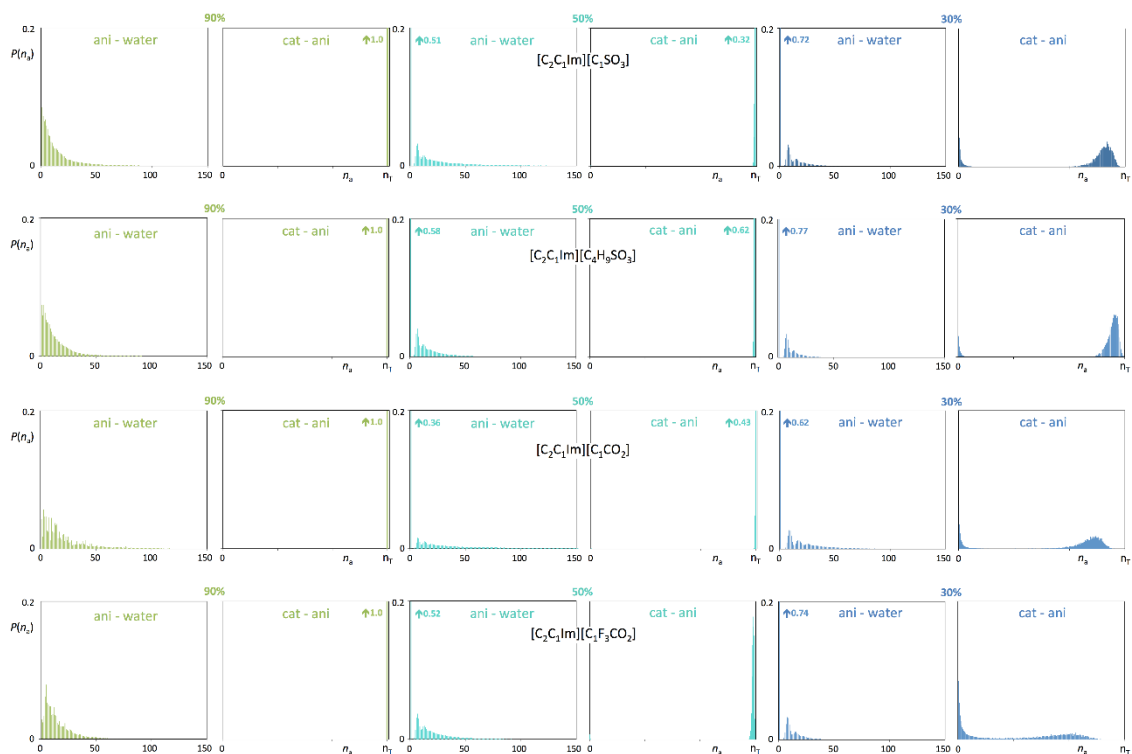


Figure 2.S7 Discrete probability distribution functions of water aggregate sizes, $P(n_a)$, for different compositions of water-IL mixtures.

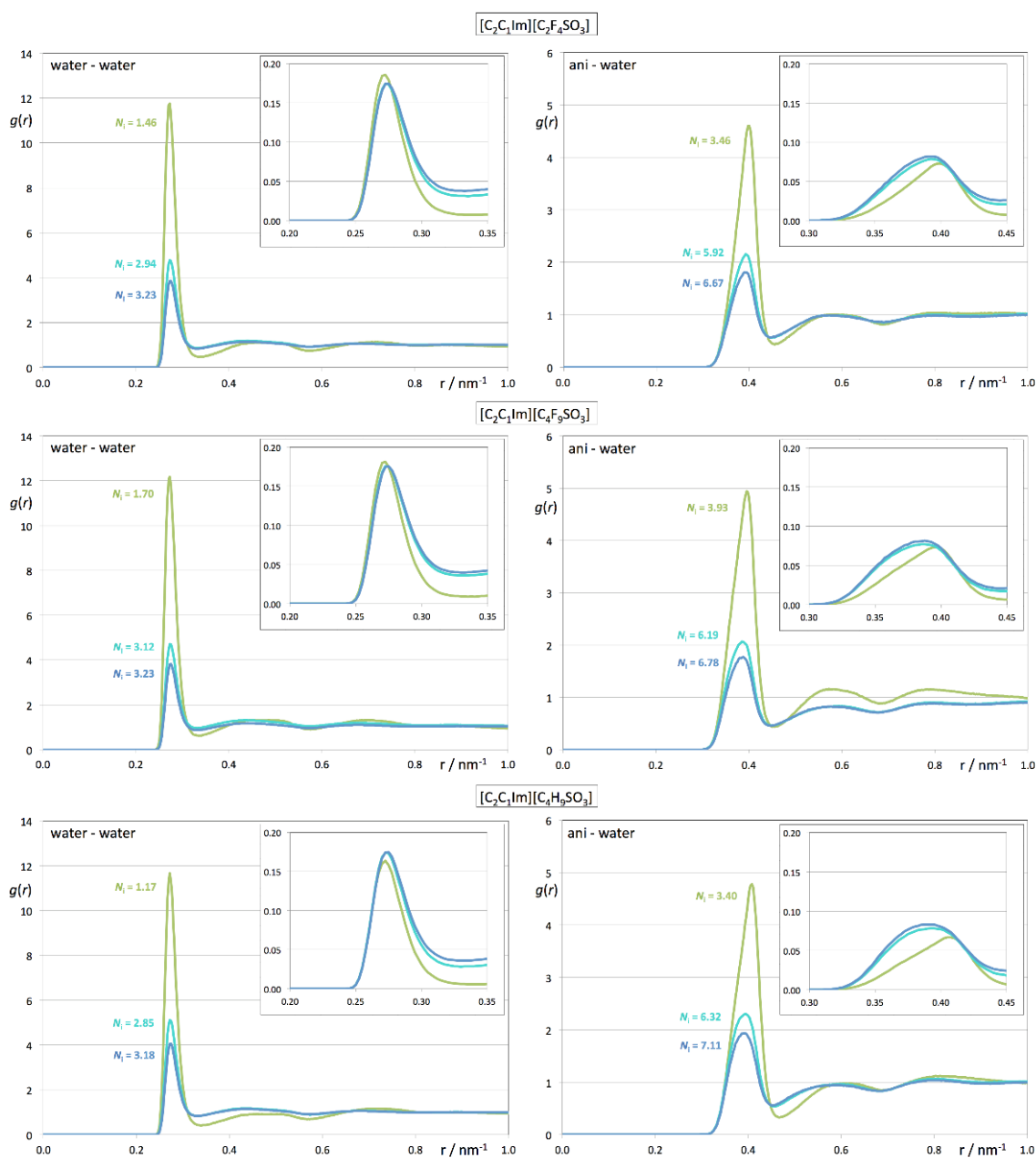


Figure 2.S8 Pair radial distribution functions, $g(r)$, between oxygen atoms in water (left column), and between sulphur atoms in the anion and oxygen atoms in water (right column) for different compositions of water-IL mixtures (green, cyan and blue represent 90, 50 and 30 wtIL% compositions, respectively). To have a fair comparison between the first peaks in the different water-IL mixtures, the RDFs were multiplied by the corresponding numerical density (inset). The average size of contact neighbours, N_i , in the water aggregates and anion-water aggregates are also presented in the figure and were calculated from the integration of the first peaks of the corresponding $g(r)$ functions.

References

- S1. N. S. M. Vieira, P. M. Reis, K. Shimizu, O. A. Cortes, I. M. Marrucho, J. M. M. Araújo, J. M. S. S. Esperança, J. N. C. Lopes, A. B. Pereiro and L. P. N. Rebelo, *RSC Adv.*, 2015, 5, 65337.

- S2. A. B. Pereiro, J. M. M. Araújo, F. S. Teixeira, I. M. Marrucho, M. M. Piñeiro and L. P. N. Rebelo, *Langmuir*, 2015, 31, 1283.
- S3. M. A. Ab Rani, A. Brant, L. Crowhurst, A. Dolan, M. Lui, N. H. Hassan, J. P. Hallett, P. A. Hunt, H. Niedermeyer, J. M. Perez-Arlandis, M. Schrems, T. Welton, R. Wilding, *Phys. Chem. Chem. Phys.*, 2011, 13, 16831.
- S4. A. B. Pereiro, J. M. M. Araújo, F. S. Teixeira, I. M. Marrucho, M. M. Piñeiro and L. P. N. Rebelo, *Langmuir*, 2015, 31, 1283.
- S5. C. Zhong, F. Cheng, Y. Zhu, Z. Gao, H. Jia and P. Wei, *Carbohydrate Polymers*, 2017, 174, 400.
- S6. T. V. Doherty, M. Mora-Pale, S. E. Foley, R. J. Linhardt and, J. S. Dordick, *Green Chem.*, 2010, 12, 1967.
- S7. D. L. Minnick, R. A. Flores, M. R. DeStefano and A. M. Scurto, *J. Phys. Chem. B*, 2016, 120, 7906.
- S8. M. Praprotnik, D. Janežič and J. Mavri, *J. Phys. Chem. A*, 2004, 108, 11056.
- S9. J. N. Canongia Lopes, J. Deschamps and A. A. H. Pádua, *J. Phys. Chem. B*, 2004, 108, 2038.
- S10. J. N. Canongia Lopes and A. A. H. Pádua, *J. Phys. Chem. B*, 2004, 108, 16893.
- S11. J. N. Canongia Lopes, A. A. H. Pádua and K. Shimizu, *J. Phys. Chem. B*, 2008, 112, 5039.
- S12. Smith, W.; Forester, T. R. *The DL_POLY Package of Molecular Simulation Routines (v.2.2)*; The Council for The Central Laboratory of Research Councils. Warrington: Daresbury Laboratory, 2006.
- S13. H. J. C. Berendsen, D. van der Spoel and R. van Drunen, *Comput. Phys. Commun.*, 1995, 91, 43.
- S14. S. Páll, M. J. Abraham, C. Kutzner, B. Hess and E. Lindahl, in *Solving Software Challenges for Exascale*. Vol. 8759, Springer, Cham, 2015, pp. 3–27.
- S15. M. J. Abraham, T. Murtola, R. Schulz, S. Páll, J. C. Smith, B. Hess and E. Lindahl, *SoftwareX*, 2015, 1-2, 19.
- S16. L. Martínez, R. Andrade, E. G. Birgin and J. M. Martínez, *J. Comput. Chem.*, 2009, 30, 2157.
- S17. A. F. M. Claudio, M. C. Neves, K. Shimizu, J. N. Canongia Lopes, M. G. Freire and J. A. P. Coutinho, *Green Chem.*, 2015, 17, 3948.
- S18. K. Shimizu, C. E. S. Bernardes and J. N. Canongia Lopes, *J. Phys. Chem. B*, 2014, 118, 567.

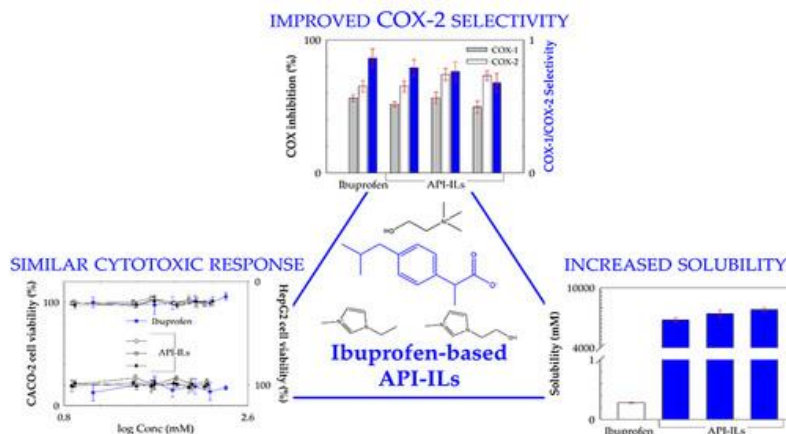
- S19. C. E. S. Bernardes, K. Shimizu, A. I. M. C. Lobo Ferreira, L. M. N. B. F. Santos and J. N. Canongia, *J. Phys. Chem. B*, 2014, 118, 6885.

**HUMAN CYTOTOXICITY, HEMOLYTIC ACTIVITY,
ANTI-INFLAMMATORY ACTIVITY AND AQUEOUS
SOLUBILITY OF IBUPROFEN-BASED IONIC
LIQUIDS**

3.1 Abstract

Ionic liquids (ILs) are a potential solution to the general problem of low solubility, polymorphism and low bioavailability of active pharmaceutical ingredients (APIs). In this work, we report on the synthesis of three pharmaceutically active ILs (API-ILs) based on ibuprofen, one of the most commonly available over-the-counter nonsteroidal anti-inflammatory drugs (NSAIDs), with imidazolium cations ($[C_2C_1Im][Ibu]$ and $[C_{2(OH)}C_1Im][Ibu]$) and a cholinium cation ($[N_{1112(OH)}][Ibu]$). An upgrade to the aqueous solubility (water and biological simulated fluids) for the ibuprofen-based ILs relative to the ibuprofen's neutral and salt form (sodium ibuprofen) was verified. The cytotoxic profiles of the synthesized API-ILs were characterized using two human cells lines, Caco-2 colon carcinoma cells and HepG-2 hepatocellular carcinoma cells, up to ibuprofen's maximum plasma concentration (C_{max}) without impairing their cytotoxicity response. Additionally, the EC_{50} in the Caco-2 cell line revealed similar results for both parent APIs and API-ILs. The biocompatibility of the ibuprofen-based ILs was also evaluated through a hemolytic activity assay, and the results showed that all the ILs were hemocompatible at concentrations higher than the ibuprofen C_{max} . Moreover, the anti-inflammatory properties of the API-ILs were assessed through the inhibition of bovine serum albumin (BSA) denaturation and inhibition of cyclooxygenases (COX-1 and COX-2). The results showed that $[C_2C_1Im][Ibu]$, $[C_{2(OH)}C_1Im][Ibu]$ and $[N_{1112(OH)}][Ibu]$ maintained their anti-inflammatory response to ibuprofen, with improved selectivity towards COX-2, allowing the development of safer NSAIDs and the recognition of new avenues for selective COX-2 inhibitors in cancer chemotherapy and neurological diseases such as Alzheimer's and Parkinson's.

Keywords: ionic liquids; ibuprofen; bioavailability; cytotoxicity; HepG2; Caco-2; BSA denaturation; hemocompatibility; cyclooxygenase inhibitors; COX-1; COX-2.



Published in: [Joana C. Bastos](#), Nicole S. M. Vieira, Maria Manuela Gaspar, Ana B. Pereiro, João M. M. Araújo. Human Cytotoxicity, Hemolytic Activity, Anti-Inflammatory Activity and Aqueous Solubility of Ibuprofen-Based Ionic Liquids. *Sustain. Chem.* **2022**, 3(3), 358-375.

Own experimental contribution: Ibu-based ILs synthesis, NMR and DSC sample preparation, solubility assay, cytotoxicity assay, protein denaturation assay, cyclooxygenases (COX-1 and COX-2) inhibition assay.

Own written contribution: NMR and DSC analysis, solubility assay, cytotoxicity assay, protein denaturation assay, hemocompatibility assay, cyclooxygenases (COX-1 and COX-2) inhibition assay.

Other contributions: Experimental design and data analysis.

3.2 Introduction

The pharmaceutical industry has resorted to several strategies to improve drugs that present major physicochemical problems such as polymorphism, low solubility and low bioavailability [1]. Since most pharmaceutical compounds are obtained in a crystalline solid form, polymorphism often represents a crucial complication. Polymorphism can be defined as the ability of a solid material to exist in two or more crystalline forms; although chemically the same, the polymorphs present different lattice structures and, consequently, different physicochemical and biological properties. Thus, polymorphism can significantly influence the properties of an active pharmaceutical ingredient (API) such as the dissolution rate, solubility, stability and, therefore, its bioavailability [2]. Strategies, such as solid dispersions, cyclodextrin inclusions, nanoemulsions, micelles and nanoparticles, were widely adopted to deliver poorly water-soluble drugs [3]. However, one of the most used approaches by pharmaceutical companies to overcome the low bioavailability problem is to redesign drugs in their respective salt forms [4], for example, in the context of nonsteroidal anti-inflammatory drugs (NSAIDs), the commercially used sodium ibuprofen, sodium naproxen and sodium diclofenac.

Ionic liquids (ILs), in agreement with the usually accepted definition, are salts comprising cations and anions with a melting point below the conventional temperature of 100 °C [5]. The large number of possible cation/anion combinations allows for a great variety of tunable properties. The key physicochemical properties, such as melting point, density, viscosity, surface tension, thermal stability, solubility, hygroscopicity and even toxicity and biodegradability [6,7,8], can be tailored, making ILs task-specific designer materials suitable for the biotechnology and pharmaceutical areas [9,10]. The development of ILs based on active pharmaceutical ingredients (API-ILs) has arisen as a possible solution to some of the problems that crystalline solid APIs present [1,11], leading to APIs with lower melting temperatures and improved bioavailability [4].

For example, the API-IL approach has been applied to increase the solubility in aqueous media (water and simulated biological fluids) of the APIs nalidixic acid and niflumic

acid by their conversion into cholinium-based ILs ($[N_{1112(OH)}][NaI]$ and $[N_{1112(OH)}][Nif]$) successfully, allowing for increases of 3300-fold and 53,000-fold of the solubility in water at 25 °C, respectively. Furthermore, an in vitro study on two human cell lines, Caco-2 colon carcinoma cells and HepG2 hepatocellular carcinoma cells, revealed that the cytotoxicity of these APIs was preserved upon their conversion into ILs [12]. Fernández-Stefanuto and coworkers synthesized alverine-based ILs with a water solubility up to 39,937-fold higher than the parent API, a widely known smooth muscle relaxant. Additionally, they managed to synthesize API-ILs that were liquid at room temperature, avoiding any limitations related to polymorphism [13]. In addition, Florindo et al. reported the conversion of the antibiotic ampicillin into ampicillin-based ILs, namely, 1-ethyl-3-methylimidazolium ampicillin ($[C_2C_1Im][Amp]$), 1-hydroxy-ethyl-3-methylimidazolium ampicillin ($[C_{2(OH)}C_1Im][Amp]$) and cholinium ampicillin ($[N_{1112(OH)}][Amp]$), and an enhancement in the octanol–water partition coefficient was verified [14]. Although an API is converted into an IL, the API-ILs platform allows to maintain or even improve the pharmacological profile of the parent API. Zhao et al. developed a cholinium-based derivative of betulinic acid with higher solubility in water than betulinic acid (by 100-fold) and improved the biological activity for inhibition of HIV-1 protease [15]. Moreover, Demurtas and coworkers developed cholinium-based ILs from hydroxycinnamic acids with higher solubility and free radical scavenging activity than the parent hydroxycinnamic acids as well as negligible cytotoxicity activity [16].

NSAIDs are the most used pharmaceutical ingredients for inflammation relief [17]. Their main action is through the inhibition of cyclooxygenase (COX), minimizing the production of prostaglandins, which is responsible for pain and inflammation responses [18]. Most NSAIDs are poorly water-soluble, which is a major drawback when envisaging their incorporation into hydrophilic matrices for drug release or their bioavailability [19]. The oral administration of NSAIDs is currently the most used route [20]; however, this type of administration presents several drawbacks including possible side effects such as gastrointestinal [21] and renal [18] toxicity. Therefore, whenever

possible, topical administration of anti-inflammatory drugs is an efficient way to reduce some of the side effects. The therapeutic anti-inflammatory action of NSAIDs is produced by the inhibition of COX-2, while the undesired side effects arise from inhibition of COX-1 activity. Thus, more selective COX-2 inhibitors have reduced side effects [22].

The API-ILs platform has already been implemented to tackle some of the NSAIDs' drawbacks. Wu et al. successfully improved ibuprofen aqueous solubility by its conversion into imizazolium- and phosphonium-based ILs [23], and Santos and coworkers [24] prepared a set of ibuprofen-based ILs with different organic cations (e.g., cholinium, imidazolium and acetylpyridine) with increased solubility in aqueous media and negligible cytotoxicity towards human dermal fibroblasts and ovarian carcinoma cells. Stocker and coworkers [25] successfully spray-dried an imidazolium-based ibuprofen IL into a polymer carrier in loadings of up to 75% w/w in order to transform it into a solid powder suitable for oral solid dosage formulation, and they demonstrated that aqueous solutions of this API-IL has the potential to offer thermodynamic stability upon release, avoiding in vivo recrystallization issues that can limit the bioavailability of amorphous solid dispersions and some high-energy crystalline forms. Chantereau et al. [26] increased the solubility in aqueous media (up to 100-fold) of different NSAIDs, such as ibuprofen, naproxen and ketoprofen, via the preparation of cholinium-based ILs, and incorporated these API-ILs into bacterial nanocellulose membranes envisaging their use in transdermal drug delivery systems. Ibuprofen-based ILs conjugated with pyrrolidonium and cholinium cations were prepared by Moshidur et al. [27] as effective biocompatible formulations for topical drug delivery. Abednejad and coworkers [28] exploited the dual nature of ILs by combining an analgesic licocainium cation with anti-inflammatory NSAID-based anions, namely, ibuprofen, naproxen and diclofenac, obtaining liquid API-ILs at 25 °C with higher solubility in aqueous media and higher permeation than the parent APIs, without impairing their anti-inflammatory activity. The dual nature of ILs was also explored by Panic' et al. [29], who modified the local anesthetic drug, procaine, into ionic liquids combined with distinct pharmaceutically

active anions such as ibuprofenate, salicylate and docusate. Dual pharmaceutically active protic ILs containing NSAIDs (i.e., ibuprofen or naproxen) as anions and diphenhydramine, an H1-receptor antagonist, as the cation were developed by Wang and coworkers [30] and loaded into a mesoporous carrier for novel formulation development. Recently, ibuprofen-based ILs with diphenhydramine and ranitidine cations were prepared by Frizzo et al. [31], and antifungal activity that was not present in the precursor salts was observed in the ILs. Wust and coworkers [32] showed that the API-IL, diphenhydraminium ibuprofenate, supported onto mesoporous silicas, can be obtained through a simple and efficient process (i.e., adsorption from solution), and they determined the release profiles of the supported API-IL, which were dependent on the pore size of the silicas. Additionally, the API-IL had an antinociceptive effect greater than sodium ibuprofen; thus, the authors concluded that the diphenhydramine potentiates the antinociceptive effect of ibuprofen. Further, the development of ibuprofen-based API-ILs conjugated with amino acid derivatives were also attained in different works for improved solubility and permeability of the parent API [33,34].

Herein, we report on the synthesis, characterization and thermal properties of three API-ILs based on the imidazolium and cholinium cations with the ibuprofenate anion: 1-ethyl-3-methylimidazolium ibuprofenate ($[\text{C}_2\text{C}_1\text{Im}][\text{Ibu}]$), 1-(2-hydroxyethyl)-3-methylimidazolium ibuprofenate ($[\text{C}_{2(\text{OH})}\text{C}_1\text{Im}][\text{Ibu}]$) and cholinium ibuprofenate ($[\text{N}_{1112(\text{OH})}][\text{Ibu}]$). Further, the solubility in water (all three ibuprofen-based ILs, ibuprofen and sodium ibuprofen) and buffer solutions suitable to dissolution testing ($[\text{N}_{1112(\text{OH})}][\text{Ibu}]$, ibuprofen and sodium ibuprofen) at 25 °C were evaluated. The studied buffer solutions included simulated gastric fluid without enzymes (interchangeable with 0.1 N HCl pH 1.0), simulated intestinal fluid without enzymes (interchangeable with phosphate standard buffer pH 6.8) and 0.15 M NaCl (isotonic ionic strength solution). Additionally, to ascertain the biocompatibility of the ibuprofen-based ILs, we performed in vitro cytotoxicity assays with two different human cells lines, namely, Caco-2 colon carcinoma cells and HepG2 hepatocellular carcinoma cells, as well as hemocompatibility assays. Finally, the anti-inflammatory activity of the API-ILs was assessed by the

inhibition of bovine serum albumin (BSA) denaturation and the inhibition of cyclooxygenases (COX-1 and COX-2) enzymes using a colorimetric COX (COX-2, human; COX-1, ovine) inhibitor screening assay kit, to evaluate the potential of the API-ILs platform to maintain/upgrade the pharmacological activity of the parent API and to improve selectivity towards COX-2.

3.3 Materials and Methods

3.3.1 Materials

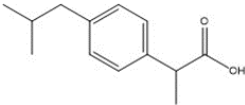
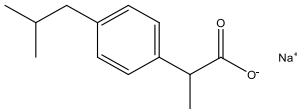
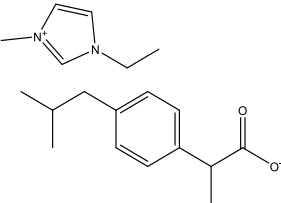
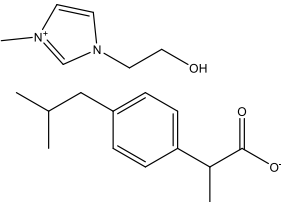
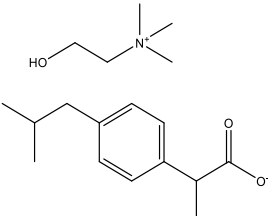
Ibuprofen (>98% mass fraction purity) was purchased from TCI and ibuprofen sodium salt ($\geq 98\%$ mass fraction purity) from Sigma-Aldrich. Both APIs were used without further purification. The ionic liquids, 1-ethyl-3-methylimidazolium chloride ($[\text{C}_2\text{C}_1\text{Im}]\text{Cl}$; >98% mass fraction purity) and 1-(2-Hydroxyethyl)-3-methylimidazolium chloride ($[\text{C}_{2(\text{OH})}\text{C}_1\text{Im}]\text{Cl}$; >99% mass fraction purity), were acquired at IoLiTec. Cholinium chloride ($[\text{N}_{1112(\text{OH})}]\text{Cl}$; $\geq 98\%$ mass fraction purity) was purchased at Sigma-Aldrich. To avoid volatile impurities, the ionic liquids and cholinium chloride were dried under a 3×10^{-2} Torr vacuum for at least 48 h prior to any use. Additionally, the water content was determined by Karl Fischer coulometric titration, and it was 0.05 wt%.

Through a two-step anion exchange reaction methodology proposed in previous works [6,12], three ibuprofen-based ionic liquids were synthesized: 1-ethyl-3-methylimidazolium ibuprofenate ($[\text{C}_2\text{C}_1\text{Im}][\text{Ibu}]$), 1-(2-hydroxyethyl)-3-methylimidazolium ibuprofenate ($[\text{C}_{2(\text{OH})}\text{C}_1\text{Im}][\text{Ibu}]$) and cholinium ibuprofenate ($[\text{N}_{1112(\text{OH})}][\text{Ibu}]$). Neat ibuprofen-based ionic liquids were obtained after eliminating the excess water and API by evaporation and washing, respectively. Their chemical structures and respective acronyms are shown in **Table 3.1**. More experimental details on the synthesis can be found in the **Supplementary Materials**. Additionally, the ionic liquids were characterized by ^1H and ^{13}C NMR and elemental analysis in order to examine their expected structures and final purities. The water content, determined by

Karl Fischer titration, was less than 0.05 wt%. The prepared ibuprofen-based ionic liquids were further characterized by differential scanning calorimetry (DSC).

In all experiments throughout the work, Milli-Q water (Milli-Q Integral Water Purification System, Merck, Darmstadt, Germany) was used. The simulated gastric fluid without enzymes (interchangeable with 0.1 N HCl at pH 1.0) was acquired from Carlo Erba Reagents, and the simulated intestinal fluid without enzymes (interchangeable with phosphate standard buffer at pH 6.8) from Honeywell. The sodium chloride physiological solution (0.15 M NaCl isotonic ionic strength) was purchased from Sigma-Aldrich. Tablets for the phosphate-buffered saline (PBS) solution preparation were purchased from PanReac Applichem ITW Reagents Division (Chicago, IL, USA).

Table 3.1. Chemical structures and respective acronyms and molecular weights of ibuprofen, sodium ibuprofen and the ibuprofen-based API-ILs.

Chemical Structure	Designation and Acronym	Mw (g/mol)
	2-(4-Isobutylphenyl) propionic acid Ibuprofen (Ibu)	206.29
	Sodium 2-(4-isobutylphenyl) propanoate Sodium ibuprofen salt (Na[Ibu])	228.26
	1-Ethyl-3-methylimidazolium Ibuprofenate [C ₂ C ₁ Im][Ibu]	316.44
	1-(2-Hydroxyethyl)-3-methylimidazolium Ibuprofenate [C _{2(OH)} C ₁ Im][Ibu]	332.44
	Cholinium Ibuprofenate [N _{1112(OH)}][Ibu]	309.44

3.3.2 Nuclear Magnetic Resonance (NMR)

The prepared ibuprofen-based ILs were completely characterized by ^1H and ^{13}C NMR (Bruker Avance III 400) in order to determine their expected structures. The integration of the API-ILs characteristic ^1H NMR and ^{13}C NMR resonance peaks confirmed the expected cation/anion ratios. All characterizations are depicted in **Supporting Information**.

3.3.3 Differential Scanning Calorimetry (DSC)

The experiments were performed using a TA Instrument DSC Q200 Differential Scanning Calorimeter. Cooling was accomplished using a refrigerated cooling system capable of controlling the temperature down to $-90\text{ }^\circ\text{C}$. The sample was continuously purged with $50\text{ mL}\cdot\text{min}^{-1}$ nitrogen. Approximately 5 mg of sample was crimped in a standard aluminum hermetic sample pan. Indium ($T_m = 157.61\text{ }^\circ\text{C}$) was used as the standard compound for the calibration of the DSC. The samples were cooled to $-90\text{ }^\circ\text{C}$, tempered (30 min) and, finally, heated to $100\text{ }^\circ\text{C}$. The cooling–heating cycles were repeated three times at different rates (i.e., 10, 5 and $1\text{ }^\circ\text{C}/\text{min}$). The transition temperatures obtained from the second and subsequent cycles at the same rate were reproducible. The DSC curves of ibuprofen, $[\text{C}_2\text{C}_1\text{Im}][\text{Ibu}]$, $[\text{C}_2(\text{OH})\text{C}_1\text{Im}][\text{Ibu}]$ and $[\text{N}_{1112}(\text{OH})][\text{Ibu}]$ are presented in the **Supporting Information (Figures 3.S1–S4)**.

3.3.4 Solubility Studies

An excess of ibuprofen, ibuprofen sodium salt and ibuprofen-based ILs were added in 1.5 mL safe-lock microtubes with 1.5 mL of each solvent (Milli-Q water and buffer solutions suitable for dissolution testing, such as simulated intestinal fluid without enzymes (interchangeable with phosphate buffer at pH 6.8), simulated gastric fluid without enzymes (interchangeable with 0.1 N HCl at pH 1.0) and a 0.15 M NaCl isotonic ionic strength solution. The test samples were placed in an accuTherm (Labnet) microtube shaking incubator and kept under a controlled temperature of $25\text{ }^\circ\text{C}$ ($\pm 1\text{ }^\circ\text{C}$) while stirring up to 1000 rpm. A study of the amount of ibuprofen solubilized in the

solvents over time ensured that the equilibrium was achieved. Before sampling, each solution was centrifugated (VWR® Mega Star 600 R) at isothermal conditions to enhance the physical separation of the two phases. Concentrations were determined by UV-Vis spectroscopy using a VWR® spectrophotometer, model UV-6300PC, after appropriate dilution and interpolation from previously acquired calibration curves. All the solubilities experiments were repeated at least two times.

3.3.5 Cytotoxicity Assays

To screen the cytotoxicity of the ibuprofen-based ILs two different cell lines were chosen: human colon carcinoma cells, Caco-2, and the hepatocellular carcinoma cell line, HepG2. The Caco-2 cell line was grown in RPMI 1640 medium supplemented with 10% of inactivated fetal bovine serum (FBS) and 1% penicillin–streptomycin, and the HepG2 cells were cultured in MEM medium with 10% inactivated FBS, 2 mM glutamine, 1% MEM-NEAA and 1% sodium pyruvate. All media and supplements were supplied by Gibco from Thermo Fisher Scientific. Both cell lines were kept at 37 °C in a humidified incubator (Smart Biotherm S-Bt, bioSan) with 5% CO₂ and routinely grown in 175 cm² culture flasks. Caco-2 cells were seeded at a density of 2×10^5 cells per well in 96-well plates, and the experiments were performed using cells after reaching a 90% confluence, 96 h after seeding. The HepG2 cells were seeded at a density of 6×10^5 cells per well, and the experiments were performed at a confluence of 80%, 24 h after seeding. Each ibuprofen-based IL was tested in a concentration range above/in the maximum plasma concentration (C_{\max}) of ibuprofen: 0.175 mM [26]. Additionally, the half maximal effective concentration (EC_{50}) was determined for the Caco-2 cell line within concentrations ranging from 0.012 up to 4.8 mM for ibuprofen, 0.008 up to 7.5 mM for the API-ILs and 0.008 up to 320 mM for the ILs. All the stock solutions were homogenously prepared and diluted in 0.5% FBS culture media and added to a 96-well plate that was previously seeded. All cell lines were incubated for 24 h. Negative control cells were prepared containing culture medium with 0.25% (*v/v*) DMSO and the positive control cells only containing DMSO. To perform the cytotoxicity assay, an CyQUANT™ XTT Cell Viability test kit (Invitrogen, Waltham, MA, USA) was used. A preworking

solution was prepared using an electron coupling reagent and the XTT reagent ((2,3-bis-(2-methoxy-4-nitro-5-sulfophenyl)-2H-tetrazolium-5-carboxanilide) according to the manufacturer's instructions. After the incubation period, all samples were removed and 100 μ L of the working solution was added to each well and left to react for 4 h. The XTT reagent is sensitive to cellular redox potential; thus, actively respiring cells convert the water-soluble XTT compound into an orange-colored formazan product. The amount of formazan product that was soluble in the culture medium was proportional to the number of viable cells, and it was quantified spectrophotometrically at 450 nm in a Multiskan GO (ThermoFisher Scientific) microplate reader. Each sample was incubated in three different wells, and the obtained value was the average of three independent assays. Cell viability was determined by the ratio between the measured test compound-contacted cells and the measured absorbance of the control cells treated only with culture medium. Dose-independent viability curves were determined using the cell viability trends. Nonlinear regression analysis was used to determine the EC₅₀ values for ibuprofen, ibuprofen-based ILs and IL/salt cation "suppliers" (i.e., [C₂C₁Im]Cl, [C_{2(OH)}C₁Im]Cl and [N_{1112(OH)}]Cl).

3.3.6 Hemolytic Activity

The hemolytic activity was assessed according to the method optimized by Gaspar and coworkers [35]. Ethylene diamine tetraacetic acid (EDTA), preserved peripheral human blood obtained from voluntary donors, was used on the same day of all experiments. Briefly, the erythrocytes were centrifugated at 1000 \times g for 10 min to separate them from the serum and washed three times in a PBS solution. The ibuprofen-based ILs and sodium ibuprofen were prepared in PBS with a final concentration of 6 mM and ibuprofen, due to the fact of its low solubility, with a final concentration of 3 mM. The assay was performed in 96-well plates in which 100 μ L/well of sample were diluted with 100 μ L of the erythrocyte suspension. Moreover, the microplates were incubated at 37 $^{\circ}$ C for 1 h followed by a centrifugation at 800 \times g for 10 min. The supernatant absorbance was measured at 570 nm with a reference filter at 600 nm. The percentage of the hemolytic activity was calculated according to **Equation 3.1**:

$$\text{Hemolytic Activity (\%)} = \frac{\text{AbsS} - \text{AbsN}}{\text{AbsP} - \text{AbsN}} \times 100 \quad (\text{Equation 3.1})$$

where AbsS is the average absorbance of the sample; AbsN is the average absorbance of the negative control; AbsP is the average absorbance of the positive control. All the compounds were tested in triplicate.

3.3.7 Protein Albumin Denaturation Assay

The inhibition of protein denaturation by the three ibuprofen-based ILs was evaluated according to the method described by Mizushima and Kobayashi [36] with slight modifications, and it was implemented to assess the anti-inflammatory activity of the API-ILs. Briefly, a 2% bovine serum albumin (BSA) solution was prepared in PBS at pH 7.4. Ibuprofen and sodium ibuprofen were used as positive control drugs. A solution of only PBS and 2% BSA was used as the negative control. Solutions of each API-IL and control drugs were also prepared in PBS. The reaction mixture containing 0.5 mL of 2% BSA and 1.5 mL of each test compound was incubated at 37 °C for 15 min and cooled at room temperature. Denaturation was induced by maintaining the mixtures at 80 °C ± 1 °C in a dry bath for 15 min. The turbidity of the solutions represented the level of protein precipitation. Thus, in the manual centrifuge, all samples were centrifuged and then measured at 660 nm. Each sample concentration consisted of at least two independent replicates.

3.3.8 Cyclooxygenases (COX-1 and COX-2) Inhibition Assays

The anti-inflammatory activity was directly determined by measuring the inhibition of the COX enzymes using a colorimetric COX (COX-1, ovine; COX-2, human) inhibitor screening assay kit (Cayman Chemical Co., No. 701050, Ann Arbor, MI, USA). The assay was conducted according to the manufacturer's instructions. Briefly, a reaction mixture containing 150 µL of assay buffer, 10 µL of heme, 10 µL of enzyme (either COX-1 or COX-2) and 10 µL of ibuprofen or ibuprofen-based ILs at 3 mM were added to the plate. To evaluate the 100% initial activity, a solution of 150 µL of assay buffer, 10 µL of heme, 10 µL of enzyme (either COX-1 or COX-2) and 10 µL of a solution 50/50 H₂O and EtOH

was added to the plate. The nonenzymatic solution designated as background contained 160 μL of assay buffer, while 10 μL of heme and 10 μL of a solution of 50/50 H_2O and EtOH were also added to the plate. Cayman's COX colorimetric inhibitor screening assay measures the peroxidase component of COXs. The peroxidase activity was assayed colorimetrically by monitoring the appearance of oxidized N, N, N' and N'-tetramethylphenylenediamine (TMPD) at 590 nm [37]. Each plate was firstly incubated for 5 min at 25 $^\circ\text{C}$ and then 20 μL TMPD, and 20 μL of arachidonic acid was added to start the reaction. For a more accurate determination of the reaction rates, the samples were measured kinetically for precisely 2 min at 25 $^\circ\text{C}$. All samples were assayed in triplicate. The COX-1 and COX-2 percent inhibition was calculated using **Equation 3.2**:

$$\text{COX inhibition activity (\%)} = \frac{T}{C} \times 100 \quad (\text{Equation 3.2})$$

where C is absorbance of the 100% initial activity sample; T is the subtraction of each inhibitor sample from the 100% initial activity sample. The absorbances are the average of all samples, and one must subtract the absorbance of the background wells from the absorbances of the 100% initial activity and the inhibitor wells.

3.4 Results and Discussion

3.4.1 Characterization of the Ibuprofen-Based Ionic Liquids

The ^1H and ^{13}C NMR spectra were acquired for the API-ILs sodium ibuprofen and ibuprofen. The ibuprofen-based ILs presented the expected chemical shifts from the anion and the corresponding cation, meaning that the reactions were complete, and only one highly pure product was formed in each reaction. In agreement with the intended stoichiometry, a strict 1:1 proportion was always observed in the ^1H NMR spectra (see the **Supplementary Materials**). The hydroxyl group ($-\text{COOH}$) ^1H NMR chemical shift for the ibuprofen acid formed was detected at 12.15 ppm in DMSO and, as expected, no peak was observed in the ibuprofen-based ILs (the neutralization step in the two-step anion exchange reaction; see Section 3.4.1) and sodium ibuprofen ^1H NMR spectra in the same deuterated solvent. Additionally, there was a clear change in the chemical shifts

upfield for protons 2 and 3 of ibuprofen for the APIs' salt forms in DMSO (see **Table 3.2**), corroborating the cations and API-based anion interactions. The same trend was observed in D₂O, and it is depicted in **Table 3.S1** in the **Supplementary Materials**. The chemical shift deviations were more significant for the API-ILs, which is supported by the interionic hydrogen-bonded network in the ILs, verified by experimental measurements and computer simulations [38,39].

The melting temperatures (T_m) and glass transition temperatures (T_g) of ibuprofen-based ILs and ibuprofen determined by DSC are summarized in **Table 3.3**. Both [C₂C₁Im][Ibu] and [N_{1112(OH)}][Ibu] were solid ($T_m = 72.44$ °C and 70.89 °C, respectively), whereas [C_{2(OH)}C₁Im][Ibu] was liquid, at room temperature. The addition of a hydroxyl group connected to the aromatic imidazolium ring seemed to strongly decrease the melting temperature. The same was observed by Ferreira et al. with fluorinated ionic liquids based on an imidazolium cation, where it was inferred that both structural features (i.e., hydroxyl group and anion) highly influence the thermal properties of ILs [40]. Although the API-IL [C₂C₁Im][Ibu] was not liquid at room temperature or even at body temperature (a more relevant temperature for pharmaceutical applications; the T_m cut-off of API-ILs for use within the body should be approximately 37 °C), and the API-IL platform was not effective in reducing the melting point of the parent API in this IL (see **Table 3**), the DSC trace at a scan rate of 1 °C/min (see **Figure 3.S2** in the **Supporting Information**) indicated that [C₂C₁Im][Ibu] exhibited a cold crystallization temperature (26.98 °C) and, thus, depending on the cooling–heating cycles, this API-IL can easily be handled as a liquid at room temperature. This is advantageous for the development of new drug delivery systems such as the adsorption of API-ILs onto mesoporous silica-based materials for the controlled delivery of APIs [41] and incorporation of API-ILs into bacterial nanocellulose membranes for transdermal drug delivery systems [26].

Table 3.2. Chemical shifts for the hydrogens in positions 2 and 3 (as depicted in the chemical structure of ibuprofen on the bottom) for ibuprofen, sodium ibuprofen and API-ILs in DMSO.

Compounds	H2 (δ /ppm)	H3 (δ /ppm)
Ibuprofen	3.63	1.35
Na[Ibu]	3.21	1.22
[C ₂ C ₁ Im][Ibu]	3.15	1.19
[C _{2(OH)} C ₁ Im][Ibu]	3.18	1.19
[N _{1112(OH)}][Ibu]	3.18	1.20

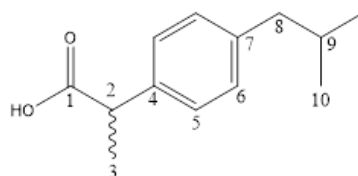


Table 3.3. Glass transition temperatures (T_g) and melting temperatures (T_m) of ibuprofen and ibuprofen-based ILs determined by DSC at a heating rate of 1 °C/min.

Compound	T_g (°C)	T_m (°C)
Ibuprofen	-43.57	74.89
[C ₂ C ₁ Im][Ibu]	-30.55	72.44
[C _{2(OH)} C ₁ Im][Ibu]	–	-13.97
[N _{1112(OH)}][Ibu]	–	70.89

3.4.2 Equilibrium Solubility in Water and Simulated Biological Fluids

A poor water solubility is a limiting factor in the efficacy and bioavailability of an API. The solubilities of the ibuprofen-based ILs, ibuprofen and ibuprofen sodium salt determined in the present work (see **Section 3.4.4**) are listed in **Table 3.4**. Ibuprofen, itself, by being an acid drug, has a low solubility in water (0.297 mM), a simulated gastric fluid solution at pH 1.0 (0.215 mM) and in the buffer, NaCl, a physiological solution mimicking the isotonic ionic strength in the bloodstream (0.353 mM). In the simulated intestinal fluid at pH 6.8, it had an increased solubility (20.21 mM) compared to the previous buffers and water.

Table 3.4. Solubility of ibuprofen, sodium ibuprofen and ibuprofen-based ILs in water and the solubility of ibuprofen, ibuprofen sodium and cholinium-based API-IL in buffer solutions suitable for dissolution testing, isotonic ionic strength aqueous solution (0.15 M NaCl), simulated gastric fluid (pH 1.0) and simulated intestinal fluid (pH 6.8). All experiments were performed at 25 °C ± 0.1 °C. The solubility was the overall mean of at least two independent experiments ± standard deviation.

Compound	Solubility (mM) at 25 °C			
	Water	0.15 M NaCl	pH 1.0	pH 6.8
Ibuprofen	0.2791 ± 0.0068 (0.3259 [23], 0.3394 [43])	0.3530 ± 0.0131	0.2146 ± 0.0053	20.21 ± 0.58
Sodium ibuprofen	1762 ± 52	1506 ± 30	1173 ± 57	1907 ± 11
[N ₁₁₁₂ (OH)][Ibu]	6783 ± 226	2519 ± 45	3159 ± 84	11,074 ± 438
[C ₂ C ₁ Im][Ibu]	7817 ± 160	-†	-†	-†
[C ₂ (OH)C ₁ Im][Ibu]	7426 ± 357	-†	-†	-†

† Not determined.

The replacement of an acidic proton in ibuprofen by sodium significantly increases the Lewis-based properties of sodium ibuprofen [42]. Through the enhancement of basic properties, ibuprofen sodium salt presented a higher solubility and within the same order of magnitude in water (1761.97 mM), 0.15 M NaCl solution (1505.67 mM), simulated gastric fluid (1172.85 mM) and simulated intestinal fluid (1906.65 mM) at 25 °C when compared to ibuprofen.

Due to the anion–cation interactions, the solubilities of the API-ILs were much higher than those found for ibuprofen in the neutral and salt forms. The solubility studies attained in this work are illustrated in **Figure 3.1**, and **Figure 3.1A** depicts the solubility of ibuprofen, sodium ibuprofen and all three ibuprofen-based ILs in water, while **Figure 3.1B** depicts the solubility of ibuprofen, sodium ibuprofen and cholinium-based API-IL in buffer solutions suitable for dissolution testing, *viz.*, simulated gastric fluid without enzymes (interchangeable with 0.1 N HCl pH 1.0), simulated intestinal fluid without enzymes (interchangeable with phosphate standard buffer pH 6.8) and a 0.15 M NaCl (isotonic ionic strength solution). The solubility of [N₁₁₁₂(OH)][Ibu], [C₂C₁Im][Ibu] and [C₂(OH)C₁Im][Ibu] in water at 25 °C were similar, and much higher (up to 28,000-fold) than ibuprofen, and higher (up to 4.4-fold) than the commercialized salt formulation, sodium ibuprofen. The same trend was observed by Viciosa et al., who demonstrated

that the richness of the possible interactions between imidazolium cations vs. ibuprofenate anions favor the interaction with water molecules, leading to a much more soluble material compared to the original molecular drug, which only interacts by hydrogen bonding. These authors reported the solubility in water and phosphate buffer at pH 7.54 for $[C_{2(OH)}C_1Im][Ibu]$ at 9845.39 and 9965.71 mM, respectively, in accordance with the values reported in this study [44]. Recently, Wu and coworkers also reported an increased water solubility of imidazolium-based ibuprofen ILs ($[C_4C_1Im][Ibu]$ and $[C_{2(OH)}C_1Im][Ibu]$) and correlated the higher solubility of the API-ILs to the higher permeability results and higher bioavailability [23].

Cholinium benefits many physiological functions due to the fact of its incorporation into neurotransmitters, signaling molecules and membrane components [12]. In addition to imidazolium-based ibuprofen IL, cholinium-based ibuprofen IL was also prepared and investigated in this work for their potential use in pharmaceutical applications due to the prevalence of cholinium in the human body. Additionally, cholinium salts, such as chloride ($[N_{1112(OH)}]Cl$ —the cation “supplier” for $[N_{1112(OH)}][Ibu]$ in the implemented two-step anion exchange synthetic procedure, see **Section 3.4.1**), are currently cost-efficient chemicals, produced on a scale of millions per year. Accordingly, cholinium-based API-ILs propound biocompatibility and economic advantages. Thus, the solubility of $[N_{1112(OH)}][Ibu]$ in simulated biological fluids at 25 °C were determined as well as for ibuprofen (parent API) and sodium ibuprofen (commercial salt form of the API). The results are depicted in **Table 3.4** and **Figure 3.1B**, clearly demonstrating the superiority of the API-ILs platform. Santos et al. determined the solubility for $[N_{1112(OH)}][Ibu]$ in water and 0.1 M phosphate-buffered solution at 37 °C, 8111.43 and 8085.57 mM, respectively [24], in agreement with the results presented herein.

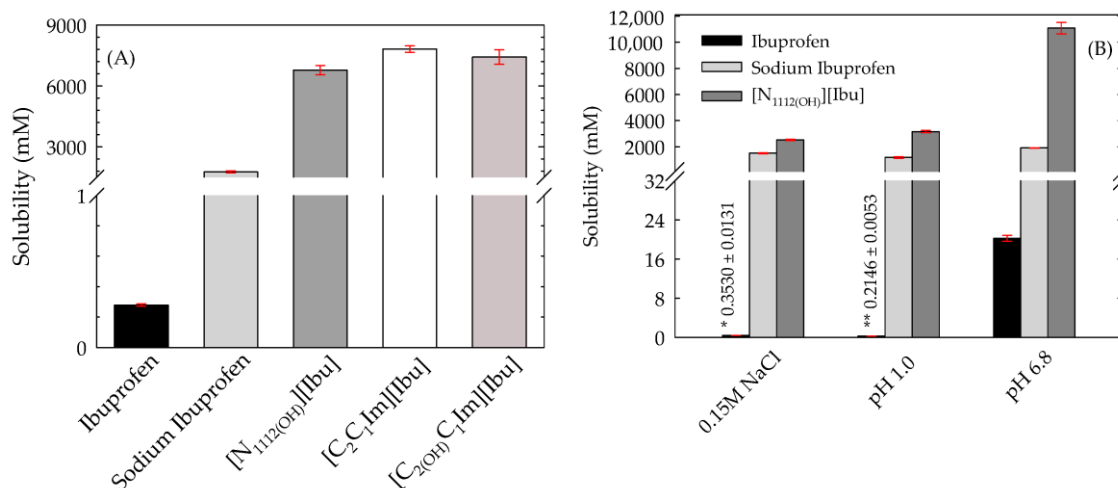


Figure 3.1. Solubility of ibuprofen, ibuprofen sodium salt and ibuprofen-based ILs in water (A). Solubility of ibuprofen, ibuprofen sodium salt and cholinium-based API-ILs in isotonic ionic strength aqueous solution (0.15 M NaCl), simulated gastric fluid (pH 1.0) and simulated intestinal fluid (pH 6.8) (B). All experiments were performed at 25 °C. * $p < 0.05$, ** $p < 0.01$.

The overall solubility results clearly demonstrate that the cholinium- and imidazolium-based API-ILs strategy was appropriate to twist the solubility in water and buffer solutions suitable for dissolution testing of the parent API and, consequently, enhanced the efficacy, bioavailability and potential membrane permeability. Solving the bioavailability problems of APIs is one of the critical challenges of the pharmaceutical industry, since nearly half of the new active substances being identified in high-throughput screening are either insoluble or poorly soluble in water [12].

3.4.3 Cytotoxicity Profile in Human Cell Lines

The cytotoxicity profiles of ibuprofen-based API-ILs as well as ibuprofen and sodium ibuprofen were accessed in the human colon carcinoma cell line, Caco-2, and the hepatocellular carcinoma cell line, HepG2. The studied concentrations were above/in the range of the pharmacokinetic parameter maximum plasma concentration of ibuprofen (C_{max} , 0.175 mM; the highest level of ibuprofen that can be obtained in the blood usually following multiple doses) [45], which is above the possible intracellular concentrations. The dose–response cytotoxicity curves are depicted in **Figure 3.2**. Comparing the viability curves of ibuprofen, sodium ibuprofen and ibuprofen-based ILs, no significant changes were verified, indicating that the use of a modular IL strategy based on the

cations $[N_{1112(OH)}]^+$, $[C_2C_1Im]^+$ and $[C_{2(OH)}C_1Im]^+$ produced no significant effect on the ibuprofen system cytotoxicity.

NSAIDs are mainly associated with gastrointestinal problems [21]. Thus, to evaluate the relative toxicity in the in gastrointestinal tract, the EC_{50} (i.e., effective concentration reducing cell viability to 50%) in the Caco-2 cell line was acquired and is depicted in **Table 3.5**. In **Figure 3.S5**, the nonlinear regression curves used to obtain the EC_{50} values are illustrated. In addition to API-ILs and parent API, the EC_{50} in the Caco-2 cell line was determined for IL/salt cation “suppliers” for the API-ILs (i.e., $[C_2C_1Im]Cl$, $[C_{2(OH)}C_1Im]Cl$ and $[N_{1112(OH)}]Cl$).

The EC_{50} values for ibuprofen and the three ibuprofen-based API-ILs were at the mM level (see **Table 3.5**). All four ibuprofen formulations (neutral and API-ILs) showed low toxicity against Caco-2 cells. $[C_2C_1Im][Ibu]$, $[C_{2(OH)}C_1Im][Ibu]$ and $[N_{1112(OH)}][Ibu]$ showed similar EC_{50} values, all slightly higher than ibuprofen (approximately 1.4-fold), implying a similar toxicity or safety profile with ibuprofen. The IL/salt cation “suppliers” for the API-ILs (i.e., $[C_2C_1Im]Cl$, $[C_{2(OH)}C_1Im]Cl$ and $[N_{1112(OH)}]Cl$) also showed low toxicity, lower than the ibuprofen-based counterparts, which is in agreement with previous literature that compared the cytotoxicity of ibuprofen API-ILs and the corresponding precursor halide salts in different cell lines [23,24,48]. The EC_{50} for the precursor halide salts followed the trend: $[N_{1112(OH)}]Cl > [C_{2(OH)}C_1Im]Cl > [C_2C_1Im]Cl$ (see **Table 3.5** and **Figure 3.S6**), supporting the higher biocompatibility of the cholinium cation as discuss above (see Section 3.5.2) and indicating that the incorporation of a hydroxyl group in the alkyl substituent of the imidazolium ring significantly decreases the toxicity of imidazolium-based ILs ($[C_2C_1Im]^+$ versus $[C_{2(OH)}C_1Im]^+$) [49]. The overall analysis of the in vitro cytotoxicity assays indicates the suitability and biocompatibility of the proposed cholinium- and imidazolium-based API-ILs for pharmaceutical formulations.

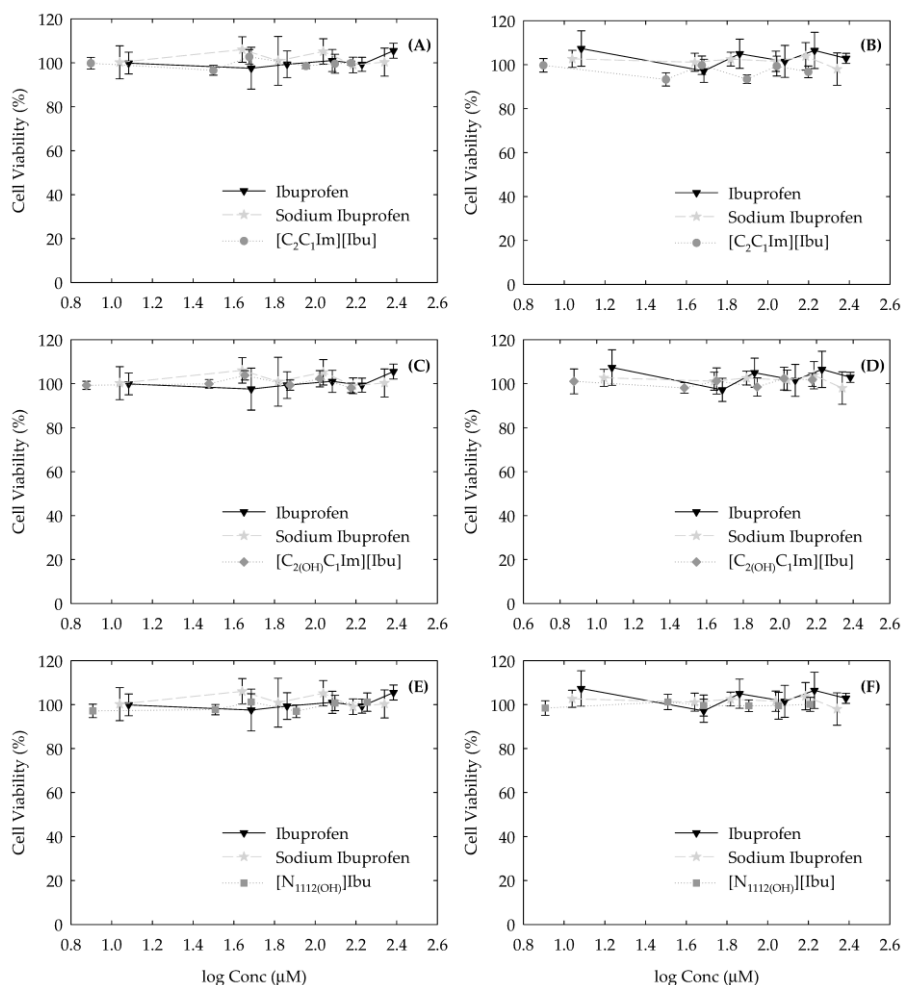


Figure 3.2. Cytotoxicity profiles of ibuprofen in the neutral and sodium salt forms compared with [C₂C₁Im][Ibu] in Caco-2 (A) and HepG2 (B) with [C₂(OH)C₁Im][Ibu] in Caco-2 (C) and HepG2 (D) and with [N₁₁₂(OH)][Ibu] in Caco-2 (E) and HepG2 (F). Both Caco-2 and HepG2 cells were exposed for 24 h to the respective API-ILs and parent API at the concentrations shown.

Table 3.5. EC₅₀ values of ibuprofen, ibuprofen-based ILs and IL/salt cation “suppliers” for the API-ILs (i.e., [C₂C₁Im]Cl, [C₂(OH)C₁Im]Cl and [N₁₁₂(OH)]Cl) in the Caco-2 cell line exposed to the compounds for 24 h. The R-squared was greater than 0.9540 and *p* < 0.0001 for all fitted curves.

Compound	EC ₅₀ (mM)
Ibuprofen	4.052 ± 0.010 (2.893 ± 0.059 [46])
[C ₂ C ₁ Im][Ibu]	5.683 ± 0.001
[C ₂ (OH)C ₁ Im][Ibu]	5.523 ± 0.001
[N ₁₁₂ (OH)][Ibu]	5.508 ± 0.001
[C ₂ C ₁ Im]Cl	70.66 ± 0.011 (32.10 ± 1.84 [47])
[C ₂ (OH)C ₁ Im]Cl	137.5 ± 0.001
[N ₁₁₂ (OH)]Cl	178.1 ± 0.001

3.4.4 Hemolytic Activity

Drug-induced immune hemolytic anemia is a serious condition that can be a rare side effect of commonly used over-the-counter medications such as NSAIDs [50,51]. Thus, an *in vitro* hemolysis study was performed prior to any pharmaceutical application to ensure that there was no serious potential pharmacologically mediated toxicity according to the guidelines of the European Medicines Agency (EMA) [52]. In this study, the red blood cell lysis through the hemoglobin release in the plasma was evaluated. Ibuprofen did not reveal hemolytic activity in the range of concentrations studied up to 1.5 mM. Additionally, ibuprofen sodium salt and ibuprofen-based ILs also displayed no hemolytic activity against human erythrocytes up to 3 mM. The studied concentration range for ibuprofen was limited to 1.5 mM due to the lower solubility in PBS (see **Section 3.4.6**). Still, the studied concentrations were above the C_{max} of ibuprofen (0.175 mM) [45], which was above the possible intracellular concentrations. The structure–activity correlation suggests that an aromatic ring with a side chain containing a carbonyl group attached to a nitrogen atom is a requirement for stabilizing the erythrocyte membrane [53]. Additionally, our group reported the hemolytic activity of several ionic liquids and demonstrated that imidazolium and cholinium-based ILs are considered hemocompatible with ~0% hemolytic activity up to 3 mM [54]. Hemolysis also represents the most employed initial toxicity assessment in drug development that could be correlated to cytotoxicity assays, since the main reason for toxicity can be related to the disruption of cell membranes [55]. The hemocompatibility results agree with the cytotoxicity evaluation. Ibuprofen and ibuprofen API-ILs showed low toxicity against Caco-2 cells, their EC_{50} were at the mM level (see **Table 3.5**), higher than 4.0 mM for ibuprofen and 5.5 mM for the API-ILs.

3.4.5 Protein Albumin Denaturation Assay

Protein denaturation has been correlated with the formation of inflammatory disorders, such as rheumatoid arthritis, diabetes and cancer, since proteins lose their biological activity. Therefore, the ability of a substance to prevent protein denaturation may also

help to prevent the inflammatory conditions [56]. Serum albumins are the most abundant proteins in plasma and are responsible for the movement of drugs through the blood stream. BSA is widely used as a model protein in many areas of research, because it holds similar properties to those of human serum albumin [57]. Herein, BSA was used to assess the ability of ibuprofen, ibuprofen sodium salt and ibuprofen-based ILs to prevent protein denaturation and, consequently, to evaluate their anti-inflammatory properties.

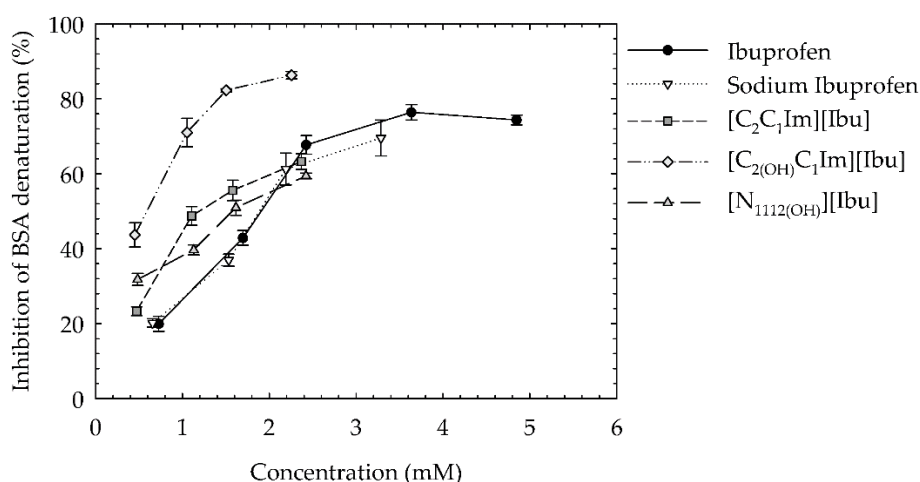


Figure 3.3. Inhibition profile of BSA denaturation by ibuprofen, ibuprofen sodium salt, [C₂C₁Im][Ibu], [C₂(OH)C₁Im][Ibu] and [N₁₁₂(OH)][Ibu].

Ibuprofen, ibuprofen sodium salt, [C₂C₁Im][Ibu] and [N₁₁₂(OH)][Ibu] exhibited similar profiles, without significant differences, while [C₂(OH)C₁Im][Ibu] presented an increased inhibition of BSA denaturation (see **Figure 3.3** and **Table 3.S2**). Cholinium cations can be considered as chaotropic agents [58,59] while imidazolium cations as kosmotropic agents [59,60]. A chaotropic agent can reduce the amount of order in the structure of a protein formed by water molecules, whereas a kosmotropic agent can cause water molecules to favorably interact which, in effect, stabilizes the intramolecular interactions in macromolecules such as proteins [61]. Additionally, Pace et al. [62] investigated the contribution of polar groups and their hydrogen bonds to the conformational stability of proteins and disclosed that hydrogen bonds by side chain hydroxyl groups make a favorable contribution to protein stability. The hydrogen bonding and other interactions of –OH groups in folded proteins can be sometimes more favorable than interactions with water in the unfolded protein. Consequently, the hydroxyl group presented in the

[C_{2(OH)}C_{1Im}][Ibu] API-ILs (see **Table 3.1**) contributed to stabilizing the BSA, preventing its denaturation in the tested conditions.

3.4.6 Cyclooxygenases (COX-1 and COX-2) Inhibition Assay

Cyclooxygenase (COX, also called prostaglandin H synthase (PGHS)) is a bifunctional enzyme exhibiting both COX and peroxidase activities. The COX component converts arachidonic acid to a hydroperoxyl endoperoxide (PGG₂), and the peroxidase component reduced the endoperoxide to the corresponding alcohol (PGH₂), the precursor of PGs, prostacyclins and thromboxanes [63,64]. Currently, it is well established that there are two distinct isoforms of COX. COX-1 is constitutively expressed in a variety of cell types and is involved in normal cellular homeostasis. The expression of a second isoform of COX, COX-2, is induced by a variety of mitogenic stimuli such as phorbol esters, lipopolysaccharides, and cytokines. COX-2 is responsible for the biosynthesis of PGs under acute inflammatory conditions [65]. All NSAIDs are essentially COX-2 inhibitors with differing degrees of COX-1 inhibition as a side effect. NSAIDs act by inhibiting these enzymes, which are involved in prostaglandin synthesis, resulting in their antipyretic, analgesic and anti-inflammatory effects. Drugs that inhibit COX-1 and COX-2 with comparable potency (non-selective NSAIDs, e.g., ibuprofen and ketoprofen) will not spare COX-1 activity after dosing, while drugs with intermediate COX-2 selectivity (e.g., diclofenac and nimesulide) or highly selective COX-2 inhibitors (e.g., rofecoxib and etoricoxib) have greater potential for sparing COX-1 activity [66]. In the gastrointestinal (GI) track, kidneys, and platelets, COX-1 is a commonly present enzyme responsible for the synthesis of prostaglandins, mainly in the GI mucosa and platelets. The produced prostaglandins help to maintain the GI mucosal integrity and renal blood flow as well as platelet activation. Symptomatic ulcers and ulcer complications associated with the use of nonselective NSAIDs is a very common side effect and may occur in approximately 1% of patients treated for three to six months and in 2–4% of patients treated for one year. Additionally, platelet function may also be impaired because of NSAIDs' inhibitory effect on thromboxane, a potent aggregating agent, resulting in bleeding [67]. Otherwise, COX-2 is primarily found at sites of

inflammation. Additionally, the use of selective COX-2 inhibitors, as demonstrated by Simon and coworkers in long-term rheumatoid arthritis patients [68], allowed a significant reduction in pre-existing conditions, such as perforation and hemorrhages in the GI, alongside anti-inflammatory and analgesic activity. Accordingly, it is advantageous to develop selective COX-2 NSAIDs with minimal COX-1 inhibition after dosing, allowing pain relief and inflammation reduction without no disruption of platelet and a lower risk for GI toxicity. Ibuprofen (nonselective NSAIDs) that inhibit COX-1 and COX-2 with comparable potency, which is observed in the relative COX-1/COX-2 selectivity [69], will not spare COX-1 activity after dosing, with all the unwanted side effects [70,71].

Ibuprofen-based ILs, as well as ibuprofen, were evaluated for their ability to inhibit cyclooxygenases (COX-1, ovine; COX-2, human) using a COX colorimetric inhibitor assay kit (see Section 3.4.8), providing direct insight into their anti-inflammatory properties. The results obtained are depicted in **Figure 3.4** and **Table 3.6**.

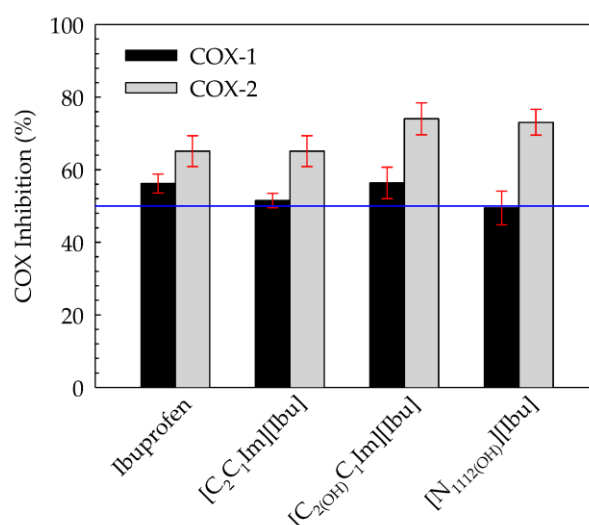


Figure 3.4. Selective inhibition of COX-1 and COX-2 enzymes for ibuprofen and ibuprofen-based ILs at 3 mM. The YY axis guideline corresponds to 50% COX inhibition.

It was found that under the same experimental conditions, the ibuprofen-based ILs maintained/upgraded the anti-inflammatory activity of ibuprofen (% COX inhibition). The COX-1/COX-2 selectivity followed the order: ibuprofen > [C₂C₁Im][Ibu] > [C₂(OH)C₁Im][Ibu] > [N₁₁₂(OH)][Ibu]. Lower COX-1/COX-2 selectivity values indicate a

greater selectivity for COX-2, and higher values indicate greater selectivity for COX-1. This trend shows that ibuprofen-based API-ILs improve the selectivity towards COX-2. These results clearly demonstrate the potential of the API-ILs platform in the development of safer NSAIDs with improved gastric and renal safety profiles and the recognition of new avenues for selective COX-2 inhibitors in cancer chemotherapy and neurological diseases such as Alzheimer's and Parkinson's.

Table 3.6. Inhibition of COX-1 (ovine) and COX-2 (human) and COX-1/COX-2 selectivity for 3 mM ibuprofen and ibuprofen-based ILs.

Compound	Inhibition of COX-1 (Ovine) (%)	Inhibition of COX-2 (Human) (%)	COX-1/COX-2 Selectivity
Ibuprofen	56.18 ± 2.60	65.13 ± 4.25	0.863 ± 0.069
[C ₂ C ₁ Im][Ibu]	51.50 ± 1.98	65.13 ± 4.27	0.791 ± 0.060
[C _{2(OH)} C ₁ Im][Ibu]	56.35 ± 4.35	74.04 ± 4.42	0.761 ± 0.074
[N _{1112(OH)}][Ibu]	49.48 ± 4.64	73.07 ± 3.55	0.677 ± 0.071

3.5 Conclusions

In the present work, we reported on the synthesis of three NSAID-based ionic liquids, conjugating the ibuprofenate anion (derived from ibuprofen, one of the most commonly available over-the-counter NSAIDs) with imidazolium cations (i.e., [C₂C₁Im][Ibu] and [C_{2(OH)}C₁Im][Ibu]) and a cholinium cation (i.e., [N_{1112(OH)}][Ibu]). An upgrade to the aqueous solubility (i.e., water and biological simulated fluids) for the ibuprofen-based ILs relative to the ibuprofen neutral and commercial ibuprofen salt form (i.e., sodium ibuprofen) was verified. Cytotoxicity tests on human cell lines and hemocompatibility assays substantiated the biocompatibility of the ibuprofen-based ILs, viz., ibuprofen-based ILs, sodium ibuprofen and ibuprofen, which displayed similar cytotoxic responses and all forms were hemocompatible, which boosts opportunities for creating advances in pharmaceutical challenges. The pharmacological action of the prepared API-ILs were tested to validate if a potential synergetic effect between the ion pairs existed, consequently conducting novel therapeutic advantages. Accordingly, the anti-inflammatory properties of the ibuprofen-based ILs were assessed through the inhibition of BSA denaturation and inhibition of cyclooxygenases (i.e., COX-1 and COX-

2), showing that all prepared API-ILs, [C₂C₁Im][Ibu], [C_{2(OH)}C₁Im][Ibu] and [N_{1112(OH)}][Ibu], maintained the anti-inflammatory response of ibuprofen with improved selectivity towards COX-2, allowing for the development of safer NSAIDs and the recognition of new avenues for selective COX-2 inhibitors in cancer chemotherapy and neurological diseases such as Alzheimer's and Parkinson's. The development of API-ILs represents a paradigm that poses diverse opportunities to drug development and delivery, which may play a relevant role in the future of healthcare, taking ILs from the benchtop to the bedside.

Funding

This research was funded by FCT/MCTES (Portugal), through grants PD/BD/135078/2017 and COVID/BD/151824/2021 (J.C.B.), the Individual Call to Scientific Employment Stimulus 2020.00835.CEECIND (J.M.M.A.) and 2021.01432.CEECIND (A.B.P.), and the project PTDC/EQU-EQU/2223/2021. This work was also supported by the Associate Laboratory for Green Chemistry—LAQV which was financed by national funds from FCT/MCTES (UIDB/50006/2020 and UIDP/50006/2020).

Conflicts of Interest

The authors declare no conflict of interest.

3.6 References

1. Egorova, K.S.; Gordeev, E.G.; Ananikov, V.P. Biological Activity of Ionic Liquids and Their Application in Pharmaceuticals and Medicine. *Chem. Rev.* **2017**, *117*, 7132–7189.
2. Maurya, P.; Tiwari, R.; Tiwari, G.; Yadav, P.; Shukla, Pharmaceutical polymorphism: The phenomenon affecting the performance of drug and an approach to enhance drug solubility, stability and bioavailability. *P. World J. Pharm. Sci.* **2016**, *4*, 411–419.
3. Huang, W.; Wu, X.; Qi, J.; Zhu, Q.; Wu, W.; Lu, Y.; Chen, Z. Ionic liquids: Green and tailor-made solvents in drug delivery. *Drug Discov. Today.* **2020**, *5*, 901–908.
4. Pedro, S.N.; R Freire, C.S.; Silvestre, A.; Freire, M.G. The Role of Ionic Liquids in the Pharmaceutical Field: An Overview of Relevant Applications. *Int. J. Mol. Sci.* **2020**, *21*, 8298.

5. MacFarlane, D.R.; Seddon, K.R. Ionic Liquids—Progress on the Fundamental Issues. *Aust. J. Chem.* **2007**, *60*, 3–5.
6. Ferraz, R.; Branco, L.C.; Marrucho, I.M.; Araújo, J.M.M.; Rebelo, L.P.N.; da Ponte, M.N.; Prudêncio, C.; Noronha, J.P.; Petrovski, Z. Development of novel ionic liquids based on ampicillin. *Med. Chem. Commun.* **2012**, *3*, 494–497.
7. Vieira, N.S.M.; Stolte, S.; Araújo, J.M.M.; Rebelo, L.P.N.; Pereiro, A.B.; Markiewicz, M. Acute Aquatic Toxicity and Biodegradability of Fluorinated Ionic Liquids. *ACS Sustain. Chem. Eng.* **2019**, *7*, 3733–3741.
8. Vieira, N.S.M.; Bastos, J.C.; Rebelo, L.P.N.; Matias, A.; Araújo, J.M.M.; Pereiro, A.B. Human cytotoxicity and octanol/water partition coefficients of fluorinated ionic liquids. *Chemosphere* **2019**, *216*, 576–586.
9. Vieira, N.S.; Castro, P.J.; Marques, D.F.; Araújo, J.M.M.; Pereiro, A.B. Tailor-Made Fluorinated Ionic Liquids for Protein Delivery. *Nanomaterials*. **2020**, *10*, 1594–1610.
10. Zhuang, W.; Hachem, K.; Bokov, D.; Ansari, M.J.; Nakhjiri, A.T. Ionic liquids in pharmaceutical industry: A systematic review on applications and future perspectives. *J. Mol. Liq.* **2022**, *349*, 118145.
11. Balk, A.; Widmer, T.; Wiest, J.; Bruhn, H.; Rybak, J.C.; Matthes, P.; Müller-Buschbaum, K.; Sakalis, A.; Lühmann, T.; Berghausen, J.; et al. Ionic liquid versus prodrug strategy to address formulation challenges. *Pharm. Research*. **2015**, *32*, 2154–2167
12. Araújo, J.M.M.; Florindo, C.; Pereiro, A.B.; Vieira, N.S.M.; Matias, A.A.; Duarte, C.M.M.; Rebelo, P.N.; Marrucho, I.M. Cholinium-based ionic liquids with pharmaceutically active anions. *RSC Adv.* **2014**, *4*, 28126–28132.
13. Fernández-Stefanuto, V.; Esteiro, P.; Santiago, R.; Moreno, D.; Palomar, J.; Tojo, E. Design and synthesis of alverine-based ionic liquids to improve drug water solubility. *New J. Chem.*, **2020**, *44*, 20428–20433.
14. Florindo, C.; Araújo, J.M.M.; Alves, F.; Matos, C.; Ferraz, R.; Prudêncio, C.; Marrucho, I.M. Evaluation of solubility and partition properties of ampicillin-based ionic liquids. *Int. J. Pharm.* **2013**, *456*, 553–559.
15. Zhao, H.; Holmes, S.S.; Baker, G.A.; Challa, S.; Bose, H.S.; Song, Z. Ionic derivatives of betulinic acid as novel HIV-1 protease inhibitors. *J. Enzyme Inhib. Med. Chem.* **2012**, *27*, 715–721.
16. Demurtas, M.; Onnis, V.; Zucca, P.; Rescigno, A.; Lachowicz, J.I.; Engelbrecht, L.D.V.; Nieddu, M.; Ennas, G.; Scano, A.; Mocci, F.; et al. Cholinium-Based Ionic Liquids from Hydroxycinnamic Acids as New Promising Bioactive Agents: A Combined Experimental and Theoretical Investigation. *ACS Sustain. Chem. Eng.* **2021**, *9*, 2975–2986.
17. Wongrakpanich, S.; Wongrakpanich, A.; Melhado, K. A Comprehensive Review of Non-Steroidal Anti- Inflammatory Drug Use in The Elderly. *Aging Dis.* **2018**, *9*, 143–150.
18. Bessone, F. Non-Steroidal Anti-inflammatory Drugs: What Is the Actual Risk of Liver Damage? *World J. Gastroenterol.* **2010**, *16*, 5651–5661.

19. Lipinski, C. A. Poor Aqueous Solubility—An Industry Wide Problem in ADME Screening. *Am. Pharm. Rev.* **2002**, *5*, 82–85.
20. Stolberg, V.B. *Painkillers: History, Science, and Issues*, 1st ed.; ABC-CLIO, Ed.; Greenwood: Santa Barbara, CA, USA, 2016.
21. Sostres, C.; Gargallo, C. J.; Arroyo, M.T.; Lanas, A. Adverse Effects of Non-Steroidal Anti-Inflammatory Drugs (NSAIDs, Aspirin and Coxibs) on Upper Gastrointestinal Tract. *Best Pract. Res. Clin. Gastroenterol.* **2010**, *24*, 121–132.
22. Zarghi, A.; Arfaei, S. Selective COX-2 Inhibitors: A Review of Their Structure-Activity Relationships. *Iran J Pharm Res.* **2011**, *10*, 655–683.
23. Wu, H.; Deng, Z.; Zhou, B.; Qi, M.; Hong, M.; Ren, G. Improved transdermal permeability of ibuprofen by ionic liquid technology: Correlation between counterion structure and the physicochemical and biological properties. *J. Mol. Liq.* **2019**, *283*, 399–409.
24. Santos, M.M.; Raposo, L.R.; Carrera, G.V.S.M.; Costa, A.; Dionísio, M.; Baptista, P.V.; Fernandes, A.R.; Branco, L.C. Ionic Liquids and Salts from Ibuprofen as Promising Innovative Formulations of an Old Drug. *Chem. Med. Chem.* **2019**, *14*, 907–911.
25. Stockerm, M.W.; Healy, A.M.; Ferguson, S. Spray Encapsulation as a Formulation Strategy for Drug-Based Room Temperature Ionic Liquids: Exploiting Drug–Polymer Immiscibility to Enable Processing for Solid Dosage Forms. *Mol. Pharm.* **2020**, *17*, 3412–3424.
26. Chantereau, G.; Sharma, M.; Abednejad, A.; Neves, B.M.; Se, G.; Freire, M.G.; Freire, C.S.R.; Silvestre, A.J.D. Design of Nonsteroidal Anti-Inflammatory Drug-Based Ionic Liquids with Improved Water Solubility and Drug Delivery. *ACS Sustain. Chem. Eng.* **2019**, *7*, 14126–14134.
27. Moshikur, R.M.; Chowdhury, M.R.; Wakabayashi, R.; Tahara, Y.; Kamiya, N.; Moniruzzaman, M.; Goto, M. Ionic liquids with N-methyl-2-pyrrolidonium cation as an enhancer for topical drug delivery: Synthesis, characterization, and skin-penetration evaluation. *J. Mol. Liq.* **2020**, *299*, 167–7322.
28. Abednejad, A.; Ghaee, A.; Morais, E.S.; Sharma, M.; Neves, B.M.; Freire, M.G.; Nourmohammadi, J.; Mehrizi, A.A. Polyvinylidene fluoride–Hyaluronic acid wound dressing comprised of ionic liquids for controlled drug delivery and dual therapeutic behavior. *Acta Biomater.* **2019**, *100*, 142–157.
29. Panić, J.J.; Tot, A.; Drid, P.; Gadžurić, S.; Vraneš, M. Design and analysis of interactions in ionic liquids based on procaine and pharmaceutically active anions. *Eur. J. Pharm. Sci.* **2021**, *166*, 105966.
30. Wang, C.; Chopade, S.A.; Guo, Y.; Early, J.T.; Tang, B.; Wang, E.; Hillmyer, M.A.; Lodge, T.P.; Sun, C.C. Preparation, Characterization, and Formulation Development of Drug–Drug Protic Ionic Liquids of Diphenhydramine with Ibuprofen and Naproxen. *Mol. Pharm.* **2018**, *15*, 4190–4201.
31. Frizzo, C.P.; Wust, K.; Tier, A.Z.; Beck, T.S.; Rodrigues, L.V.; Vaucher, R.A.; Bolzan, L.P.; Terra, S.; Soares, F.; Martins, M.A.P. Novel ibuprofenate-and docusate-based ionic liquids: Emergence of antimicrobial activity. *RSC Adv.* **2016**, *6*, 100476–100486.

32. Wust, K.M.; Beck, T.S.; Burrow, R.A.; Oliveira, S.M.; Brum, E.S.; Brusco, I.; Machado, G.; Bianchi, O.; Villetti, M.A.; Frizzo, C.P. Physicochemical characterization, released profile, and antinociceptive activity of diphenhydraminium ibuprofenate supported on mesoporous silica. *Mater. Sci. Eng. C.* **2020**, *108*, 110194.
33. Janus, E.; Ossowicz, P.; Klebeko, J.; Nowak, A.; Duchnik, W.; Kucharski, Ł.; Klimowicz, A. Enhancement of ibuprofen solubility and skin permeation by conjugation with l-valine alkyl esters. *RSC Adv.* **2020**, *10*, 7570–7584.
34. Ossowicz-Rupniewska, P.; Klebeko, J.; Świątek, E.; Biliska, K.; Nowak, A.; Duchnik, W.; Kucharski, Ł.; Struk, Ł.; Wenelska, K.; Klimowicz, A.; et al. Influence of the Type of Amino Acid on the Permeability and Properties of Ibuprofenates of Isopropyl Amino Acid Esters. *Int. J. Mol. Sci.* **2022**, *23*, 4158.
35. Gaspar, M.M.; Calado, S.; Pereira, J.; Ferronha, H.; Correia, I.; Castro, H.; Tomás, A.M.; Cruz, M.E.M. Targeted delivery of paromomycin in murine infectious diseases through association to nano lipid systems. *Nanomedicine* **2015**, *11*, 1851–1860.
36. Mizushima, Y.; Kobayashi, M. Interaction of anti-inflammatory drugs with serum proteins, especially with some biologically active proteins. *J. Pharm. Pharmacol.*, **1968**, *20*, 169–173.
37. Kulmacz, R.J.; Lands, W.E.M. Requirements for Hydroperoxide by the Cyclooxygenase and Peroxidase Activities of Prostaglandin H Synthase. *Prostaglandins.* **1983**, *25*, 531–540.
38. Araújo, J.M.M.; Ferreira, R.; Marrucho, I.M.; Rebelo, L.P.N. Solvation of Nucleobases in 1,3-Dialkylimidazolium Acetate Ionic Liquids: NMR Spectroscopy Insights into the Dissolution Mechanism. *Phys. Chem. B.* **2011**, *115*, 10739–10749.
39. Araújo, J.M.M.; Pereiro, A.B.; Lopes, J.N.C.; Rebelo, L.P.N.; Marrucho, I.M. Hydrogen-Bonding and the Dissolution Mechanism of Uracil in an Acetate Ionic Liquid: New Insights from NMR Spectroscopy and Quantum Chemical Calculations. *J. Phys. Chem. B.* **2013**, *117*, 4109–4120.
40. Ferreira, M.L.; Araújo, J.M.M.; Vega, L.F.; Llovel, F.; Pereiro, A.B. Functionalization of fluorinated ionic liquids: A combined experimental-theoretical study. *J. Mol. Liq.*, **2020**, *302*, 112489.
41. Bica, K.; Rodríguez, H.; Gurau, G.; Cojocar, O.A.; Riisager, A.; Fehrmann, R.; Rogers, R.D. Pharmaceutically active ionic liquids with solids handling, enhanced thermal stability, and fast release. *Chem. Commun.* **2012**, *48*, 5422–5424
42. Bustamante, P.; Pena, M.A.; Barra, J. The modified extended Hansen method to determine partial solubility parameters of drugs containing a single hydrogen bonding group and their sodium derivatives: Benzoic acid/Na and ibuprofen/Na. *Int. J. Pharm.* **2000**, *194*, 117–124.
43. Lu, C.; Cao, J.; Wanga, N.; Su, E. Significantly improving the solubility of non-steroidal anti-inflammatory drugs in deep eutectic solvents for potential non-aqueous liquid administration. *Med. Chem. Commun.* **2016**, *7*, 955–959.

44. Viciosa, M.T.; Santos, G.; Costa, A.; Danède, F.; Branco, L.C.; Jordão, N.; Correia, N.T.; Dionísio, M. Dipolar motions and ionic conduction in an ibuprofen derived ionic liquid. *Phys. Chem. Chem. Phys.* **2015**, *17*, 24108–24120.
45. Dewland, P.M.; Reader, S.; Berry, P. Bioavailability of ibuprofen following oral administration of standard ibuprofen, sodium ibuprofen or ibuprofen acid incorporating poloxamer in healthy volunteers. *BMC Clin. Pharmacol.* **2009**, *9*, 1–10.
46. Pereira, C.V.; Silva, J.M.; Rodrigues, L.; Reis, R.L.; Paiva, A.; Duarte, A.R.C.; Matias, A. Unveil the anticancer potential of limonene based therapeutic deep eutectic solvents. *Scientific reports.* **2019**, *9*, 1–11.
47. Egorova, K.S.; Seitkalieva, M.M.; Posvyatenkob, A.V.; Ananikov, V.P. An unexpected increase of toxicity of amino acid-containing ionic liquids. *Toxicol. Res.* **2015**, *4*, 152–159
48. Dobler, D.; Schmidts, T.; Klingenhöfer, I.; Runkel, F. Ionic liquids as ingredients in topical drug delivery systems. *Int. J. Pharm.* **2013**, *441*, 620–627.
49. Hernández-Fernández, F.J.; Bayo, J.; Pérez de los Ríos, A.; Vicente, M.A.; Bernal, F.J.; Quesada-Medina, J. Discovering Less Toxic Ionic Liquids by Using the Microtox® Toxicity Test. *Ecotoxicol. Environ. Saf.* **2015**, *116*, 29–33.
50. Iyinagoro, C.; Nwankwo, N.; Ali, A.M.; Saba, R.; Kwatra, S.G.; Hussain, N.; Uzoka, C.C.; Prueksaritanond, S.; Mirrakhimov, A.E. Ibuprofen-induced hemolytic anemia. *Case Rep. Hematol.* **2013**, *2013*.
51. Garratty, G. Immune hemolytic anemia associated with drug therapy. *Blood Rev.* **2010**, *24*, 143–150.
52. European Medicines Agency. *Guideline on Strategies to Identify and Mitigate Risks for First-in-Human and Early Clinical Trials with Investigational Medicinal Products*. EMEA/CHMP/SWP/28367/07 Rev. 1; Committee for Medicinal Products for Human Use (CHMP): Amsterdam, The Netherlands, 2017.
53. Orhan, H.; Sahi'n, G. In vitro effects of NSAIDs and paracetamol on oxidative stress-related parameters of human erythrocytes. *Exp. Toxic. Pathol.* **2001**; *53*, 133–140.
54. Vieira, N.S.; Oliveira, A.L.; Araújo, J.M.M.; Gaspar, M.M.; Pereiro, A.B. Ecotoxicity and Hemolytic Activity of Fluorinated Ionic Liquids. *Sustain. Chem.* **2021**, *2*, 115–126.
55. Greco, I.; Molchanova, N.; Holmedal, E.; Jenssen, H.; Hummel, B.D.; Watts, J. L.; Håkansson, J.; Hansen, P.R.; Svenson, J. Correlation between hemolytic activity, cytotoxicity and systemic in vivo toxicity of synthetic antimicrobial peptides. *Sci. Rep.* **2020**, *10*, 1–13.
56. Sangeetha, G.; Vidhya, R. In vitro anti-inflammatory activity of different parts of *Petalium murex* (L.). *Inflammation*, **2016**, *4*, 31–36.
57. Douadi, K.; Chafaa, S.; Douadi, T.; Al-Noaimi, M.; Kaabi, I. Azoimine quinoline derivatives: Synthesis, classical and electrochemical evaluation of antioxidant, anti-inflammatory, antimicrobial activities and the DNA/BSA binding. *J. Mol. Struct.* **2020**, *1217*, 128305.

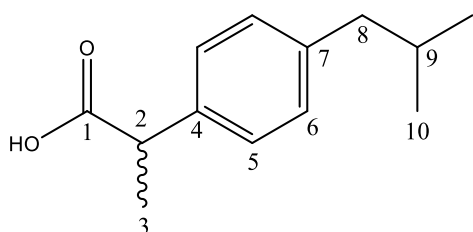
58. Kumar, A.; Rani, A.; Venkatesu, P. A comparative study of the effects of the Hofmeister series anions of the ionic salts and ionic liquids on the stability of α -chymotrypsin. *New J. Chem.* **2015**, *39*, 938–952.
59. Bisht, M.; Venkatesu, P. Influence of cholinium-based ionic liquids on the structural stability and activity of α -chymotrypsin. *New J. Chem.* **2017**, *41*, 13902.
60. Lange, C.; Patil, G.; Rudolph, R. Ionic liquids as refolding additives: N'-alkyl and N'-(ω -hydroxyalkyl) N-methylimidazolium chlorides. *Protein Sci.* **2005**, *14*, 2693–2701.
61. Moelbert, S.; Normand, B.; De Los Rios, P. Kosmotropes and chaotropes: Modelling preferential exclusion, binding and aggregate stability. *Biophys. Chem.* **2004**, *112*, 45–57.
62. Pace, C.N.; Fu, H.; Fryar, K.L.; Landua, J.; Trevino, S.R.; Schell, D.; Thurlkill, R.L.; Imura, S.; Scholtz, J.M.; Gajiwala, K.; et al. Contribution of hydrogen bonds to protein stability. *Protein Sci.* **2014**, *23*, 652–661.
63. Nugteren, D.H.; Hazelhof, E. Isolation and properties of intermediates in prostaglandin biosynthesis. *Biochim. Biophys. Acta, Lipids Lipid Metab.* **1973**, *326*, 448–461.
64. Hamberg, M.; Samuelsson, B. Detection and isolation of an endoperoxide intermediate in prostaglandin biosynthesis. *Proc. Natl. Acad. Sci. USA* **1973**, *70*, 899–903.
65. Xie, W.L.; Chipman, J.G.; Robertson, D.L.; Erikson, R.L.; Simmons, D.L. Expression of a mitogen-responsive gene encoding prostaglandin synthase is regulated by mRNA splicing. *Proc. Natl. Acad. Sci. USA* **1991**, *88*, 2692–6.
66. Patrignani, P.; Tacconelli, S.; Bruno, A.; Sostres, C.; Lanas, A. Managing the adverse effects of nonsteroidal anti-inflammatory drugs. *Expert. Rev. Clin. Pharmacol.* **2011**, *4*, 605–621.
67. Hutchison, R. COX-2-selective NSAIDs. *Am. J. Nurs. Sci.* **2004**, *10*, 52–56.
68. Simon, L.S.; Weaver, A.L.; Graham, D.Y.; Kivitz, A.J.; Lipsky, P.E.; Hubbard, R.C.; Isakson, P.C.; Verburg, K.M.; Yu, S.S.; Zhao, W.W.; et al. Anti-inflammatory and Upper Gastrointestinal Effects of Celecoxib in Rheumatoid Arthritis: A Randomized Controlled Trial. *JAMA.* **1999**, *282*, 1921–1928.
69. Brune, K.; Patrignani, P. New insights into the use of currently available non-steroidal anti-inflammatory drugs. *J. Pain Res.* **2015**, *8*, 105–118.
70. Bruno, A.; Tacconelli, S.; Patrignani, P. Variability in the response to non-steroidal anti-inflammatory drugs: Mechanisms and perspectives. *BCPT* **2014**, *114*, 56–63.
71. Mazaleuskaya, L.L.; Theken, K.N.; Gong, L.; Thorn, C.F.; FitzGerald, G.A.; Altman, R.B.; Klein, T.E. PharmGKB summary: Ibuprofen pathways. *Pharm. Genom.* **2015**, *25*, 96.

3.7 Supporting Information

Characterization of the Ibuprofen-based Ionic Liquids

The prepared ibuprofen-based ionic liquids, ibuprofen and ibuprofen sodium salt were completely characterized by ^1H and ^{13}C NMR in order to check their expected structures. Additionally, the quantitative integration of their characteristic ^1H NMR resonance peaks unfold the expected cation/anion correlations. Also, there were no peaks assigned to impurities in the ^1H NMR spectra.

Ibuprofen

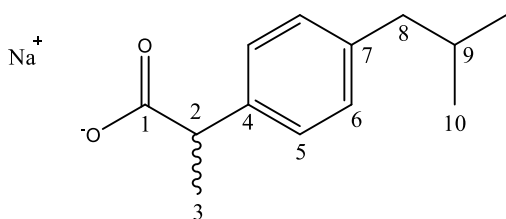


^1H NMR (400 MHz, D_2O): $\delta/\text{ppm} = 7.20$ (d, $J = 8.0$ Hz, 2H, 6), 7.15 (d, $J = 8.3$ Hz, 2H, 5), 3.58 (m, 1H, 2), 2.40 (d, $J = 7.1$ Hz, 2H, 8), 1.75 (dd, $J = 13.5, 6.6$ Hz, 1H, 9), 1.33 (d, $J = 7.2$ Hz, 3H, 3), 0.79 (d, $J = 6.6$ Hz, 6H, 10).

^1H NMR (400 MHz, DMSO): $\delta/\text{ppm} = \delta 12.25$ (s, 1H, OH), 7.19 (d, $J = 7.9$ Hz, 2H, 6), 7.11 (d, $J = 7.9$ Hz, 2H, 5), 3.63 (q, $J = 7.1$ Hz, 1H, 2), 2.42 (d, $J = 7.1$ Hz, 2H, 8), 1.81 (dp, $J = 13.5, 6.9$ Hz, 1H, 9), 1.35 (d, $J = 7.1$ Hz, 3H, 3), 0.86 (d, $J = 6.6$ Hz, 6H, 10). ^{13}C NMR (101 MHz, DMSO): $\delta/\text{ppm} = 175.95$ (s, 1), 140.02 (s, 7), 138.94 (s, 4), 129.43 (s, 6), 127.57 (s, 5), 44.74 (s, 8), 44.68 (s, 2), 30.03 (d, $J = 8.9$ Hz, 9), 22.42 (d, $J = 43.1$ Hz, 10), 18.91 (d, $J = 16.1$ Hz, 3).

^1H NMR (400 MHz, CDCl_3): $\delta/\text{ppm} = \delta 7.25$ (d, $J = 7.8$ Hz, 2H, 6), 7.13 (d, $J = 7.8$ Hz, 2H, 5), 3.74 (q, $J = 7.1$ Hz, 1H, 2), 2.48 (d, $J = 7.1$ Hz, 2H, 8), 1.87 (tt, $J = 13.4, 6.7$ Hz, 1H, 9), 1.52 (s, 3H, 3), 0.93 (d, $J = 6.6$ Hz, 6H, 10). ^{13}C NMR (101 MHz, CDCl_3): $\delta/\text{ppm} = 180.61$ (s, 1), 140.87 (s, 7), 137.00 (s, 4), 129.40 (s, 6), 127.29 (s, 5), 45.05 (s, 8), 44.94 (s, 2), 30.17 (s, 9), 22.40 (s, 10), 18.11 (s, 3).

Sodium Ibuprofen



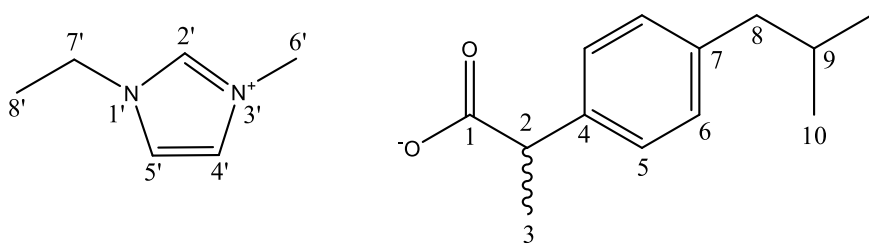
Chapter 3 | Human Cytotoxicity, Hemolytic Activity, Anti-Inflammatory Activity and Aqueous Solubility of Ibuprofen-Based Ionic Liquids

^1H NMR (500 MHz, D_2O): δ/ppm = 7.19 (d, J = 8.0 Hz, 2H, 6), 7.13 (d, J = 7.9 Hz, 2H, 5), 3.53 (q, J = 7.1 Hz, 1H, 2), 2.40 (d, J = 7.1 Hz, 2H, 8), 1.82–1.69 (m, 1H, 9), 1.31 (d, J = 7.2 Hz, 3H, 3), 0.79 (d, J = 6.6 Hz, 6H, 10). ^{13}C NMR (126 MHz, D_2O): δ/ppm = 183.98 (d, J = 3.0 Hz, 1), 140.67 (s, 7), 140.44 (s, 4), 129.41 (s, 6), 127.10 (s, 5), 48.12 (d, J = 3.9 Hz, 8), 44.15 (d, J = 3.9 Hz, 2), 29.68 (s, 9), 21.56 (s, 10), 18.41 (s, 3).

^1H NMR (500 MHz, DMSO): δ/ppm = 7.17 (d, J = 8.0 Hz, 2H, 6), 6.96 (d, J = 8.0 Hz, 2H, 5), 3.21 (q, J = 7.1 Hz, 1H, 2), 2.37 (d, J = 7.1 Hz, 2H, 8), 1.87–1.70 (m, 1H, 9), 1.22 (t, J = 8.2 Hz, 3H, 3), 0.86 (d, J = 6.6 Hz, 6H, 10). ^{13}C NMR (101 MHz, DMSO) : δ/ppm = 177.55 (s, 1), 143.79 (s, 7), 137.88 (s, 4), 128.48 (s, 6), 127.68 (s, 5), 49.04 (s, 8), 44.84 (s, 2), 30.19 (s, 9), 22.69 (s, 10), 20.74 (s, 3).

^1H NMR (400 MHz, CDCl_3): δ/ppm = 7.24 (d, J = 8.0 Hz, 2H, 6), 7.12 (d, J = 8.0 Hz, 2H, 5), 3.74 (q, J = 7.0 Hz, 1H, 2), 2.47 (d, J = 7.2 Hz, 2H, 8), 1.94–1.75 (m, 1H, 9), 1.52 (d, J = 7.2 Hz, 3H, 3), 0.92 (d, J = 6.6 Hz, 6H, 10). ^{13}C NMR (101 MHz, CDCl_3): δ/ppm = 179.40–176.46 (m, 1), 142.58–138.96 (m, 7), 137.83–135.65 (m, 4), 129.42 (s, 6), 127.25 (s, 5), 45.04 (s, 8), 44.74–44.31 (m, 2), 30.16 (s, 9), 22.38 (s, 10), 18.20 (s, 3).

1-Ethyl-3-methylimidazolium ibuprofenate ($[\text{C}_2\text{C}_1\text{Im}][\text{Ibu}]$)

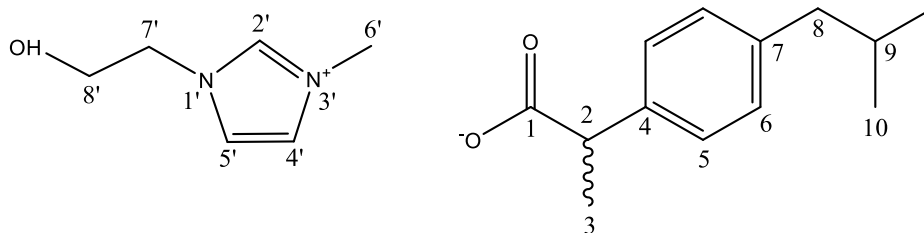


^1H NMR (400 MHz, D_2O): δ/ppm = 8.58 (s, 1H, 2'), 7.37 (s, 1H, 4'), 7.30 (s, 1H, 5'), 7.18 (d, J = 7.9 Hz, 2H, 6), 7.12 (d, J = 7.9 Hz, 2H, 5), 4.11 (q, J = 7.4 Hz, 2H, 7'), 3.77 (s, 3H, 6'), 3.53 (m, 1H, 2), 2.38 (d, J = 7.1 Hz, 2H, 8), 1.74 (dp, J = 13.5, 6.7 Hz, 1H, 9), 1.39 (t, J = 7.4 Hz, 3H, 8'), 1.30 (d, J = 7.2 Hz, 3H, 3), 0.78 (d, J = 6.6 Hz, 6H, 10). ^{13}C NMR (101 MHz, DMSO): δ/ppm = 183.92 (s, 1), 140.71 (s, 7), 140.42 (s, 4), 129.40 (s, 6), 127.12 (s, 5), 123.36 (s, 4'), 121.78 (s, 5'), 48.18 (s, 7'), 44.70 (s, 8), 44.17 (s, 2), 35.49 (s, 6'), 29.69 (s, 9), 21.58 (s, 10), 18.43 (s, 3), 14.40 (s, 8').

^1H NMR (400 MHz, DMSO): δ/ppm = 9.48 (s, 1H, 2'), 7.79 (s, 1H, 4'), 7.70 (s, 1H, 5'), 7.14 (d, J = 7.8 Hz, 2H, 5), 6.94 (d, J = 7.8 Hz, 2H, 6), 4.18 (q, J = 7.3 Hz, 2H, 7'), 3.84 (s, 3H, 6'), 3.15 (q, J = 7.1 Hz, 1H, 2), 2.37 (d, J = 7.1 Hz, 2H, 8), 1.78 (dp, J = 13.3, 6.8 Hz, 1H, 9), 1.40 (t, J = 7.3 Hz, 3H, 8'), 1.19 (d, J = 7.1 Hz, 3H, 3), 0.86 (d, J = 6.6 Hz, 6H, 10). ^{13}C NMR (101 MHz, DMSO): δ/ppm = 175.76 (s, 1), 144.45 (s, 2'), 137.55 (s, 7), 137.27 (s, 4), 128.35 (s, 6), 127.64 (s, 5), 123.97 (s, 4'), 122.38 (s, 5'), 49.65 (s, 7'), 44.86 (s, 8), 44.50 (s, 2), 36.06 (s, 6'), 30.19 (s, 9), 22.69 (s, 10), 20.86 (s, 3), 15.60 (s, 8').

1-(2-Hydroxyethyl)-3-methylimidazolium ibuprofenate ($[\text{C}_{2(\text{OH})}\text{C}_1\text{Im}][\text{Ibu}]$)

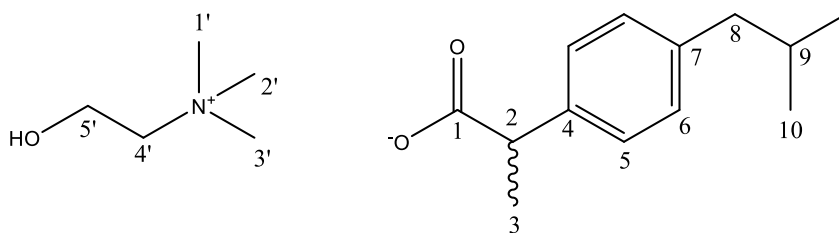
Chapter 3 | Human Cytotoxicity, Hemolytic Activity, Anti-Inflammatory Activity and Aqueous Solubility of Ibuprofen-Based Ionic Liquids



^1H NMR (500 MHz, D_2O): δ/ppm = 7.41 (d, J = 1.9 Hz, 1H, 4'), 7.36 (d, J = 1.8 Hz, 1H, 5'), 7.18 (dd, J = 4.7, 3.2 Hz, 2H, 6), 7.12 (dd, J = 4.9, 3.0 Hz, 2H, 5), 4.26 – 4.19 (m, 2H, 7'), 3.88 – 3.78 (m, 5H, 6', 8'), 3.51 (m, 1H, 2), 2.39 (dd, J = 6.9, 3.5 Hz, 2H, 8), 1.75 (ddd, J = 20.1, 10.1, 4.9 Hz, 1H, 9), 1.30 (dd, J = 7.1, 3.6 Hz, 3H, 3), 0.91 – 0.68 (m, 6H, 10). ^{13}C NMR (126 MHz, D_2O) : δ/ppm = 183.97 (s, 2'), 140.68 (s, 7), 140.44 (s, 4), 129.39 (s, 6), 127.09 (s, 5), 123.52 (s, 4'), 122.35 (s, 5'), 59.70 (s, 7'), 51.45 (s, 8), 48.15 (s, 2), 44.15 (s, 8'), 35.61 (s, 6'), 29.67 (s, 9), 21.55 (s, 10), 18.40 (s, 3).

^1H NMR (400 MHz, DMSO): δ/ppm = 9.31 (s, 1H, 2'), 7.73 (s, 1H, 4'), 7.67 (s, 1H, 5'), 7.15 (d, J = 7.8 Hz, 2H, 6), 6.96 (d, J = 7.8 Hz, 2H, 5), 4.21 (t, J = 4.9 Hz, 2H, 7'), 3.83 (s, 3H, 6'), 3.69 (dd, J = 13.8, 8.9 Hz, 2H, 8'), 3.18 (q, J = 7.1 Hz, 1H, 2), 2.36 (t, J = 8.1 Hz, 2H, 8), 1.87 – 1.68 (m, 1H, 9), 1.19 (d, J = 7.1 Hz, 3H, 3), 0.85 (d, J = 6.6 Hz, 6H, 10). ^{13}C NMR (101 MHz, DMSO) : δ/ppm = 176.29 (s, 1), 144.09 (s, 2'), 137.75 (s, 7), 137.62 (s, 4), 128.45 (s, 6), 127.64 (s, 5), 123.62 (s, 4'), 123.14 (s, 5'), 59.66 (s, 7'), 52.02 (s, 8), 49.39 (s, 2), 44.84 (s, 8'), 36.05 (s, 6'), 30.20 (s, 9), 22.70 (s, 10), 20.77 (s, 3).

Cholinium ibuprofenate ($[\text{N}_{1112}(\text{OH})][\text{Ibu}]$)



^1H NMR (500 MHz, D_2O): δ/ppm = 7.19 (d, J = 8.1 Hz, 2H, 6), 7.13 (d, J = 8.0 Hz, 2H, 5), 4.01 – 3.91 (m, 2H, 5'), 3.60 – 3.46 (m, 1H, 2), 3.46 – 3.36 (m, 2H, 4'), 3.10 (s, 9H, 1', 2', 3'), 2.40 (d, J = 7.1 Hz, 2H, 8), 1.82 – 1.67 (m, 1H, 9), 1.30 (d, J = 7.2 Hz, 3H, 3), 0.79 (d, J = 6.6 Hz, 6H, 10). ^{13}C NMR (126 MHz, D_2O) : δ/ppm = 183.96 (s, 1), 140.69 (s, 7), 140.43 (s, 4), 129.41 (s, 6), 127.10 (s, 5), 68.57 – 65.25 (m, 5'), 55.55 (s, 4'), 54.66 – 53.28 (m, 1', 2', 3'), 48.15 (s, 8), 44.15 (s, 2), 29.68 (s, 9), 21.56 (s, 10), 18.41 (s, 3).

^1H NMR (500 MHz, DMSO): δ/ppm = 7.15 (d, J = 8.0 Hz, 2H, 5), 6.96 (d, J = 8.0 Hz, 2H, 6), 3.90 – 3.73 (m, 2H, 5'), 3.18 (q, J = 7.1 Hz, 1H, 2), 3.09 (s, 9H, 1', 2', 3'), 2.37 (d, J = 7.1 Hz, 2H, 8), 1.77 (dq, J = 20.1, 6.7 Hz, 1H, 9), 1.20 (d, J = 7.1 Hz, 3H, 3), 0.86 (d, J = 6.6 Hz, 6H, 10). ^{13}C NMR (126 MHz, DMSO) : δ/ppm = 176.34 (s, 1),

Chapter 3 | Human Cytotoxicity, Hemolytic Activity, Anti-Inflammatory Activity and Aqueous Solubility of Ibuprofen-Based Ionic Liquids

144.07 (s, 7), 137.77 (s, 4), 128.46 (s, 6), 127.64 (s, 5), 67.68 (s, 5'), 55.43 (s, 4'), 54.01 – 53.24 (m, 1', 2', 3'), 49.35 (s, 8), 44.84 (s, 2), 30.19 (s, 9), 22.70 (s, 10), 20.79 (s, 3).

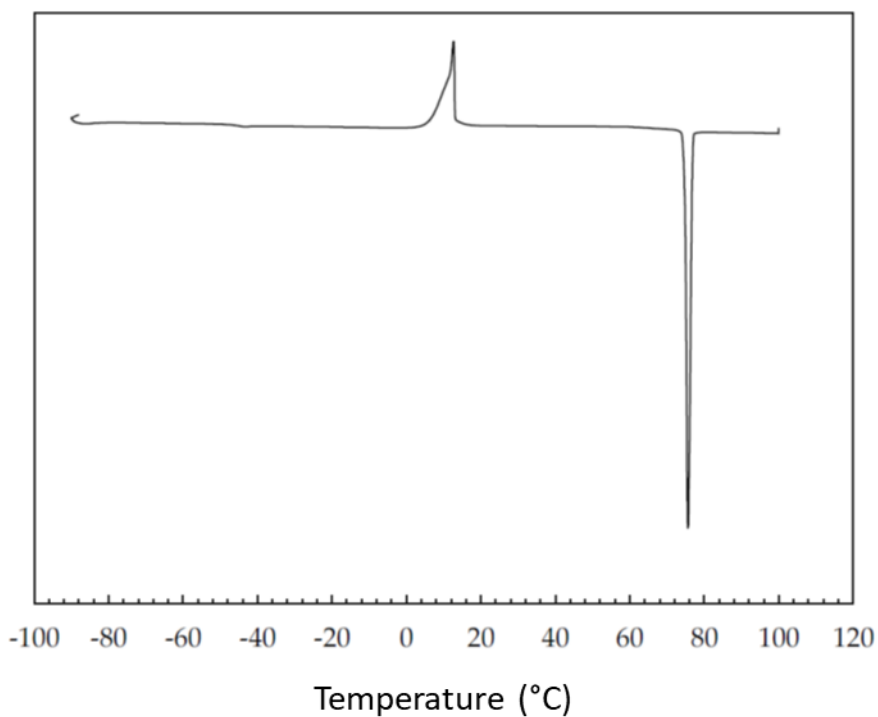


Figure 3.S1. DSC profile and analysis with TA Instruments Universal Analysis V4.5A software at 1°C/min of ibuprofen.

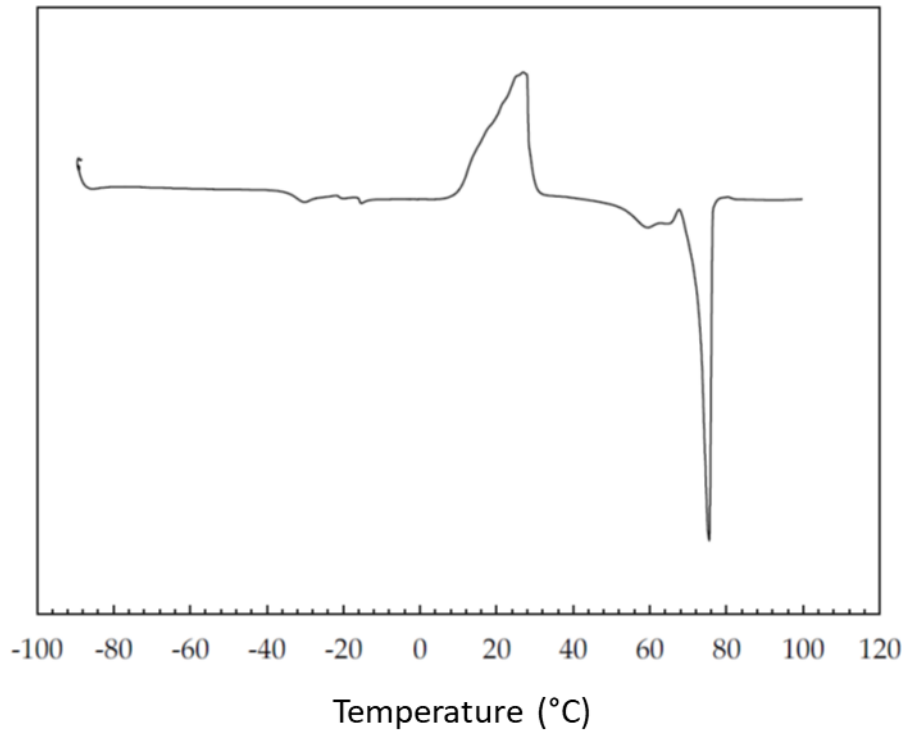


Figure 3.S2. DSC profile and analysis with TA Instruments Universal Analysis V4.5A software at 1°C/min of [C₂C₁Im][Ibu].

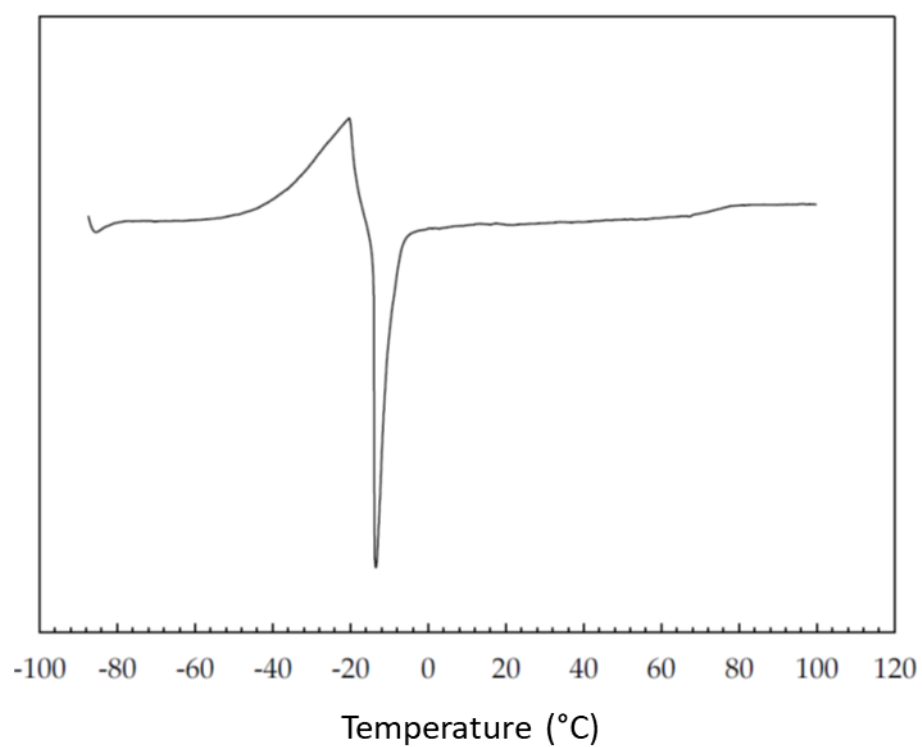


Figure 3.S3. DSC profile and analysis with TA Instruments Universal Analysis V4.5A software at 1°C/min of [C₂(OH)C₁Im][Ibu].

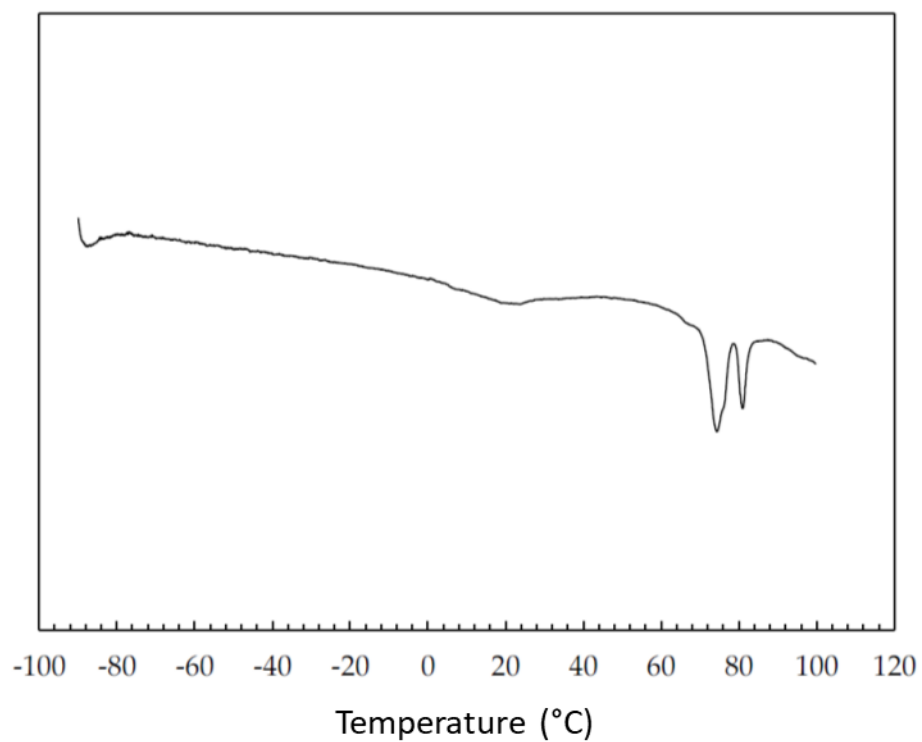
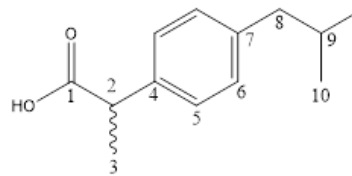


Figure 3.S4. DSC profile and analysis with TA Instruments Universal Analysis V4.5A software at 1°C/min of [N₁₁₁₂(OH)][Ibu].

Table 3.S1. Chemical shifts for the hydrogens in the position 2 and 3 (as depicted chemical structure of ibuprofen on the right) for ibuprofen, sodium ibuprofen and API-ILs in D₂O.

Compounds	H2 (δ /ppm)	H3 (δ /ppm)
Ibuprofen	3.58	1.33
Na[Ibu]	3.53	1.31
[C ₂ C1Im][Ibu]	3.53	1.30
[C _{2(OH)} C1Im][Ibu]	3.51	1.30
[N _{1112(OH)}][Ibu]	3.53	1.30



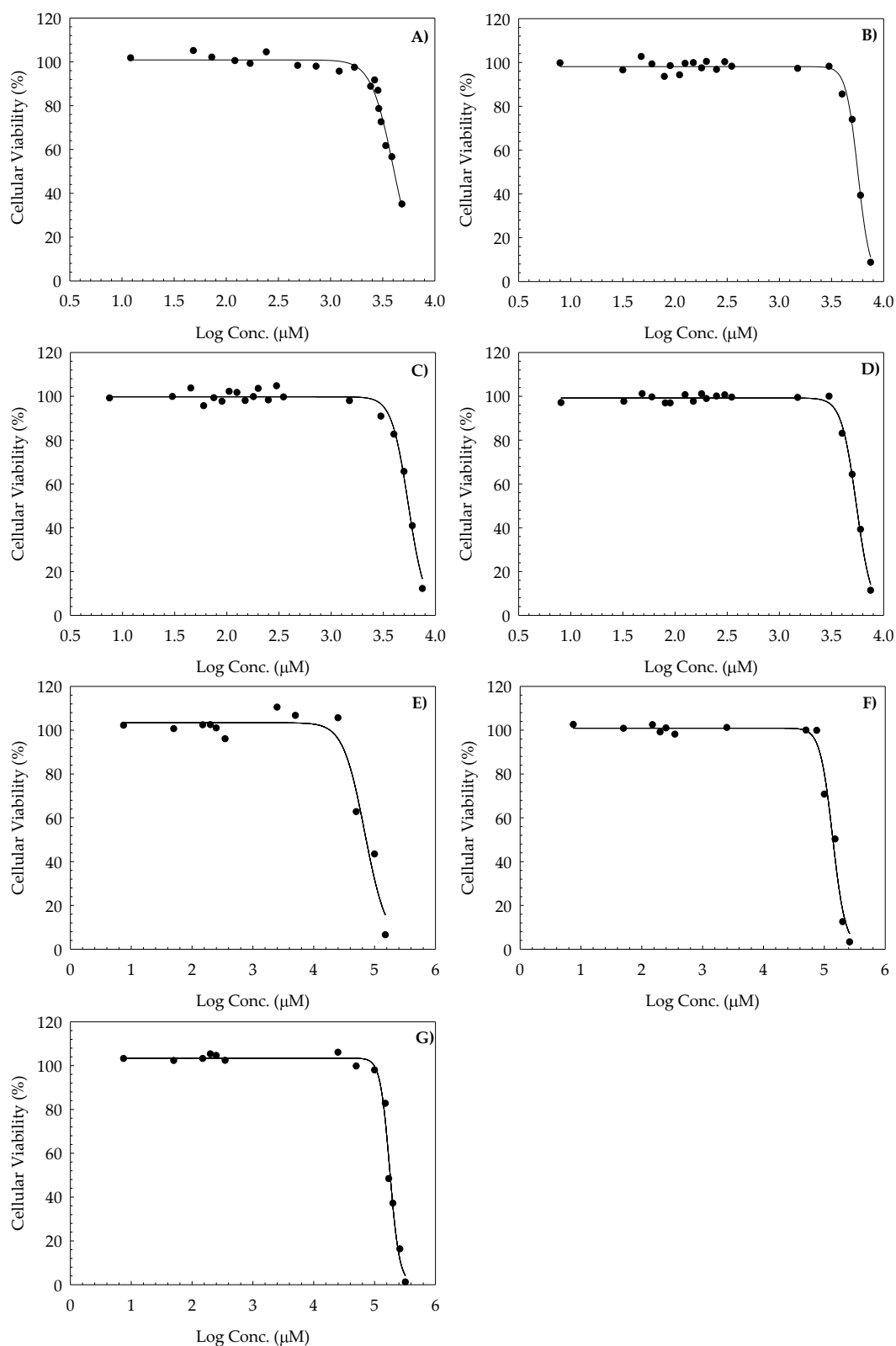


Figure 3.S5. Non-linear regression fitting curves, calculated Log EC₅₀ ± standard deviation and respective R-squared and p-value for ibuprofen (A), [C₂C₁Im][Ibu] (B), [C₂(OH)C₁Im][Ibu] (C), [N₁₁₁₂(OH)][Ibu] (D), [C₂C₁Im]Cl (E), [C₂(OH)C₁Im]Cl (F) and [N₁₁₁₂(OH)]Cl (G) in Caco-2 cell line.

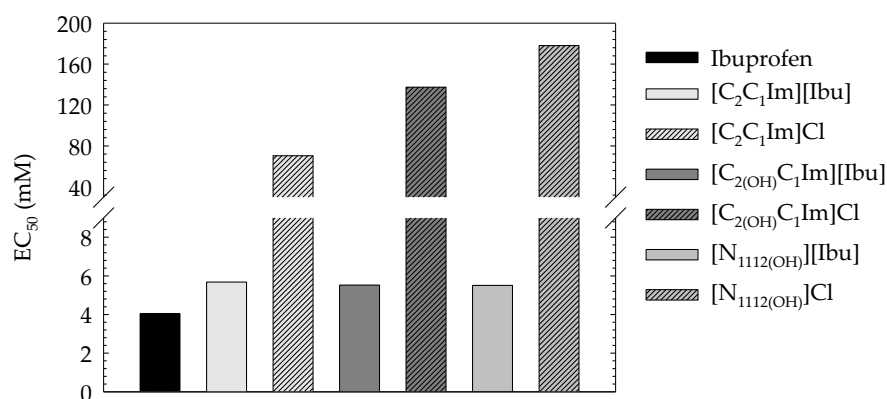


Figure 3.S6. EC₅₀ values of ibuprofen, ibuprofen-based ILs and IL/salt cation “suppliers” for the API-ILs ([C₂C₁Im]Cl, [C_{2(OH)}C₁Im]Cl, [N_{1112(OH)}]Cl) in Caco-2 cell line exposed to the compounds for 24h. The R-squared was greater than 0.9540 and P < 0.0001 for all fitted curves.

Table 3.S2. Inhibition of BSA denaturation in PBS pH 7.4 at different concentrations for the neutral and salt form of ibuprofen and API-ILs. The presented value is the mean of at least two independent measures ± standard deviation.

Concentration (mM)	Inhibition of BSA denaturation (%)	Concentration (mM)	Inhibition of BSA denaturation (%)
Ibuprofen		Sodium Ibuprofen	
0.727	19.93 ± 2.00	0.657	20.15 ± 1.10
1.697	42.85 ± 1.97	1.533	36.97 ± 1.61
2.424	67.66 ± 2.49	2.190	61.24 ± 4.24
3.636	76.40 ± 1.32	3.286	69.54 ± 4.81
4.848	74.34 ± 1.32		
[C₂C₁Im][Ibu]		[C_{2(OH)}C₁Im][Ibu]	
0.474	23.30 ± 1.15	0.451	43.67 ± 3.21
1.106	48.77 ± 2.52	1.053	70.99 ± 3.81
1.580	55.56 ± 2.73	1.504	82.25 ± 0.44
2.370	63.27 ± 2.08	2.256	86.27 ± 0.95
[N_{1112(OH)}][Ibu]			
0.485	31.79 ± 1.57		
1.131	39.66 ± 1.33		
1.616	50.93 ± 2.00		
2.424	59.41 ± 0.79		

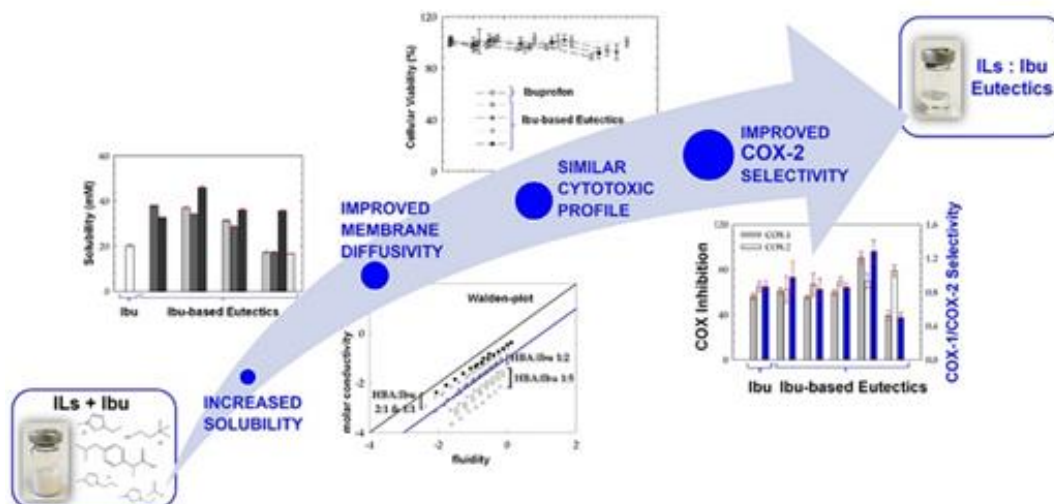
IBUPROFEN-BASED EUTECTIC SYSTEMS

4.1 Role of Ionic Liquids in Ibuprofen-based Eutectic Systems: Aqueous Solubility, Permeability, Human Cytotoxicity, Hemolytic Activity and Anti-Inflammatory Activity

4.1.1 Abstract

Eutectic systems, as well as ionic liquids (ILs), offer a potential solution to the challenges associated with low solubility, polymorphism, and limited bioavailability of active pharmaceutical ingredients (APIs). Herein, we prepared twelve pharmaceutically active eutectics based on ibuprofen (Ibu), a widely accessible without prescription non-steroidal anti-inflammatory drug (NSAID), and imidazolium-based ILs ($[\text{C}_2\text{C}_1\text{Im}]\text{Cl}$, $[\text{C}_{2(\text{OH})}\text{C}_1\text{Im}]\text{Cl}$ and $[\text{C}_2\text{C}_1\text{Im}][\text{C}_1\text{CO}_2]$) and cholinium salt ($[\text{N}_{1112(\text{OH})}]\text{Cl}$) at different molar ratio (2:1, 1:1, 1:2 and 1:5). All eutectic systems were characterized by DSC and NMR, and their polarity was assessed using the Kamlet-Taft approach to characterize the non-specific (polarity/polarizability) and specific (hydrogen bonding ability) interactions. An upgrade of the aqueous solubility (water and biological simulated fluids) for the Ibu-based eutectics relatively to ibuprofen was verified. Also, the assessment of ionicity (viscosity, conductivity, and density) was attained, confirming the formation of ion-pairs or clusters, that increase the potential of these liquids to be more membrane diffusive. The biocompatibility of the Ibu-based eutectics was evaluated up to 3mM (well above the ibuprofen maximum plasma concentration) through a hemolytic activity assay and in vitro cytotoxicity assays with two human cell lines (Caco-2 colon carcinoma cells and HepG2 hepatocellular carcinoma cells), without impairing their hemolytic and cytotoxic response. Additionally, the anti-inflammatory activity was evaluated by the inhibition of bovine serum albumin (BSA) denaturation and inhibition of cyclooxygenases (COX-1 and COX-2) enzymes, showing that the ibuprofen eutectic formulations maintain the anti-inflammatory response of ibuprofen with the opportunity to improve the selectivity towards COX-2, allowing the development of safer NSAIDs.

Keywords: Ibuprofen; Ionic Liquids; Eutectic Systems; Bioavailability; Walden plot; Ionicity; Polarity; Hydrogen bonding; Cytotoxicity; Hemocompatibility; Anti-inflammatory activity.



Published in: Joana C. Bastos, Maria Manuela Gaspar, Ana B. Pereiro, João M. M. Araújo. Role of Ionic Liquids in Ibuprofen-based Eutectic Systems : Aqueous Solubility, Permeability, Human Cytotoxicity, Hemolytic Activity and Anti-Inflammatory Activity. *Pharmaceuticals* 2023. (*In press*)

Own experimental contribution: Ibu-based eutectic systems synthesis, NMR and DSC sample preparation, solubility assay, cytotoxicity assay, protein denaturation assay, cyclooxygenases (COX-1 and COX-2) inhibition assay.

Own written contribution: NMR and DSC analysis, solubility assay, cytotoxicity assay, protein denaturation assay, hemocompatibility assay, ionicity analysis, solvatochromic parameters assay, cyclooxygenases (COX-1 and COX-2) inhibition assay.

Other contributions: Experimental design and data analysis.

4.1.2 Introduction

Currently, one of the major issues regarding active pharmaceutical ingredients (APIs) applications is poor water solubility, which leads to low bioavailability and permeation. At least 90% of the drugs currently in development and 40% of the ones already available in the market are poorly water soluble. Thus, improving the efficiency of the current tried-and-tested APIs is a better alternative rather than developing new drugs [1]. To overcome the problem of low solubility and/or low permeability of drugs, higher dosages are administrated leading to severe side effects. Pharmaceutical research and development rely mostly on crystal engineering strategies coupled with new delivery systems able to provide a more effective therapy. However, polymorphic conversion associated with the solid form of the drugs can lead to the loss of the drug therapeutic effect and even potentialize their systemic toxicity. Several strategies, namely creation of metastable polymorphs, salt formation, microemulsions and self-emulsifying drug delivery systems have been proposed to improve the APIs dissolution and permeability [1].

Non-steroidal anti-inflammatory drugs (NSAIDs) are the most prominent and widely used medicines for the treatment of pain, fever and inflammation among children, adults and elders. The arylpropionic acid derivatives (e.g. fenbufen, fenoprofen, flurbiprofen, ibuprofen, indoprofen, ketoprofen and naproxen) constitute an important group of the NSAIDs for the treatment of common acute pain, fever and inflammation but also for musculoskeletal traumatism, chronic rheumatoid arthritis and osteoarthritis [2]. Ibuprofen (Ibu), chemically known as 2-(4-isobutylphenyl) propionic acid and is one of the most prescribed NSAIDs. According to the biopharmaceutics classification system (BSC), Ibu falls in Class II type of drugs [3] with low solubility and high permeability (0.067 ± 0.0066 mg/mL at 25 °C; $\text{LogP} = 1.89 \pm 0.03$) [4]. The low aqueous solubility limits the expected therapeutic outcome in pharmaceutical dosage form. Therefore, enhancement of ibuprofen solubility is still a challenge faced by the pharmaceutical industries [4].

Eutectic systems have emerged in the past decade as an analogue class of ionic liquids (ILs). Although they share many features with ILs, the terms are not interchangeable, and they can offer several other advantages [5]. ILs are defined as salts with melting points below 100°C (some of them liquid at room temperature) and composed by an organic cation and an organic or inorganic anion. They own peculiar physical features such as high thermal and chemical stability, lack of inflammability, low volatility, and tunable properties, such as solubility, lipophilicity and cytotoxicity [6,7]. Recently, Vieira et al. [8,9] disclosed that the human cytotoxicity and hydrophilic/lipophilic balance of ILs and their biodegradability can be designed. These studies were performed in several families of ILs based on imidazolium, pyridinium, ammonium, cholinium and pyrrolidinium cations. The results established that compounds with short hydrogenated moieties in the ILs cation can possess a negligible cytotoxicity [9] and biodegradability [8]. Moreover, ILs can be designed to reduce the impact of the addition of water upon the ILs hydrogen-bond acceptance ability which is crucial once most biological applications involve aqueous solutions (water and biological fluids) [10]. By taking advantage of their unique characteristics, ILs have been studied as enhancers of properties for several biological compound [11]. In the past decades, were proposed as solvents or co-solvents to increase solubility of drugs [12,13] and biomolecules [14] and some works have taken a further step into developing ILs with a pharmaceutical effect, such as anti-bacterial [7], anti-inflammatory [4,6,15] and anesthetic [16,17]. Chantereau et al. [15] demonstrated that the conversion of ibuprofen into cholinium-based ILs allows an increase in solubility by 2 orders of magnitude, which is highly beneficial to improve their bioavailability. Additionally, by incorporating the cholinium-based ILs with ibuprofen into bacterial cellulose membranes, the API transdermal release was faster and complete. Recently, we have developed ibuprofen-based ILs (with imidazolium and cholinium cations) with upgraded aqueous solubility (water and biological simulated fluids), and similar biocompatibility profiles (assessed by cytotoxicity test on human cell lines and hemocompatibility assays), relatively to the ibuprofen neutral and sodium ibuprofen (commercial ibuprofen salt form). Additionally, all the Ibu-based ILs

maintained the anti-inflammatory response of ibuprofen (parent API) with improved selectivity towards COX-2, allowing the development of safer NSAIDs [18].

On the other hand, eutectic systems have been gaining attention in the academic and pharmaceutical research due to their properties, such as lower toxicity, higher biodegradability, and easy preparation in comparison to ILs [5]. Eutectic systems are a mixture of at least two compounds, a salt (hydrogen bond acceptor, HBA) and a hydrogen bond donor (HBD), which can self-associate and it is characterized by a depression in the melting temperature in comparison to each individual components [5]. These eutectic mixtures often convert a solid API in a liquid formulation which can increase the drug bioavailability. Recently, Abbott et al. [19] disclosed that a wide variety of pharmaceutical agents can be formulated into liquids as eutectic solvents with improved solubility. By converting paracetamol into a eutectic formulation, the API solubility increased up to 10-folds. Moreover, aspirin which is solid at room temperature became a liquid formulation with increased solubility [19]. Morrison and coworkers [20] also reported that benzoic acid, griseofulvin, danazol and itraconazole exhibited a 5- to 22,000-fold enhancement of their solubilities in eutectic formulation when compared to water. The first pharmaceutically active eutectic system, composed by ibuprofen and menthol, was first described in the 90's [21]. Since then, several studies have been made using this strategy, whether formulating eutectic systems to have a direct pharmacological effect [3,22,23], or as solvent enhancers for API solubility [19,20,24], or even as precursors in the synthesis of pharmaceutically active biopolymers [25–28].

In the present work, we have further investigated the benefits of using eutectic systems to modulate the bioavailability of ibuprofen. Thus, cholinium chloride and imidazolium chloride and acetate based-ILs were used as HBA and ibuprofen as HBD at different molar ratio, namely 2:1, 1:1, 1:2, and 1:5. The ibuprofen-based eutectic systems were characterized by DSC and NMR to validate the eutectic formation. Also, the polarity of the Ibu-based eutectics was studied using the Kamlet-Taft approach to characterize the non-specific (polarity/polarizability) and specific (hydrogen bonding ability) interactions. The solubility of the prepared eutectic formulations and ibuprofen at 25°C

were obtained in water, simulated gastric fluid, simulated intestinal fluid and in 0.15 M NaCl (isotonic ionic strength solution). Further, the Ibu-based eutectics were characterized in terms of viscosity, conductivity, density and ionicity (via Walden plot), to probe the formation of larger charged or non-charged aggregates, or the existence of ionic networks, that increase the possibility for these liquids to penetrate membranes more efficiently than ibuprofen (parent solid API). Additionally, to realize the biocompatibility of the ibuprofen-based eutectics, we have performed in vitro cytotoxicity assays with two different human cells lines, namely Caco-2 colon carcinoma cells and HepG2 hepatocellular carcinoma cells, and hemocompatibility assays. Besides, the anti-inflammatory activity of the Ibu-based eutectic systems was evaluated by the inhibition of bovine serum albumin (BSA) denaturation and the inhibition of cyclooxygenases (COX-1 and COX-2) enzymes, to evaluate the potential of the ibuprofen eutectic formulations to maintain/upgrade the pharmacological activity of ibuprofen.

4.1.3 Materials and Methods

4.1.3.1 Materials

Ibuprofen (>98% mass fraction purity) was purchased from TCI and used without further purification. The ionic liquids 1-ethyl-3-methylimidazolium chloride ($[\text{C}_2\text{C}_1\text{Im}]\text{Cl}$; >98% mass fraction purity); 1-(2-hydroxyethyl)-3-methylimidazolium chloride ($[\text{C}_{2(\text{OH})}\text{C}_1\text{Im}]\text{Cl}$; >99% mass fraction purity); 1-ethyl-3-methylimidazolium acetate ($[\text{C}_2\text{C}_1\text{Im}][\text{C}_1\text{CO}_2]$; > 95 % mass fraction purity) were acquired at IoLiTec and cholinium chloride ($[\text{N}_{1112(\text{OH})}]\text{Cl}$; $\geq 98\%$ mass fraction purity) T² Torr vacuum for at least 48 hours to avoid volatile impurities. The water content was determined using Karl Fischer coulometric titration method (Metrohm 831 KF Coulometer) and it was less than 0.05wt%. The structures, acronyms and molecular masses of ionic liquids, cholinium chloride and ibuprofen are listed in **Table 4.1**. The buffer solutions suitable for dissolution testing, simulated intestinal fluid without enzymes-interchangeable with phosphate standard buffer pH 6.8 was purchased from Honeywell, simulated gastric fluid without enzymes-interchangeable with 0.1 N HCl (pH 1.0) was acquired at Carlo Erba Reagents, and sodium chloride physiological solution (0.15M NaCl–isotonic ionic

strength) was purchased from Sigma-Aldrich. Milli-Q water (Milli-Q Integral Water Purification System) was used in all experiments throughout the work. Tablets for the phosphate buffered saline (PBS) solution preparation were purchased from PanReac Applichem ITW Reagents Division (Chicago, IL, USA).

Table 4.1. Designation, chemical structure, and molecular weight (Mw) of ibuprofen, cholinium salt and imidazolium-based ILs used along this work.

Structure	Designation and acronym	M _w (g/mol)
	2-(4-Isobutylphenyl) propionic acid Ibuprofen (Ibu)	206.29
	1-Ethyl-3-methylimidazolium chloride [C ₂ C ₁ Im]Cl	146.62
	1-(2-hydroxyethyl)-3-methylimidazolium chloride [C _{2(OH)} C ₁ Im]Cl	162.62
	1-Ethyl-3-methylimidazolium acetate [C ₂ C ₁ Im][C ₁ CO ₂]	170.21
	Cholinium chloride [N _{1112(OH)}]Cl	139.62

4.1.3.2 Preparation of Ibuprofen-based eutectic systems

For the preparation of pharmaceutically active eutectic systems we have used a similar procedure to the one recently implemented by us [29], mixing a ionic liquid ([C₂C₁Im]Cl, [C_{2(OH)}C₁Im]Cl and [C₂C₁Im][C₁CO₂]) or a cholinium salt ([N_{1112(OH)}]Cl), used as hydrogen-bond acceptors (HBA), with ibuprofen as hydrogen-bond donor (HBD). The HBA:Ibu systems were prepared by mixing the counterparts at different molar ratio, namely 2:1, 1:1, 1:2, and 1:5 (Table 4.S1 in Supporting Information). The mixtures were prepared in crimped seal glass vials using an analytical high precision balance (Sartorius, Germany) with 0.01 mg resolution and sealed under nitrogen atmosphere. Three heating (up to 85°C ±2°C) / cooling (down to 5°C ±2°C) cycles were performed

under constant stirring, to guarantee that all components were blended. ^1H NMR technique was used to verify that the HBA (imidazolium-based ILs or cholinium chloride) and ibuprofen (HBD) have not reacted, and to check the molar ratio.

A dynamic visual method (lab benchtop procedure) was attained, after the three heating/cooling cycles, to determine the solid-liquid transitions of the prepared mixtures, i.e. the temperatures at which a liquid phase appears and the last crystal disappears. First, the mixtures were cooled down to $-40\text{ }^\circ\text{C}$, maintained at this temperature for at least 30 min, and examined. If the mixture remained in the liquid state, the melting temperature was considered below -40°C . If crystals were detected, the mixtures were heated up to achieve a complete liquid phase. For this last case, a second run was attained to confirm the solid-liquid transition. This procedure was carried out with successive increment of 5°C in the heating/cooling runs until the solid-liquid transition was determined, and the prepared mixtures pre-validated as eutectic mixtures (**Table 4.S1** in Supporting Information).

The ibuprofen-based eutectic systems were synthesized at atmospheric pressure and under control of moisture content. Samples were kept in well-sealed glass vials after preparation and fresh samples were always used for analysis to avoid structural change or environmental effects on their physical properties.

4.1.3.3 Nuclear magnetic resonance (NMR)

The prepared ibuprofen-based eutectic systems and their individual components were characterized by ^1H NMR (Bruker Avance III 400). The NMR spectroscopy disclosed that there were no individual functional group modifications on the ibuprofen-based eutectic systems, being indeed a eutectic combination. All characterization is appended in Supporting Information.

4.1.3.4 Differential Scanning Calorimetry (DSC)

The DSC traces of all prepared mixtures, hydrogen-bond acceptors ($[\text{C}_2\text{C}_1\text{Im}]\text{Cl}$; $[\text{C}_2(\text{OH})\text{C}_1\text{Im}]\text{Cl}$; $[\text{C}_2\text{C}_1\text{Im}][\text{C}_1\text{CO}_2]$; $[\text{N}_{1112}(\text{OH})]\text{Cl}$) and hydrogen-bond donor (ibuprofen) were

acquired using a TA Instrument DSC Q200 Differential Scanning Calorimeter with a refrigerated cooling system capable of controlling the temperature down to -90°C . Indium ($T_m=157.61^{\circ}\text{C}$) was used as standard for the DSC calibration. Around 5-10mg of sample was crimped in a standard aluminum hermetic sample pan and continuously purged with $50\text{ mL}\cdot\text{min}^{-1}$ nitrogen. The samples were cooled to -90°C for 30 min and then heated to 100°C . The cooling-heating cycles were repeated three times at different rates ($10^{\circ}\text{C}/\text{min}$, $5^{\circ}\text{C}/\text{min}$ and $1^{\circ}\text{C}/\text{min}$). The transition temperatures obtained from the second and subsequent cycles at the same rate were reproducible. The glass transition temperature (T_g) and melting temperature (T_m) of each eutectic system were determined using the DSC traces. The standard uncertainty was estimated as $\pm 1^{\circ}\text{C}$. Universal Analysis 2000 v. 4.5A software (TA Instruments) was used to integrate the peaks to determine the different phase transitions.

4.1.3.5 Solubility in water and simulated biological fluids

The determination of the solubility in water and buffer solutions suitable for dissolution testing (simulated gastric fluid without enzymes-interchangeable with 0.1 N HCl (pH 1.0); simulated intestinal fluid without enzymes-interchangeable with phosphate standard buffer pH 6.8; 0.15 M NaCl-isotonic ionic strength solution) of the ibuprofen-based eutectic mixtures (the non-eutectic mixtures were also analysed) was conducted at room temperature and atmospheric pressure according to the detailed procedure described in previous work [29]. Briefly, an excess of compound is added to a 1.5 mL safe-lock microtubes with 1.5 ml of Mili-Q water or buffer. Then the amount solubilized ibuprofen in each solution is followed over time through UV-Vis (VWR® spectrophotometer, model UV-6300PC). The presented solubilities were repeated at least three times and the available data is the average value.

4.1.3.6 Density, Viscosity and Conductivity

Measurements of viscosity and density were performed at atmospheric pressure in the temperature range of 15°C to 80°C using an automated SVM 3000 Anton Paar rotational Stabinger (Viscosimeter and Densimeter). The SVM 3000 uses a Peltier with an error on

temperature of $\pm 0.02\text{ C}^\circ$. The reproducibility of the dynamic viscosity and the density is $\pm 1\%$ and $\pm 0.0002\text{g}\cdot\text{cm}^{-3}$, respectively. For each sample, duplicates were measured, and the reported result is the average value. The expanded uncertainty with 0.95 level of confidence of the measurements is estimated to be 2% for the viscosity and 0.1% for the density. A METTLER TOLEDO FiveEasy plus Model FP30 was used to measure the conductivities of the eutectic mixtures in a glass cell containing a magnetic stirrer. The cell was flushed with dry nitrogen to prevent humidity uptake. The conductivity cell was calibrated at each temperature with certified 0.01 D and 0.1 D KCl (D = demal) standard solutions supplied by Radiometer Analytical. The conductivity cell uses an alternating current of 9 to 12 V and a frequency of 1 W in the range of conductivities measured in this work. Every conductivity value was determined at least two times with an estimated expanded uncertainty with 0.95 level of confidence of $\pm 2\%$ in the temperature range of 15°C to $50^\circ\text{C} \pm 0.3^\circ\text{C}$. The reported results are the average for all measurements.

4.1.3.7 Kamlet-Taft solvatochromic parameter: Hydrogen-bond acceptor ability (β)

A eutectic system is normally prepared by mixing an organic salt and a hydrogen-bond donor (HBD) in which the melting point can be lower than the individual components [5]. Therefore, the formation of a stable eutectic depends on the strength of the HBD and hydrogen-bond acceptor (HBA) and the physicochemical properties of the system can be tuned depending on the molar composition of the respective components. The combination between both counterparts gives the eutectic formulation the ability to accept and donate protons during solvation and thus form a hydrogen bond with the solute [10].

One of the most important properties of a solvent is polarity which defines the possible interactions between a solute and a solvent. Additionally, the polarity of a solvent influences the reaction rate, mechanism, solvation ability, and product yield being an important parameter in drug development & discovery [30]. A simplistic multiparametric model to scale polarity was developed by Kamlet and Taft using a set of solvatochromic probes to assess the ability of HBD (acidity) and HBA (basicity) and

polarity/polarizability of the same solvent [10]. The polarity/polarizability (π^* value) is a well-founded scale of solvent strength to characterize dipolar interactions important to predict the solute-solvent dissolution [31]. The hydrogen-bond basicity (β value) is one of the most important parameters, reflecting the hydrogen bond accepting ability of an IL [32] since a high β parameter imply anions that can strongly interact with the H-bond donator groups of a solute, promoting its dissolution [33,34].

4-Nitroaniline and N,N-diethyl-4-nitroaniline are traditionally being used for the experimental measurement of the Kamlet-Taft parameters, namely the hydrogen-bond basicity and polarity/polarizability [32]. The stock solutions of 4-nitroaniline and N,N-diethyl-4-nitroaniline dye were prepared using ± 0.010 g of dried dye and mixed with 10 mL of dichloromethane. An additional 1:10 dilution with dichloromethane (DCM) was made to ensure an absorbance in accordance with Lambert-Beer law. Roughly 0.35 mL of 4-nitroaniline or N-N-diethyl-4-nitroaniline dye stock solution were added to a glass vial with an open top screw-caped sealed with a silicone skewered with a 0.8 x 30 mm regular needle. The glass vials with the dye stock solutions were submitted to a $3 \cdot 10^{-2}$ Torr at room temperature for 30 minutes to remove the DCM. Thus, 0.4 mg of sample is added to the vial and vigorously stirred in a vortex until all blended. Kamlet-Taft solvatochromic parameter β was obtained using an UV-Vis VWR® spectrophotometer, model UV- 6300PC. Each sample was loaded into a dry cuvette and measured in a scan range of 250 to 800 nm at 100.00 nm/min. In order to obtain a high spectra resolution, a 0.1 nm interval was chosen. The spectrum for each sample was recorded three times and the wavelengths in which the absorbance was maximum were acquired. All spectra were analyzed using the UV-Vis Analyst Software according to the methodology of previous work [10].

4.1.3.8 Cytotoxicity assays

Human colon carcinoma cell line (Caco-2) and hepatocellular carcinoma cell line (HepG2) were used to evaluate the ibuprofen-based eutectic systems cytotoxicity. The HepG2 cell line grown in MEM medium with 10% of inactivated FBS, 2mM glutamine, 1% MEM-NEAA and 1% sodium pyruvate and the Caco-2 cell line grown in RPMI 1640

medium supplemented with 10% of inactivated fetal bovine serum (FBS) and 1% of penicillin-streptomycin. All the supplements and media were provided by Gibco from Thermo Fisher Scientific. Both cells lines were kept at 37°C in a humidified incubator (Smart Biotherm S-Bt, bioSan) with 5% CO₂ and consistently grown in 175 cm² culture flasks. The HepG2 cells were seeded at a density of 6x10⁵ cells per well in a 96-well plates and used after 24 hours with a 80% confluence. The Caco-2 cells were seeded at a density of 2x10⁵ cells per well in a 96-well plates and used after 96 hours with a 90% confluence. Each ibuprofen-based system was tested in concentrations ranging from 0.12 mM to 3.00 mM, lying above/in the maximum plasma concentration (C_{max}) of ibuprofen, 0.175 mM [35], and further compared to neat ibuprofen obtained in our previous work [18]. The stock solutions were prepared and diluted in 0.5% FBS culture media, added to a seeded 96-well plate and incubated for 24h. DMSO was used as positive control and a culture media solution with 0.25% (*v/v*) DMSO was used as negative control. A CyQUANT™ XTT Cell Viability test kit (Invitrogen, Waltham, MA, USA) was used to access the cytotoxicity assay. A working solution was prepared using an XTT reagent ((2,3-bis-(2-methoxy-4-nitro-5-sulfophenyl)-2H-tetrazolium-5-carboxanilide) and an electron coupling reagent according to the manufacturer's instructions. After the incubation period, the samples were removed and 100 μ L of the working solution was added and left to react for 4h. The water-soluble XTT compound is sensitive to cellular redox potential and when in contact with viable cells it is converted to an orange-coloured formazan product is formed being proportional to the number of viable cells which can be quantified spectrophotometrically at 450 nm in a micro-plate reader (Multiskan GO from ThermoFisher Scientific). Each sample was incubated in three different wells and the obtained value was the average of three independent assays. Cell viability was determined by the ratio between the measured test compounds-contacted cells and the measured absorbance of the control cells treated only with culture medium. Dose-independent viability curves were determined using the cell viability trends.

4.1.3.9 Hemolytic Activity

The hemolytic activity assay was performed according to the method optimized by Gaspar and coworkers [31]. Peripheral human blood obtained from voluntary donors and preserved in ethylene diamine tetraacetic acid (EDTA), was used on the same day of all experiments. Briefly, the erythrocytes were centrifugated at $1000 \times g$ for 10 min to separate them from the serum and then washed three times with a PBS solution. The ibuprofen-based systems were prepared in PBS with a final concentration of 6 mM. The assay was performed in 96-well plates in which 100 μL /well of sample were diluted with 100 μL of the erythrocyte suspension. Then, the microplates were incubated at 37 °C for 1 h followed by a centrifugation at $800 \times g$ for 10 min. The supernatant absorbance was measured at 570 nm with a reference filter at 600 nm. The percentage of the hemolytic activity was calculated according to **Equation (4.1)**:

$$\text{Hemolytic Activity (\%)} = \frac{\text{AbsS} - \text{AbsN}}{\text{AbsP} - \text{AbsN}} \times 100 \quad (4.1)$$

Where AbsS is the average absorbance of the sample, AbsN is the average absorbance of the negative control and AbsP is the average absorbance of the positive control. All the compounds were tested in triplicate.

4.1.3.10 Protein albumin denaturation assay

The inhibition of protein denaturation was evaluated according to the method described by Mizushima and Kobayashi [37] with slight modifications to assess the anti-inflammatory activity of the ibuprofen-based eutectic systems. Briefly, a 2 %bovine serum albumin (BSA) solution was prepared in a PBS buffer with a pH 7.4. Ibuprofen was used as positive control drug and was accessed in our previous work [18]. A solution of only PBS and 2% BSA was used as the negative control. The sample solutions of ibuprofen-based eutectic systems were prepared also in PBS ranging from of 0.75 to 4.5 mM. The reaction mixture composed of 0.5 mL of 2% BSA and 1.5 mL of each test compound was incubated at 37 °C for 15 min and cooled at room temperature. Denaturation was induced by kept the samples at $80^{\circ}\text{C} \pm 1^{\circ}$ in a dry bath for 15 min and then the turbidity of the solutions represented the level of protein precipitation. All the samples were centrifuged in a manual centrifuge and then measured at 660 nm. Each sample concentration consisted of at least two independent replicates.

4.1.3.11 Cyclooxygenases (COX-1, COX-2) inhibition assay

The anti-inflammatory activity of the ibuprofen-based eutectic systems was evaluated through the direct inhibition of the COX enzymes by using a colorimetric COX (COX-2, human; COX-1, ovine) inhibitor screening assay kit (Cayman Chemical Co., No.701050). The assay was conducted according to the manufacturer's instructions. Briefly, a reaction mixture was prepared containing 150 μl of assay buffer, 10 μl of heme, 10 μl of enzyme (either COX-2 or COX-1) and 10 μl of each eutectic system at 3mM. The 100% initial activity was accessed with a solution of 150 μL of assay buffer, 10 μL of heme, 10 μL of enzyme (either COX-1 or COX-2) and 10 μL of a solution 50/50 H_2O and EtOH. The background contained 160 μL of assay buffer, while 10 μL of heme and 10 μL of a solution of 50/50 H_2O and EtOH. By monitoring the appearance of oxidized N, N, N, N'-tetramethyl-phenylenediamine (TMPD) at 590 nm it is possible to assay colorimetrically the peroxidase activity which corresponds to the COX's catalytic domain. The samples plate was firstly incubated for 5 min at 25 °C and then 20 μL TMPD, and 20 μL of arachidonic acid was added to start the reaction. The samples were measured kinetically for precisely 2 min at 25° C for a more accurate determination of the reaction rates. All samples were assayed in triplicate. The COX-1 and COX-2 percent inhibition was calculated using **Equation 4.2**:

$$\text{COX inhibition activity (\%)} = \frac{T}{C} \times 100 \quad (4.2)$$

where C is absorbance of the 100% initial activity sample; T is the subtraction of each inhibitor sample from the 100% initial activity sample. The absorbances are the average of all samples, and one must subtract the absorbance of the background wells from the absorbances of the 100% initial activity and the inhibitor wells.

4.1.4 Results

4.1.4.1 Characterization of ibuprofen-based eutectic systems

Eutectic systems are formed from Lewis or Bronsted acids and bases which can have a variety of anionic and cationic species. They contain nonsymmetric ions that have low

lattice energy, and consequently, low melting points, and usually obtained by the complexation of a salt acting as a hydrogen-bond acceptor with a hydrogen-bond donor. The charge delocalization occurring through hydrogen bonding between the salt and the hydrogen bond donor is responsible for decreasing the melting point of the mixture relative to the melting points of the individual components or that expected for an ideal liquid phase [38]. Most studies have focused on quaternary ammonium and imidazolium cations, with particular emphasis being placed on systems using cholinium chloride, a cost-efficient chemical produced on a scale of millions per year, as an animal feed supplement [39]. An upmost within the scope of the development of pharmaceutically active eutectic systems, due to the prevalence of cholinium in the human body, once cholinium serves many physiological functions due to its incorporation in membrane components, neurotransmitters, and signaling molecules [6].

All the 16 binary mixtures (HBA:IBU) studied in this work were prepared as described in Section 2.2, and their validation as eutectic mixtures were firstly achieved implementing the described lab benchtop procedure (dynamic visual method; Section 2.2), prior to DSC validation. 12 out of the 16 prepared binary mixtures were validated as pharmaceutically active eutectic systems, and all were liquid at room temperature. This temperature is much lower than the melting temperature of the neat ibuprofen (**Table 4.3**). For the cholinium-based systems ($[N_{1112(OH)}]Cl:Ibu$) only the molar ratio 1:5 was validated as eutectic system. Regarding the mixtures containing imidazolium-based ILs ($[C_{2(OH)}C_1Im]Cl$, $[C_2C_1Im]Cl$, and $[C_2C_1Im][C_1CO_2]$), only the mixture $[C_{2(OH)}C_1Im]Cl:Ibu$ 2:1 was not validated as a pharmaceutically active eutectic system. All these results are summarized in **Table 4.S1** of the Supporting Information.

The eutectic systems, the neat hydrogen-bond donor (ibuprofen) and hydrogen-bond acceptors ($[C_{2(OH)}C_1Im]Cl$, $[C_2C_1Im]Cl$, $[C_2C_1Im][C_1CO_2]$, and $[N_{1112(OH)}]Cl$) were analyzed by 1H NMR. The 1H NMR has been previously used to characterize H-bonds interaction in eutectic systems and ionic liquids showing its utility to investigate structures and interactions at molecular level [41–43]. All the ibuprofen-based eutectic systems showed

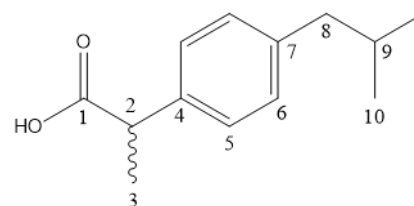
sharp and well-defined signals allowing to confirm the ratios of the counterparts, to verify that ibuprofen and the HBA have not reacted, and to study intermolecular interactions. It is well known that the strength of H-bonds affects the chemical shifts, therefore the chemical shifts in the vicinity of ibuprofen carboxyl group (-COOH), *viz.* position 2 and 3 of the chemical structure depicted in **Table 4.2**, were analyzed. As can be seen in **Table 4.2**, the eutectic systems presented similar chemical shifts for both positions 2 and 3 with the exception of [C₂C₁Im][C₁CO₂]-based systems, where a clear change in the chemical shifts upfield with the increase of HBA molar ratio was verified. Additionally, deviations of the chemical shifts of the most acidic proton in the imidazolium ring of the [C₂C₁Im][C₁CO₂] (HBA) as well as the -CH₃ presented on the acetate anion, *viz.* position 2' and 10', respectively, was verified (**Table 4.S2** in Supporting Information). The H₂' proton of the imidazolium cation shows a upfield shift, while the methyl protons H₁₀' of the acetate anion presented a downfield shift. All the deviations of the proton resonance verified in the HBD and HBA corroborate the major role of H-bonding in the IL:API eutectic systems formation. Also, the hydroxyl group (-COOH) of ibuprofen was not detected in the ¹H NMR in DMSO of the [C₂C₁Im][C₁CO₂]-based eutectic systems, while the others eutectic systems showed one sharp chemical shift at 12-13 ppm, indicative of the stronger H-bonding in the [C₂C₁Im][C₁CO₂]:Ibu eutectic systems. The full ¹H NMR characterization of all eutectic systems is available in Supporting Information.

Table 4.3 summarized the glass transition temperature (*T_g*) and melting temperature (*T_m*) of the ibuprofen-based eutectic systems, ibuprofen, and all hydrogen-bond acceptors. All the mixtures validated as eutectic system using the lab benchtop procedure were confirmed by DSC at heating/cooling rate of 1°C/min. No *T_m* was determined for [N_{1112(OH)}]Cl in the range of temperatures tested by DSC ([-90°C, 100°C]), since the melting temperature is higher than 300°C with decomposition (e.g. *T_m* = 302°C [40]). Plus, decomposition prevents, or at least strongly hinders, the use of direct techniques for the measurement of the melting temperature. The DSC of [N_{1112(OH)}]Cl presents a sharp endothermic peak (solid-solid transition, *T_{S-S}*) at 79.2°C (*c.f.* **Figure 1**), that results from a crystallographic arrangement phase transition [44]. The reported

solid-solid transition, in agreement with previous studies [44,45], is listed in **Table 4.3** alongside the T_m reported by Abbott and co-workers [40], to validate the eutectic systems in the range of temperatures tested by DSC. **Figure 4.1** shows the DSC traces for all the prepared mixtures $[N_{1112(OH)}]Cl:Ibu$ at $1^\circ C/min$ rate. $[N_{1112(OH)}]Cl:Ibu$ 1:5, the only eutectic of the four $[N_{1112(OH)}]Cl:Ibu$ molar ratio prepared (2:1, 1:1, 1:2 and 1:5), remains liquid upon cooling (subcooled liquid state) until it reaches a vitreous transition at low temperature. The glass transition with enthalpic relaxation is achieved at $-50.11^\circ C$ in the heating part of the cycle. On heating above the T_g , $[N_{1112(OH)}]Cl:Ibu$ 1:5 exhibits an exothermic broaden crystallization peak (cold crystallization temperature) followed by an endothermic melting peak at $13.87^\circ C$. This eutectic shows thermal hysteresis.

Table 4.2. 1H NMR chemical shifts for the position 2 and 3 according to the chemical structure of ibuprofen (right) for all the eutectic systems in DMSO.

Compounds	2 (δ/ppm)	3 (δ/ppm)
Ibuprofen [30]	3.63	1.35
$[C_2C_1Im]Cl:Ibu$ 2:1	3.64	1.34
$[C_2C_1Im]Cl:Ibu$ 1:1	3.63	1.33
$[C_2C_1Im]Cl:Ibu$ 1:2	3.63	1.34
$[C_2C_1Im]Cl:Ibu$ 1:5	3.63	1.34
$[C_{2(OH)}C_1Im]Cl:Ibu$ 1:1	3.63	1.34
$[C_{2(OH)}C_1Im]Cl:Ibu$ 1:2	3.63	1.35
$[C_{2(OH)}C_1Im]Cl:Ibu$ 1:5	3.63	1.34
$[C_2C_1Im][C_1CO_2]:Ibu$ 2:1	3.31	1.22
$[C_2C_1Im][C_1CO_2]:Ibu$ 1:1	3.41	1.25
$[C_2C_1Im][C_1CO_2]:Ibu$ 1:2	3.49	1.27
$[C_2C_1Im][C_1CO_2]:Ibu$ 1:5	3.57	1.31
$[N_{1112(OH)}]Cl:Ibu$ 1:5	3.63	1.34



The $[N_{1112(OH)}]Cl:Ibu$ molar ratio 2:1, 1:1 and 1:2 were not validated as eutectics using the lab benchtop procedure, which was corroborated by the DSC traces depicted in **Figure 4.1**. Despite, $[N_{1112(OH)}]Cl:Ibu$ 1:1 and 1:2 exhibit cold crystallization temperature (broaden band) and thus depending on the cooling-heating cycles these mixtures can be easily handled as liquid at room temperature, which is beneficial for the development of new drug delivery systems that are emerging as good candidates for controlled delivery of APIs, e.g. incorporation of APIs into bacterial nanocellulose membranes for transdermal drug delivery systems [15], and adsorption of APIs onto mesoporous silica-based

materials [46]. The DSC trace for the molar ratio 2:1 is not shown since a liquid mixture was not attained.

The DSC traces at 1°C/min for the imidazolium-based systems (eutectics, non-eutectics, and individual compounds) can be found in Supporting Information (**Figure 4.S1-S3**). All the prepared eutectics containing imidazolium-based ILs ($C_{2(OH)}C_1Im$]Cl, $[C_2C_1Im]Cl$, and $[C_2C_1Im][C_1CO_2]$) are liquid at room temperature (**Table 4.3**), and show no melting or freezing behavior in the DSC measurements, even when slowly heated and cooled at a scan rate of 1°C/min. For all the ibuprofen-based eutectics studied in this work, conjugated with imidazolium-based ILs or cholinium chloride, a discontinuity in the heat flux is observed at lower temperatures, due to the glass transition. This second order transition, with no latent heat associated, unfolds in the DSC as a step transition. It denotes a change in the structure of the material from a glass-like state to a rubber-like state, or vice-versa, imaged in a jump in heat capacity. The observed glass transition allows the determination of the glass transition temperature (T_g) and the classification of all the prepared ibuprofen-based eutectics as glass formers. This is also true only for ibuprofen (HBD; parent API). Particularly relevant is the decrease of the initial melting point and glass transition temperature of the parent-API (ibuprofen; listed in **Table 4.3**) by its conjugation with the imidazolium-based ILs and cholinium salt. All the prepared pharmaceutically active eutectics are liquid at room temperature.

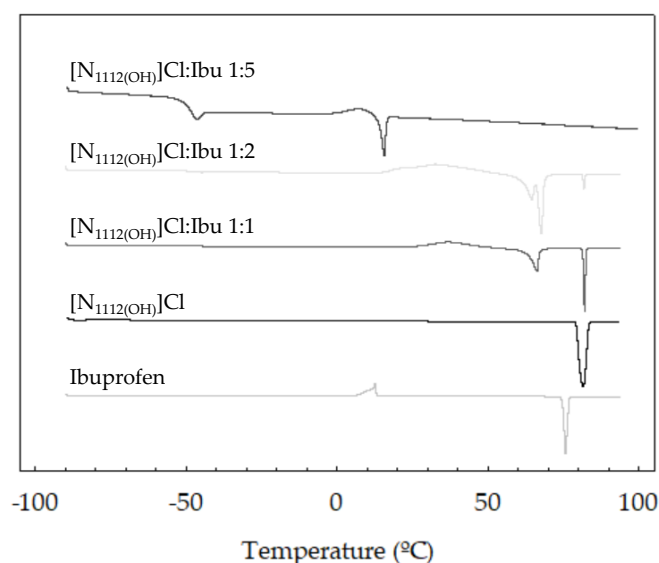


Figure 4.1. DSC curves at 1° C/min for $[N_{1112(OH)}]Cl$: Ibu systems, ibuprofen (HBD) and $[N_{1112(OH)}]Cl$ (HBA). Exo up in all thermograms.

Table 4.3. Thermal properties (T_g and T_m) of the ibuprofen-based eutectic systems, ibuprofen (HBD) and hydrogen-bond acceptors, determined by DSC at a heating rate of 1°C/min. A solid-solid transition is reported for [N_{1112(OH)}]Cl for eutectics validation in the range of temperatures tested by DSC.

	T_g (C°)	T_m (C°)
Ibuprofen [30]	-43.57	74.89
[C _{2(OH)} C _{1Im}]Cl	-	77.48
[C ₂ C _{1Im}]Cl	-	71.39
[C ₂ C _{1Im}][C ₁ CO ₂]	-	-76.16
[N _{1112(OH)}]Cl	-	302 [38] (T_{s-s} , 79.20)
[C _{2(OH)} C _{1Im}]Cl:Ibu 1:1	-48.27	-
[C _{2(OH)} C _{1Im}]Cl:Ibu 1:2	-46.96	-
[C _{2(OH)} C _{1Im}]Cl:Ibu 1:5	-48.33	-
[C ₂ C _{1Im}]Cl:Ibu 2:1	-54.35	-
[C ₂ C _{1Im}]Cl:Ibu 1:1	-56.27	-
[C ₂ C _{1Im}]Cl:Ibu 1:2	-48.80	-
[C ₂ C _{1Im}]Cl:Ibu 1:5	-54.14	-
[C ₂ C _{1Im}][C ₁ CO ₂]:Ibu 2:1	-66.76	-
[C ₂ C _{1Im}][C ₁ CO ₂]:Ibu 1:1	-69.50	-
[C ₂ C _{1Im}][C ₁ CO ₂]:Ibu 1:2	-52.74	-
[C ₂ C _{1Im}][C ₁ CO ₂]:Ibu 1:5	-50.61	-
[N _{1112(OH)}]Cl:Ibu 1:5	-50.11	13.87

4.1.4.2 Hydrogen-bond acceptor ability (β) and dipolarity/polarizability (π^*) of Ibuprofen-based eutectics

The unique properties of ILs are related to their ionic nature and their ability to form varied type of interactions, dipolar, dispersion or hydrogen-bonding [47,48]. The existence of functional groups in a drug that can form hydrogen bonds, can increase its solubility and the ability to establish important interactions with its biomolecular targets, driving the binding and selectivity. Herein, imidazolium-based ILs ([C₂C_{1Im}]Cl, [C_{2(OH)}C_{1Im}]Cl, [C₂C_{1Im}][C₁CO₂]) and cholinium chloride were combined with ibuprofen (Table 4.1 for all the structures) at the molar ratio of 2:1, 1:1, 1:2 and 1:5 to prepare pharmaceutically active eutectics (Table 4.3 and Table 4.S1 in Supporting Information), exploiting the eutectics easy preparation without purification steps and the ILs nanostructured character, higher polarity and wide hydrophilicity-hydrophobicity range. In fact, the weaker hydration of hydrogen bond donors implies that attempts to

address polarity surfeit in the optimization of permeability in drug formulations should be focused on hydrogen bond acceptors [49]. Which is one of the motives in applying ILs as HBA in the formulation of ibuprofen-based eutectics.

Understanding the interactions of a drug molecule with its microenvironment, which greatly affects the physico-chemical properties of a solute molecule, is relevant in different fields such as biology, biochemistry, physics, pharmacy, and medicine [49]. Further, drugs change their environments many times before reaching the target receptor (from polar aprotic – physiologic fluids to a relatively non-polar receptor hilus). Polarity (the sum of all possible interactions between a solvent and any potential solute [10,50]), is a complex property once different intra- and inter-aggregate/ion pair interactions (e.g. hydrogen bonding, π -interactions, van der Waals forces) are involved, plays an important role in solvation phenomena. Accordingly, the polarity of the developed ibuprofen eutectic formulations was studied through solvatochromic responses of UV-vis absorption probes, namely the Kamlet-Taft (KT) approach (Section 2.7) [10,51]. This approach assumes that the solute-solvent interactions are of two kinds, non-specific (polarity/polarizability) and specific (hydrogen bond donor and hydrogen bond acceptor complexing) interactions.

In this work two of the Kamlet-Taft parameters, specifically KT β parameter (the H-bond basicity or the H-bond acceptor ability) and KT π^* parameter (polarity/polarizability), were determined for the twelve ibuprofen-based eutectic systems (Table 4.3). Most of the relevant properties of ILs regarding biological applications depend on solute-solvent interactions that are usually determined by the nature of the anion rather than the cation [52]. The hydrogen-bond basicity (β value) is one of the most important parameters reflecting the hydrogen bond accepting ability of the IL anion [32]. Further, almost all biological applications involve aqueous solutions (water and biological fluids). The addition of water into ILs has a great impact on the β parameter [53], mainly due to the water's relatively hydrogen bond basicity ($\beta = 0.13 \pm 0.014$ [10]). The KT β and π^* parameters were determined for all the twelve Ibu-based eutectic systems (all liquid) at 25°C (Table S3 in Supporting Information). The values for

the same solvatochromic parameters for $[\text{C}_2\text{C}_1\text{Im}][\text{C}_1\text{CO}_2]$, only HBA liquid at 25°C, and water are also included for comparison purposes (with the same dyes). Ibuprofen (HBD) is solid at 25°C, so the determination of the solvatochromic parameters is not possible at room temperature. Our experimental method (Section 4.1.4.7.) was validated in a previous work by measuring the three Kamlet-Taft parameters (α , β and π^*) of two ILs ($[\text{C}_4\text{C}_1\text{Im}][\text{NTf}_2]$ and $[\text{C}_4\text{C}_1\text{Im}][\text{C}_1\text{F}_3\text{SO}_3]$) and water, obtaining a good agreement with those reported in literature [10].

The experimental KT β parameter at 25°C, for the Ibu-based eutectics are plotted in Figure 4.2 and depicted in Table 4.S3 in Supporting Information. The KT β parameter describes the material capacity to accept protons or its hydrogen-bond basicity. The β parameter of the all Ibu-based eutectics ranges between 0.662 ($[\text{C}_2\text{C}_1\text{Im}][\text{C}_1\text{CO}_2]$: Ibu 1:5) and 1.048 ($[\text{C}_2\text{C}_1\text{Im}][\text{C}_1\text{CO}_2]$: Ibu 2:1). The minimum and maximum value of β parameter is attained for the eutectics $[\text{C}_2\text{C}_1\text{Im}][\text{C}_1\text{CO}_2]$: Ibu depending on the molar ratio. Considering the values depicted in Table 4.S3 for the pure $[\text{C}_2\text{C}_1\text{Im}][\text{C}_1\text{CO}_2]$ (HBA), it is clear that the hydrogen-bond basicity of the Ibu-based eutectics is mainly governed by the HBA, the imidazolium-based ILs and cholinium chloride. For the Ibu-based eutectics composed of imidazolium-based ILs as HBA, the β value increases with the increase of HBA molar ratio. The KT β values reported in the literature for methanol, ethanol and glycerol are 0.66, 0.75 and 0.51, respectively [54,55], meaning that the Ibu-based eutectics display a higher ability to accept protons than these solvents. KT β values up to 1.15 have been reported for ILs composed of anions with high ability to accept protons, such as $[\text{C}_2\text{C}_1\text{Im}][\text{C}_1\text{CO}_2]$ [10]. For one of the most studied eutectics, $[\text{N}_{1112}(\text{OH})]\text{Cl}$ and glycerol in a 1:2 molar ratio, it was reported a β value of 0.544 [56]. For all the Ibu-based eutectics developed in this work, KT β values higher than 0.66 were obtained, confirming thus their high ability to establish hydrogen bonds.

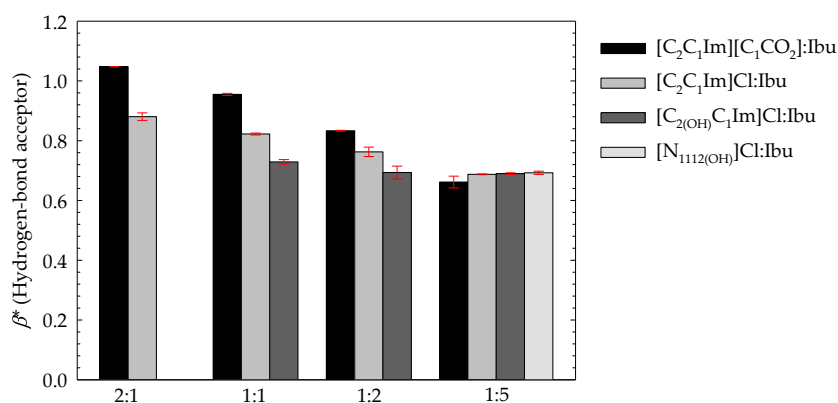


Figure 4.2. Hydrogen-bond acceptance ability (β) of ibuprofen-based eutectic systems. All β values are the average of three independent measurements.

The experimental KT π^* parameter at 25°C, for the Ibu-based eutectics are plotted in **Figure 4.3** and depicted in **Table 4.S3** of Supporting Information. The KT π^* parameter is related to non-specific interactions (polarizability, and dipole-dipole and dipole-induced dipole interactions) occurring between the solute and the solvent. The π^* parameter of the all Ibu-based eutectics ranges between 0.715 ([N_{1112(OH)}]Cl: Ibu 1:5) and 1.008 ([C₂C₁Im]Cl:Ibu 2:1). For the Ibu-based eutectics composed of imidazolium-based ILs as HBA, the π^* value increases with the increase of HBA molar ratio. Considering the values depicted in **Table 4.S3** for the pure [C₂C₁Im][C₁CO₂] (HBA), it is clear that the dipolarity/polarizability of the Ibu-based eutectics is mainly governed by the HBA, the imidazolium-based ILs and cholinium chloride. The π^* values reported in the literature for methanol, ethanol and glycerol are 0.58, 0.51 and 0.62, respectively [54,55], meaning that the Ibu-based eutectics display a higher ability to establish non-specific with a solute than organic molecular solvents. Further, this parameter presents a similar magnitude to that found in pure ILs ($\pi^* = 1.05$ for [C₂C₁Im][C₁CO₂] [10]) as well as in one of the most studied eutectics ($\pi^* = 1.161$ for [N_{1112(OH)}]Cl:Glycerol in a 1:2 molar ratio [56]). For all the Ibu-based eutectics developed in this work, π^* values higher than 0.71 were obtained, confirming thus their high polarity and ability to establish dipole-dipole and dipole-induced dipole interactions. This similarity to ILs results from the presence of ions in both classes of compounds. Alike, the KT π^* increases with the salt content in the eutectic composition (higher amount of ionic species).

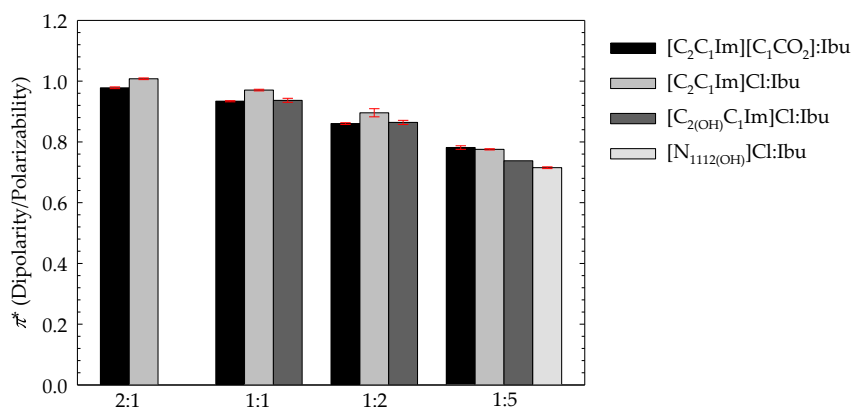


Figure 4.3. Dipolarity/polarizability (π^*) of ibuprofen-based eutectic systems at 25°C. All π^* values are the average of three independent measurements.

4.1.4.3 Solubility of ibuprofen-based eutectics in water and biological simulated

The solubility behavior of drugs plays a major role in bioavailability and often is a limiting factor for the drug therapeutic effectiveness [19]. The conversion of ibuprofen into pharmaceutical active ionic liquids (API-ILs) significantly increased the parent API solubility in water and buffer solutions suitable for dissolution testing as described in our previous work [18]. The use of ILs as HBAs in pharmaceutically active eutectics has never, to the best of our knowledge, been previously described or investigated. Still, two recent contributions from two of the coauthors of the present work address the absorption of fluorinated gases in eutectic systems synthesized using ILs as HBAs and perfluorinated acids as HBDs [29,57]. In the present work, imidazolium-based ILs ([C₂C₁Im]Cl, [C₂(OH)C₁Im]Cl, [C₂C₁Im][C₁CO₂]; **Table 4.1**) and cholinium chloride were combined with ibuprofen at the molar ratio of 2:1, 1:1, 1:2 and 1:5 to prepare pharmaceutically active eutectics (**Table 4.3**), exploiting the eutectics easy preparation without purification steps and the ILs nanostructured character, higher polarity and wide hydrophilicity-hydrophobicity range. Differences in solubility would be expected as the API is in a different state, in the eutectic formulation ibuprofen is in the liquid state while naturally the parent API is found to be in the powder/solid form. Accordingly, we evaluated the aqueous solubility, water and buffer solutions under physiological pH conditions (simulated gastric without enzymes – interchangeable with 0.1 N HCl (pH 1.0), simulated intestinal fluid without enzymes – interchangeable with

phosphate standard buffer pH 6.8, and 0.15 M NaCl – isotonic ionic strength), of the synthesized ibuprofen-based eutectics and neat ibuprofen. Further, the non-eutectic formulations were also analyzed, playing with the hydrotrophy phenomenon, first reported by Neuberg in 1916 [58], that demonstrated the increased solubility of sparingly soluble compounds in water by addition of alkali metal salts of short alkyl chain organic acids. More recent studies [59,60] proposed that the formation of co-aggregates between the solute and the hydrotropes is the main driver to the enhanced solubilization observed. Recently, Cláudio and co-workers [61] studied the ability of ILs to act as hydrotropes, enhancing the solubility in water of two phenolic compounds, namely gallic acid and vanillin, and establishing ILs as a new class of catanionic hydrotropes with a superior performance since both the IL cation and anion may contribute to enhance the solubility of poorly soluble compounds in aqueous solution. The potential of ILs to act as hydrotropes was here investigated based on their ability to enhance the aqueous solubility of ibuprofen, using the molar ratios not validated as eutectics (Table S1 in Supporting Information). Fresh samples were used to avoid structural changes or environmental effects on the physical properties of all the studied systems (eutectics and non-eutectics) and to prevent moisture formation. The increase of ibuprofen molar ratio (HBA:IBU 2:1, 1:1, 1:2 and 1:5) and the influence of HBA ($[\text{C}_{2(\text{OH})}\text{C}_1\text{Im}]\text{Cl}$, $[\text{C}_2\text{C}_1\text{Im}]\text{Cl}$, $[\text{C}_2\text{C}_1\text{Im}][\text{C}_1\text{CO}_2]$, and $[\text{N}_{1112(\text{OH})}]\text{Cl}$) in the formation and properties of eutectic systems, as well as in the non-eutectic systems characteristics as hydrotropes, were evaluated. The solubilities in water and simulated biological fluids at 25°C for the eutectic and non-eutectic systems are listed in **Table 4.4**.

The solubilities of ibuprofen in water and buffer solutions under physiological pH conditions, determined in our previous work [18], are as follow, 0.279 ± 0.007 mM (water), 0.353 ± 0.013 mM (0.15M NaCl), 20.2 ± 0.6 mM (pH 6.8) and 0.215 ± 0.005 mM (pH 1.0). All the ibuprofen-based eutectics increased the solubility in all aqueous media, except for the molar ratio 1:5 in simulated intestinal fluid (pH 6.8) for the following three HBA, $[\text{C}_{2(\text{OH})}\text{C}_1\text{Im}]\text{Cl}$, $[\text{C}_2\text{C}_1\text{Im}]\text{Cl}$ and $[\text{N}_{1112(\text{OH})}]\text{Cl}$ (**Figure 4.4**), which present slightly lower solubilities than neat ibuprofen (lower up to 1.2-fold). The most evident increase in solubility is observed for the eutectic $[\text{C}_2\text{C}_1\text{Im}][\text{C}_1\text{CO}_2]:\text{Ibu}$ 2:1 in

water and in isotonic ionic strength aqueous solution (0.15M NaCl), which presents a 38-fold increase (from 0.279 mM to 10.6 mM) and a 30-fold increase (from 0.353 mM to 10.7 mM), respectively. In simulated intestinal fluid (pH 6.8), the highest increase is observed for [C₂C₁Im][C₁CO₂]:Ibu 1:1, which presents a 2.3-fold increase in the solubility from 20.2 mM to 46.0 mM. In simulated gastric fluid (pH 1.0), the highest increase in the solubility is observed for the eutectic [C_{2(OH)}C₁Im]Cl:Ibu 1:1, up to 4.9-fold increase from 0.215 mM to 1.06 mM. Abbott and co-workers also successfully increased the solubility of aspirin, a carboxylic acid API, in water, using the eutectics approach combining the API with cholinium chloride [19]. A similar behavior in the solubility at pH 7 was observed by Duarte et al. [3], where the increased solubility of ibuprofen, benzoic acid and phenylacetic acid was achieved by the formulation of a eutectic system with menthol.

The 1:5 molar ratio is the unique HBA:Ibu molar ratio that is a eutectic for all the four studied HBA, [C_{2(OH)}C₁Im]Cl, [C₂C₁Im]Cl, [C₂C₁Im][C₁CO₂] and [N_{1112(OH)}]Cl (**Table 4.3** and **Table 4.S1** in Supporting Information), allowing to assess the effect of the different HBA's (**Table 4.S4** in Supporting Information). The trend of the aqueous solubilities of the HBA:Ibu 1:5 eutectics is as follow (t-test, 1 tailed, confidence level 90%, p<0.05):

Water: [C₂C₁Im][C₁CO₂] > [N_{1112(OH)}]Cl ≈ [C_{2(OH)}C₁Im]Cl > [C₂C₁Im]Cl.

pH 1.0: [N_{1112(OH)}]Cl ≈ [C₂C₁Im][C₁CO₂] > [C_{2(OH)}C₁Im]Cl > [C₂C₁Im]Cl.

pH 6.8: [C₂C₁Im][C₁CO₂] > [C_{2(OH)}C₁Im]Cl ≈ [C₂C₁Im]Cl ≈ [N_{1112(OH)}]Cl.

0.15 M NaCl: [C₂C₁Im][C₁CO₂] > [N_{1112(OH)}]Cl > [C_{2(OH)}C₁Im]Cl > [C₂C₁Im]Cl.

The major impact in aqueous solubility is attained by the HBA's [C₂C₁Im][C₁CO₂] and [N_{1112(OH)}]Cl, where [C₂C₁Im][C₁CO₂] has the highest impact. Generally, the 1:5 molar ratio presented a similar trend for water, isotonic ionic strength solution (0.15 M NaCl) and simulated gastric fluid (pH 1.0). For simulated intestinal fluid (pH 6.8), the highest impact in the ibuprofen solubility is also attained by [C₂C₁Im][C₁CO₂], although the other 3 HBA's ([C_{2(OH)}C₁Im]Cl, [C₂C₁Im]Cl and [N_{1112(OH)}]Cl) has similar impact, there's no

significant difference between the solubilities, all the eutectics present slightly lower solubilities than neat ibuprofen (lower up to 1.2-fold).

Table 4.4. Solubility of ibuprofen-based eutectic and non-eutectic systems in water, isotonic ionic strength aqueous solution (0.15 M NaCl), simulated intestinal fluid (pH 6.8) and simulated gastric fluid (pH 1.0) at 25°C. The solubility is the overall mean of three independent experiments \pm standard deviation.

Eutectic systems	Solubility (mM)			
	Water	0.15M NaCl	pH 6.8	pH 1.0
Ibuprofen [30]	0.279 \pm 0.007	0.353 \pm 0.013	20.2 \pm 0.6	0.215 \pm 0.005
[C _{2(OH)} C ₁ Im]Cl:Ibu 1:1	1.00 \pm 0.01	1.49 \pm 0.01	37.0 \pm 0.4	1.06 \pm 0.02
[C _{2(OH)} C ₁ Im]Cl:Ibu 1:2	0.649 \pm 0.013	0.698 \pm 0.012	31.3 \pm 0.4	0.778 \pm 0.022
[C _{2(OH)} C ₁ Im]Cl:Ibu 1:5	0.828 \pm 0.017	1.42 \pm 0.04	17.3 \pm 0.4	0.668 \pm 0.016
[C ₂ C ₁ Im]Cl:Ibu 2:1	0.941 \pm 0.037	1.37 \pm 0.02	37.9 \pm 0.6	0.676 \pm 0.009
[C ₂ C ₁ Im]Cl:Ibu 1:1	0.642 \pm 0.017	0.987 \pm 0.024	34.1 \pm 0.4	0.695 \pm 0.011
[C ₂ C ₁ Im]Cl:Ibu 1:2	0.806 \pm 0.022	0.794 \pm 0.020	28.7 \pm 0.5	0.960 \pm 0.028
[C ₂ C ₁ Im]Cl:Ibu 1:5	0.787 \pm 0.007	0.963 \pm 0.013	17.3 \pm 0.4	0.596 \pm 0.010
[C ₂ C ₁ Im][C ₁ CO ₂]:Ibu 2:1	10.6 \pm 0.2	10.7 \pm 0.1	32.7 \pm 0.5	0.889 \pm 0.009
[C ₂ C ₁ Im][C ₁ CO ₂]:Ibu 1:1	9.56 \pm 0.10	6.66 \pm 0.09	46.0 \pm 0.6	0.852 \pm 0.017
[C ₂ C ₁ Im][C ₁ CO ₂]:Ibu 1:2	4.32 \pm 0.04	4.91 \pm 0.07	36.2 \pm 0.7	0.705 \pm 0.005
[C ₂ C ₁ Im][C ₁ CO ₂]:Ibu 1:5	1.75 \pm 0.01	5.03 \pm 0.09	35.7 \pm 0.5	0.714 \pm 0.007
[N _{1112(OH)}]Cl:Ibu 1:5	0.833 \pm 0.010	2.69 \pm 0.04	16.7 \pm 0.04	0.766 \pm 0.020
Non-eutectic systems	Solubility (mM)			
	Water	0.15M NaCl	pH 6.8	pH 1.0
[N _{1112(OH)}]Cl:Ibu 2:1	1.07 \pm 0.01	0.961 \pm 0.012	41.6 \pm 0.4	0.612 \pm 0.015
[N _{1112(OH)}]Cl:Ibu 1:1	0.837 \pm 0.023	0.555 \pm 0.006	31.0 \pm 0.3	0.313 \pm 0.011
[N _{1112(OH)}]Cl:Ibu 1:2	0.720 \pm 0.009	0.562 \pm 0.006	23.6 \pm 0.2	0.255 \pm 0.009
[C _{2(OH)} C ₁ Im]Cl:Ibu 2:1	1.37 \pm 0.02	1.01 \pm 0.02	48.9 \pm 0.9	0.986 \pm 0.010

Only for the HBA's [C₂C₁Im]Cl and [C₂C₁Im][C₁CO₂] (Table 4.3 and Table 4.S1 in Supporting Information), one can assess the effect of the increasing ibuprofen molar ratio of the eutectics for all the four studied ratios (HBA:Ibu 2:1, 1:1, 1:2 and 1:5), in the aqueous solubility of ibuprofen. The trend of the solubilities in water and buffer solutions under physiological conditions for the eutectics [C₂C₁Im]Cl:Ibu and [C₂C₁Im][C₁CO₂]:Ibu are depicted in Table 4.S4 of the Supporting Information, denoting that the aqueous solubilities are HBA-dependent.

Although [N_{1112(OH)}]Cl:Ibu 2:1, 1:1 and 1:2 and [C_{2(OH)}C₁Im]Cl:Ibu 2:1 are non-eutectic formulations (Table 4.3 and Table 4.S1 in Supporting Information), solubility studies

were performed to assess the hydrotrophy phenomenon [59,60]. The solubility results of the non-eutectic systems are summarized in **Table 4.4** and illustrated in **Figure 4.4**, alongside the eutectic systems results. All the ibuprofen-based non-eutectic formulations increased the ibuprofen solubility in all aqueous media (**Figure 4.4**). The higher increase in ibuprofen solubility is attained for the non-eutectic formulation $[C_{2(OH)}C_1Im]Cl:Ibu$ 2:1 in water, 0.15M NaCl, pH 6.8 and pH 1.0, which presents a 4.9-fold increase (from 0.279 mM to 1.37 mM), a 2.9-fold increase (from 0.353 mM to 1.01 mM), a 2.4-fold increase (from 20.2 mM to 48.9 mM) and a 4.6-fold increase (from 0.215 mM to 0.986 mM), respectively. The effect of the different HBA's in ibuprofen solubility, eutectic and non-eutectic formulations, is summarized in **Table 4.S5** of Supporting Information. The trend of the aqueous solubilities of the HBA:Ibu 2:1 formulations (t-test, 1 tailed, confidence level 90%, $p < 0.05$), indicates that the higher ibuprofen solubility is achieved by the non-eutectic formulation in simulated intestinal fluid (pH 6.8) and simulated gastric fluid (pH 1.0). Additionally, the effect of increasing ibuprofen molar ratio in the aqueous solubility of ibuprofen for all the four studied ratios (HBA:Ibu 2:1, 1:1, 1:2 and 1:5), eutectic and non-eutectic formulations, is summarized in **Table 4.S5** of Supporting Information. The trend of the solubilities of $[C_{2(OH)}C_1Im]Cl:Ibu$ and $[N_{1112(OH)}]Cl:Ibu$ formulations (t-test, 1 tailed, confidence level 90%, $p < 0.05$) in water and simulated intestinal fluid (pH 6.8), indicates that the higher ibuprofen solubility is achieved by the non-eutectic formulation HBA:Ibu 2:1. The results denote that the aqueous solubilities are HBA-dependent, similarly to the observed for the eutectics.

Overall, the solubility results show that the impact of the eutectic and non-eutectic formulations are similar, once both formulations are playing with the hydrotrophy phenomenon to enhance the solubility of ibuprofen in water and simulated biological fluids. A defining characteristic of type III eutectics (HBD mixed with an organic salt; the eutectics prepared herein) is likely hydrogen bonding [39]. Computational studies, including MD, have elucidated the nanostructure of various eutectics and eutectics-water mixtures and supported the contribution of hydrogen bonding to the depression of the melting temperatures [62,63]. Additionally, many authors have addressed the nanostructure of eutectics-water mixtures to understand the interaction between water

and the hydrogen bond network within eutectics. Showing that low quantities of water strengthen the hydrogen bond within the eutectic, and that the increase of water concentration weakens the interaction between the eutectic components, up to a behavior typical of solutes in aqueous solution [62,64,65]. In this work, all the solutions (Table 4.4) have a concentration greater or equal than 99.9 mol% of water, and at this water concentration the whole system simple behaves as a pool of aqueous solution containing its constituents species [64,66–68]. Despite the similar solubility enhancement for both eutectics and non-eutectics formulations when compared to the parent API (ibuprofen; Figure 4.4), the non-eutectics systems are solid at room temperature contributing to a main disadvantage for APIs bioavailability [1]. The solubility of ibuprofen increased significantly for the eutectics, and its formulation could be handled in a liquid state, which significantly influence the dissolution rate (not discussed in the present work), membrane permeation, activity and stability.

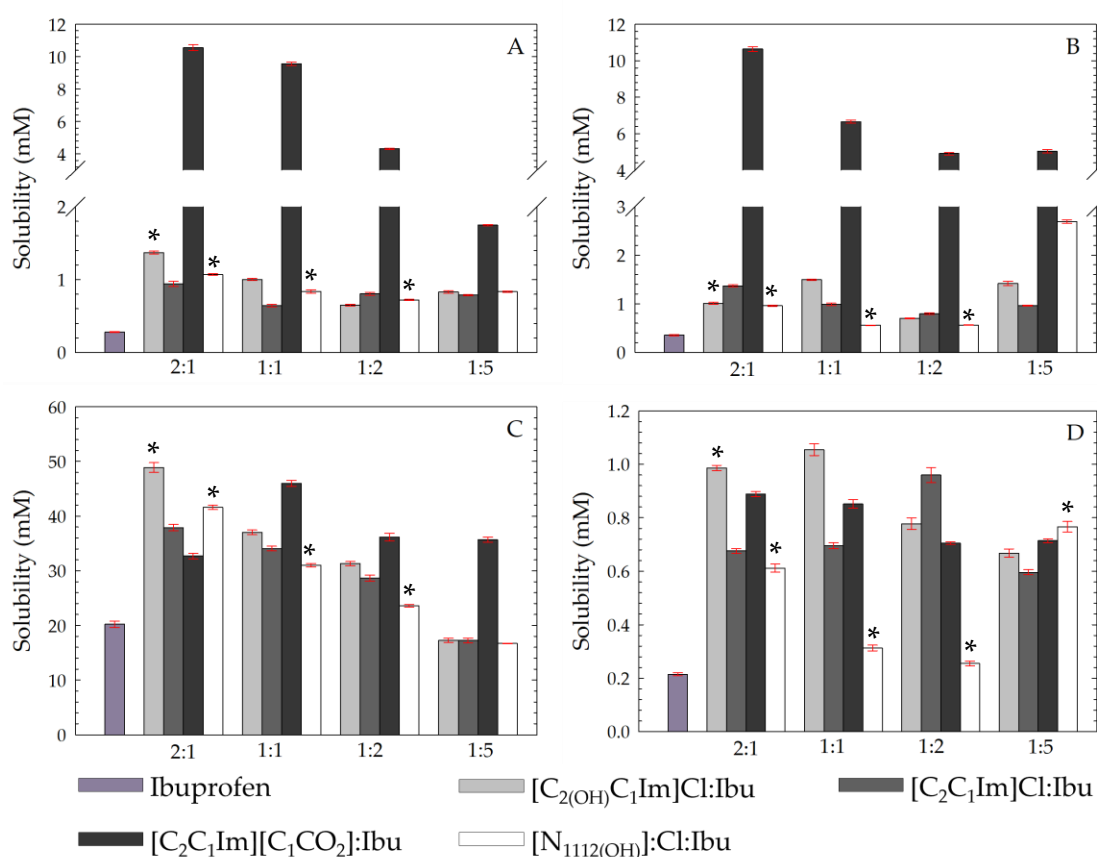


Figure 4.4. Solubility of the ibuprofen-based eutectics, non-eutectics and neat ibuprofen in (A) water and buffer solutions suitable for dissolution testing, (B) isotonic ionic strength aqueous solution (0.15 M NaCl), simulated intestinal fluid (pH 6.8), and (D) simulated gastric fluid (pH 1.0), at 25°C. The * represents the non-eutectic systems.

4.1.4.4 Ionicity *versus* permeation potential of ibuprofen-based eutectic systems

One of the most attractive advantages of API-based eutectics is that the properties of the parent API could be fine-tuned by changing the components and the molar ratio of HBA to HBD. Although ideal eutectic systems consist of non-associated ions, due to the relative high concentration of salts, the ions in the liquid may not diffuse independently of each other, and to some extent the occurrence of aggregates or clusters is verified [69]. In this context, the concept of ionicity, as the effective fraction of ions available to participate in conduction, is of utmost relevance. Ionic interactions could significantly affect other physical properties, such as mobility, which is one of the factors that influences the efficiency of permeation of pharmaceutical formulations for transmembrane transport. For example, the regulations proposed by the FDA suggest that ionicity is responsible for the different behavior of one class of compounds over another [70].

The Walden plot is a convenient and versatile tool for ionicity studies [71,72], since it correlates molar conductivity and viscosity, two properties that are directly related to the occurrence of ion pairs, the formation of larger charged or non-charged aggregates, or the existence of ionic networks. It is mainly used as a qualitative and semi-quantitative measurement, that can be implemented in this field to evaluate the ionicity of eutectics [73,74]. Furthermore, the validity of applying the Walden plot to address the ionicity of eutectics was proven by comparing these values with the ionicity calculated by using the self-diffusion coefficients using the PFG-NMR method [75]. **Figure 4.5** is a plot based on the classical concept of the Walden plot for the twelve ibuprofen-based eutectics (**Table 4.3** and **Table 4.S1** in Supporting Information). Angel and coworkers [71,72] introduced the ΔW value, the vertical deviation to the reference (ideal) line of slope 1 (black line in **Figure 4.5**) that indicates the region of fully dissociated ions like a dilute solution of 0.01 M KCl, to characterize the medium according to this value. In this framework, “good ionic” liquids are fully dissociated and show a $\Delta W < 1$. ILs with $\Delta W = 1$ exhibit only 10% of the ionic conductivity as would have been expected at the ideal line of 0.01 M KCl (blue line in **Figure 4.5**).

Eutectics systems show IL-like behavior, but they cannot be purely ionic because eutectics form across a range of stoichiometries (**Table 4.3** and **Table 4.S1** in Supporting Information). MacFarlane et al [76] identified the existence of ion pairs and clusters in protic pharmaceutically active ILs, supported by a crystal structure analysis of analogous compounds [77], that strongly enhanced the permeation of both ions. Further, the authors verified that the enhanced permeation and the formation of associated species is related to the position of these ILs, sitting well below, relative to ideal line on the Walden plot. The authors hypothesize that these paired compounds behave more like “neutral” species and hence cross the membrane faster than the more “ionic” APIs. Additionally, Peng and coworkers [78,79] reported that IL-ionicity was key to enhance the intestinal absorption of macromolecular drugs such as insulin and immunoglobulin, improving API delivery in the skin, buccal membrane, and small intestine.

The ibuprofen-based eutectics (**Table 4.3** and **Table 4.S1** in Supporting Information) were characterized in terms of their viscosity, conductivity, density and ionicity (*via* Walden plot), to assess their permeation potential.

Viscosity is one of the most important parameters for flow behavior, influencing the mass transport and the hydrodynamic application of eutectics. Generally, eutectics exhibit a relatively high viscosity, which could be attributed to the extensive hydrogen bond network causing lower mobility of the species. In this framework, viscosity is necessary for the calculation of ionicity using the Walden plot. Accordingly, the viscosities of all twelve Ibu-based eutectics were measured in a range of temperatures from 15°C to 80°C (**Section 4.1.4.6**), and all the values are reported in **Table 4.S6-S9** and **Figures 4.S4-S7** of Supporting Information. The viscosity of all ibuprofen-based eutectic system (Table S6-S9) resulted quite high (> 100 mPa.s) at 25°C, probably due to the network of intramolecular hydrogen bonds and to molecular packing formed in these systems originates a reduced mobility of the free species. Temperature-dependent viscosity data is depicted in **Figures 4.S4-S7**. The viscosity of all ibuprofen-based eutectics decreases with increasing temperature over the temperature range studied. The decrease in viscosity with the increasing temperature comes from the weakening of van

der Waals forces and hydrogen bond interactions, and the molecules and ions move easily.

The conductivity of eutectic systems is relevant for their pharmaceutical or electrochemical applications. Also, conductivity is necessary to address the ionicity of eutectics using the Walden plot. For that, the conductivities of all twelve Ibu-based eutectics were measured in a range of temperatures from 15°C to 50°C (Section 4.1.4.6; upper temperature is limited by the conductivity standards), and all the values are reported in Table 4.S6-S9 and Figures 4.S4-S7 of Supporting Information. The conductivity of all Ibu-based eutectics increases as the temperature increases. Conductivity depends on the amount of free charges and on their mobility. The conductivity of the eutectics is diminished by limited free charges and high viscosities.

Density and its temperature dependence are relevant thermophysical properties, and in this context for the calculation of molar conductivity, which is further used to achieve ionicity by Walden plot. Therefore, the densities of all Ibu-based eutectics were measured in a range of temperatures from 15°C to 80°C (Section 4.1.4.6), and all the values are reported in Table 4.S6-S9 and Figures 4.S4-S7 of Supporting Information. All the Ibu-based eutectics showed a linear dependence of density with temperature. The density of all eutectics decreases with increasing temperature due to the thermal expansion, in agreement with previously reported eutectics [75,78,79].

The points depicted in Figure 4.5 (Walden plot) represent the temperature dependent molar conductivities and fluidities (reciprocal viscosity) of the twelve Ibu-based eutectics (Table 4.3 and Table 4.S1 in Supporting Information). The eutectics with molar ratio HBA:Ibu 2:1 and HBA:Ibu 1:1 are visible very close to the ideal line of the Walden plot ($\Delta W \approx 0.5$) and are fully dissociated and behave like “good ionic” liquids, and none or only a few ion pairs are expected to exist. The vertical deviation for all the eutectics HBA:Ibu 1:2 are around 1.0 ($\Delta W \approx 1.0$). In this second group the eutectics behave like “poor ionic” liquids, where hydrogen-bonds and other specific interactions are more pronounced. For the eutectics HBA:Ibu 1:5 the vertical deviation is greater than 1.0, and the deviation increase in the following order of HBA, $[N_{1112(OH)}]Cl < [C_2C_1Im][C_1CO_2] <$

$[C_2C_1Im]Cl < [C_{2(OH)}C_1Im]Cl$. The HBA:Ibu 1:5 eutectics are described as liquid ions pairs or “subionic liquids”. In these liquids, ion conductivity is substantially less, based on ion pairs, the formation of larger charged or non-charged aggregates, or the existence of ionic networks.

From the previous discussion on the deviation from the ideal 0.01 M KCl line, the ionicity would decrease in the following order of HBA:Ibu molar ratio, $2:1 \approx 1:1 > 1:2 > 1:5$, which depends on the increase of aggregates or clusters. In the cases such as the HBA:Ibu 1:5 eutectics where the Walden plot indicates large negative deviations from the ideal line, one needs to consider the possibility of much stronger correlations that are not present in the ideal cases, such ion pairing or even large aggregates or networks of ions. The low ionicity observed for the formulations HBA:Ibu1:5 in comparison to fully ionized salts provide the possibility for these liquids to penetrate membranes more efficiently and for the possible future use in transdermal drug delivery and local anti-inflammatory action. One of the advantages of these ibuprofen-based eutectics approach is that active formulations can be designed to be more membrane diffusive in a way that is not otherwise possible.

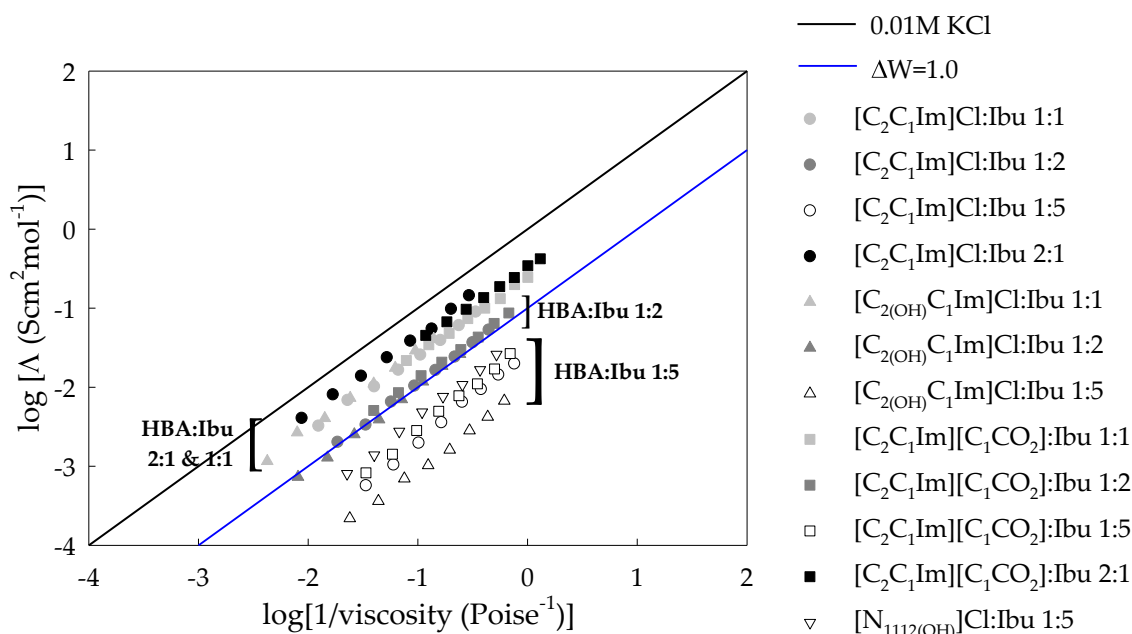


Figure 4.5. Walden plot of ibuprofen-based eutectic systems.

4.1.4.5 Hemolytic activity and cytotoxic profile of ibuprofen-based eutectic systems

The ease associated with isolating erythrocytes makes the hemolytic activity assay a versatile tool for rapid initial toxicity assessment often included in several studies of drug development [80,81]. According to the guidelines of the European Medicines Agency (EMA), an *in vitro* hemolysis study is recommended to ensure that there is no serious potential of pharmacologically mediated toxicity such as drug-induced hemolysis [82]. Additionally, hemolysis represents the most employed initial toxicity assessment in drug development that could be correlated to cytotoxicity assays, since the main reason for toxicity can be related to the disruption of cell membranes [83]. In a previous work, we have evaluated the red blood cell lysis through the hemoglobin release in the plasma for ibuprofen and ibuprofen based ILs [18]. Ibuprofen and ibuprofen-based ILs did not reveal hemolytic activity against human erythrocytes up to 1.5 mM and 3 mM, respectively. In this study, the twelve ibuprofen-based eutectic formulations (**Table 4.3** and **Table 4.S1** in Supporting Information) were analyzed, displaying no hemolytic activity against human erythrocytes up to 3 mM. These results are in line with the results of the ibuprofen-based ILs, once the cations of the HBA used in this work are the same of the ibuprofen-based ILs [18]. Also, we have demonstrated that several imidazolium and cholinium-based ILs are hemocompatible with ~0% hemolytic activity up to 3 mM [83]. Orhan et al. [84] developed a structure–activity correlation suggesting that an aromatic ring with a side chain containing a carbonyl group attached to a nitrogen atom is a requirement for stabilizing the erythrocyte membrane.

Recently, Radošević et al. [35] examined the cytotoxic profile of [N_{1112(OH)}]Cl:Glucose, [N_{1112(OH)}]Cl:Glycerol, and [N_{1112(OH)}]Cl:Oxalic acid eutectic systems on channel catfish ovary fish cell line and the human breast adenocarcinoma cell line. Their results showed that the [N_{1112(OH)}]Cl:Oxalic acid eutectic exhibited a significantly higher toxicity (EC₅₀ < 5 mM) compared to the remaining [N_{1112(OH)}]Cl-based eutectics (EC₅₀ > 10 mM), emphasizing the importance of a careful selection of the eutectics constituents (HBA and/or HBD)[85]. Herein, ibuprofen (parent API) is the HBD of the pharmaceutical

active eutectic formulations (**Table 4.3** and **Table 4.S1** in Supporting Information), with a maximum plasma concentration of 0.175 mM (C_{\max} ; pharmacokinetic parameter), which is the highest level of ibuprofen that can be obtained in the blood usually following multiple doses, above the possible intracellular concentrations. Accordingly, the ibuprofen-based eutectic formulations were tested above/in the range of the ibuprofen C_{\max} to evaluate the cytotoxic profile in the human colon carcinoma cell line, Caco-2, and the hepatocellular carcinoma cell line, HepG2. The results are depicted in **Figure 4.6**. At ibuprofen C_{\max} , all the eutectic formulations present 100% of cellular viability in both HepG2 and Caco-2 cell lines. Additionally, it was not possible to determine the EC_{50} (i.e., effective concentration reducing cell viability to 50%) in both HepG2 and Caco-2 cell lines up to 3 mM. Both cytotoxicity and hemocompatibility results of the studied ibuprofen-based eutectic formulations agree, indicating the suitability and biocompatibility of the cholinium- and imidazolium-based HBA:IBU eutectics for pharmaceutical formulations.

The influence of the molar ratio (2:1, 1:1, 1:2 and 1:5) in the eutectic formulations was evaluated for [C₂C₁Im]Cl:Ibu in HEPG2 (**Figure 4.6 A**) and Caco-2 (**Figure 4.6 C**) cell lines. Comparing the viability curves of ibuprofen and the four [C₂C₁Im]Cl:IBU eutectics in Caco-2 cell line up to 3 mM, no significant changes were observed by increasing the ibuprofen molar ratio. The dose-response cytotoxicity curves in HEPG2 cell line up to 3 mM, indicates that the increase in ibuprofen molar ratio slightly decreases the cellular viability. For the molar ratio 2:1 and 1:1, no significant differences in the viability curves of ibuprofen and [C₂C₁Im]Cl:Ibu eutectics were observed. Similarly, no significant differences were verified for the viability curve between ibuprofen and the ibuprofen-based IL [C₂C₁Im][Ibu] [18]. For the [C₂C₁Im]Cl:Ibu 1:2 and 1:5 eutectics, the cellular viability decreases down to ~80%, having the 1:5 molar ratio the greater impact. The effect of the different HBA's ([C_{2(OH)}C₁Im]Cl, [C₂C₁Im]Cl, [C₂C₁Im][C₁CO₂] and [N_{1112(OH)}]Cl) in the cytotoxicity profiles was evaluated with HBA:Ibu 1:5 molar ratio eutectic formulations (1:5 is only molar ratio that is a eutectic for all the four studied HBA's) in HEPG2 (**Figure 4.6 B**) and Caco-2 (**Figure 4.6 D**) cell lines. Comparing the viability curves of ibuprofen and the four HBA:IBU 1:5 eutectics in Caco-2 cell line up to

3 mM, no significant changes were observed by changing the HBA in the eutectic formulation. The dose-response cytotoxicity curves of HBA:Ibu 1:5 eutectics in HEPG2 cell line up to 3 mM, indicates that the cellular viability is HBA-dependent. For the HBA $[\text{C}_{2(\text{OH})}\text{C}_1\text{Im}]\text{Cl}$ no significant difference in the viability curves of ibuprofen and $[\text{C}_{2(\text{OH})}\text{C}_1\text{Im}]\text{Cl}:\text{Ibu}$ 1:5 eutectic was observed. For the HBA's $[\text{C}_2\text{C}_1\text{Im}]\text{Cl}$, $[\text{C}_2\text{C}_1\text{Im}][\text{C}_1\text{CO}_2]$ and $[\text{N}_{1112(\text{OH})}]\text{Cl}$, the cellular viability decreases down to ~80%, having the $[\text{C}_2\text{C}_1\text{Im}]\text{Cl}:\text{Ibu}$ and $[\text{C}_2\text{C}_1\text{Im}][\text{C}_1\text{CO}_2]:\text{Ibu}$ 1:5 eutectics the greater impact.

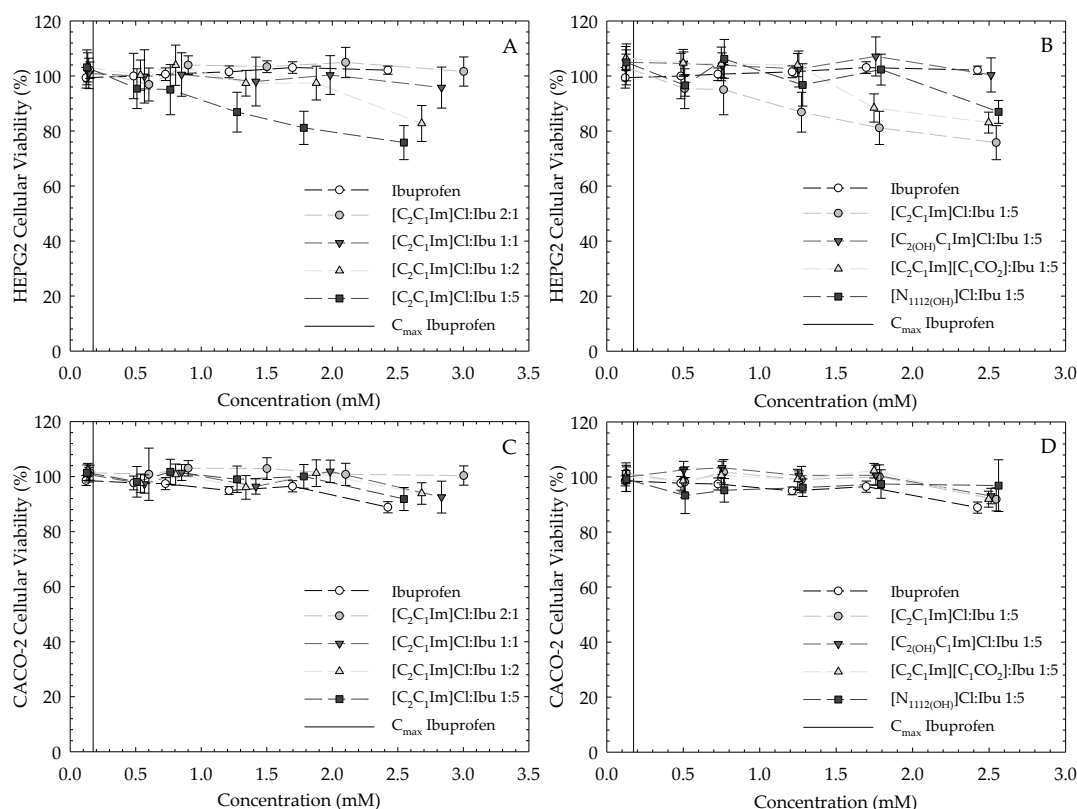


Figure 4.6. Cytotoxicity profile of ibuprofen [18] compared with $[\text{C}_2\text{C}_1\text{Im}]\text{Cl}$ -based eutectics in HEPG2 (A), HBA:Ibu 1:5 molar ratio eutectics in HEPG2 (B), $[\text{C}_2\text{C}_1\text{Im}]\text{Cl}$ -based eutectics in Caco-2 (C) and HBA:Ibu 1:5 molar ratio eutectics in Caco-2 (D). Both cell lines were exposed for 24 h to the eutectic formulations prior to the cytotoxicity assessment. The XX axis guideline corresponds to the pharmacokinetic parameter maximum plasma concentration of ibuprofen (C_{max} , 0.175 mM; [35])

4.1.4.6 Anti-inflammatory activity of ibuprofen-based eutectic systems

The anti-inflammatory activity of the ibuprofen-based eutectic formulations was evaluated against ibuprofen using the inhibition profile of BSA denaturation and the degree of cyclooxygenases (COX-1 and COX-2) inhibition.

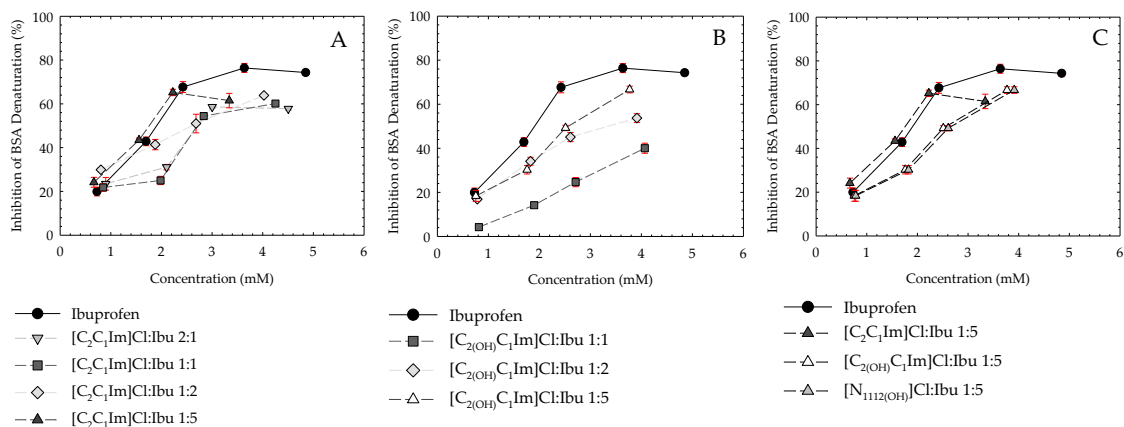


Figure 4.7. Inhibition profile of BSA denaturation by the ibuprofen-based eutectic systems with the HBD [C₂C₁Im]Cl (A), the HBD [C₂(OH)C₁Im]Cl (B), and the HBD [N₁₁₁₂(OH)]Cl (C). The profile of ibuprofen (parent-API) is also displayed [29].

The ability of a substance to prevent protein denaturation may also help to prevent an inflammatory process, since protein biological activity loss has been correlated with the formation of inflammatory disorders like rheumatoid arthritis, diabetes and cancer [86]. Serum albumins are the most abundant proteins in plasma and are responsible for the movement of drugs through the blood stream. BSA has similar properties to those of human serum albumin, thus is widely used as a model protein [87]. In this study, BSA was used to evaluate the ability of the ibuprofen-based eutectic formulations to prevent protein denaturation, and consequently assess their anti-inflammatory properties. **Figure 4.7** compares the inhibition profile of BSA denaturation of ibuprofen (parent-API) [18] with ibuprofen-based eutectics based on the HBA [C₂C₁Im]Cl, [C₂(OH)C₁Im]Cl, and [N₁₁₁₂(OH)]Cl (**Table 4.S10**). Unlike the ibuprofen API-ILs based on the same cations ([C₂C₁Im]⁺, [C₂(OH)C₁Im]⁺, and [N₁₁₁₂(OH)]⁺) [29], that exhibited similar profiles to the parent-API, or even presented an increased inhibition of BSA denaturation ([C₂(OH)C₁Im][Ibu]), all the 8 studied Ibu-based eutectics generally exhibited a reduced inhibition of BSA denaturation (**Figure 4.7** and **Table 4.S10**). Although, for the 1:5 molar ratio the 3 analyzed eutectics ([C₂C₁Im]Cl:Ibu, [C₂(OH)C₁Im]Cl:Ibu, [N₁₁₁₂(OH)]Cl:Ibu) the inhibition profile is more similar to ibuprofen, indicating that with a fine-tuning of the molar ratio, a eutectic system may present similar anti-inflammatory properties of the parent API.

Cyclooxygenase (COX; also called prostaglandin H synthase, PGHS) is a bifunctional enzyme exhibiting both COX and peroxidase activities. There are two distinct isoforms of COX, COX-1 and COX-2, that are responsible for prostaglandin biosynthesis involved in the anti-inflammatory process (more details on COX-1 and COX-2 can be found elsewhere [88]). Fundamentally, NSAIDs are COX-2 inhibitors with differing degrees of COX-1 inhibition as a side effect. Non-selective NSAIDs, such as ibuprofen, inhibit COX-1 and COX-2 with comparable potency ([18,89]), not sparing COX-1 activity after dosing with all the unwanted side effects [90,91]. Clearly, it is advantageous to develop selective COX-2 NSAIDs with minimal COX-1 inhibition after dosing, allowing pain relief and inflammation reduction with less adverse effects [92]. The following ibuprofen-based eutectic formulations, [C₂C₁Im]Cl:Ibu 1:1, [C₂C₁Im]Cl:Ibu 1:5 [C_{2(OH)}C₁Im]Cl:Ibu 1:1, [C_{2(OH)}C₁Im]Cl:Ibu 1:5, and [N_{1112(OH)}]Cl:Ibu 1:5, as well as ibuprofen [18], were evaluated for their ability to inhibit cyclooxygenases (COX-1, ovine; COX-2, human) using a COX colorimetric inhibitor assay kit (**Section 4.1.4.11**), providing direct insight into their anti-inflammatory properties. The results obtained are depicted in **Figure 4.8** and **Table 4.5**, indicating that under the same experimental conditions, the ibuprofen-based eutectics generally maintained the anti-inflammatory activity of ibuprofen (% COX inhibition).

A closer look to the results, through the COX-1/COX-2 selectivity, once all NSAIDs are essentially COX-2 inhibitors with differing degrees of COX-1 inhibition as side effect, is attained to better understand the effect of the HBA and HBA:Ibu molar ratio in the COX-1/COX-2 selectivity of the ibuprofen-based eutectic systems (**Figure 4.8** and **Table 4.5**), and to assess the fine-tuning of these parameters to optimize the anti-inflammatory activity of ibuprofen, a non-selective NSAID that inhibit COX-1 and COX-2 with comparable potency, as observed in the relative COX-1/COX-2 selectivity [18,89], and do not spare COX-1 activity after dosing, with all the unwanted side effects [89,90]. Both [C₂C₁Im]Cl-based eutectics (1:1 and 1:5) and [C_{2(OH)}C₁Im]Cl:Ibu 1:1 eutectic presented a similar COX-1/COX-2 selectivity to ibuprofen (t-test, 1 tailed, confidence level 90%, p<0.05). Differently, [C_{2(OH)}C₁Im]Cl:Ibu 1:5 eutectic upgraded the activity (% COX inhibition), with a higher increase of the inhibition of COX-1 (%), increasing the COX-1/COX-2 selectivity relatively to ibuprofen (t-test, 1 tailed, confidence level 90%, p<0.05).

The $[N_{1112(OH)}]Cl:Ibu$ 1:5 eutectic presented the lower COX-1/COX-2 selectivity (Table 5), indicating a greater selectivity for COX-2 than ibuprofen (t-test, 1 tailed, confidence level 90%, $p < 0.05$).

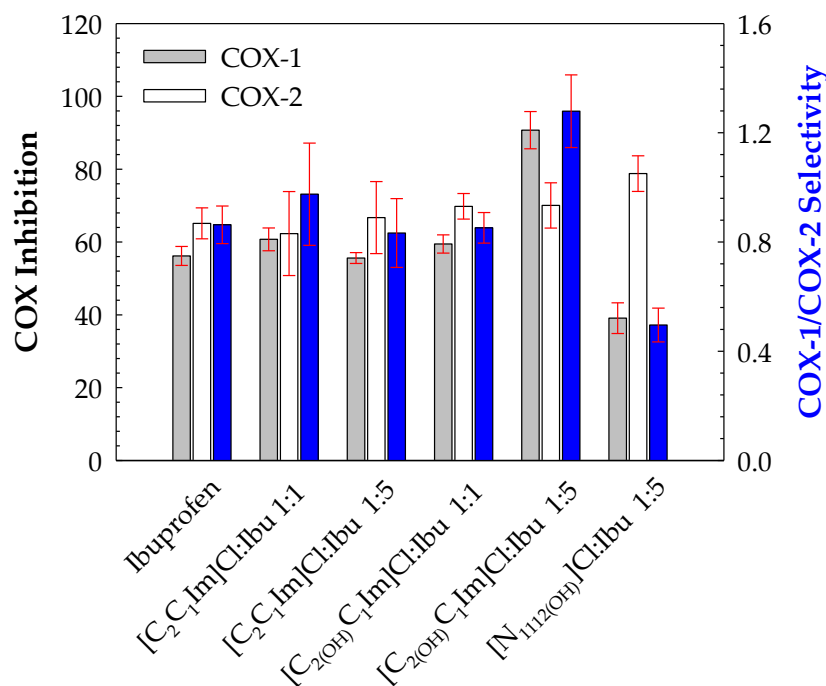


Figure 4.8. Selective inhibition of of COX-1 (ovine) and COX-2 (human) and COX-1/COX-2 selectivity for 3 mM ibuprofen [30] and ibuprofen-based eutectics

The COX-1/COX-2 selectivity of the ibuprofen-based eutectics and ibuprofen (Table 5) follows the order (t-test, 1 tailed, confidence level 90%, $p < 0.05$): $[C_2(OH)C_1Im]Cl:Ibu$ 1:5 > ibuprofen $\approx [C_2C_1Im]Cl$ 1:1 $\approx [C_2C_1Im]Cl$ 1:5 $\approx [C_2(OH)C_1Im]Cl:Ibu$ 1:1 > $[N_{1112(OH)}]Cl:Ibu$ 1:5. Lower COX-1/COX-2 selectivity values indicate a greater selectivity for COX-2, and higher values indicate greater selectivity for COX-1. Similar results were obtained for ibuprofen-based ionic liquids [18], a comparison between the ibuprofen-based eutectics and the ibuprofen API-ILs is depicted in **Figure 4.S8**. Globally, the ibuprofen-based API-ILs, sharing the same cation with the HBA's of the eutectics developed in this work, have a greater impact in the improvement of the selectivity towards COX-2. Although, the $[N_{1112(OH)}]Cl:Ibu$ 1:5 eutectic surpasses the $[N_{1112(OH)}][Ibu]$ ionic liquid, the API-IL with the better COX-1/COX-2 selectivity (t-test, 1 tailed, confidence level 80%, $p < 0.1$). These results provide strong evidence of the API-based eutectics platform's potential for

facilitating the development of safer NSAIDs with improved gastric and renal safety profiles. Additionally, the study reveals new avenues for selective COX-2 inhibitors in cancer chemotherapy and neurological diseases such as Alzheimer's and Parkinson's.

Table 4.5. Inhibition of COX-1 (ovine) and COX-2 (human) and COX-1/COX-2 selectivity for 3 mM ibuprofen [30] and ibuprofen-based eutectics.

Compound	Inhibition of COX-1 (ovine) (%)	Inhibition of COX-2 (human) (%)	COX-1/COX-2 selectivity
Ibuprofen	56.18 ± 2.60	65.13 ± 4.25	0.863 ± 0.069
[C ₂ C ₁ Im]Cl:Ibu 1:1	60.74 ± 3.13	62.32 ± 11.53	0.975 ± 0.187
[C ₂ C ₁ Im]Cl:Ibu 1:5	55.60 ± 1.49	66.71 ± 9.89	0.833 ± 0.126
[C _{2(OH)} C ₁ Im]Cl:Ibu 1:1	59.47 ± 2.51	69.80 ± 3.51	0.852 ± 0.056
[C _{2(OH)} C ₁ Im]Cl:Ibu 1:5	90.73 ± 5.12	70.95 ± 6.22	1.279 ± 0.133
[N _{1112(OH)}]Cl:Ibu 1:5	39.09 ± 4.21	78.79 ± 4.90	0.496 ± 0.062

4.1.5 Conclusions

In this work, we developed twelve NSAID-based eutectic formulations, conjugating ibuprofen (HBD) with three imidazolium-based ILs ([C₂C₁Im]Cl, [C_{2(OH)}C₁Im]Cl and [C₂C₁Im][C₁CO₂]) and cholinium salt ([N_{1112(OH)}]Cl) in different molar ratio, namely 2:1, 1:1, 1:2 and 1:5. All eutectic systems were characterized by DSC and NMR, and their polarity was assessed using the Kamlet-Taft approach. The KT β and π^* values obtained confirmed that the developed Ibu-based eutectics have high ability to establish hydrogen bonds (specific interactions) and high polarity and ability to establish dipole-dipole and dipole-induced dipole interactions (non-specific interactions). An upgrade of the aqueous solubility (water and biological simulated fluids) for the Ibu-based eutectics relatively to ibuprofen was verified. Also, the Ibu-based eutectics were characterized in terms of viscosity, conductivity, density and ionicity (via Walden plot), confirming the formation of large charged or non-charged aggregates, or the existence of ionic networks, that increase the potential for these liquids to penetrate membranes more efficiently than ibuprofen (parent solid API). The ibuprofen-based eutectics and ibuprofen display similar cytotoxic response (with two human cell lines, Caco-2 colon carcinoma cells and HepG2 hepatocellular carcinoma cells) and all forms are hemocompatible. The pharmacological action of the prepared Ibu-based eutectic formulations were examined to ascertain the presence of a potential synergistic

interaction between ionic liquids (HBA) and ibuprofen (HBD), which could lead to novel therapeutic benefits. Subsequently, the anti-inflammatory properties of the Ibu-based eutectics were evaluated through the inhibition of BSA denaturation and inhibition of cyclooxygenases (COX-1 and COX-2) enzymes, showing that the ibuprofen eutectic formulations maintain the anti-inflammatory response of ibuprofen with the opportunity to improve the selectivity towards COX-2, allowing the development of safer NSAIDs. These results reveal significant potential in the use of eutectic formulations combining NSAIDs and ionic liquids, presenting novel opportunities for the development of selective COX-2 inhibitors in cancer chemotherapy and neurodegenerative diseases such as Alzheimer's and Parkinson's. The development of pharmaceutically active eutectics using ionic liquids as HBA represents a paradigm offering diverse opportunities for drug development and delivery, potentially playing a significant role in the future of healthcare by taking both eutectics and ILs from the laboratory to patient care.

Funding

This research was funded by FCT/MCTES (Portugal), through grants PD/BD/135078/2017 and COVID/BD/151824/2021 (J.C.B.), the Individual Call to Scientific Employment Stimulus 2020.00835.CEECIND (J.M.M.A.) and 2021.01432.CEECIND (A.B.P.), and the project PTDC/EQU-EQU/2223/2021. This work was also supported by the Associate Laboratory for Green Chemistry—LAQV which was financed by national funds from FCT/MCTES (UIDB/50006/2020 and UIDP/50006/2020).

Conflicts of Interest

The authors declare no conflict of interest.

4.1.6 References

1. Kalepu, S.; Nekkanti, V. Insoluble Drug Delivery Strategies: Review of Recent Advances and Business Prospects. *Acta Pharm Sin B* **2015**, *5*, 442–453, doi:10.1016/j.apsb.2015.07.003.

2. Rainsford, K.D. Ibuprofen: Pharmacology, Efficacy and Safety. *Inflammopharmacology* 2009, 17, 275–342.
3. Duarte, A.R.C.; Ferreira, A.S.D.; Barreiros, S.; Cabrita, E.; Reis, R.L.; Paiva, A. A Comparison between Pure Active Pharmaceutical Ingredients and Therapeutic Deep Eutectic Solvents: Solubility and Permeability Studies. *European Journal of Pharmaceutics and Biopharmaceutics* 2017, 114, 296–304, doi:10.1016/j.ejpb.2017.02.003.
4. Wu, H.; Deng, Z.; Zhou, B.; Qi, M.; Hong, M.; Ren, G. Improved Transdermal Permeability of Ibuprofen by Ionic Liquid Technology: Correlation between Counterion Structure and the Physicochemical and Biological Properties. *J Mol Liq* 2019, 283, 399–409, doi:10.1016/j.molliq.2019.03.046.
5. Tomé, L.I.N.; Baião, V.; da Silva, W.; Brett, C.M.A. Deep Eutectic Solvents for the Production and Application of New Materials. *Appl Mater Today* 2018, 10, 30–50.
6. Araújo, J.M.M.; Florindo, C.; Pereira, A.B.; Vieira, N.S.M.; Matias, A.A.; Duarte, C.M.M.; Rebelo, L.P.N.; Marrucho, I.M. Cholinium-Based Ionic Liquids with Pharmaceutically Active Anions. *RSC Adv* 2014, 4, 28126–28132, doi:10.1039/c3ra47615d.
7. Florindo, C.; Araújo, J.M.M.; Alves, F.; Matos, C.; Ferraz, R.; Prudêncio, C.; Noronha, J.P.; Petrovski, Ž.; Branco, L.; Rebelo, L.P.N.; et al. Evaluation of Solubility and Partition Properties of Ampicillin-Based Ionic Liquids. *Int J Pharm* 2013, 456, 553–559, doi:10.1016/j.ijpharm.2013.08.010.
8. Vieira, N.S.M.; Stolte, S.; Araújo, J.M.M.; Rebelo, L.P.N.; Pereira, A.B.; Markiewicz, M. Acute Aquatic Toxicity and Biodegradability of Fluorinated Ionic Liquids. *ACS Sustain Chem Eng* 2019, 7, 3733–3741, doi:10.1021/acssuschemeng.8b03653.
9. Vieira, N.S.M.; Bastos, J.C.; Rebelo, L.P.N.; Matias, A.; Araújo, J.M.M.; Pereira, A.B. Human Cytotoxicity and Octanol/Water Partition Coefficients of Fluorinated Ionic Liquids. *Chemosphere* 2019, 216, 576–586, doi:10.1016/j.chemosphere.2018.10.159.

10. Bastos, J.C.; Carvalho, S.F.; Welton, T.; Canongia Lopes, J.N.; Rebelo, L.P.N.; Shimizu, K.; Araújo, J.M.M.; Pereiro, A.B. Design of Task-Specific Fluorinated Ionic Liquids: Nanosegregation: Versus Hydrogen-Bonding Ability in Aqueous Solutions. *Chemical Communications* **2018**, *54*, 3524–3527, doi:10.1039/c8cc00361k.
11. Tang, J.; Song, H.; Feng, X.; Yohannes, A.; Yao, S. Ionic Liquid-Like Pharmaceutical Ingredients and Applications of Ionic Liquids in Medicinal Chemistry: Development, Status and Prospects. *Curr Med Chem* **2018**, *26*, 5947–5967, doi:10.2174/0929867325666180605123436.
12. Huang, W.; Wu, X.; Qi, J.; Zhu, Q.; Wu, W.; Lu, Y.; Chen, Z. Ionic Liquids: Green and Tailor-Made Solvents in Drug Delivery. *Drug Discov Today* **2020**, *25*, 901–908.
13. Jin, W.; Yang, Q.; Zhang, Z.; Bao, Z.; Ren, Q.; Yang, Y.; Xing, H. Self-Assembly Induced Solubilization of Drug-like Molecules in Nanostructured Ionic Liquids. *Chemical Communications* **2015**, *51*, 13170–13173, doi:10.1039/c5cc03463a.
14. Alves, M.; Vieira, N.S.M.; Rebelo, L.P.N.; Araújo, J.M.M.; Pereiro, A.B.; Archer, M. Fluorinated Ionic Liquids for Protein Drug Delivery Systems: Investigating Their Impact on the Structure and Function of Lysozyme. *Int J Pharm* **2017**, *526*, 309–320, doi:10.1016/j.ijpharm.2017.05.002.
15. Chantereau, G.; Sharma, M.; Abednejad, A.; Neves, B.M.; Sèbe, G.; Coma, V.; Freire, M.G.; Freire, C.S.R.; Silvestre, A.J.D. Design of Nonsteroidal Anti-Inflammatory Drug-Based Ionic Liquids with Improved Water Solubility and Drug Delivery. *ACS Sustain Chem Eng* **2019**, *7*, 14126–14134, doi:10.1021/acssuschemeng.9b02797.
16. Jiang, Q.; Yu, S.; Li, X.; Ma, C.; Li, A. Evaluation of Local Anesthetic Effects of Lidocaine-Ibuprofen Ionic Liquid Stabilized Silver Nanoparticles in Male Swiss Mice. *J Photochem Photobiol B* **2018**, *178*, 367–370, doi:10.1016/j.jphotobiol.2017.11.028.
17. Hough, W.L.; Smiglak, M.; Rodríguez, H.; Swatloski, R.P.; Spear, S.K.; Daly, D.T.; Pernak, J.; Grisel, J.E.; Carliss, R.D.; Soutullo, M.D.; et al. The Third Evolution of Ionic

Liquids: Active Pharmaceutical Ingredients. *New Journal of Chemistry* **2007**, *31*, 1429–1436, doi:10.1039/b706677p.

18. Bastos, J.C.; Vieira, N.S.M.; Gaspar, M.M.; Pereiro, A.B.; Araújo, J.M.M. Human Cytotoxicity, Hemolytic Activity, Anti-Inflammatory Activity and Aqueous Solubility of Ibuprofen-Based Ionic Liquids. *Sustainable Chemistry* **2022**, *3*, 358–375, doi:10.3390/suschem3030023.
19. Abbott, A.P.; Ahmed, E.I.; Prasad, K.; Qader, I.B.; Ryder, K.S. Liquid Pharmaceuticals Formulation by Eutectic Formation. *Fluid Phase Equilib* **2017**, *448*, 2–8, doi:10.1016/j.fluid.2017.05.009.
20. Morrison, H.G.; Sun, C.C.; Neervannan, S. Characterization of Thermal Behavior of Deep Eutectic Solvents and Their Potential as Drug Solubilization Vehicles. *Int J Pharm* **2009**, *378*, 136–139, doi:10.1016/j.ijpharm.2009.05.039.
21. Stott, P.W.; Williams, A.C.; Barry, B.W. *Transdermal Delivery from Eutectic Systems: Enhanced Permeation of a Model Drug, Ibuprofen*; 1998; Vol. 50;.
22. Lu, C.; Cao, J.; Wang, N.; Su, E. Significantly Improving the Solubility of Non-Steroidal Anti-Inflammatory Drugs in Deep Eutectic Solvents for Potential Non-Aqueous Liquid Administration. *Medchemcomm* **2016**, *7*, 955–959, doi:10.1039/c5md00551e.
23. Aroso, I.M.; Silva, J.C.; Mano, F.; Ferreira, A.S.D.; Dionísio, M.; Sá-Nogueira, I.; Barreiros, S.; Reis, R.L.; Paiva, A.; Duarte, A.R.C. Dissolution Enhancement of Active Pharmaceutical Ingredients by Therapeutic Deep Eutectic Systems. *European Journal of Pharmaceutics and Biopharmaceutics* **2016**, *98*, 57–66, doi:10.1016/j.ejpb.2015.11.002.
24. Li, Z.; Lee, P.I. Investigation on Drug Solubility Enhancement Using Deep Eutectic Solvents and Their Derivatives. *Int J Pharm* **2016**, *505*, 283–288, doi:10.1016/j.ijpharm.2016.04.018.

25. Pradeepkumar, P.; Subbiah, A.; Rajan, M. Synthesis of Bio-Degradable Poly(2-Hydroxyethyl Methacrylate) Using Natural Deep Eutectic Solvents for Sustainable Cancer Drug Delivery. *SN Appl Sci* **2019**, *1*, doi:10.1007/s42452-019-0591-4.
26. García-Argüelles, S.; Serrano, M.C.; Gutiérrez, M.C.; Ferrer, M.L.; Yuste, L.; Rojo, F.; del Monte, F. Deep Eutectic Solvent-Assisted Synthesis of Biodegradable Polyesters with Antibacterial Properties. *Langmuir* **2013**, *29*, 9525–9534, doi:10.1021/la401353r.
27. Serrano, M.C.; Gutiérrez, M.C.; Jiménez, R.; Ferrer, M.L.; del Monte, F. Synthesis of Novel Lidocaine-Releasing Poly(Diol-Co-Citrate) Elastomers by Using Deep Eutectic Solvents. *Chemical Communications* **2012**, *48*, 579–581, doi:10.1039/c1cc15284j.
28. Sánchez-Leija, R.J.; Pojman, J.A.; Luna-Bárceñas, G.; Mota-Morales, J.D. Controlled Release of Lidocaine Hydrochloride from Polymerized Drug-Based Deep-Eutectic Solvents. *J Mater Chem B* **2014**, *2*, 7495–7501, doi:10.1039/c4tb01407c.
29. Castro, P.J.; Redondo, A.E.; Sosa, J.E.; Zakrzewska, M.E.; Nunes, A.V.M.; Araújo, J.M.M.; Pereiro, A.B. Absorption of Fluorinated Greenhouse Gases in Deep Eutectic Solvents. *Ind Eng Chem Res* **2020**, *59*, 13246–13259, doi:10.1021/acs.iecr.0c01893.
30. Kundu, D.; Rao, P.S.; Banerjee, T. First-Principles Prediction of Kamlet–Taft Solvatochromic Parameters of Deep Eutectic Solvent Using the COSMO-RS Model. *Ind Eng Chem Res* **2020**, *59*, 11329–11339, doi:10.1021/acs.iecr.0c00574.
31. Cheong, W.Jo.; Carr, P.W. Kamlet-Taft π^* Polarizability/Dipolarity of Mixtures of Water with Various Organic Solvents. *Anal Chem* **1988**, *60*, 820–826, doi:10.1021/ac00159a018.
32. Kurnia, K.A.; Lima, F.; Cláudio, A.F.M.; Coutinho, J.A.P.; Freire, M.G. Hydrogen-Bond Acidity of Ionic Liquids: An Extended Scale. *Physical Chemistry Chemical Physics* **2015**, *17*, 18980–18990, doi:10.1039/C5CP03094C.

33. Zhang, S.; Qi, X.; Ma, X.; Lu, L.; Deng, Y. Hydroxyl Ionic Liquids: The Differentiating Effect of Hydroxyl on Polarity Due to Ionic Hydrogen Bonds between Hydroxyl and Anions. *J Phys Chem B* **2010**, *114*, 3912–3920, doi:10.1021/jp911430t.
34. Zhang, J.; Zhang, H.; Wu, J.; Zhang, J.; He, J.; Xiang, J. NMR Spectroscopic Studies of Cellobiose Solvation in EmimAc Aimed to Understand the Dissolution Mechanism of Cellulose in Ionic Liquids. *Physical Chemistry Chemical Physics* **2010**, *12*, 1941, doi:10.1039/b920446f.
35. Dewland, P.M.; Reader, S.; Berry, P. Bioavailability of Ibuprofen Following Oral Administration of Standard Ibuprofen, Sodium Ibuprofen or Ibuprofen Acid Incorporating Poloxamer in Healthy Volunteers. *BMC Clin Pharmacol* **2009**, *9*, doi:10.1186/1472-6904-9-19.
36. Gaspar, M.M.; Calado, S.; Pereira, J.; Ferronha, H.; Correia, I.; Castro, H.; Tomás, A.M.; Cruz, M.E.M. Targeted Delivery of Paromomycin in Murine Infectious Diseases through Association to Nano Lipid Systems. *Nanomedicine* **2015**, *11*, 1851–1860, doi:10.1016/j.nano.2015.06.008.
37. Mizushima, Y.; Kobayashi, M. Interaction of Anti-inflammatory Drugs with Serum Proteins, Especially with Some Biologically Active Proteins. *Journal of Pharmacy and Pharmacology* **1968**, *20*, 169–173, doi:10.1111/j.2042-7158.1968.tb09718.x.
38. Abbott, A.P.; Capper, G.; Davies, D.L.; Munro, H.L.; Rasheed, R.K.; Tambyrajah, V. Preparation of Novel, Moisture-Stable, Lewis-Acidic Ionic Liquids Containing Quaternary Ammonium Salts with Functional Side Chains. *Chemical Communications* **2001**, *1*, 2010–2011, doi:10.1039/b106357j.
39. Smith, E.L.; Abbott, A.P.; Ryder, K.S. Deep Eutectic Solvents (DESs) and Their Applications. *Chem Rev* **2014**, *114*, 11060–11082.
40. Abbott, A.P.; Capper, G.; Davies, D.L.; Rasheed, R.K.; Tambyrajah, V. Novel Solvent Properties of Choline Chloride/Urea Mixtures. *Chemical Communications* **2003**, 70–71, doi:10.1039/b210714g.

41. Araújo, J.M.M.; Ferreira, R.; Marrucho, I.M.; Rebelo, L.P.N. Solvation of Nucleobases in 1,3-Dialkylimidazolium Acetate Ionic Liquids: NMR Spectroscopy Insights into the Dissolution Mechanism. *Journal of Physical Chemistry B* **2011**, *115*, 10739–10749, doi:10.1021/jp203282k.
42. Araújo, J.M.M.; Pereiro, A.B.; Canongia Lopes, J.N.; Rebelo, L.P.N.; Marrucho, I.M. Hydrogen-Bonding and the Dissolution Mechanism of Uracil in an Acetate Ionic Liquid: New Insights from NMR Spectroscopy and Quantum Chemical Calculations. *Journal of Physical Chemistry B* **2013**, *117*, 4109–4120, doi:10.1021/jp400749j.
43. Gabriele, F.; Chiarini, M.; Germani, R.; Tiecco, M.; Spreti, N. Effect of Water Addition on Choline Chloride/Glycol Deep Eutectic Solvents: Characterization of Their Structural and Physicochemical Properties. *J Mol Liq* **2019**, *291*, doi:10.1016/j.molliq.2019.111301.
44. Collin, R.L. Polymorphism and Radiation Decomposition of Choline Chloride. *J. Am. Chem. Soc.* **1957**, *22*, 79.
45. Petrouleas, V.; Lemmon, R.M. Calorimetric Studies of Choline Chloride, Bromide, and Iodide. *J Chem Phys* **1978**, *69*, 1315–1316, doi:10.1063/1.436673.
46. Bica, K.; Rodríguez, H.; Gurau, G.; Andreea Cojocaru, O.; Riisager, A.; Fehrmann, R.; Rogers, R.D. Pharmaceutically Active Ionic Liquids with Solids Handling, Enhanced Thermal Stability, and Fast Release. *Chemical Communications* **2012**, *48*, 5422–5424, doi:10.1039/c2cc30959a.
47. Plechkova, N. v.; Seddon, K.R. Applications of Ionic Liquids in the Chemical Industry. *Chem. Soc. Rev.* **2008**, *37*, 123–150, doi:10.1039/b006677j.
48. Welton, T. Room-Temperature Ionic Liquids. Solvents for Synthesis and Catalysis. *Chem Rev* **1999**, *99*, 2071–2083, doi:10.1021/cr980032t.
49. Lakowicz, J.R. *Principles of Fluorescence Spectroscopy*; Springer, 2006;
50. Reichardt, C.; Welton, T. *Solvents and Solvent Effects in Organic Chemistry*; John Wiley & Sons, 2011; ISBN 3527642137.

51. Taft, R.W.; Kamlet, M.J. The Solvatochromic Comparison Method. *J. Am. Chem. Soc.* **1975**, *99*, 377.
52. Cláudio, A.F.M.; Swift, L.; Hallett, J.P.; Welton, T.; Coutinho, J.A.P.; Freire, M.G. Extended Scale for the Hydrogen-Bond Basicity of Ionic Liquids. *Physical Chemistry Chemical Physics* **2014**, *16*, 6593, doi:10.1039/c3cp55285c.
53. Doherty, T. V.; Mora-Pale, M.; Foley, S.E.; Linhardt, R.J.; Dordick, J.S. Ionic Liquid Solvent Properties as Predictors of Lignocellulose Pretreatment Efficacy. *Green Chemistry* **2010**, *12*, 1967, doi:10.1039/c0gc00206b.
54. Marcus, Y. The Properties of Organic Liquids That Are Relevant to Their Use as Solvating Solvents. *Chem Soc Rev* **1993**, *22*, 409–416.
55. Reichardt, C.; Welton, T. *Solvents and Solvent Effects in Organic Chemistry*; John Wiley & Sons, 2011; ISBN 3527642137.
56. Kim, S.H.; Park, S.; Yu, H.; Kim, J.H.; Kim, H.J.; Yang, Y.-H.; Kim, Y.H.; Kim, K.J.; Kan, E.; Lee, S.H. Effect of Deep Eutectic Solvent Mixtures on Lipase Activity and Stability. *J Mol Catal B Enzym* **2016**, *128*, 65–72.
57. Jovell, D.; B. Gómez, S.; Zakrzewska, M.E.; Nunes, A.V.M.; Araújo, J.M.M.; Pereiro, A.B.; Llorell, F. Insight on the Solubility of R134a in Fluorinated Ionic Liquids and Deep Eutectic Solvents. *J Chem Eng Data* **2020**, *65*, 4956–4969, doi:10.1021/acs.jced.0c00588.
58. Neuberg, C. Hydrotropy. *Biochem. Z.* **1916**, *76*, 107–108.
59. Booth, J.J.; Abbott, S.; Shimizu, S. Mechanism of Hydrophobic Drug Solubilization by Small Molecule Hydrotropes. *Journal of Physical Chemistry B* **2012**, *116*, 14915–14921, doi:10.1021/jp309819r.
60. Shimizu, S.; Matubayasi, N. Hydrotropy: Monomer-Micelle Equilibrium and Minimum Hydrotrope Concentration. *Journal of Physical Chemistry B* **2014**, *118*, 10515–10524, doi:10.1021/jp505869m.

61. Cláudio, A.F.M.; Neves, M.C.; Shimizu, K.; Canongia Lopes, J.N.; Freire, M.G.; Coutinho, J.A.P. The Magic of Aqueous Solutions of Ionic Liquids: Ionic Liquids as a Powerful Class of Catanionic Hydrotropes. *Green Chemistry* **2015**, *17*, 3948–3963, doi:10.1039/c5gc00712g.
62. Hammond, O.S.; Bowron, D.T.; Edler, K.J. Liquid Structure of the Choline Chloride-Urea Deep Eutectic Solvent (Reline) from Neutron Diffraction and Atomistic Modelling. *Green Chemistry* **2016**, *18*, 2736–2744, doi:10.1039/C5GC02914G.
63. Sun, H.; Li, Y.; Wu, X.; Li, G. Theoretical Study on the Structures and Properties of Mixtures of Urea and Choline Chloride. *J Mol Model* **2013**, *19*, 2433–2441, doi:10.1007/s00894-013-1791-2.
64. Ahmadi, R.; Hemmateenejad, B.; Safavi, A.; Shojaeifard, Z.; Shahsavar, A.; Mohajeri, A.; Heydari Dokoohaki, M.; Zolghadr, A.R. Deep Eutectic–Water Binary Solvent Associations Investigated by Vibrational Spectroscopy and Chemometrics. *Physical Chemistry Chemical Physics* **2018**, *20*, 18463–18473, doi:10.1039/C8CP00409A.
65. Weng, L.; Toner, M. Janus-Faced Role of Water in Defining Nanostructure of Choline Chloride/Glycerol Deep Eutectic Solvent. *Physical Chemistry Chemical Physics* **2018**, *20*, 22455–22462, doi:10.1039/C8CP03882A.
66. Gabriele, F.; Chiarini, M.; Germani, R.; Tiecco, M.; Spreti, N. Effect of Water Addition on Choline Chloride/Glycol Deep Eutectic Solvents: Characterization of Their Structural and Physicochemical Properties. *J Mol Liq* **2019**, *291*, 111301, doi:10.1016/j.molliq.2019.111301.
67. Dai, Y.; Witkamp, G.-J.; Verpoorte, R.; Choi, Y.H. Tailoring Properties of Natural Deep Eutectic Solvents with Water to Facilitate Their Applications. *Food Chem* **2015**, *187*, 14–19, doi:10.1016/j.foodchem.2015.03.123.
68. Hammond, O.S.; Bowron, D.T.; Edler, K.J. The Effect of Water upon Deep Eutectic Solvent Nanostructure: An Unusual Transition from Ionic Mixture to Aqueous Solution. *Angewandte Chemie International Edition* **2017**, *56*, 9782–9785, doi:10.1002/anie.201702486.

69. D'Agostino, C.; Harris, R.C.; Abbott, A.P.; Gladden, L.F.; Mantle, M.D. Molecular Motion and Ion Diffusion in Choline Chloride Based Deep Eutectic Solvents Studied by ¹H Pulsed Field Gradient NMR Spectroscopy. *Physical Chemistry Chemical Physics* **2011**, *13*, 21383–21391, doi:10.1039/c1cp22554e.
70. Food and Drug Administration Guidance for Industry: Regulatory Classification of Pharmaceutical Co-Crystals. *Silver Spring, MD* 2018.
71. Angell, C.A.; Byrne, N.; Belieres, J.-P. Parallel Developments in Aprotic and Protic Ionic Liquids: Physical Chemistry and Applications. *Acc Chem Res* **2007**, *40*, 1228–1236.
72. Pereiro, A.B.; Araújo, J.M.M.; Oliveira, F.S.; Bernardes, C.E.S.; Esperança, J.M.S.S.; Canongia Lopes, J.N.; Marrucho, I.M.; Rebelo, L.P.N. Inorganic Salts in Purely Ionic Liquid Media: The Development of High Ionicity Ionic Liquids (HIILs). *Chemical Communications* **2012**, *48*, 3656, doi:10.1039/c2cc30374d.
73. Xu, W.; Cooper, E.I.; Angell, C.A. Ionic Liquids: Ion Mobilities, Glass Temperatures, and Fragilities. *Journal of Physical Chemistry B* **2003**, *107*, 6170–6178, doi:10.1021/jp0275894.
74. Schreiner, C.; Zugmann, S.; Hartl, R.; Gores, H.J. Fractional Walden Rule for Ionic Liquids: Examples from Recent Measurements and a Critique of the So-Called Ideal KCl Line for the Walden Plot. *J Chem Eng Data* **2010**, *55*, 1784–1788, doi:10.1021/jc900878j.
75. Wang, Y.; Chen, W.; Zhao, Q.; Jin, G.; Xue, Z.; Wang, Y.; Mu, T. Ionicity of Deep Eutectic Solvents by Walden Plot and Pulsed Field Gradient Nuclear Magnetic Resonance (PFG-NMR). *Physical Chemistry Chemical Physics* **2020**, *22*, 25760–25768, doi:10.1039/D0CP01431A.
76. Stoimenovski, J.; MacFarlane, D.R. Enhanced Membrane Transport of Pharmaceutically Active Protic Ionic Liquids. *Chemical Communications* **2011**, *47*, 11429, doi:10.1039/c1cc14314j.

77. Stoimenovski, J.; Dean, P.M.; Izgorodina, E.I.; MacFarlane, D.R. Protic Pharmaceutical Ionic Liquids and Solids: Aspects of Protonics. *Faraday Discuss.* **2012**, *154*, 335–352, doi:10.1039/C1FD00071C.
78. Dyshin, A.A.; Eliseeva, O. V; Kiselev, M.G. Density and Viscosity of Zinc Chloride Solution in N-Methylacetamide over the Temperature Range from 308.15 to 328.15 K at Atmospheric Pressure. *J Chem Eng Data* **2018**, *63*, 3130–3135, doi:10.1021/acs.jced.8b00399.
79. Agieienko, V.; Buchner, R. Densities, Viscosities, and Electrical Conductivities of Pure Anhydrous Reline and Its Mixtures with Water in the Temperature Range (293.15 to 338.15) K. *J Chem Eng Data* **2019**, *64*, 4763–4774, doi:10.1021/acs.jced.9b00145.
80. Pagano, M.; Faggio, C. The Use of Erythrocyte Fragility to Assess Xenobiotic Cytotoxicity. *Cell Biochem Funct* **2015**, *33*, 351–355, doi:10.1002/cbf.3135.
81. Farag, M.R.; Alagawany, M. Erythrocytes as a Biological Model for Screening of Xenobiotics Toxicity. *Chem Biol Interact* **2018**, *279*, 73–83.
82. European Medicines Agency. Guideline on Strategies to Identify and Mitigate Risks for First-in-Human and Early Clinical Trials With Investigational Medicinal Products; EMEA/CHMP/SWP/28367/07 Rev. 1; Committee for Medicinal Products for Human Use (CHMP): Amsterdam, The Netherlands, 2017.
83. Vieira, N.S.M.; Oliveira, A.L.S.; Araújo, J.M.M.; Gaspar, M.M.; Pereira, A.B. Ecotoxicity and Hemolytic Activity of Fluorinated Ionic Liquids. *Sustainable Chemistry* **2021**, *2*, 115–126, doi:10.3390/suschem2010008.
84. Orhan, H.; Şahin, G. In Vitro Effects of NSAIDs and Paracetamol on Oxidative Stress-Related Parameters of Human Erythrocytes. *Experimental and Toxicologic Pathology* **2001**, *53*, 133–140, doi:10.1078/0940-2993-00179.
85. Radošević, K.; Cvjetko Bubalo, M.; Gaurina Srček, V.; Grgas, D.; Landeka Dragičević, T.; Redovniković, R.I. Evaluation of Toxicity and Biodegradability of Choline Chloride

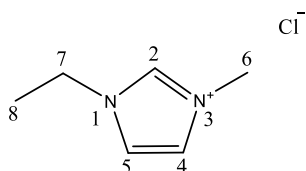
Based Deep Eutectic Solvents. *Ecotoxicol Environ Saf* **2015**, *112*, 46–53, doi:10.1016/j.ecoenv.2014.09.034.

86. Sangeetha, G.; Vidhya, R. In Vitro Anti-Inflammatory Activity of Different Parts of *Pedaliium Murex* (L.). ~ 31 ~ *International Journal of Herbal Medicine* **2016**, *4*.
87. Douadi, K.; Chafaa, S.; Douadi, T.; Al-Noaimi, M.; Kaabi, I. Azoimine Quinoline Derivatives: Synthesis, Classical and Electrochemical Evaluation of Antioxidant, Anti-Inflammatory, Antimicrobial Activities and the DNA / BSA Binding. *J Mol Struct* **2020**, *1217*, 128305, doi:10.1016/j.molstruc.2020.128305.
88. Zidar, N.; Odar, K.; Glavac, D.; Jerse, M.; Zupanc, T.; Stajer, D. Cyclooxygenase in Normal Human Tissues - Is COX-1 Really a Constitutive Isoform, and COX-2 an Inducible Isoform? *J Cell Mol Med* **2009**, *13*, 3753–3763, doi:10.1111/j.1582-4934.2008.00430.x.
89. Brune; Patrignani, P. New Insights into the Use of Currently Available Non-Steroidal Anti-Inflammatory Drugs. *J Pain Res* **2015**, *105*, doi:10.2147/JPR.S75160.
90. Patrignani, P.; Tacconelli, S.; Bruno, A.; Sostres, C.; Lanas, A. Managing the Adverse Effects of Nonsteroidal Anti-Inflammatory Drugs. *Expert Rev Clin Pharmacol* **2011**, *4*, 605–621, doi:10.1586/ecp.11.36.
91. Mazaleuskaya, L.L.; Theken, K.N.; Gong, L.; Thorn, C.F.; Fitzgerald, G.A.; Altman, R.B.; Klein, T.E. PharmGKB Summary: Ibuprofen Pathways. *Pharmacogenet Genomics* **2015**, *25*, 96–106, doi:10.1097/FPC.0000000000000113.
92. Dionne, R. Relative Efficacy of Selective COX-2 Inhibitors Compared with over-the-Counter Ibuprofen. *Int J Clin Pract Suppl* **2003**, *18*–22.

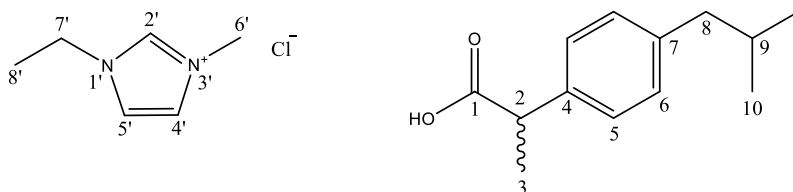
4.1.7 Supplementary Materials

Characterization of the Ibuprofen-based eutectic systems

The prepared ibuprofen-based eutectic systems were completely characterized by ^1H and ^{13}C NMR. Additionally, the hydrogen bond donors were also analysed.

1-Ethyl-3-methylimidazolium chloride ($[\text{C}_2\text{C}_1\text{Im}]\text{Cl}$)

^1H NMR (400 MHz, DMSO): $\delta/\text{ppm} = 9.44$ (s, 1H, 2), 7.86 (s, 1H, 4), 7.77 (s, 1H, 5), 4.22 (q, $J = 7.3$ Hz, 2H, 7), 3.87 (s, 3H, 6), 1.41 (t, $J = 7.3$ Hz, 3H, 8).

 $[\text{C}_2\text{C}_1\text{Im}]\text{Cl}$: Ibuprofen

2:1 ^1H NMR (400 MHz, DMSO): $\delta/\text{ppm} = 12.27$ (s, 1H, OH), 9.22 (s, 2H, 2'), 7.80 (s, 2H, 4'), 7.72 (s, 2H, 5'), 7.19 (d, $J = 7.9$ Hz, 2H, 6), 7.10 (d, $J = 7.9$ Hz, 2H, 5), 4.20 (q, $J = 7.3$ Hz, 4H, 7'), 3.86 (s, 6H, 6'), 3.69 – 3.58 (m, 1H, 2), 2.41 (d, $J = 7.1$ Hz, 2H, 8), 1.87 – 1.73 (m, 1H, 9), 1.42 (t, $J = 7.3$ Hz, 6H, 8'), 1.34 (d, $J = 7.1$ Hz, 3H, 3), 0.86 (d, $J = 6.6$ Hz, 6H, 10).

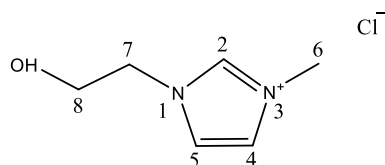
1:1 ^1H NMR (400 MHz, DMSO): $\delta/\text{ppm} = 12.25$ (s, 1H, OH), 9.16 (s, 1H, 2'), 7.79 (s, 1H, 4'), 7.70 (s, 1H, 5'), 7.19 (d, $J = 8.0$ Hz, 2H, 6), 7.10 (d, $J = 8.0$ Hz, 2H, 5), 4.20 (q, $J = 7.3$ Hz, 2H, 7'), 3.85 (s, 3H, 6'), 3.63 (q, $J = 7.1$ Hz, 1H, 2), 2.41 (d, $J = 7.1$ Hz, 2H, 8), 1.89 – 1.70 (m, 1H, 9), 1.42 (t, $J = 7.3$ Hz, 3H, 8'), 1.33 (s, 3H, 3), 0.86 (d, $J = 6.6$ Hz, 6H, 10).

1:2 ^1H NMR (400 MHz, DMSO): $\delta/\text{ppm} = 12.25$ (s, 1H, OH), 9.18 (s, 0.5H, 2'), 7.79 (s, 0.5H, 4'), 7.71 (s, 0.5H, 5'), 7.19 (d, $J = 8.0$ Hz, 2H, 6), 7.10 (d, $J = 8.0$ Hz, 2H, 5), 4.20 (q, $J = 7.3$ Hz, 1H, 7'), 3.85 (s, 1.5H, 6'), 3.63 (q, $J = 7.1$ Hz, 1H, 2), 2.41 (d, $J = 7.1$ Hz, 2H, 8), 1.81 (dp, $J = 13.4, 6.7$ Hz, 1H, 9), 1.42 (t, $J = 7.3$ Hz, 1.5H, 8'), 1.34 (d, $J = 7.1$ Hz, 3H, 3), 0.86 (d, $J = 6.6$ Hz, 6H, 10).

1:5 ^1H NMR (400 MHz, DMSO): $\delta/\text{ppm} = 12.25$ (s, 1H, OH), 9.14 (s, 0.2H, 2'), 7.79 (s, 0.2H, 4'), 7.70 (s, 0.2H, 5'), 7.19 (d, $J = 8.0$ Hz, 2H, 6), 7.10 (d, $J = 8.0$ Hz, 2H, 5), 4.19 (q, $J = 7.3$ Hz, 0.4H, 7'), 3.85 (s, 0.6H, 6'), 3.63 (q, $J = 7.1$ Hz, 1H, 2), 2.41 (d, $J = 7.1$ Hz, 2H, 8), 1.81 (dp, $J = 13.5, 6.7$ Hz, 1H, 9), 1.42 (t, $J = 7.3$ Hz, 0.6H, 8'), 1.34 (d, $J = 7.1$ Hz, 3H, 3), 0.86 (d, $J = 6.6$ Hz, 6H, 10).

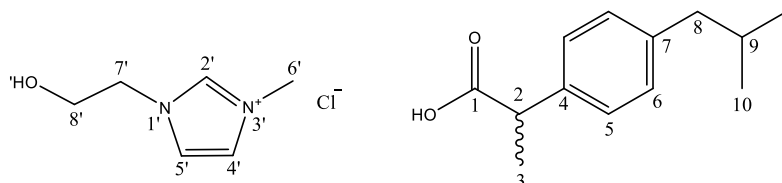
1-(2-Hydroxyethyl)-3-methylimidazolium chloride ($[\text{C}_2(\text{OH})\text{C}_1\text{Im}]\text{Cl}$)

Chapter 4 | Ibuprofen-based Eutectic Systems



^1H NMR (400 MHz, DMSO): $\delta/\text{ppm} = 9.23$ (s, 1H, 2), 7.77 (s, 1H, 4), 7.73 (s, 1H, 5), 5.41 (t, $J = 5.1$ Hz, 1H, OH), 4.24 (t, $J = 4.9$ Hz, 2H, 7), 3.88 (s, 3H, 6), 3.72 (dd, $J = 9.5, 4.7$ Hz, 2H, 8).

$[\text{C}_{2(\text{OH})}\text{C}_1\text{Im}]\text{Cl}$: Ibuprofen

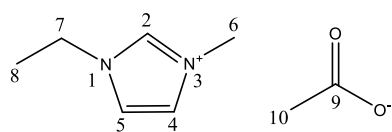


1:1 ^1H NMR (400 MHz, DMSO): $\delta/\text{ppm} = 12.26$ (s, 1H, OH), 9.15 (s, 1H, 2'), 7.75 (s, 1H, 4'), 7.71 (s, 1H, 5'), 7.19 (d, $J = 8.0$ Hz, 2H, 6), 7.10 (d, $J = 7.9$ Hz, 2H, 5), 5.30 (s, 1H, OH'), 4.30 – 4.15 (m, 2H, 7'), 3.87 (s, 3H, 6'), 3.72 (d, $J = 4.6$ Hz, 2H, 8'), 3.63 (q, $J = 7.1$ Hz, 1H, 2), 2.41 (d, $J = 7.1$ Hz, 2H, 8), 1.81 (dp, $J = 13.3, 6.7$ Hz, 1H, 9), 1.34 (d, $J = 7.1$ Hz, 3H, 3), 0.86 (d, $J = 6.6$ Hz, 6H, 10).

1:2 ^1H NMR (400 MHz, DMSO): $\delta/\text{ppm} = 12.25$ (s, 1H, OH), 9.14 (s, 0.5H, 2'), 7.74 (s, 0.5H, 4'), 7.71 (s, 0.5H, 5'), 7.19 (d, $J = 8.0$ Hz, 2H, 6), 7.10 (d, $J = 8.0$ Hz, 2H, 5), 5.28 (s, 0.5H, OH'), 4.27 – 4.18 (m, 1H, 7'), 3.87 (s, 1.5H, 6'), 3.76 – 3.68 (m, 1H, 8'), 3.63 (q, $J = 7.1$ Hz, 1H, 2), 2.41 (d, $J = 7.1$ Hz, 2H, 8), 1.81 (dp, $J = 13.4, 6.7$ Hz, 1H, 9), 1.35 (t, $J = 6.4$ Hz, 3H, 3), 0.86 (d, $J = 6.6$ Hz, 6H, 10).

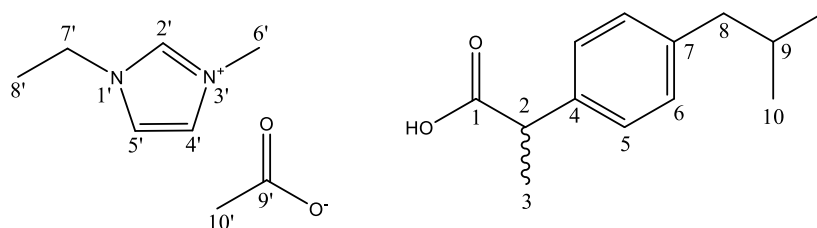
1:5 ^1H NMR (400 MHz, DMSO): $\delta/\text{ppm} = 12.26$ (s, 1H, OH), 9.11 (s, 0.2H, 2'), 7.73 (s, 0.2H, 4'), 7.70 (s, 0.2H, 5'), 7.19 (d, $J = 8.0$ Hz, 2H, 6), 7.10 (d, $J = 8.0$ Hz, 2H, 5), 5.12 (s, 0.2H, OH'), 4.26 – 4.18 (m, 0.4H, 7'), 3.87 (s, 0.6H, 6'), 3.75 – 3.70 (m, 0.4H, 8'), 3.63 (q, $J = 7.1$ Hz, 1H, 2), 2.41 (d, $J = 7.1$ Hz, 2H, 8), 1.81 (dp, $J = 13.6, 6.7$ Hz, 1H, 9), 1.34 (d, $J = 7.1$ Hz, 3H, 3), 0.86 (d, $J = 6.6$ Hz, 6H, 10).

1-Ethyl-3-methylimidazolium acetate ($[\text{C}_2\text{C}_1\text{Im}][\text{C}_1\text{CO}_2]$)



^1H NMR (400 MHz, DMSO): $\delta/\text{ppm} = 9.96$ (s, 1H, 2), 7.86 (s, 1H, 4), 7.77 (s, 1H, 5), 4.22 (q, $J = 7.3$ Hz, 2H, 7), 3.87 (s, 3H, 6), 1.56 (s, 3H, 10), 1.41 (t, $J = 7.3$ Hz, 3H, 8).

$[\text{C}_2\text{C}_1\text{Im}][\text{C}_1\text{CO}_2]$:Ibu



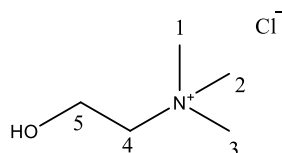
2:1 ^1H NMR (400 MHz, DMSO): $\delta/\text{ppm} = 9.44$ (s, 2H, 2'), 7.79 (s, 2H, 4'), 7.71 (s, 2H, 5'), 7.16 (d, $J = 7.9$ Hz, 2H, 5), 6.98 (d, $J = 7.9$ Hz, 2H, 6), 4.19 (dd, $J = 14.6, 7.3$ Hz, 4H, 7'), 3.84 (s, 6H, 6'), 3.31 (q, $J = 7.1$ Hz, 1H, 2), 2.36 (t, $J = 8.8$ Hz, 2H, 8), 1.84 – 1.72 (m, 1H, 9), 1.70 (s, 6H, 10'), 1.40 (t, $J = 7.3$ Hz, 6H, 8'), 1.22 (d, $J = 7.1$ Hz, 3H, 3), 0.85 (d, $J = 6.6$ Hz, 6H, 10).

1:1 ^1H NMR (400 MHz, DMSO): $\delta/\text{ppm} = 9.29$ (s, 1H, 2'), 7.78 (s, 1H, 4'), 7.69 (s, 1H, 5'), 7.16 (d, $J = 7.9$ Hz, 2H, 6), 7.00 (d, $J = 7.9$ Hz, 2H, 5), 4.19 (m, 2H, 7'), 3.83 (s, 3H, 6'), 3.41 (q, $J = 7.0$ Hz, 1H, 2), 2.37 (t, $J = 11.1$ Hz, 2H, 8), 1.76 (s, 3H, 10'), 1.40 (t, $J = 7.3$ Hz, 3H, 8'), 1.25 (d, $J = 7.1$ Hz, 3H, 3), 0.85 (d, $J = 6.6$ Hz, 6H, 10).

1:2 ^1H NMR (400 MHz, DMSO): $\delta/\text{ppm} = 9.18$ (s, 0.5H, 2'), 7.78 (s, 0.5H, 4'), 7.69 (s, 0.5H, 5'), 7.17 (d, $J = 8.0$ Hz, 2H, 6), 7.03 (d, $J = 8.0$ Hz, 2H, 5), 4.18 (dd, $J = 14.6, 7.3$ Hz, 1H, 7'), 3.84 (s, 1.5H, 6'), 3.49 (q, $J = 7.1$ Hz, 1H, 2), 2.39 (d, $J = 7.1$ Hz, 2H, 8), 1.82 (s, 1.5H, 10'), 1.41 (t, $J = 7.3$ Hz, 1.5H, 8'), 1.27 (d, $J = 7.1$ Hz, 3H, 3), 0.85 (d, $J = 6.6$ Hz, 6H, 10).

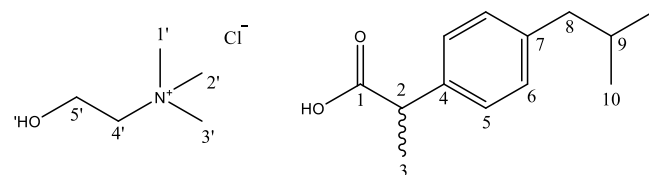
1:5 ^1H NMR (400 MHz, DMSO): $\delta/\text{ppm} = 9.14$ (s, 0.2H, 2'), 7.77 (s, 0.2H, 4'), 7.69 (s, 0.2H, 5'), 7.18 (d, $J = 7.9$ Hz, 2H, 6), 7.07 (d, $J = 7.9$ Hz, 2H, 5), 4.18 (dd, $J = 14.6, 7.3$ Hz, 0.4H, 7'), 3.84 (s, 0.6H, 6'), 3.57 (q, $J = 7.1$ Hz, 1H, 2), 2.40 (d, $J = 7.1$ Hz, 2H, 8), 1.87 (s, 0.6H, 10'), 1.86 – 1.74 (m, 1H, 9), 1.41 (t, $J = 7.3$ Hz, 2H, 8'), 1.31 (d, $J = 7.1$ Hz, 3H, 3), 0.86 (d, $J = 6.6$ Hz, 6H, 10).

Cholinium chloride ($[\text{N}_{1112}(\text{OH})]\text{Cl}$)



^1H NMR (400 MHz, DMSO): $\delta/\text{ppm} = 5.46$ (t, $J = 4.9$ Hz, 1H, OH), 3.87 – 3.78 (m, 2H, 5), 3.44 – 3.38 (m, 2H, 4), 3.13 (s, 9H, 1,2,3).

$[\text{N}_{1112}(\text{OH})]\text{Cl}$: Ibuprofen



1:5 ^1H NMR (400 MHz, DMSO): $\delta/\text{ppm} = 12.27$ (s, 1H, OH), 7.25 – 7.14 (m, 2H, 6), 7.11 (t, $J = 7.8$ Hz, 2H, 5), 3.84 (dd, $J = 9.8, 5.4$ Hz, 0.4H, 5'), 3.63 (q, $J = 7.1$ Hz, 1H, 2), 3.12 (s, 1.8H, 1',2',3'), 2.41 (d, $J = 7.1$ Hz, 2H, 8), 1.81 (dp, $J = 13.4, 6.6$ Hz, 1H, 9), 1.34 (d, $J = 7.1$ Hz, 3H, 3), 0.86 (d, $J = 6.6$ Hz, 6H, 10).

Table 4.S1. Validation of the prepared ibuprofen-based mixtures as eutectic mixtures based on the Lab benchtop procedure (dynamic visual method) used to determine the liquid-solid transition of the prepared mixtures. All mixtures validated as eutectic systems were liquid at room temperature (RT).

	Eutectic systems			
	2:1	1:1	1:2	1:5
[C ₂ (OH)C ₁ Im]Cl:Ibu	✗	✓	✓	✓
[C ₂ C ₁ Im]Cl:Ibu	✓	✓	✓	✓
[C ₂ C ₁ Im][C ₁ CO ₂]:Ibu	✓	✓	✓	✓
[N ₁₁₁₂ (OH)]Cl:Ibu	✗	✗	✗	✓

Table 4.S2. ¹H NMR chemical shifts for the position 2' and 3' according to the chemical structure of [C₂C₁Im][C₁CO₂] (right) for all the eutectic systems.

Compounds	2' (δ/ppm)	3' (δ/ppm)
[C ₂ C ₁ Im][C ₁ CO ₂]	9.96	1.56
[C ₂ C ₁ Im][C ₁ CO ₂]:Ibu 2:1	9.44	1.70
[C ₂ C ₁ Im][C ₁ CO ₂]:Ibu 1:1	9.29	1.76
[C ₂ C ₁ Im][C ₁ CO ₂]:Ibu 1:2	9.18	1.82
[C ₂ C ₁ Im][C ₁ CO ₂]:Ibu 1:5	9.14	1.87

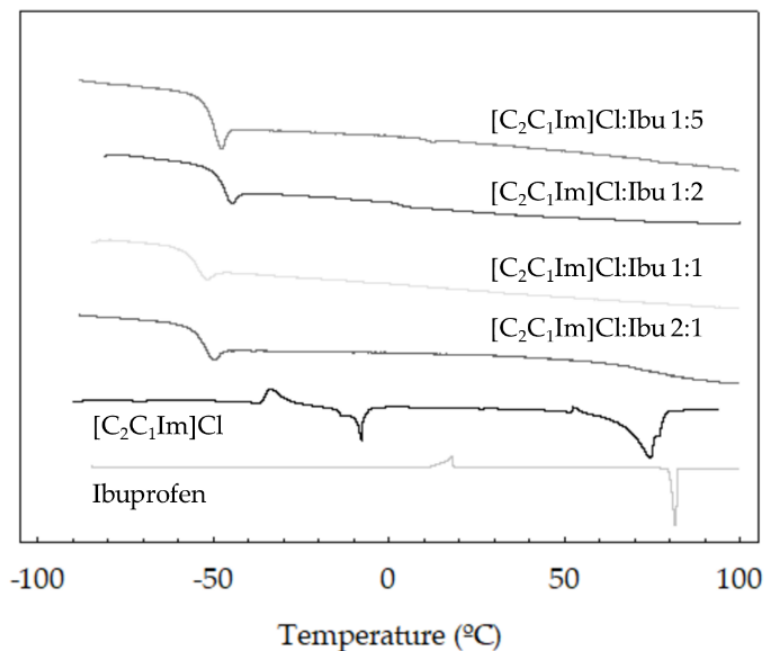
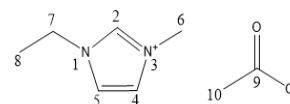


Figure 4.S1. DSC curves at 1° C/min for [C₂C₁Im]Cl: Ibu systems, ibuprofen (HBD) and [C₂C₁Im]Cl (HBA). Exo up in all thermograms.

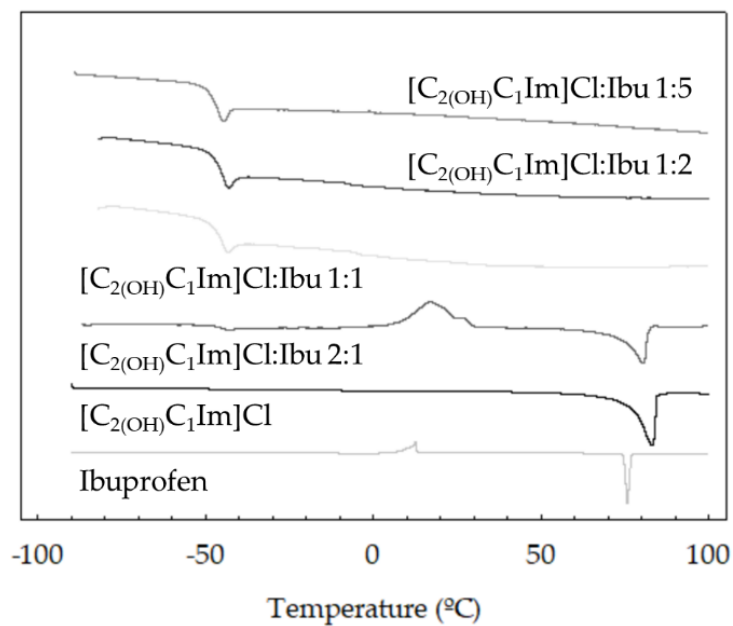


Figure 4.S2. DSC curves at 1° C/min for $[C_{2(OH)}C_1Im]Cl$:Ibu systems, ibuprofen (HBD) and $[C_{2(OH)}C_1Im]Cl$ (HBA). Exo up in all thermograms.

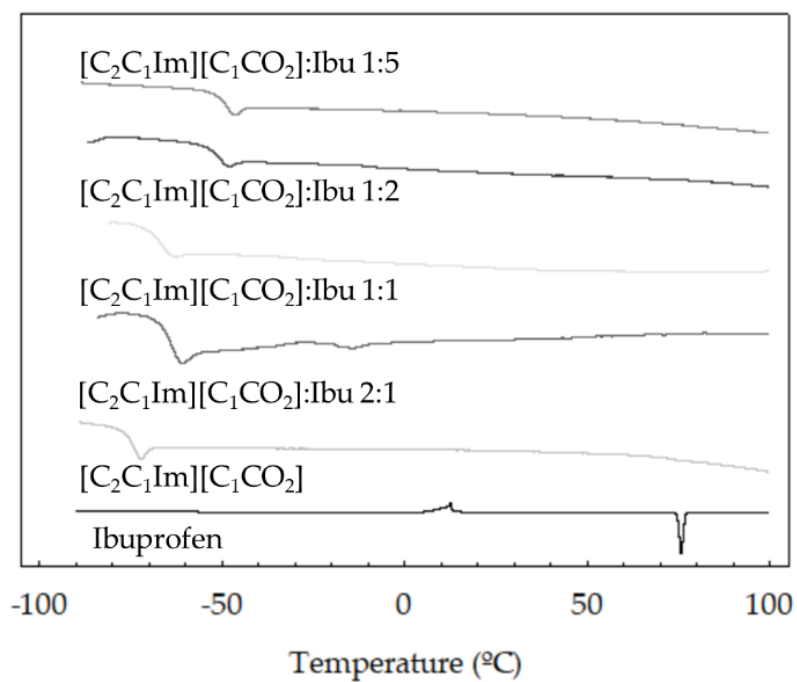


Figure 4.S3. DSC curves at 1° C/min for $[C_2C_1Im][C_1CO_2]$:Ibu systems, ibuprofen (HBD) and $[C_2C_1Im][C_1CO_2]$ (HBA). Exo up in all thermograms.

Table 4.S3. Kamlet-Taft parameters, hydrogen-bond acceptor (β) and dipolarity/polarizability (π^*) with their corresponding standards deviations determined for the eutectic systems studied in this work.

Eutectic Systems	Hydrogen-bond acceptor (β)	Dipolarity/polarizability (π^*)
[C ₂ C ₁ Im][C ₁ CO ₂]:Ibu 2:1	1.048 ± 0.000	0.978 ± 0.006
[C ₂ C ₁ Im][C ₁ CO ₂]:Ibu 1:1	0.955 ± 0.003	0.934 ± 0.002
[C ₂ C ₁ Im][C ₁ CO ₂]:Ibu 1:2	0.833 ± 0.001	0.860 ± 0.003
[C ₂ C ₁ Im][C ₁ CO ₂]:Ibu 1:5	0.662 ± 0.020	0.781 ± 0.006
[C ₂ C ₁ Im]Cl:Ibu 2:1	0.880 ± 0.012	1.008 ± 0.003
[C ₂ C ₁ Im]Cl:Ibu 1:1	0.822 ± 0.003	0.971 ± 0.003
[C ₂ C ₁ Im]Cl:Ibu 1:2	0.763 ± 0.016	0.915 ± 0.013
[C ₂ C ₁ Im]Cl:Ibu 1:5	0.688 ± 0.001	0.776 ± 0.002
[C _{2(OH)} C ₁ Im]Cl:Ibu 1:1	0.729 ± 0.008	0.937 ± 0.007
[C _{2(OH)} C ₁ Im]Cl:Ibu 1:2	0.693 ± 0.022	0.864 ± 0.007
[C _{2(OH)} C ₁ Im]Cl:Ibu 1:5	0.690 ± 0.003	0.738 ± 0.000
[N _{1112(OH)}]Cl:Ibu 1:5	0.692 ± 0.005	0.715 ± 0.003
[C ₂ C ₁ Im][C ₁ CO ₂] [S1]	1.15 ± 0.040	1.05 ± 0.002
Water [S1]	0.130 ± 0.014	1.34 ± 0.001

Table 4.S4. The effect of the different HBA's in ibuprofen solubility, eutectic and non-eutectic formulations, in water and simulated fluids (pH 1.0, pH 6.8 and 0.15M NaCl).

HBA:Ibu 2:1	
Water	$[C_2C_1Im][C_1CO_2] > [C_{2(OH)}C_1Im]Cl^* > [N_{1112(OH)}]Cl^* > [C_2C_1Im]Cl$
pH 1.0	$[C_{2(OH)}C_1Im]Cl^* > [C_2C_1Im][C_1CO_2] > [C_2C_1Im]Cl > [N_{1112(OH)}]Cl^*$
pH 6.8	$[C_{2(OH)}C_1Im]Cl^* > [N_{1112(OH)}]Cl^* > [C_2C_1Im]Cl > [C_2C_1Im][C_1CO_2]$
0.15M NaCl	$[C_2C_1Im][C_1CO_2] > [C_2C_1Im]Cl > [C_{2(OH)}C_1Im]Cl^* \approx [N_{1112(OH)}]Cl^*$
HBA:Ibu 1:1	
Water	$[C_2C_1Im][C_1CO_2] > [C_{2(OH)}C_1Im]Cl > [N_{1112(OH)}]Cl^* > [C_2C_1Im]Cl$
pH 1.0	$[C_{2(OH)}C_1Im]Cl > [C_2C_1Im][C_1CO_2] > [C_2C_1Im]Cl > [N_{1112(OH)}]Cl^*$
pH 6.8	$[C_2C_1Im][C_1CO_2] > [C_{2(OH)}C_1Im]Cl > [C_2C_1Im]Cl > [N_{1112(OH)}]Cl^*$
0.15M NaCl	$[C_2C_1Im][C_1CO_2] > [C_{2(OH)}C_1Im]Cl > [C_2C_1Im]Cl > [N_{1112(OH)}]Cl^*$
HBA:Ibu 1:2	
Water	$[C_{2(OH)}C_1Im]Cl > [C_2C_1Im]Cl > [N_{1112(OH)}]Cl^* > [C_2C_1Im][C_1CO_2]$
pH 1.0	$[C_2C_1Im]Cl > [C_2C_1Im][C_1CO_2] > [C_{2(OH)}C_1Im]Cl > [N_{1112(OH)}]Cl^*$
pH 6.8	$[C_{2(OH)}C_1Im]Cl > [C_2C_1Im][C_1CO_2] > [C_2C_1Im]Cl > [N_{1112(OH)}]Cl^*$
0.15M NaCl	$[C_{2(OH)}C_1Im]Cl > [C_2C_1Im]Cl > [C_2C_1Im][C_1CO_2] > [N_{1112(OH)}]Cl^*$
HBA:Ibu 1:5	
Water	$[C_2C_1Im][C_1CO_2] > [N_{1112(OH)}]Cl \approx [C_{2(OH)}C_1Im]Cl > [C_2C_1Im]Cl$
pH 1.0	$[N_{1112(OH)}]Cl \approx [C_2C_1Im][C_1CO_2] > [C_{2(OH)}C_1Im]Cl > [C_2C_1Im]Cl$
pH 6.8	$[C_2C_1Im][C_1CO_2] > [C_{2(OH)}C_1Im]Cl \approx [C_2C_1Im]Cl \approx [N_{1112(OH)}]Cl$
0.15M NaCl	$[C_2C_1Im][C_1CO_2] > [N_{1112(OH)}]Cl > [C_{2(OH)}C_1Im]Cl > [C_2C_1Im]Cl$

* non-eutectic system

Table 4.S5. The effect of the molar ratio in ibuprofen solubility, eutectic and non-eutectic formulations, in water and simulated fluids (pH 1.0, pH 6.8 and 0.15M NaCl).

[C₂C₁Im]Cl	
Water	2:1 > 1:2 ≈ 1:5 > 1:1
pH 1.0	1:2 > 1:1 ≈ 2:1 > 1:5
pH 6.8	2:1 > 1:1 > 1:2 > 1:5
0.15M NaCl	2:1 > 1:1 ≈ 1:5 > 1:2
[C₂C₁Im][C₁CO₂]	
Water	2:1 > 1:1 > 1:2 > 1:5
pH 1.0	2:1 ≈ 1:1 > 1:5 ≈ 1:2
pH 6.8	1:1 > 1:2 ≈ 1:5 > 2:1
0.15M NaCl	2:1 > 1:1 > 1:5 ≈ 1:2
[C_{2(OH)}C₁Im]Cl	
Water	2:1* > 1:1 > 1:5 > 1:2
pH 1.0	1:1 > 2:1* > 1:2 > 1:5
pH 6.8	2:1* > 1:1 > 1:2 > 1:5
0.15M NaCl	1:1 ≈ 1:5 > 2:1* > 1:2
[N_{1112(OH)}]Cl	
Water	2:1* > 1:1* > 1:5 > 1:2*
pH 1.0	1:5 > 2:1* > 1:1* > 1:2*
pH 6.8	2:1* > 1:1* > 1:2* > 1:5
0.15M NaCl	1:5 > 2:1* > 1:2* ≈ 1:1*

* non-eutectic system

Table 4.S6. Density, ρ , dynamic viscosity, η , and ionic conductivity, k , as a function of temperature of ibuprofen-based systems with [C₂C₁Im]Cl as hydrogen bond acceptor.

$T/^\circ\text{C}$	$\rho/\text{g}\cdot\text{cm}^{-3}$	$\eta/\text{m}\cdot\text{Pa}\cdot\text{s}$	$k/\text{mS}\cdot\text{cm}^{-1}$	$T/^\circ\text{C}$	$\rho/\text{g}\cdot\text{cm}^{-3}$	$\eta/\text{m}\cdot\text{Pa}\cdot\text{s}$	$k/\text{mS}\cdot\text{cm}^{-1}$
[C₂C₁Im]Cl:Ibu 2:1				[C₂C₁Im]Cl:Ibu 1:1			
15	1.09315	11455.5	0.027	15	1.07050	8067.4	0.020
20	1.08995	5965.3	0.053	20	1.06740	4373.0	0.042
25	1.08690	3296.4	0.091	25	1.06420	2506.1	0.062
30	1.08395	1919.2	0.156	30	1.06110	1510.0	0.100
35	1.08095	1173.3	0.251	35	1.05800	951.3	0.155
40	1.07795	749.5	0.357	40	1.05490	623.8	0.237
45	1.07505	497.9	0.632	45	1.05190	424.1	0.364
50	1.07220	342.6	0.937	50	1.04890	297.7	0.537
55	1.06940	243.2		55	1.04590	215.1	
60	1.06670	177.5		60	1.04310	159.5	
65	1.06390	132.9		65	1.04030	121.0	
70	1.06115	101.7		70	1.03740	93.70	
75	1.05840	79.45		75	1.03450	73.94	
80	1.05550	63.34		80	1.03130	59.34	
[C₂C₁Im]Cl:Ibu 1:2				[C₂C₁Im]Cl:Ibu 1:5			
15	1.04840	5406.5	0.011	15	1.02750	2979.6	0.003
20	1.04510	2998.2	0.019	20	1.02343	1669.7	0.005
25	1.04180	1755.9	0.037	25	1.01933	987.2	0.010
30	1.03850	1079.4	0.058	30	1.01560	612.2	0.019
35	1.03520	692.6	0.092	35	1.01233	396.0	0.034
40	1.03190	461.7	0.135	40	1.00920	266.2	0.049
45	1.02870	318.5	0.204	45	1.00627	185.0	0.074
50	1.02570	226.5	0.293	50	1.00343	132.6	0.102
55	1.02270	165.5		55	1.00080	97.63	
60	1.01970	124.0		60	0.99807	73.65	
65	1.01670	94.89		65	0.99547	56.78	
70	1.01380	74.10		70	0.99233	44.69	
75	1.01070	58.88		75	0.98910	35.73	
80	1.00740	47.57		80	0.98577	29.08	

Table 4.S7. Density, ρ , dynamic viscosity, η , and ionic conductivity, k , as a function of temperature of ibuprofen-based systems with $[\text{C}_{2(\text{OH})}\text{C}_1\text{Im}]\text{Cl}$ as hydrogen bond acceptor.

T/C°	$\rho/\text{g}\cdot\text{cm}^{-3}$	$\eta/\text{m}\cdot\text{Pa}\cdot\text{s}$	$k/\text{mS}\cdot\text{cm}^{-1}$	T/C°	$\rho/\text{g}\cdot\text{cm}^{-3}$	$\eta/\text{m}\cdot\text{Pa}\cdot\text{s}$	$k/\text{mS}\cdot\text{cm}^{-1}$
$[\text{C}_{2(\text{OH})}\text{C}_1\text{Im}]\text{Cl}:\text{Ibu}$ 1:1				$[\text{C}_{2(\text{OH})}\text{C}_1\text{Im}]\text{Cl}:\text{Ibu}$ 1:2			
15	1.10705	23604.3	0.007	15	1.07350	12385.0	0.004
20	1.10350	12597.0	0.016	20	1.07010	6669.7	0.007
25	1.10065	7058.3	0.024	25	1.06680	3789.8	0.014
30	1.09790	4135.3	0.043	30	1.06350	2254.9	0.022
35	1.09508	2528.4	0.066	35	1.06020	1398.9	0.039
40	1.09200	1604.9	0.104	40	1.05700	901.1	0.065
45	1.09023	1054.8	0.172	45	1.05380	600.7	0.102
50	1.08688	715.1	0.240	50	1.05050	413.2	0.144
55	1.08410	499.0		55	1.04740	292.4	
60	1.08125	357.3		60	1.04430	212.3	
65	1.07830	262.1		65	1.04120	157.8	
70	1.07530	196.4		70	1.03820	119.8	
75	1.07218	150.1		75	1.03510	92.769	
80	1.06890	117.0		80	1.03170	73.085	
$[\text{C}_{2(\text{OH})}\text{C}_1\text{Im}]\text{Cl}:\text{Ibu}$ 1:5							
15	1.04127	4169.1	0.001				
20	1.03760	2287.9	0.002				
25	1.03410	1326.0	0.004				
30	1.03010	806.6	0.005				
35	1.02663	512.3	0.008				
40	1.02323	338.1	0.015				
45	1.01957	231.1	0.022				
50	1.01640	162.9	0.034				
55	1.01367	118.1					
60	1.01043	87.78					
65	1.00727	66.74					
70	1.00413	51.84					
75	1.00157	40.99					

Table 4.S8. Density, ρ , dynamic viscosity, η , and ionic conductivity, k , as a function of temperature of ibuprofen-based systems with $[\text{C}_2\text{C}_1\text{Im}][\text{C}_1\text{CO}_2]$ as hydrogen bond acceptor.

T/C°	$\rho/\text{g}\cdot\text{cm}^{-3}$	$\eta/\text{m}\cdot\text{Pa}\cdot\text{s}$	$k/\text{mS}\cdot\text{cm}^{-1}$	T/C°	$\rho/\text{g}\cdot\text{cm}^{-3}$	$\eta/\text{m}\cdot\text{Pa}\cdot\text{s}$	$k/\text{mS}\cdot\text{cm}^{-1}$
$[\text{C}_2\text{C}_1\text{Im}][\text{C}_1\text{CO}_2]:\text{Ibu } 2:1$				$[\text{C}_2\text{C}_1\text{Im}][\text{C}_1\text{CO}_2]:\text{Ibu } 1:1$			
15	1.07298	848.318	0.267	15	1.05970	1271.5	0.123
20	1.06980	543.498	0.395	20	1.05650	795.4	0.193
25	1.06658	362.840	0.568	25	1.05320	518.8	0.269
30	1.06350	251.188	0.795	30	1.04990	351.3	0.411
35	1.06048	179.503	1.09	35	1.04680	245.9	0.556
40	1.05740	131.925	1.42	40	1.04370	177.3	0.733
45	1.05450	99.407	1.99	45	1.04070	131.3	1.10
50	1.05163	76.590	2.43	50	1.03780	99.52	1.35
55	1.04873	60.183		55	1.03480	77.06	
60	1.04583	48.155		60	1.03190	60.82	
65	1.04295	39.145		65	1.02900	48.83	
70	1.04003	32.279		70	1.02610	39.81	
75	1.03713	26.967		75	1.02310	32.92	
80	1.07298	22.792		80	1.02000	27.57	
$[\text{C}_2\text{C}_1\text{Im}][\text{C}_1\text{CO}_2]:\text{Ibu } 1:2$				$[\text{C}_2\text{C}_1\text{Im}][\text{C}_1\text{CO}_2]:\text{Ibu } 1:5$			
15	1.04410	2526.6	0.027	15	1.02703	2974.9	0.004
20	1.04100	1501.8	0.046	20	1.02350	1703.6	0.007
25	1.03780	933.7	0.075	25	1.01997	1025.9	0.014
30	1.03450	605.0	0.111	30	1.01647	645.5	0.025
35	1.03120	406.4	0.159	35	1.01297	422.6	0.039
40	1.02810	282.2	0.228	40	1.00967	286.4	0.056
45	1.02490	201.7	0.338	45	1.00640	200.3	0.086
50	1.02190	148.1	0.457	50	1.00317	144.1	0.134
55	1.01880	111.3		55	0.99997	106.4	
60	1.01580	85.4		60	0.99703	80.29	
65	1.01270	66.8		65	0.99335	61.52	
70	1.00950	53.2		70	0.99060	48.65	
75	1.00630	43.1		75	0.98723	38.83	
80	1.00300	35.3		80	0.98243	31.50	

Table 4.S9. Density, ρ , dynamic viscosity, η , and ionic conductivity, k , as a function of temperature of [N₁₁₁₂(OH)]Cl:Ibu 1:5.

$T/^\circ\text{C}$	$\rho/\text{g}\cdot\text{cm}^{-3}$	$\eta/\text{mPa}\cdot\text{s}$	$k/\text{mS}\cdot\text{cm}^{-1}$
15	1.02567	4433.7	0.004
20	1.02207	2503.2	0.007
25	1.01850	1483.0	0.014
30	1.01493	917.5	0.025
35	1.01130	591.0	0.039
40	1.00773	394.2	0.056
45	1.00427	271.5	0.086
50	1.00103	192.5	0.134
55	0.99807	140.0	
60	0.99503	104.3	
65	0.99180	79.36	
70	0.98860	61.56	
75	0.98527	48.57	

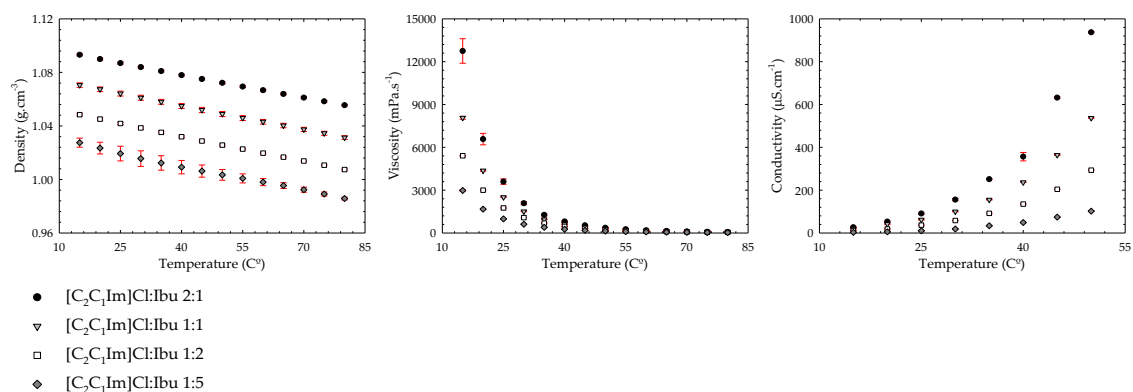


Figure 4.S4. Density, viscosity and conductivity of the Ibuprofen-based eutectic systems based with [C₂C₁Im]Cl as hydrogen bond acceptor.

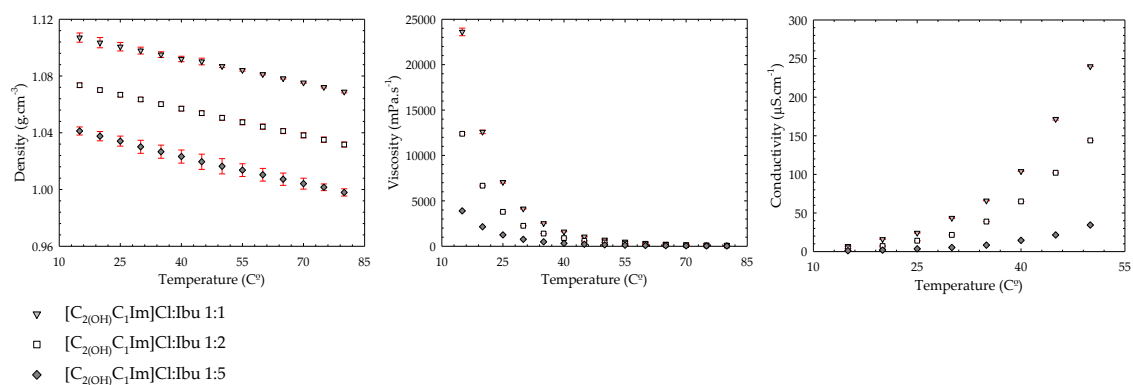


Figure 4.S5. Density, viscosity and conductivity of the Ibuprofen-based eutectic systems based with [C_{2(OH)}C₁Im]Cl as hydrogen bond acceptor.

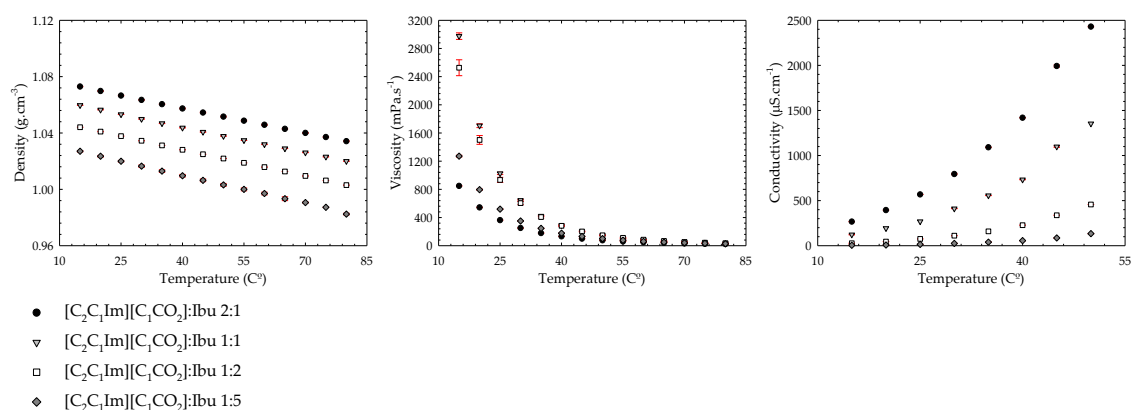


Figure 4.S6. Density, viscosity and conductivity of the Ibuprofen-based eutectic systems based with [C₂C₁Im][C₁CO₂] as hydrogen bond acceptor.

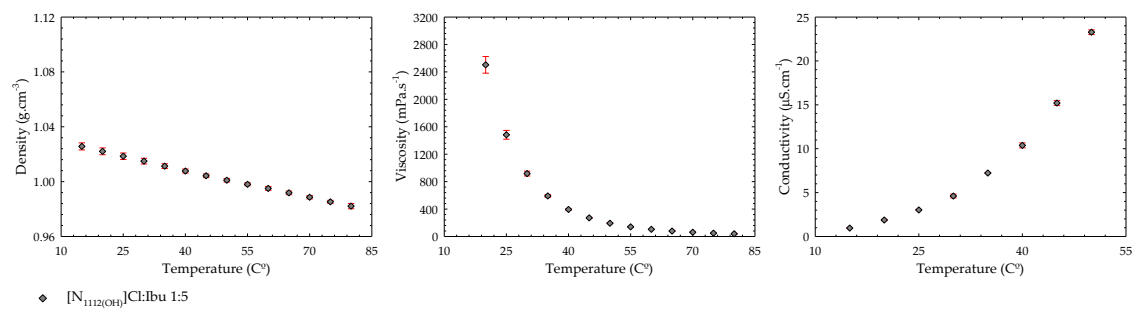


Figure 4.S7. Density, viscosity and conductivity of the Ibuprofen-based eutectic systems based with [N₁₁₁₂(OH)]Cl as hydrogen bond acceptor.

Table 4.S10. Inhibition of BSA denaturation in PBS pH 7.4 at different concentrations for ibuprofen-based eutectic systems. The presented value is the mean of at least two independent measures \pm standard deviation.

Concentration (mM)	Inhibition of BSA denaturation (%)	Concentration (mM)	Inhibition of BSA denaturation (%)
[C₂C₁Im]Cl:Ibu 2:1		[C₂C₁Im]Cl:Ibu 1:1	
0.901	23.48 \pm 2.90	0.850	21.79 \pm 1.67
2.102	31.08 \pm 1.24	1.984	25.00 \pm 1.90
3.003	58.61 \pm 0.48	2.834	54.39 \pm 1.49
4.505	57.77 \pm 1.09	4.251	60.14 \pm 1.04
[C₂C₁Im]Cl:Ibu 1:2		[C₂C₁Im]Cl:Ibu 1:5	
0.805	29.90 \pm 0.96	0.764	4.22 \pm 0.41
1.878	41.39 \pm 2.35	1.783	15.03 \pm 2.04
2.683	51.01 \pm 4.25	2.547	35.64 \pm 0.41
4.024	63.85 \pm 0.63	3.820	45.10 \pm 0.63
[C_{2(OH)}C₁Im]Cl:Ibu 1:1		[C_{2(OH)}C₁Im]Cl:Ibu 1:2	
0.813	4.22 \pm 0.51	0.782	16.89 \pm 0.83
1.898	14.19 \pm 0.63	1.826	34.12 \pm 1.80
2.711	24.66 \pm 2.08	2.608	45.10 \pm 2.08
4.066	40.03 \pm 2.28	3.912	53.72 \pm 1.96
[C₂C₁Im]Cl:Ibu 1:5		[N_{1112(OH)}]Cl:Ibu 1:5	
0.754	18.36 \pm 2.52	0.769	6.25 \pm 0.41
1.759	30.25 \pm 1.90	1.793	26.35 \pm 1.26
2.513	49.23 \pm 1.22	2.562	47.13 \pm 2.42
3.769	66.67 \pm 1.51	3.843	52.20 \pm 3.05

Table 4.S11. Inhibition of COX-1 (ovine) and COX-2 (human) and COX-1/COX-2 selectivity for 3 mM ibuprofen [S1], ibuprofen-based ionic liquids and ibuprofen-based eutectics.

Compound	Inhibition of COX-1 (ovine) (%)	Inhibition of COX-2 (human) (%)	COX-1/COX-2 selectivity
Ibuprofen	56.18 \pm 2.60	65.13 \pm 4.25	0.863 \pm 0.069
[C ₂ C ₁ Im]Cl:Ibu 1:1	60.74 \pm 3.13	62.32 \pm 11.53	0.975 \pm 0.187
[C ₂ C ₁ Im]Cl:Ibu 1:5	55.60 \pm 1.49	66.71 \pm 9.89	0.833 \pm 0.126
[C _{2(OH)} C ₁ Im]Cl:Ibu 1:1	59.47 \pm 2.51	69.80 \pm 3.51	0.852 \pm 0.056
[C _{2(OH)} C ₁ Im]Cl:Ibu 1:5	90.73 \pm 5.12	70.95 \pm 6.22	1.279 \pm 0.133
[N _{1112(OH)}]Cl:Ibu 1:5	39.09 \pm 4.21	78.79 \pm 4.90	0.496 \pm 0.062

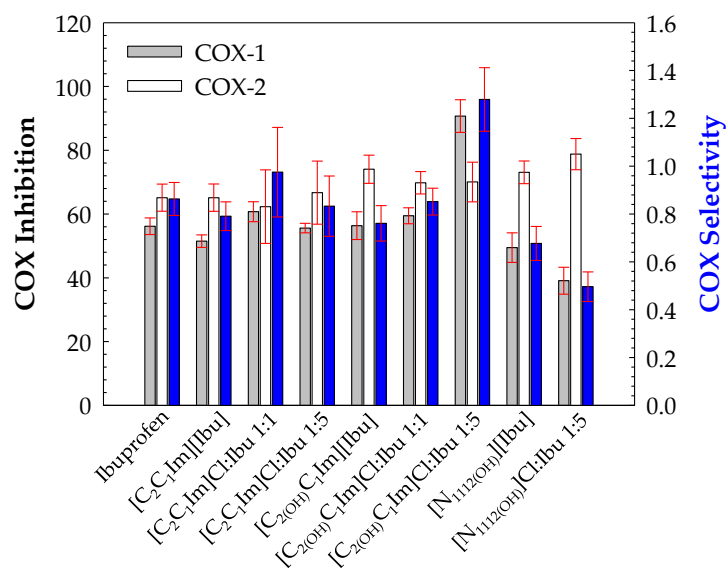


Figure 4.S8. Selective inhibition of COX-1 (ovine) and COX-2 (human) and COX-1/COX-2 selectivity for 3 mM ibuprofen [S2], ibuprofen-based ionic liquids [S2] and ibuprofen-based eutectics.

References

- S1. Bastos, J.C.; Carvalho, S.F.; Welton, T.; Canongia Lopes, J.N.; Rebelo, L.P.N.; Shimizu, K.; Araújo, J.M.M.; Pereira, A.B. Design of Task-Specific Fluorinated Ionic Liquids: Nanosegregation: Versus Hydrogen-Bonding Ability in Aqueous Solutions. *Chemical Communications* **2018**, *54*, 3524–3527, doi:10.1039/c8cc00361k.
- S2. Bastos, J.C.; Vieira, N.S.M.; Gaspar, M.M.; Pereira, A.B.; Araújo, J.M.M. Human Cytotoxicity, Hemolytic Activity, Anti-Inflammatory Activity and Aqueous Solubility of Ibuprofen-Based Ionic Liquids. *Sustainable Chemistry* **2022**, *3*, 358–375, doi:10.3390/suschem3030023.

4.2 Liquid Ibuprofen Formulations by Eutectic Formation Between Ibuprofen-based Ionic Liquids and Ibuprofen: Human Cytotoxicity, Hemolytic Activity and Anti-Inflammatory Activity

4.2.1 Abstract

The low solubility of active pharmaceutical ingredients (APIs) is a problem in pharmaceutical development. Several methodologies can be used to improve API solubility, including the use of eutectic systems in which one of the constituents is the API. Herein we exploit for the first time the synthesis of eutectic systems combining ibuprofen-based ionic liquids as hydrogen-bond acceptor (HBA) and neat ibuprofen as hydrogen-bond donor (HBD) at the molar ratios 2:1, 1:1, 1:2 and 1:5. Firstly, a thermal behavior analysis was conducted by differential scanning calorimetry (DSC) to confirm the eutectic formation and the interactions between the components that constitute the systems were studied by NMR corroborating that the eutectic system is formed by H-bonds between the ibuprofen-based ionic liquids and the neat ibuprofen. An in vitro cytotoxicity assessment was accessed in two different human cells lines, namely in colon carcinoma cells (Caco-2) and hepatocellular carcinoma cells (HepG2). The anti-inflammatory properties were also achieved through the inhibition of the bovine serum albumin (BSA) denaturation and confirmed by the direct evaluation of COX-1(ovine) and COX-2(human) inhibition. The results prove that it is possible to formulate a eutectic system with ibuprofen-based ionic liquids and neat ibuprofen with low hepatic and intestinal cytotoxicity yet maintaining, and in some cases improving, the pharmacological activity of the parent API.

Keywords: Ibuprofen; Eutectic Systems; Ionic Liquids; Bioavailability; Cytotoxicity; HepG2; Caco-2; Anti-inflammatory Activity; Protein denaturation inhibition; COX-1 (human); COX-2 (bovine).

To be published in: Joana C. Bastos, Ana B. Pereiro, João M. M. Araújo. Liquid Ibuprofen Formulations by Eutectic Formation Between Ibuprofen-based Ionic Liquids and Ibuprofen: Human Cytotoxicity, Hemolytic Activity and Anti-Inflammatory Activity. *Pharmaceuticals* 2023 (*Submitted*)

Own experimental contribution: API-ILs-based eutectics synthesis, NMR and DSC sample preparation, cytotoxicity assay, protein denaturation assay, cyclooxygenases (COX-1 and COX-2) inhibition assay.

Own written contribution: NMR and DSC analysis, cytotoxicity assay, protein denaturation assay, hemocompatibility assay, cyclooxygenases (COX-1 and COX-2) inhibition assay.

Other contributions: Experimental design and data analysis.

4.2.2 Introduction

Improving the efficiency of the existing drugs is currently one of the major goals of pharmaceutical industries [1]. Rather than developing new drugs with higher bioavailability, there are undisputable assurances and profits in improving the already tried-and-tested drugs [1]. To improve their pharmacological action, drugs can suffer incremental changes, such as the modification of the drug's form and formulation, assessment of new combinations, and the use of different dosages or novel administration routes. One of the characteristics with great ceiling for improvement is hydrophilicity; approximately 40% of the approved drugs and nearly 90% of the drugs under development are poorly water-soluble, which leads to low bioavailability and permeation [2]. Innovation in drug efficacy improvement has been constrained by the common use of solid forms of active pharmaceutical ingredients (APIs), often associated with physical and chemical instability in their final dosage [3]. These concerns can be due to their polymorphism and dissolution and oral drug absorption in humans, thereby conditioning the drug's bioavailability [4]. An alternative to overcome these concerns is to convert the API into a liquid formulation. Contrarily to solid forms, liquids display a higher solubility in water since the energy barrier associated with the enthalpy of fusion is overwhelmed, providing a higher therapeutic response [5]. However, the manufacturing of APIs in the liquid form must ensure safety, efficacy, and stability of the final drug product.

One helpful example of the development of liquid forms of APIs is their conversion into ionic liquids, constituted by anionic and/or cationic active ingredients (API-ILs) [6]. Ionic liquids (ILs) present unique physicochemical properties, such as low melting point (less than 100°C), negligible vapor pressure, wide liquid range, nonflammability, high thermal stability, *etc* [6]. It has been shown that the combination of poorly water-soluble APIs with suitable counter-ions to give liquid forms can resolve the limitations of low solubility and polymorphism [7]. Some successful examples involve the preparation of API-ILs from sulfasalazine [8], paclitaxel [9], salicylic acid [10], methotrexate [11], selurampanel [12] and ibuprofen [6].

Recently four ibuprofen-based ionic liquids were developed, namely, 1-ethyl-3-methylimidazolium ibuprofenate ($[\text{C}_2\text{C}_1\text{Im}][\text{Ibu}]$), 1-(2-hydroxyethyl)-3-methylimidazolium ibuprofenate ($[\text{C}_{2(\text{OH})}\text{C}_1\text{Im}][\text{Ibu}]$) and cholinium ibuprofenate ($[\text{N}_{1112(\text{OH})}][\text{Ibu}]$) in order to improve the API efficacy. All the synthesized API-ILs demonstrated a similar cytotoxic profiles in both colon carcinoma cells, Caco-2, and hepatocellular carcinoma cells, HepG-2, and low cytotoxicity within the maximum plasma concentration (C_{max}) of ibuprofen. Moreover, the solubilities in water and simulated biological fluids increased exponentially up to four orders of magnitude always maintaining the anti-inflammatory activity [6]. Santos et al. also synthesized ibuprofenates with short-chain alcohol-functionalized imidazolium, triethylammonium, or cholinium cations with cellular viabilities up to 80% in human dermal fibroblasts ovarian carcinoma cells and enhanced water and PBS solubilities in comparison to that of the ibuprofen in neutral or sodium salt form [13]. The main disadvantage in both cases is that the API-ILs showed to be mainly solid at room temperature.

Eutectic mixtures have emerged as advantageous alternatives to incorporate APIs, being also able to produce new liquid forms to enhance the API bioavailability [14]. They are usually prepared by the combination of molecules whose toxicity profiles are already well established and whose use in pharmaceutical applications can be well accepted. Contrarily to ILs, the preparation of eutectic systems only requires the mixing of at least two species, a hydrogen-bond donor (HBD) and a hydrogen-bond acceptor (HBA), generally under stirring and moderate heating, where the temperature to which the mixture is subjected must be carefully controlled to prevent the decomposition of the individual components [14]. Since no chemical reaction is involved in the preparation process it presents 100% of the atom economy and fits within one of the Green Chemistry principles [15]. The eutectic systems deviate from the ideal thermodynamic solid-liquid phase behavior where strong hydrogen-bond interactions between the HBD and HBA species are responsible for a decrease the melting temperature to such a degree where the mixture can be liquid at room temperature [16].

The first report on eutectic systems with therapeutic purposes using non-steroidal anti-inflammatory drugs (NSAIDs) was published by Stott et al. [17] in 1998. They prepared a mixture composed of menthol and ibuprofen, envisaging the enhancement of skin permeation and development of a transdermal delivery system and found a significant increase in transdermal permeation. Since then, the production of different types of eutectic systems concerning the use NSAIDs have been reported. For instance, menthol and stearic acid were used to construct a system for wound healing [16] and a eutectic system based on choline chloride and ascorbic acid was used to create different types of drug carriers for dexamethasone [18] and a eutectic formation of naproxen and dicarboxylic acids was successfully achieved in order to develop a more efficient oral dosage for this particular poor water-soluble drug [19]. By combining several HBA with ibuprofen, namely, 1-ethyl-3-methylimidazolium chloride ($[\text{C}_2\text{C}_1\text{Im}]\text{Cl}$), 1-(2-hydroxyethyl)-3-methylimidazolium chloride ($[\text{C}_{2(\text{OH})}\text{C}_1\text{Im}]\text{Cl}$), 1-ethyl-3-methylimidazolium acetate ($[\text{C}_2\text{C}_1\text{Im}][\text{C}_1\text{CO}_2]$) and cholinium chloride ($[\text{N}_{1112(\text{OH})}]\text{Cl}$) an evident solubility enhancement in water and simulated biological fluids was observed [20]. The acid form of ibuprofen present solubilities significantly lower than its eutectic formation although maintaining the same cytotoxic and anti-inflammatory profile as the parent API.

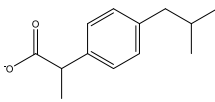
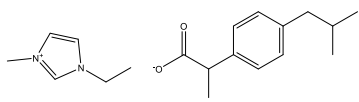
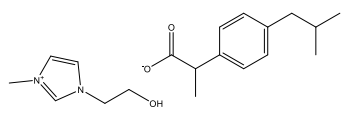
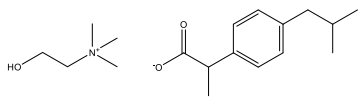
To the best of our knowledge, herein we report for the first time a study concerning the combination of ibuprofen and an ibuprofen-based IL, specifically, 1-ethyl-3-methylimidazolium ibuprofenate ($[\text{C}_2\text{C}_1\text{Im}][\text{Ibu}]$), 1-(2-hydroxyethyl)-3-methylimidazolium ibuprofenate ($[\text{C}_{2(\text{OH})}\text{C}_1\text{Im}][\text{Ibu}]$) and cholinium ibuprofenate ($[\text{N}_{1112(\text{OH})}][\text{Ibu}]$) at the molar ratios 1:1; 1:2; 1:5 and 2:1. The eutectic systems were characterized by DSC and NMR to validate the eutectic formation. We also reported the cytotoxic profiles in colon carcinoma cells, Caco-2, and hepatocellular carcinoma cells, HepG2. The pharmacological activity of the eutectic systems was attained by the protein albumin denaturation assay and by directly measuring the inhibition of COX enzymes using a colorimetric COX (human ovine) inhibitor screening assay kit. Additionally, a hemocompatibility assay was achieved to evaluate the ibuprofen-based systems biocompatibility.

4.2.3 Materials and Methods

4.2.3.1 Materials

Ibuprofen (>98% mass fraction purity) was acquired from TCI and used without further purification. The ionic liquids 1-ethyl-3-methylimidazolium ibuprofenate ($[\text{C}_2\text{C}_1\text{Im}][\text{Ibu}]$), 1-(2-hydroxyethyl)-3-methylimidazolium ibuprofenate ($[\text{C}_{2(\text{OH})}\text{C}_1\text{Im}][\text{Ibu}]$) and cholinium ibuprofenate ($[\text{N}_{1112(\text{OH})}][\text{Ibu}]$) were prepared through two-step anion exchange reaction methodology and fully characterized as described in our previous work [6]. To avoid volatile impurities the ionic liquids and cholinium chloride were dried under a $3 \cdot 10^{-2}$ Torr vacuum for at least 48 hours prior to any use and the water content, determined by Karl Fischer titration, was less than 0.05 wt%. The structures, acronyms and molecular masses of ionic liquids, cholinium chloride and ibuprofen are listed in **Table 4.6**.

Table 4.6. Designation, chemical structure, and molecular weight (M_w) of ibuprofen and cholinium- and imidazolium-based API-ILs used along this work.

Structure	Designation and acronym	M_w (g/mol)
	2-(4-Isobutylphenyl) propionic acid Ibuprofen (Ibu)	206.29
	1-Ethyl-3-methylimidazolium ibuprofenate $[\text{C}_2\text{C}_1\text{Im}][\text{Ibu}]$	316.44
	1-(2-hydroxyethyl)-3-methylimidazolium ibuprofenate $[\text{C}_{2(\text{OH})}\text{C}_1\text{Im}][\text{Ibu}]$	332.44
	Cholinium ibuprofenate $[\text{N}_{1112(\text{OH})}][\text{Ibu}]$	309.44

4.2.3.2 Preparation of pharmaceutically active eutectic systems

The pharmaceutically active eutectic systems were prepared by combining a API-IL ($[\text{C}_2\text{C}_1\text{Im}][\text{Ibu}]$, $[\text{C}_{2(\text{OH})}\text{C}_1\text{Im}][\text{Ibu}]$ and $[\text{N}_{1112(\text{OH})}][\text{Ibu}]$), used as hydrogen-bond acceptor (HBA), with ibuprofen as hydrogen-bond donor (HBD) accordingly to a procedure recently implemented by us [21]. The API-IL:Ibu systems were synthesized by mixing

the counterparts at different molar ratios such as 2:1; 1:1; 1:2 and 1:5. By using an analytical high precision balance (Sartorius, Germany) with 0.01 mg resolution, the mixtures were prepared and then sealed under nitrogen atmosphere in crimped seal glass vials. To ensure that all the counterparts were blended, three heating (up to 85°C \pm 2°C) / cooling (down to 5°C \pm 2°C) cycles were performed under constant stirring. ^1H NMR technique was used to verify that the API-ILs (HBA) and ibuprofen (HBD) had not reacted, and to check the molar ratios. A dynamic visual method (lab benchtop procedure) was attained, after the three heating/cooling cycles, to determine the solid-liquid transitions of the prepared mixtures. This procedure was carried out until the solid-liquid transition was determined, and the prepared mixtures pre-validated as eutectic mixtures. More details on eutectic systems synthesis and validation can be found in our previous work [20].

The prepared eutectic systems were synthesized at atmospheric pressure and under control of moisture content. Samples were kept in well-sealed glass vials after preparation and fresh samples were always used for analysis to avoid structural change or environmental effects on their physical properties.

4.2.3.3 Nuclear magnetic resonance (NMR)

The prepared eutectic systems were characterized by ^1H NMR (Bruker Avance III 400). The NMR spectroscopy disclosed that there were no individual functional group modifications on the ibuprofen-based eutectic systems, being indeed a eutectic combination. All characterization is appended in Supporting Information.

4.2.3.4 Differential Scanning Calorimetry (DSC)

The DSC traces of all prepared mixtures, hydrogen-bond acceptors ($[\text{C}_2\text{C}_1\text{Im}][\text{Ibu}]$; $[\text{C}_{2(\text{OH})}\text{C}_1\text{Im}][\text{Ibu}]$; $[\text{N}_{1112(\text{OH})}][\text{Ibu}]$) and hydrogen-bond donor (ibuprofen) were acquired using a TA Instrument DSC Q200 Differential Scanning Calorimeter with a refrigerated cooling system capable of controlling the temperature down to -90°C. Indium ($T_m=157.61$ C°) was used as standard for the DSC calibration. Approximately 5-10 mg of sample was crimped in a standard aluminum hermetic sample pan and continuously purged with

50 mL·min⁻¹ nitrogen. The samples were cooled to -90°C for 30 min and then heated to 100°C. The cooling-heating cycles were repeated three times at different rates (10 °C/min, 5 °C/min and 1 °C/min). The transition temperatures obtained from the second and subsequent cycles at the same rate were reproducible. The glass transition temperature (T_g) and melting temperature (T_m) of each eutectic system were determined using the DSC traces. The standard uncertainty was estimated as $\pm 1^\circ\text{C}$. Universal Analysis 2000 v. 4.5. A software (TA Instruments) was used to integrate the peaks to determine the different phase transitions.

4.2.3.5 Cytotoxicity profiles

For the cytotoxicity screening of the API-ILs:Ibu eutectic systems, human colon carcinoma cells, Caco-2, and hepatocellular carcinoma cell line, HepG2, were used. Caco-2 cell line were grown in RPMI 1640 medium supplemented with 10% of inactivated fetal bovine serum (FBS) and (1%) of penicillin-streptomycin and HepG2, were cultured in MEM medium with 10% of inactivated FBS, 2mM glutamine, 1% MEM-NEAA and 1% sodium pyruvate. All media and supplements were supplied by gibco from Thermo Fisher Scientific. Caco-2 and HepG2 were cultured at 37°C in a humidified incubator with 5% CO₂ and consistently grown in 175 cm² culture flasks. Caco-2 cells were seeded at a density of 2×10^5 cells per well, in 96-well plates and the experiments were performed using cells after reaching 90% of confluence, 96 hours after seeding. HepG2 cells were seeded at a density of 6×10^5 cells per well and experiments were performed at a confluence of 80%, 24 hours after seeding. Each eutectic system was tested in a concentration range that lie above/in the maximum plasma concentration (C_{max}) of ibuprofen, 0.175 mM [22], and further compared to neat ibuprofen obtained in our previous work [6]. The stock solutions were prepared in 0.25% (v/v) of dimethyl sulfoxide (DMSO) due to the ibuprofen poor solubility in the cell culture medium and then homogenously diluted in 0.5% FBS culture media. A culture media solution with 0.25% (v/v) DMSO was used as negative control and a solution with only DMSO was used as positive control. Additionally, both cell lines were incubated for 24h with the ibuprofen or ibuprofen-based eutectic systems. To perform the cytotoxicity, assay an

CyQUANT™ XTT Cell Viability test kit (Invitrogen) was used according to the manufacturing in-structions. Briefly, the water-soluble XTT compound is sensitive to cellular redox po-tential and when in contact with viable cells it is converted to an orange coloured formazan product that can be quantified spectrophotometrically at 450 nm in a micro-plate reader (Multiskan GO from ThermoFisher Scientific). Moreover, each sample was incubated in three different wells and the obtained value was the average of three independent assays. Cell viability was determined by the ratio between the measured test compounds-contacted cell and the measured absorbance of the control cells treated only with culture medium. Dose-independent viability curves were determined using the cell viability trends.

4.2.3.6 Haemolytic activity

To perform the hemolytic activity assays, peripheral human blood obtained from voluntary donors and preserved in ethylene diamine tetraacetic acid (EDTA) was freshly used. The erythrocytes were centrifugated at 1000× g for 10 min to separate them from the serum and washed three times in a PBS solution. The ibuprofen-based eutectic systems were prepared in PBS with a final concentration of 6 mM and ibuprofen with a final concentration of 3mM due to low solubility. According to the method optimized by Gaspar and co-workers [22,23] the assay was performed in a 96-well plates were 100 µL/well of sample were diluted with 100 µL of the erythrocyte suspension. The microplates were incubated for 1h at 37°C and then centrifugated at 800× g for 10 min. The supernatants absorbance was measured at 570nm and 600nm. The percentage of the hemolytic activity was calculated by the **Equation 4.3**:

$$\text{Hemolytic Activity (\%)} = \frac{\text{AbsS} - \text{AbsN}}{\text{AbsP} - \text{AbsN}} \times 100 \quad (\text{Equation 4.3})$$

Where AbsS is the average absorbance of the sample, AbsN is the average absorbance of the negative control and AbsP is the average absorbance of the positive control. All the compounds were tested in triplicate.

4.2.3.7 Protein albumin denaturation assay

The inhibition of protein denaturation was evaluated according to the method described by Mizushima and Kobayashi [24] with slight modifications. A 2% bovine serum albumin (BSA) solution was prepared in a PBS buffer with pH 7.4 to be used in all experiments. Stock solution of ibuprofen and ibuprofen-based eutectic systems were also prepared in PBS buffer. The reaction mixture containing 0.5mL of 2%BSA and 1.5mL of each test compound was incubated at 37°C for 15 min and cooled at room temperature. Denaturation was induced by keeping the samples at 80°C±1 in a dry bath for 15min. The turbidity of the solutions represented the level protein precipitation. Thus, in a manual centrifuge all samples were centrifuged and then measured at 660nm. For negative control a solution of PBS and 2%BSA were used. Ibuprofen was used as a positive control drug. Each sample concentration consists of at least two independent replicates.

4.2.3.8 Anti-inflammatory activity

The anti-inflammatory activity of the API-ILs-based eutectic systems was evaluated by using a colorimetric COX (human ovine) inhibitor screening assay kit (Cayman Chemical Co., No.701050) to measure the inhibition of COX enzymes. The experiment was conducted according to the manufacturer instructions. A reaction mixture was prepared containing 150 µl of assay buffer, 10 µl of heme, 10 µl of enzyme (either COX-2 or COX-1) and 10 µl of each eutectic system at 3mM. To obtain the 100% initial activity, a solution a of 150 µL of assay buffer, 10 µL of heme, 10 µL of enzyme (either COX-1 or COX-2) and 10 µL of a solution 50/50 H₂O and EtOH was prepared. By monitoring at 590 nm the oxidized N, N, N, N'-tetramethyl-phenylenediamine (TMPD) it is possible to assay colorimetrically the peroxidase activity corresponding to the COX's catalytic domain.

Initially, the samples plate was incubated at 25°C for 5 min and then 20 µL of TMPD and 20 µL of arachidonic acid was added to start the reaction. The samples were measured kinetically for precisely 2 min at 25° C for a more accurate determination of the reaction

rates. All samples were assayed in triplicate. The COX-1 and COX-2 percent inhibition was calculated using **Equation 4.4**:

$$COX \text{ inhibition activity (\%)} = \frac{T}{C} \times 100 \quad (\text{Equation 4.4})$$

where C is absorbance of the 100% initial activity sample; T is the subtraction of each inhibitor sample from the 100% initial activity sample. The absorbances are the average of all samples, and one must subtract the absorbance of the background wells from the absorbances of the 100% initial activity and the inhibitor wells.

4.2.4 Results and Discussion

4.2.4.1 Thermal and structural characterization of the eutectic systems

A binary eutectic system is a mixture of two components which do not interact to form a new chemical compound but which, at certain ratios, inhibit the crystallization process of one another resulting in a system with a lower melting point than either of the components [12]. The melting point depression is expected due to the nonsymmetric ions that have low lattice energy and charge delocalization stirring through hydrogen bonding between the salt and the hydrogen bond donor[26]. Eutectic mixtures containing APIs as part of the formulation hold excellent properties that complement some of the obstacles of existing excipients and have been applied in pharmaceutical studies to increase the drug solubility, permeation, and absorption [17]. The most used components to formulate pharmacologically active eutectics are chemicals such as sugars, alcohols, urea, natural metabolites, organic acids, and choline chloride ($[N_{1112}(\text{OH})\text{Cl}]$) [27] since cholinium serves many physiological functions due to its incorporation in membrane components, neurotransmitters, and signaling molecules [28]. Stott and co-workers used ibuprofen, along with terpenes, prepared a binary eutectic mixture which exhibited an increase in transdermal delivery across the abdominal cavity of caucasian humans. It was also observed that the eutectic formulation showed a much higher flux as compared to neat ibuprofen, stressing the importance of the HBA:HBD interactions and melting point depression [17]. Pereira et al. also successfully combined terpene limonene with ibuprofen promoting a selective

anticancer activity and increased ibuprofen solubility [29]. Recently our group observed that was possible to formulate eutectic systems combining short-chain imidazolium and cholinium-based ionic liquids with ibuprofen enhancing the NSAID solubility yet maintained their anti-inflammatory activity [20].

All the 12 binary mixtures (API-IL:Ibu) were prepared in this work according to the procedure summarized in **Section 4.2.4.3**. The eutectic system validation was first achieved through the described lab benchtop procedure (dynamic visual method; cf. **Section 4.2.4.3**) and then validated by DSC analysis. The DSC traces of all the ibuprofen-based formulations studied in this work denoted a change in the structure of the material from a glass-like state to a rubber-like state, or vice-versa, represented by a discontinuity in the heat flux observed at lower temperatures (cf. **Figure 4.9**). This second order transition allows the determination of the glass transition temperature (T_g) and the classification of all the prepared ibuprofen-based eutectics as glass formers when the melting temperatures (T_m) are not present.

The DSC results at 1°C/min for the neat hydrogen-bond donor (ibuprofen) and hydrogen-bond acceptors ([C₂C₁Im][Ibu], [C_{2(OH)}C₁Im][Ibu] and [N_{1112(OH)}][Ibu]) were previously reported by us and depicted in **Table 4.7** along with the results for the binary mixtures [C₂C₁Im][Ibu]:Ibu, [C_{2(OH)}C₁Im][Ibu]:Ibu and [N_{1112(OH)}][Ibu]:Ibu achieved in this work. 10 out of the 12 prepared binary systems were validated as eutectic combinations and were liquid at room temperature. Regarding the [C_{2(OH)}C₁Im][Ibu]:Ibu 2:1 system, upon several heating-cold cycles corresponding to the eutectic system synthesis (cf. **Section 4.2.4.3**), the two counterparts remained immiscible and the ibuprofen stayed solid under constant stirring at 85°C ±2°C making impossible its assessment. The binary system [C₂C₁Im][Ibu]:Ibu 1:5 was firstly considered a eutectic combination through the dynamic visual method procedure but the thermal characterization by DSC revealed that the system is not a eutectic formulation since presented an identical DSC profile and a very similar melting temperature to its components (cf. **Figure 4.9** and **Table 4.7**). Despite the [C₂C₁Im][Ibu]:Ibu 1:5 combination was classified as non-eutectic, it will be used along the work.

Table 4.7. Glass transition temperatures (T_g) and melting temperatures (T_m) of the neat hydrogen-bond donor (ibuprofen), hydrogen-bond acceptors ($[C_2C_1Im][Ibu]$, $[C_{2(OH)}C_1Im][Ibu]$ and $[N_{1112(OH)}][Ibu]$) and the resulted binary combinations (API-IL:Ibu) acquired at $1^\circ C/min$.

Compounds	T_g ($^\circ C$)	T_m ($^\circ C$)
Ibuprofen [6]	-43.57	74.89
$[C_2C_1Im][Ibu]$ [6]	-30.55	72.44
$[C_2C_1Im][Ibu]:Ibu$ 2:1	-37.95	
$[C_2C_1Im][Ibu]:Ibu$ 1:1	-35.64	
$[C_2C_1Im][Ibu]:Ibu$ 1:2	-37.96	
$[C_2C_1Im][Ibu]:Ibu$ 1:5	-46.41	72.00
$[C_{2(OH)}C_1Im][Ibu]$ [6]		-13.97
$[C_{2(OH)}C_1Im][Ibu]:Ibu$ 1:1	-32.27	
$[C_{2(OH)}C_1Im][Ibu]:Ibu$ 1:2	-34.53	
$[C_{2(OH)}C_1Im][Ibu]:Ibu$ 1:5	-43.45	
$[N_{1112(OH)}][Ibu]$ [6]		70.89
$[N_{1112(OH)}][Ibu]:Ibu$ 2:1	-32.50	36.55
$[N_{1112(OH)}][Ibu]:Ibu$ 1:1	-33.79	44.83
$[N_{1112(OH)}][Ibu]:Ibu$ 1:2	-37.88	
$[N_{1112(OH)}][Ibu]:Ibu$ 1:5	-41.61	

Figure 4.9. shows the DSC traces for all the prepared mixtures $[N_{1112(OH)}][Ibu]:Ibu$, $[C_2C_1Im][Ibu]:Ibu$ and $[C_{2(OH)}C_1Im][Ibu]:Ibu$ at $1^\circ C/min$ rate. $[N_{1112(OH)}][Ibu]:Ibu$ 2:1 and $[N_{1112(OH)}][Ibu]:Ibu$ 1:1 are the only solid at room temperature of the 10 eutectic formulations. The $[N_{1112(OH)}][Ibu]:Ibu$ 2:1 achieves a glass transition with enthalpic relaxation at $-32.50^\circ C$ in the heating part of the cycle. On heating above the T_g , exhibits an exothermic crystallization peak (cold crystallization temperature) followed by an endothermic melting peak at $36.55^\circ C$. The $[N_{1112(OH)}][Ibu]:Ibu$ 1:1 achieves a glass transition with enthalpic relaxation at $-33.79^\circ C$ in the heating part of the cycle. Upon heating above the T_g , exhibits a transition at $29.15^\circ C$ followed by an endothermic melting peak at $44.55^\circ C$. These eutectics show thermal hysteresis and thus, depending on the cooling-heating cycles, this mixture can be handled as liquid at room temperature. Regarding the $[N_{1112(OH)}][Ibu]:Ibu$ 1:2 and $[N_{1112(OH)}][Ibu]:Ibu$ 1:5, they only depicted a second order transition, T_g , at $-37.88^\circ C$ and $-41.61^\circ C$, respectively, which allowed the classification of these mixtures as eutectics.

The DSC traces at 1°C/min for the eutectic systems based on $[C_2C_1Im][Ibu]$ and $[C_{2(OH)}C_1Im][Ibu]$ are liquid at room temperature (*cf.* **Table 4.7.**) and show no melting or freezing behavior in the DSC measurements, even when slowly heated and cooled at a scan rate of 1°C/min. Besides, by introducing the API-ILs into the eutectic system technology it was possible to convert solid API-ILs into room temperature liquid formulations.

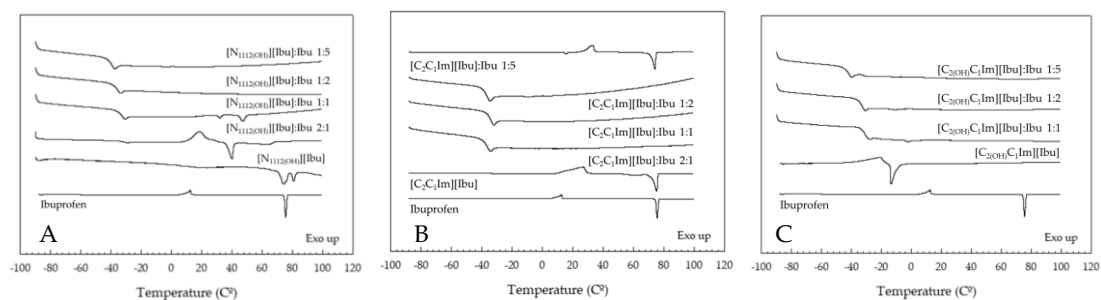


Figure 4.9. DSC profile with TA Instruments Universal Analysis V4.5A software at 1°C/min of (A) ibuprofen [6] and $N_{1112(OH)}[Ibu]$ [6] and $[N_{1112(OH)}][Ibu]$ -based systems, (B) $[C_2C_1Im][Ibu]$ [6] and $[C_2C_1Im][Ibu]$ -based systems and (C) $[C_{2(OH)}C_1Im][Ibu]$ [6] and $[C_{2(OH)}C_1Im][Ibu]$ -based systems.

The 1H NMR analysis was used to characterize the predominant hydrogen-bonding interactions responsible for the eutectic formation between the neat hydrogen-bond donor (Ibuprofen) and the hydrogen-bond acceptors ($[C_2C_1Im][Ibu]$, $[C_{2(OH)}C_1Im][Ibu]$ and $[N_{1112(OH)}][Ibu]$). The 1H NMR has been previously used to characterize H-bonds interaction in eutectic systems and ionic liquids showing its utility to investigate structures and interactions at molecular level [30–32]. All the eutectic systems presented sharp and well-defined signals allowing the confirmation of the ratios as the peak integral values vary in accordance with the proportion of the eutectic formulation. Additionally, through the 1H NMR the purity of the isolated compounds was verified since their chemical shifts are in accordance with previous reports in the literature [6]. The 1H NMR complete analysis is displayed in the Supporting Information.

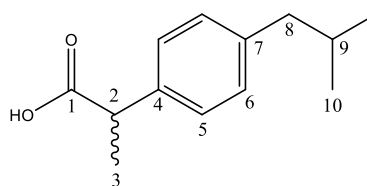
The strength of H-bonds affects the chemical shifts, therefore the chemical shifts in the vicinity of ibuprofen carboxyl group ($-COOH$), *viz.* position H2 and H3 of the chemical structure depicted in **Table 4.8.**, were analyzed. As can be seen in **Table 4.8.**, there is a clear change in the chemical shifts for the position H2 in all the imidazolium and cholinium API-ILs-based eutectics when compared to neat ibuprofen. Also, with the

increase of ibuprofen molar ratio (2:1 > 1:1 > 1:2 and 1:5) the chemical shifts move upfield. At position H3 the deviations of the chemical shifts are not so evident, yet a small change upfield with the increase of HBA molar ratio was verified. The changes in the chemical shifts corresponding to the positions H2 and H3 of the chemical structure of ibuprofen corroborate the ibuprofen and API-IL interaction, as expected.

The ^1H NMR of the neat $[\text{C}_2\text{C}_1\text{Im}][\text{Ibu}]$ and $[\text{C}_{2(\text{OH})}\text{C}_1\text{Im}][\text{Ibu}]$ has been analyzed by us in our previous work [6]. The deviations of the chemical shifts of the most acidic proton in the imidazolium ring in the imidazolium-based eutectics present in this work were also verified (cf. **Table 4.S12** in the Supporting Information). The H2' proton of the imidazolium cation in the eutectic formulations shows an upfield shift when compared to its neat corresponding HBA. The same change occurred for the $[\text{C}_2\text{C}_1\text{Im}][\text{C}_1\text{CO}_2]:\text{Ibu}$ eutectic formulations in our previous work [20]. All the deviations of the proton resonance verified in the HBD and HBA corroborate the major role of H-bonding in the API-IL:Ibu eutectic systems formation. Also, the hydroxyl group ($-\text{COOH}$) of ibuprofen was not detected in the ^1H NMR in DMSO of the all the API-ILs-based eutectic systems indicating a stronger H-bonding in these eutectic systems.

Table 4.8. ^1H NMR chemical shifts (δ) for the position H2 and H3 according to the chemical structure of ibuprofen (right) for all the eutectic systems in DMSO.

Compounds	H2 (δ/ppm)	H3 (δ/ppm)
Ibuprofen [6]	3.63	1.35
$[\text{C}_2\text{C}_1\text{Im}][\text{Ibu}]:\text{Ibu}$ 2:1	3.33	1.22
$[\text{C}_2\text{C}_1\text{Im}][\text{Ibu}]:\text{Ibu}$ 1:1	3.42	1.25
$[\text{C}_2\text{C}_1\text{Im}][\text{Ibu}]:\text{Ibu}$ 1:2	3.50	1.28
$[\text{C}_2\text{C}_1\text{Im}][\text{Ibu}]:\text{Ibu}$ 1:5	3.57	1.31
$[\text{C}_{2(\text{OH})}\text{C}_1\text{Im}][\text{Ibu}]:\text{Ibu}$ 1:1	-	1.26
$[[\text{C}_{2(\text{OH})}\text{C}_1\text{Im}][\text{Ibu}]:\text{Ibu}$ 1:2	3.57	1.32
$[\text{C}_{2(\text{OH})}\text{C}_1\text{Im}][\text{Ibu}]:\text{Ibu}$ 1:5	3.57	1.31
$[\text{N}_{1112(\text{OH})}][\text{Ibu}]:\text{Ibu}$ 2:1	3.40	1.23
$[\text{N}_{1112(\text{OH})}][\text{Ibu}]:\text{Ibu}$ 1:1	-	1.26
$[\text{N}_{1112(\text{OH})}][\text{Ibu}]:\text{Ibu}$ 1:2	3.51	1.28
$[\text{N}_{1112(\text{OH})}][\text{Ibu}]:\text{Ibu}$ 1:5	3.57	1.31



4.2.4.2 Cytotoxic profile and hemolytic activity of ibuprofen-based eutectic systems

The cytotoxicity of a eutectic system is dependent on the eutectic composition and concentration [33]. Thus, the cytotoxic profiles for the eutectic formulations $[\text{C}_2\text{C}_1\text{Im}][\text{Ibu}]:\text{Ibu}$, $[\text{C}_{2(\text{OH})}\text{C}_1\text{Im}][\text{Ibu}]:\text{Ibu}$ and $[\text{N}_{1112(\text{OH})}][\text{Ibu}]:\text{Ibu}$ were accessed in the

human colon carcinoma cell line, Caco-2 (**Figure 4.10 A, C, D**), and the hepatocellular carcinoma cell line, HepG2 (**Figure 4.10 B, D, F**).

The studied concentrations were above/in the range of the pharmacokinetic parameter maximum plasma concentration of ibuprofen (C_{\max} 0.175 mM; the highest level of ibuprofen that can be obtained in the blood usually following multiple doses [22]), which is above the possible intracellular concentrations. The dose-response cytotoxicity curves of the eutectic and non-eutectic formulations are shown in **Figure 4.10**. Comparing the viability curves of ibuprofen and the binary systems no significant changes were verified, indicating that the use of the hydrogen-bond acceptors $[C_2C_1Im][Ibu]$, $[C_{2(OH)}C_1Im][Ibu]$ and $[N_{1112(OH)}][Ibu]$ produced no significant effect on the ibuprofen cytotoxicity profile.

The half-maximal inhibitory concentration (IC_{50}) of the ibuprofen and ibuprofen-based ionic liquids and ibuprofen was previously determined by our group for the Caco-2 cell line. The IC_{50} for the acidic ibuprofen was found to be 4.051 ± 0.010 mM and for the imidazolium-based ionic liquids such as $[C_{2(OH)}C_1Im]Cl$ and $[C_2C_1Im]Cl$ was 137.4 ± 0.017 mM and 70.46 ± 0.043 mM, respectively [6]. When the chloride anion was replaced by the ibuprofenate anion the IC_{50} of the ionic liquids $[C_2C_1Im][Ibu]$ and $[C_{2(OH)}C_1Im][Ibu]$ became close to the neat ibuprofen being 5.682 ± 0.005 mM and 5.523 ± 0.007 mM accordingly [6]. Additionally, the $[N_{1112(OH)}][Ibu]$ presented a IC_{50} of 5.507 ± 0.004 mM when compared to the $[N_{1112(OH)}]Cl$ with the half-maximal inhibitory concentration being 178.1 ± 0.009 mM [6]. In our previous work we demonstrated that the ratio of ibuprofen in the imidazolium and cholinium-based ILs eutectic formulations influence the cytotoxicity in HepG2 where the cellular viability decreases upon the increase of ibuprofen[20]. In this work, in all cases the cytotoxic profile is maintained regardless of the use ratio used of API in the binary combinations and the cellular viability is preserved up to 80% (cf. **Figure 4.10**). These results suggested that cytotoxicity is influenced by the anion moiety of the IL present as HBA of the eutectic composition and the ibuprofenate-based ILs can preserve the neat ibuprofen original cytotoxic profile.

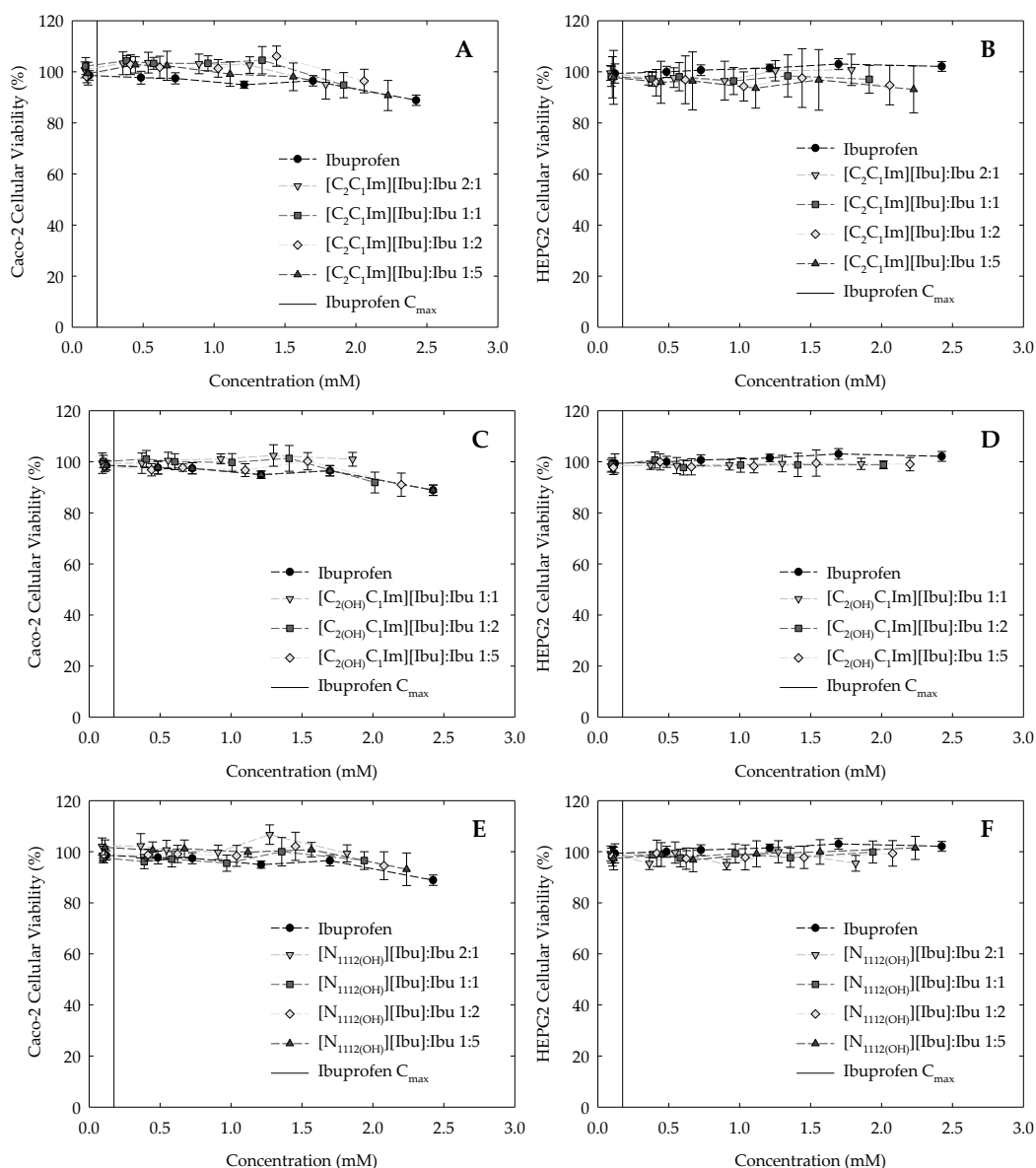


Figure 4.10. Cytotoxicity profiles for the eutectic systems containing pharmaceutically active ionic liquids in Caco-2 (A,C,E) and in HepG2 (B,D,F). Both cell lines were exposed for 24 h prior to the cytotoxicity assessment. Ibuprofen data were acquired from previous work [6]. The vertical line represents the C_{max} of ibuprofen at 0.175 mM

Drug-induced immune hemolytic anemia (DIIHA) is a serious condition that can be a rare side effect of commonly used over-the-counter medications [34]. After administration, the drugs can quickly interact with the bloodstream erythrocytes and disrupt their membranes leading to cell lysis and consequently acute toxicity [35]. Although the incidence of DIIHA is estimated to be 1 per million of the population, and NSAIDs compromise less than 15% of the reported cases worldwide [34], the assessment of hemolytic activity can lead to an understanding of what the toxic potential of a new

formulation could be [36]. According to the guidelines of the European Medicines Agency (EMA) in Europe, an *in vitro* hemolysis study is recommended to ensure that there is no serious potential of pharmacologically mediated toxicity such as DIIHA [37].

In our previous work we have evaluated the red blood cell lysis through the hemoglobin release in the plasma for ibuprofen, ibuprofen-based ILs and eutectics. Ibuprofen and ibuprofen-based ILs did not reveal hemolytic activity against human erythrocytes up to 1.5 mM and 3 mM, respectively [29]. The ibuprofen-based eutectics with $[C_2C_1Im]Cl$, $[C_{2(OH)}C_1Im]Cl$, $[C_2C_1Im][C_1CO_2]$ and $[N_{1112(OH)}]Cl$ as hydrogen-bond acceptors were previously analyzed, displaying no hemolytic activity against human erythrocytes up to 3 mM [20]. Vieira et al. [38] also disclosed that several imidazolium and cholinium-based ILs are hemocompatible with ~0% hemolytic activity up to 3 mM. With this purpose, the red blood cell lysis in peripheral human blood plasma obtained from voluntary donors was evaluated for the API-IL:Ibu eutectic systems according to the method optimized by Gaspar and co-workers [22,23]. In this study, the ibuprofen-based eutectic formulations $[C_2C_1Im][Ibu]:Ibu$, $[C_{2(OH)}C_1Im][Ibu]:Ibu$ and $[N_{1112(OH)}]:Ibu$ did not revealed hemolytic activity against human erythrocytes up to 3 mM, which is 17-fold the C_{max} of the neat ibuprofen. Moreover, a structure-activity correlation was proposed by Orhan et al. in which they suggest that an aromatic ring with a side chain containing a carbonyl group attached to a nitrogen atom is a requirement for stabilizing the erythrocyte membrane, and so chemical components with those characteristics decrease the risk of erythrocyte lysis [39]. Furthermore, both hemolysis and cytotoxic profiles of the studied ibuprofen-based eutectic systems are in agreement.

4.2.4.3 Anti-inflammatory activity: COXs and BSA inhibition

Inflammation is generally referred to as a complex biological response of vascular tissues to harmful stimuli. As well, inflammation is associated with pain, and it involves in an increase of protein denaturation, an increase of vascular permeability, and membrane alteration, among others [40]. Thus, an easy and non-invasive method to predict the anti-inflammatory effect of a new drug is to evaluate its capacity to prevent protein denaturation. In this assay the eutectic systems were assessed to inhibit the model

protein bovine serum albumin (BSA), similar to the albumin protein present in human plasma, and consequently evaluate their anti-inflammatory properties and then confirmed by the direct analysis of cyclooxygenases (COX-1 and COX-2) expression. The inhibition profile of BSA denaturation for the ibuprofen-based systems used in this work are disclosed in **Figure 4.11** and **Table 4.S11** in Supporting Information.

A recent study made by our group disclosed that the inhibition BSA profile of the API-ILs $[C_2C_1Im][Ibu]$, $[C_{2(OH)}C_1Im][Ibu]$, and $[N_{1112(OH)}][Ibu]$ exhibited a similar trend to the parent-API, or even presented an increased inhibition of BSA denaturation in the case of the $[C_{2(OH)}C_1Im][Ibu]$ [6]. Unlike the ibuprofen API-ILs based on the same cations ($[C_2C_1Im]^+$, $[C_{2(OH)}C_1Im]^+$, and $[N_{1112(OH)}]^+$), the ibuprofen-based eutectics based on the HBA $[C_2C_1Im]Cl$, $[C_{2(OH)}C_1Im]Cl$, and $[N_{1112(OH)}]Cl$ exhibited a slight reduction regarding the inhibition of BSA denaturation [20]. In this work, no significant changes were found between the inhibition profiles of BSA denaturation for the binary mixtures of API-ILs and the API-parent indicating that with a fine-tuning of HBA, a eutectic system may present similar anti-inflammatory properties of the parent API.

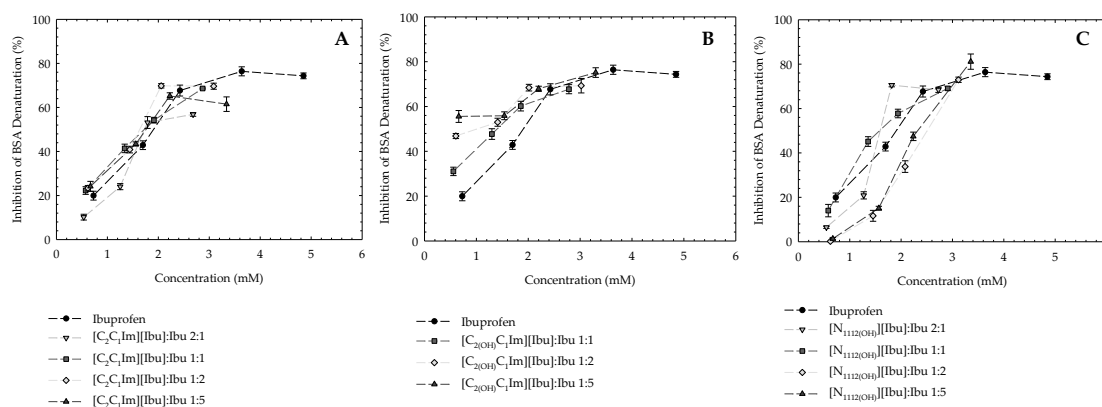


Figure 4.11 Inhibition profile of BSA denaturation in $[C_2C_1Im][Ibu]:Ibu$ (A), $[C_{2(OH)}C_1Im][Ibu]:Ibu$ (B) $[N_{1112(OH)}][Ibu]:Ibu$ (C) systems and compared to neat ibuprofen from previous work [6].

During the anti-inflammatory process elevated levels of prostaglandins (PGs) are produced as a cardinal sign of inflammation. NSAIDs reduce or prevent the production of PGs by direct inhibition of the cyclooxygenase (COX) enzymes [41]. Cyclooxygenase-1 and cyclooxygenase-2 (COX-1 and COX-2) catalyze the bis-oxygenation of free arachidonic acid to a hydroperoxyl endoperoxide (PGG_2), and the peroxidase

component reduces the endoperoxide to the corresponding alcohol (PGH₂), the precursor of PGs, prostacyclins, and thromboxanes. These lipid mediators play important roles in inflammation and pain and in normal physiological functions. While there are abundant data indicating that the inducible isoform, COX-2, is important in inflammation and pain, the constitutively expressed isoform, COX-1, has also been suggested to play a role in inflammatory processes but also as a constitutively enzyme expressed in a variety of cell types and is involved in normal cellular homeostasis [41,42].

Gastrointestinal adverse effects observed with non-selective NSAIDs are due to the inhibition of COX-1 enzyme. With the inhibition of COX-1 there is a decrease in the synthesis of prostaglandins responsible for cytoprotection [41]. Therefore, the long-term use of these drugs leads to severe gastric ulceration, hepatotoxicity, and renal dysfunction. The benefits of NSAIDs therapeutic are mainly due to the inhibition of the COX-2, while the adverse effects are observed due to COX-1 inhibition [43]. Thus, the goal of achieving anti-inflammatory efficacy with the fewest possible side effects through selectivity of COX-2 inhibition is of high significance.

The ibuprofen binary systems composed of [C₂C₁Im][Ibu], [C_{2(OH)}C₁Im][Ibu] and [N_{1112(OH)}][Ibu] at the molar ratios 1:1 and 1:5, as well as neat ibuprofen [6], were evaluated for their ability to inhibit cyclooxygenases (COX-1, ovine; COX-2, human) using a COX colorimetric inhibitor assay kit (see **Section 4.2.4.8.**), providing direct insight into their anti-inflammatory properties. The results obtained are depicted in **Figure 4.12.** and **Table 4.9.**, indicating that under the same experimental conditions, the ibuprofen-based eutectics generally maintained the anti-inflammatory activity of ibuprofen (% COX inhibition).

A closer look to the results, through the COX-1/COX-2 selectivity allow us to better understand the effect of the HBA and HBA:Ibu molar ratio in the COX-1/COX-2 selectivity of the ibuprofen-based eutectic systems. Lower COX-1/COX-2 selectivity values indicate a greater selectivity for COX-2, and higher values indicate greater selectivity for COX-1[6].

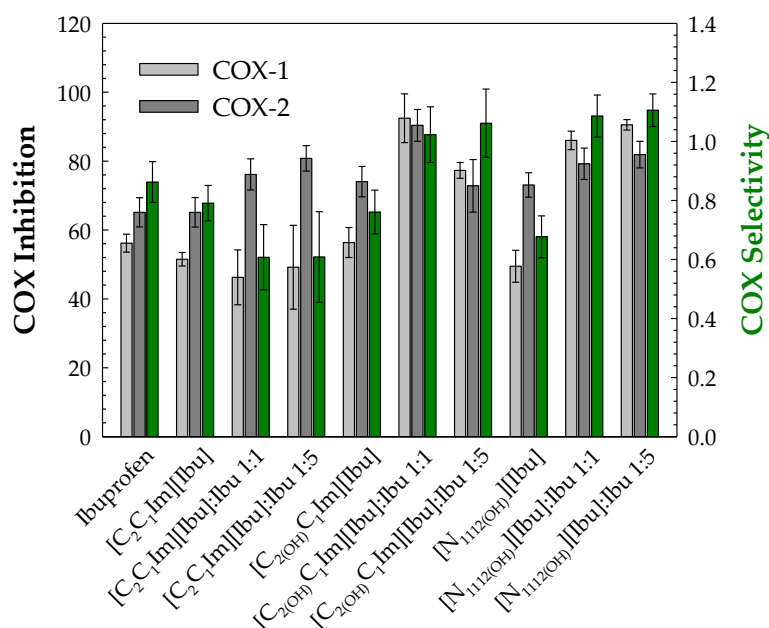


Figure 4.12. Selective inhibition of COX-1 (ovine) and COX-2 (human) and COX-1/COX-2 selectivity at 3mM for the eutectic systems and their neat hydrogen-bond donor (ibuprofen) [6] and hydrogen-bond acceptors([C₂C₁Im][Ibu], [C₂(OH)C₁Im][Ibu] and [N₁₁₂(OH)][Ibu]) [6].

In our previous work, we disclosed that, under the same experimental conditions, the ibuprofen-based ILs ([C₂C₁Im][Ibu], [C₂(OH)C₁Im][Ibu], and [N₁₁₂(OH)][Ibu]) maintained/upgraded the anti-inflammatory activity of ibuprofen [6]. Additionally, ibuprofen-based eutectic systems with ILs-based HBA ([C₂C₁Im]Cl, [C₂(OH)C₁Im]Cl and [N₁₁₂(OH)]Cl:) were also investigated. The [C₂C₁Im]Cl-based eutectics (1:1 and 1:5) and [C₂(OH)C₁Im]Cl:Ibu 1:1 presented a similar ibuprofen selectivity. However, the [C₂(OH)C₁Im]Cl:Ibu 1:5 system demonstrated a higher increase of the inhibition of COX-1 (%), increasing the COX-1/COX-2 selectivity relatively to ibuprofen. The [N₁₁₂(OH)]Cl:Ibu 1:5 eutectic presented the best outcome with a lower COX-1/COX-2 selectivity indicating a greater selectivity for COX-2 than ibuprofen [20].

In this study, the [C₂(OH)C₁Im][Ibu]:Ibu and [N₁₁₂(OH)][Ibu]:Ibu binary systems presented a similar COX-1/COX-2 selectivity (t-test, 1 tailed, confidence level 90%, p<0.05) and slightly higher than neat ibuprofen. Differently, both [C₂C₁Im][Ibu]:Ibu 1:1 and 1:5 systems presented the lowest COX-1/COX-2 selectivity (see **Table 4.9**) indicating a greater selectivity for COX-2 than ibuprofen (t-test, 1 tailed, confidence level 90%,

$p < 0.05$). Although the $[\text{C}_2\text{C}_1\text{Im}][\text{Ibu}]:\text{Ibu}$ 1:5 is not considered a eutectic formulation, it presented a similar result to $[\text{C}_2\text{C}_1\text{Im}][\text{Ibu}]:\text{Ibu}$ 1:1 implying a major rule on the HBA *vs* HBD selection instead of a eutectic formation regarding the link to COX enzymes.

Table 4.9. Inhibition of COX-1 (ovine) and COX-2 (human) and COX-1/COX-2 selectivity for 1mM of eutectic systems containing pharmacologically active ionic liquids and near ibuprofen at the molar ratios 1:1 and 1:5 at $37^\circ\text{C} \pm 1$.

Compounds	Inhibition of COX-1 (ovine) (%)	Inhibition of COX-2 (human) (%)	COX-1/-2 selectivity
Ibuprofen	56.18 ± 2.60	65.13 ± 4.25	0.863 ± 0.069
$[\text{C}_2\text{C}_1\text{Im}][\text{Ibu}]:\text{Ibu}$ 1:1	46.25 ± 7.96	76.13 ± 4.52	0.607 ± 0.111
$[\text{C}_2\text{C}_1\text{Im}][\text{Ibu}]:\text{Ibu}$ 1:5	49.19 ± 12.19	80.80 ± 3.69	0.609 ± 0.153
$[\text{C}_{2(\text{OH})}\text{C}_1\text{Im}][\text{Ibu}]:\text{Ibu}$ 1:1	92.44 ± 7.08	90.37 ± 4.63	1.023 ± 0.094
$[\text{C}_{2(\text{OH})}\text{C}_1\text{Im}][\text{Ibu}]:\text{Ibu}$ 1:5	77.31 ± 2.29	72.82 ± 7.63	1.062 ± 0.116
$[\text{N}_{1112(\text{OH})}][\text{Ibu}]:\text{Ibu}$ 1:1	86.03 ± 2.68	79.22 ± 4.57	1.086 ± 0.071
$[\text{N}_{1112(\text{OH})}][\text{Ibu}]:\text{Ibu}$ 1:5	90.53 ± 1.52	81.88 ± 3.85	1.106 ± 0.055

The COX-1/COX-2 selectivity of the ibuprofen-based eutectics and ibuprofen (see **Table 4.9.**) follows the order (t-test, 1 tailed, confidence level 90%, $p < 0.05$): $[\text{N}_{1112(\text{OH})}][\text{Ibu}]:\text{Ibu}$ 1:5 > $[\text{N}_{1112(\text{OH})}][\text{Ibu}]:\text{Ibu}$ 1:1 > $[\text{C}_{2(\text{OH})}\text{C}_1\text{Im}][\text{Ibu}]:\text{Ibu}$ 1:5 > $[\text{C}_{2(\text{OH})}\text{C}_1\text{Im}][\text{Ibu}]:\text{Ibu}$ 1:1 > Ibuprofen > $[\text{C}_2\text{C}_1\text{Im}][\text{Ibu}]:\text{Ibu}$ 1:5 \approx $[\text{C}_2\text{C}_1\text{Im}][\text{Ibu}]:\text{Ibu}$ 1:1. A lower COX-1/COX-2 selectivity value indicate a greater selectivity for COX-2 while a higher value indicate greater selectivity for COX-1. Globally, the ibuprofen-based binary systems improve, or at least maintain the COX-1/COX-2 selectivity (t-test, 1 tailed, confidence level 90%, $p < 0.05$) (cf. **Figure 4.S9** in Supporting Information). These results provide strong evidence of the API-based eutectics platform's potential for facilitating the development of safer NSAIDs with improved gastric and renal safety profiles.

4.2.5 Conclusions

In this work, ten ibuprofen-based eutectic systems were successfully synthesized conjugating ibuprofen (HBD) with three ibuprofen-based ionic liquids ($[\text{C}_2\text{C}_1\text{Im}][\text{Ibu}]$,

[C_{2(OH)}C_{1Im}][Ibu] and [N_{1112(OH)}][Ibu]) in different molar ratio, namely 2:1, 1:1, 1:2 and 1:5. All eutectic systems were characterized by DSC and NMR establishing their ability to maintain stable and liquid at room temperature. The ibuprofen and API-ILs-based eutectics and ibuprofen display similar cytocompatibility (in two human cell lines, Caco-2 colon carcinoma cells and HepG2 hepatocellular carcinoma cells) and all forms are hemocompatible. Subsequently, the anti-inflammatory properties of the eutectics API-ILs-based binary mixtures were evaluated through the inhibition of BSA denaturation and inhibition of cyclooxygenases (COX-1 and COX-2) enzymes, showing that the ibuprofen eutectic formulations maintain the anti-inflammatory response of ibuprofen with the opportunity to improve the selectivity towards COX-2 upgrading the safety of the NSAIDs. These promising findings suggest that these new pharmaceutical forms can be used for further pharmaceutical development solving the limited bioavailability of poor soluble NSAIDs without affecting its pharmacologic effect.

Funding

This research was funded by FCT/MCTES (Portugal), through grants PD/BD/135078/2017 and COVID/BD/151824/2021 (J.C.B.), the Individual Call to Scientific Employment Stimulus 2020.00835.CEECIND (J.M.M.A.) and 2021.01432.CEECIND (A.B.P.), and the project PTDC/EQU-EQU/2223/2021. This work was also supported by the Associate Laboratory for Green Chemistry – LAQV which was financed by national funds from FCT/MCTES (UIDB/50006/2020 and UIDP/50006/2020).

Conflicts of Interest

The authors declare no conflict of interest.

4.2.6 References

1. Elina Petrova *Innovation in the Pharmaceutical Industry: The Process of Drug Discovery and Development*. In *Innovation and Marketing in the Pharmaceutical Industry*; Ding M., Eliashberg J., Stremersch S., Eds.; New York: Springer Science+Business Media, 2014; Vol. Chapter 2;

2. Kalepu, S.; Nekkanti, V. Insoluble Drug Delivery Strategies: Review of Recent Advances and Business Prospects. *Acta Pharm Sin B* **2015**, *5*, 442–453, doi:10.1016/j.apsb.2015.07.003.
3. Shekunov, B.Y.; York, P. Crystallization Processes in Pharmaceutical Technology and Drug Delivery Design. *J Cryst Growth* **2000**, *211*, 122–136, doi:10.1016/S0022-0248(99)00819-2.
4. Singhal, D. Drug Polymorphism and Dosage Form Design: A Practical Perspective. *Adv Drug Deliv Rev* **2004**, *56*, 335–347, doi:10.1016/j.addr.2003.10.008.
5. Shayne Cox Gad *Pharmaceutical Manufacturing Handbook: Production and Q9690 Processes*; John Wiley Sons.Inc.: NJ, USA, 2008;
6. Bastos, J.C.; Vieira, N.S.M.; Gaspar, M.M.; Pereiro, A.B.; Araújo, J.M.M. Human Cytotoxicity, Hemolytic Activity, Anti-Inflammatory Activity and Aqueous Solubility of Ibuprofen-Based Ionic Liquids. *Sustainable Chemistry* **2022**, *3*, 358–375, doi:10.3390/suschem3030023.
7. Balk, A.; Wiest, J.; Widmer, T.; Galli, B.; Holzgrabe, U.; Meinel, L. Transformation of Acidic Poorly Water Soluble Drugs into Ionic Liquids. *European Journal of Pharmaceutics and Biopharmaceutics* **2015**, *94*, 73–82, doi:10.1016/j.ejpb.2015.04.034.
8. Shadid, M.; Gurau, G.; Shamshina, J.L.; Chuang, B.-C.; Hailu, S.; Guan, E.; Chowdhury, S.K.; Wu, J.-T.; Rizvi, S.A.A.; Griffin, R.J.; et al. Sulfasalazine in Ionic Liquid Form with Improved Solubility and Exposure. *Medchemcomm* **2015**, *6*, 1837–1841, doi:10.1039/C5MD00290G.
9. Chowdhury, Md.R.; Moshikur, R.M.; Wakabayashi, R.; Tahara, Y.; Kamiya, N.; Moniruzzaman, M.; Goto, M. Ionic-Liquid-Based Paclitaxel Preparation: A New Potential Formulation for Cancer Treatment. *Mol Pharm* **2018**, *15*, 2484–2488, doi:10.1021/acs.molpharmaceut.8b00305.
10. Moshikur, R.Md.; Chowdhury, Md.R.; Wakabayashi, R.; Tahara, Y.; Moniruzzaman, M.; Goto, M. Characterization and Cytotoxicity Evaluation of Biocompatible Amino Acid

Esters Used to Convert Salicylic Acid into Ionic Liquids. *Int J Pharm* **2018**, *546*, 31–38, doi:10.1016/j.ijpharm.2018.05.021.

11. Moshikur, R.Md.; Chowdhury, Md.R.; Wakabayashi, R.; Tahara, Y.; Moniruzzaman, M.; Goto, M. Ionic Liquids with Methotrexate Moieties as a Potential Anticancer Prodrug: Synthesis, Characterization and Solubility Evaluation. *J Mol Liq* **2019**, *278*, 226–233, doi:10.1016/j.molliq.2019.01.063.
12. Wiest, J.; Saedtler, M.; Balk, A.; Merget, B.; Widmer, T.; Bruhn, H.; Raccuglia, M.; Walid, E.; Picard, F.; Stopper, H.; et al. Mapping the Pharmaceutical Design Space by Amorphous Ionic Liquid Strategies. *Journal of Controlled Release* **2017**, *268*, 314–322, doi:10.1016/j.jconrel.2017.10.040.
13. Santos, M.M.; Raposo, L.R.; Carrera, G.V.S.M.; Costa, A.; Dionísio, M.; Baptista, P. V.; Fernandes, A.R.; Branco, L.C. Ionic Liquids and Salts from Ibuprofen as Promising Innovative Formulations of an Old Drug. *ChemMedChem* **2019**, *14*, 907–911, doi:10.1002/cmdc.201900040.
14. Tomé, L.I.N.; Baião, V.; da Silva, W.; Brett, C.M.A. Deep Eutectic Solvents for the Production and Application of New Materials. *Appl Mater Today* **2018**, *10*, 30–50, doi:10.1016/j.apmt.2017.11.005.
15. Zhang, Q.; De Oliveira Vigier, K.; Royer, S.; Jérôme, F. Deep Eutectic Solvents: Syntheses, Properties and Applications. *Chem Soc Rev* **2012**, *41*, 7108, doi:10.1039/c2cs35178a.
16. Abbott, A.P.; Capper, G.; Davies, D.L.; Rasheed, R.K.; Tambyrajah, V. Novel Solvent Properties of Choline Chloride/Urea Mixtures. *Chemical Communications* **2003**, 70–71, doi:10.1039/b210714g.
17. Stott, P.W.; Williams, A.C.; Barry, B.W. *Transdermal Delivery from Eutectic Systems: Enhanced Permeation of a Model Drug, Ibuprofen*; 1998; Vol. 50;.

18. Silva, J.M.; Reis, R.L.; Paiva, A.; Duarte, A.R.C. Design of Functional Therapeutic Deep Eutectic Solvents Based on Choline Chloride and Ascorbic Acid. *ACS Sustain Chem Eng* **2018**, *6*, 10355–10363, doi:10.1021/acssuschemeng.8b01687.
19. Kim, D.; Jang, S.; Kim, I.W. Eutectic Formation of Naproxen with Some Dicarboxylic Acids. *Pharmaceutics* **2021**, *13*, 2081, doi:10.3390/pharmaceutics13122081.
20. Bastos, J.C.; Gaspar, M.M.; Pereiro, A.B.; Araújo, J.M.M. Role of Ionic Liquids in Ibuprofen-Based Eutectic Systems: Aqueous Solubility, Permeability, Human Cytotoxicity, Hemolytic Activity and Anti-Inflammatory Activity. *Nanomaterials* **2023 (in press)**.
21. Castro, P.J.; Redondo, A.E.; Sosa, J.E.; Zakrzewska, M.E.; Nunes, A.V.M.; Araújo, J.M.M.; Pereiro, A.B. Absorption of Fluorinated Greenhouse Gases in Deep Eutectic Solvents. *Ind Eng Chem Res* **2020**, *59*, 13246–13259, doi:10.1021/acs.iecr.0c01893.
22. Dewland, P.M.; Reader, S.; Berry, P. Bioavailability of Ibuprofen Following Oral Administration of Standard Ibuprofen, Sodium Ibuprofen or Ibuprofen Acid Incorporating Poloxamer in Healthy Volunteers. *BMC Clin Pharmacol* **2009**, *9*, doi:10.1186/1472-6904-9-19.
23. Gaspar, M.M.; Calado, S.; Pereira, J.; Ferronha, H.; Correia, I.; Castro, H.; Tomás, A.M.; Cruz, M.E.M. Targeted Delivery of Paromomycin in Murine Infectious Diseases through Association to Nano Lipid Systems. *Nanomedicine* **2015**, *11*, 1851–1860, doi:10.1016/j.nano.2015.06.008.
24. Nave, M.; Castro, R.E.; Rodrigues, C.M.P.; Casini, A.; Soveral, G.; Gaspar, M.M. Nanoformulations of a Potent Copper-Based Aquaporin Inhibitor with Cytotoxic Effect against Cancer Cells. *Nanomedicine* **2016**, *11*, 1817–1830, doi:10.2217/nnm-2016-0086.
25. Mizushima, Y.; Kobayashi, M. Interaction of Anti-Inflammatory Drugs with Serum Proteins, Especially with Some Biologically Active Proteins. *Journal of Pharmacy and Pharmacology* **2011**, *20*, 169–173, doi:10.1111/j.2042-7158.1968.tb09718.x.

26. Abbott, A.P.; Capper, G.; Davies, D.L.; Munro, H.L.; Rasheed, R.K.; Tambyrajah, V. Preparation of Novel, Moisture-Stable, Lewis-Acidic Ionic Liquids Containing Quaternary Ammonium Salts with Functional Side Chains. *Chemical Communications* **2001**, *1*, 2010–2011, doi:10.1039/b106357j.
27. García, C.B.; Concha, J.; Culleré, L.; Lomba, L.; Sangüesa, E.; Ribate, M.P. Has the Toxicity of Therapeutic Deep Eutectic Systems Been Assessed? *Applied Sciences* **2023**, *13*, 5980, doi:10.3390/app13105980.
28. Araújo, J.M.M.; Florindo, C.; Pereiro, A.B.; Vieira, N.S.M.; Matias, A.A.; Duarte, C.M.M.; Rebelo, L.P.N.; Marrucho, I.M. Cholinium-Based Ionic Liquids with Pharmaceutically Active Anions. *RSC Adv* **2014**, *4*, 28126–28132, doi:10.1039/c3ra47615d.
29. Pereira, C. V.; Silva, J.M.; Rodrigues, L.; Reis, R.L.; Paiva, A.; Duarte, A.R.C.; Matias, A. Unveil the Anticancer Potential of Limonene Based Therapeutic Deep Eutectic Solvents. *Sci Rep* **2019**, *9*, doi:10.1038/s41598-019-51472-7.
30. Araújo, J.M.M.; Ferreira, R.; Marrucho, I.M.; Rebelo, L.P.N. Solvation of Nucleobases in 1,3-Dialkylimidazolium Acetate Ionic Liquids: NMR Spectroscopy Insights into the Dissolution Mechanism. *Journal of Physical Chemistry B* **2011**, *115*, 10739–10749, doi:10.1021/jp203282k.
31. Araújo, J.M.M.; Pereiro, A.B.; Canongia Lopes, J.N.; Rebelo, L.P.N.; Marrucho, I.M. Hydrogen-Bonding and the Dissolution Mechanism of Uracil in an Acetate Ionic Liquid: New Insights from NMR Spectroscopy and Quantum Chemical Calculations. *Journal of Physical Chemistry B* **2013**, *117*, 4109–4120, doi:10.1021/jp400749j.
32. Gabriele, F.; Chiarini, M.; Germani, R.; Tiecco, M.; Spreti, N. Effect of Water Addition on Choline Chloride/Glycol Deep Eutectic Solvents: Characterization of Their Structural and Physicochemical Properties. *J Mol Liq* **2019**, *291*, doi:10.1016/j.molliq.2019.111301.
33. Hayyan, M.; Hashim, M.A.; Al-Saadi, M.A.; Hayyan, A.; AlNashef, I.M.; Mirghani, M.E.S. Assessment of Cytotoxicity and Toxicity for Phosphonium-Based Deep Eutectic Solvents. *Chemosphere* **2013**, *93*, 455–459, doi:10.1016/j.chemosphere.2013.05.013.

34. Barbaryan, A.; Iyinagoro, C.; Nwankwo, N.; Ali, A.M.; Saba, R.; Kwatra, S.G.; Hussain, N.; Uzoka, C.C.; Prueksaritanond, S.; Mirrakhimov, A.E. Ibuprofen-Induced Hemolytic Anemia. *Case Rep Hematol* **2013**, *2013*, 1–3, doi:10.1155/2013/142865.
35. Jeswani, G.; Alexander, A.; Saraf, S.; Saraf, S.; Qureshi, A.; Ajazuddin Recent Approaches for Reducing Hemolytic Activity of Chemotherapeutic Agents. *Journal of Controlled Release* **2015**, *211*, 10–21, doi:10.1016/j.jconrel.2015.06.001.
36. Greco, I.; Molchanova, N.; Holmedal, E.; Jenssen, H.; Hummel, B.D.; Watts, J.L.; Håkansson, J.; Hansen, P.R.; Svenson, J. Correlation between Hemolytic Activity, Cytotoxicity and Systemic in Vivo Toxicity of Synthetic Antimicrobial Peptides. *Sci Rep* **2020**, *10*, 13206, doi:10.1038/s41598-020-69995-9.
37. EMEA Guideline on Strategies to Identify and Mitigate Risks for First-in-Human and Early Clinical Trials with Investigational Medicinal Products 2018.
38. Vieira, N.S.M.; Oliveira, A.L.S.; Araújo, J.M.M.; Gaspar, M.M.; Pereiro, A.B. Ecotoxicity and Hemolytic Activity of Fluorinated Ionic Liquids. *Sustainable Chemistry* **2021**, *2*, 115–126, doi:10.3390/suschem2010008.
39. Orhan, H.; Şahin, G. In Vitro Effects of NSAIDS and Paracetamol on Oxidative Stress-Related Parameters of Human Erythrocytes. *Experimental and Toxicologic Pathology* **2001**, *53*, 133–140, doi:10.1078/0940-2993-00179.
40. Ferrero-Miliani, L.; Nielsen, O.H.; Andersen, P.S.; Girardin, S.E. Chronic Inflammation: Importance of NOD2 and NALP3 in Interleukin-1 β Generation. *Clin Exp Immunol* **2007**, *147*, 227–235, doi:10.1111/j.1365-2249.2006.03261.x.
41. Osafo, N.; Agyare, C.; Obiri, D.D.; Antwi, A.O. Mechanism of Action of Nonsteroidal Anti-Inflammatory Drugs. In *Nonsteroidal Anti-Inflammatory Drugs*; InTech, 2017.
42. Rainsford, K.D. Ibuprofen: Pharmacology, Efficacy and Safety. *Inflammopharmacology* **2009**, *17*, 275–342.

43. Bjarnason, I.; Scarpignato, C.; Holmgren, E.; Olszewski, M.; Rainsford, K.D.; Lanas, A. Mechanisms of Damage to the Gastrointestinal Tract From Nonsteroidal Anti-Inflammatory Drugs. *Gastroenterology* **2018**, *154*, 500–514, doi:10.1053/j.gastro.2017.10.049.

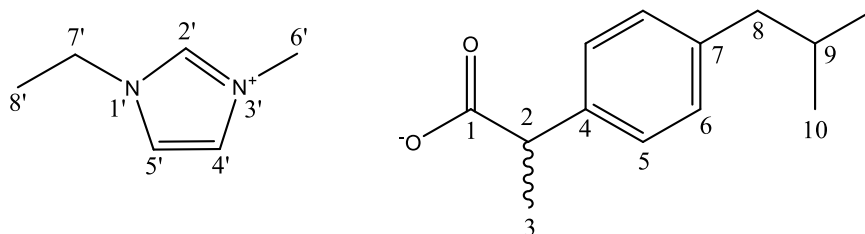
4.2.7 Supporting Information

to the loss of the drug therapeutic effect and even potentialize their systemic toxicity.

Characterization of the Ibuprofen-based Ionic Liquids

The prepared systems composed of pharmacologically active ionic liquids and ibuprofen (ILs:Ibu), at the proportions 2:1, 1:1, 1:2 and 1:5 were completely characterized by ^1H . The quantitative integration of their characteristic ^1H NMR resonance peaks unfold the expected cation/anion correlations. Also, there were no peaks assigned to impurities in the ^1H NMR spectra.

[C₂C₁Im][Ibu]-based systems



2:1

^1H NMR (400 MHz, D₂O): δ/ppm = 8.61 (s, 2H,2'), 7.39 (s, 2H,5'), 7.32 (s, 2H,4'), 7.19 (d, J = 7.9 Hz, 6H,5), 7.14 (d, J = 7.9 Hz, 6H,6), 4.13 (q, J = 7.3 Hz, 4H,7'), 3.79 (s, 6H,6'), 3.56 (q, J = 7.3 Hz, 3H,2), 2.40 (d, J = 7.1 Hz, 6H,8), 1.76 (dt, J = 13.7, 6.9 Hz, 3H,9), 1.41 (t, J = 7.4 Hz, 6H,8'), 1.31 (d, J = 7.2 Hz, 9H,3), 0.79 (d, J = 6.6 Hz, 18H,10).

^1H NMR (400 MHz, DMSO): δ/ppm = 9.24 (s, 2H,2'), 7.78 (s, 2H,5'), 7.70 (s, 2H,4'), 7.15 (d, J = 7.7 Hz, 6H,6), 6.99 (d, J = 7.8 Hz, 6H,5), 4.19 (q, J = 7.3 Hz, 4H,7'), 3.84 (s, 6H,6'), 3.33 (d, J = 7.1 Hz, 3H,2), 2.38 (d, J = 7.1 Hz, 6H,8), 1.78 (dq, J = 13.3, 6.6 Hz, 3H,9), 1.41 (t, J = 7.3 Hz, 6H,8'), 1.22 (d, J = 7.1 Hz, 9H,3), 0.86 (d, J = 6.6 Hz, 18H,10).

1:1

¹H NMR (400 MHz, D₂O): δ/ppm = 8.61 (s, 1H,2'), 7.39 (s, 1H,5'), 7.32 (s, 1H,4'), 7.19 (d, J = 7.9 Hz, 4H,5), 7.14 (d, J = 7.9 Hz, 4H,6), 4.13 (q, J = 7.3 Hz, 2H,7'), 3.79 (s, 3H,6'), 3.59 (d, J = 7.1 Hz, 2H,2), 2.40 (d, J = 7.1 Hz, 4H,8), 1.82 – 1.69 (m, 2H,9), 1.40 (t, J = 7.3 Hz, 2H,8'), 1.32 (d, J = 7.2 Hz, 6H,3), 0.79 (d, J = 6.7 Hz, 12H,10).

¹H NMR (400 MHz, DMSO): δ/ppm = 9.19 (s, 1H,2'), 7.78 (s, 1H, 5'), 7.70 (s, 1H, 4'), 7.16 (d, J = 7.8 Hz, 4H, 6), 7.02 (d, J = 7.8 Hz, 4H, 5), 4.19 (q, J = 7.3 Hz, 2H,7'), 3.84 (s, 3H, 6'), 3.42 (q, J = 7.1 Hz, 2H,2), 2.39 (d, J = 7.1 Hz, 4H,8), 1.80 (dp, J = 13.7, 6.8 Hz, 2H,9), 1.41 (t, J = 7.3 Hz, 3H,8'), 1.25 (d, J = 7.1 Hz, 6H,3), 0.86 (d, J = 6.6 Hz, 12H,10).

1:2

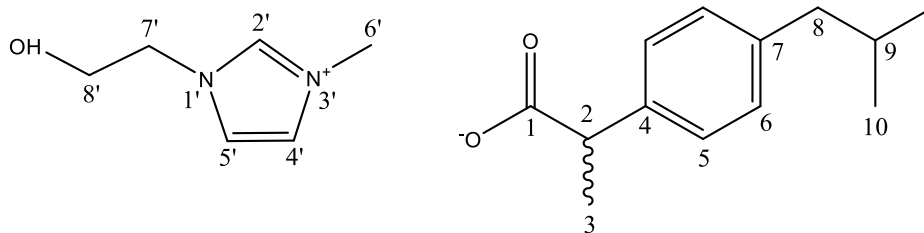
¹H NMR (400 MHz, D₂O): δ/ppm = 8.61 (s, 1H,2'), 7.39 (s, 1H,5'), 7.32 (s, 1H,4'), 7.19 (d, J = 7.8 Hz, 6H,5), 7.14 (d, J = 7.8 Hz, 6H,6), 4.13 (q, J = 7.3 Hz, 2H,7'), 3.79 (s, 3H,6'), 3.60 (t, J = 6.9 Hz, 1H,2), 2.40 (d, J = 7.2 Hz, 6H,8), 1.80 – 1.70 (m, 3H,9), 1.40 (t, J = 7.4 Hz, 3H,8'), 1.32 (d, J = 7.2 Hz,9H,3), 0.79 (d, J = 6.7 Hz, 18H,10).

¹H NMR (400 MHz, DMSO): δ/ppm = 9.16 (s, 1H,2'), 7.78 (s, 1H,5'), 7.70 (s, 1H,4'), 7.17 (d, J = 7.8 Hz, 6H,6), 7.04 (d, J = 7.8 Hz, 6H,5), 4.19 (q, J = 7.4 Hz, 2H,7'), 3.84 (s, 3H,6'), 3.50 (q, J = 7.1 Hz, 3H,2), 2.40 (d, J = 7.2 Hz, 6H,8), 1.80 (hept, J = 6.9 Hz, 3H,9), 1.41 (t, J = 7.3 Hz, 3H,8'), 1.28 (d, J = 7.1 Hz, 9H,3), 0.86 (d, J = 6.6 Hz, 18H,10).

1:5

¹H NMR (400 MHz, D₂O): δ/ppm = 8.61 (s, 1H,2'), 7.39 (s, 1H,5'), 7.32 (s, 1H,4'), 7.19 (d, J = 7.9 Hz, 12H,5), 7.13 (d, J = 7.8 Hz, 12H,6), 4.13 (q, J = 7.4 Hz, 2H,7'), 3.79 (s, 3H,6'), 3.59 – 3.52 (m, 6H,2), 2.40 (d, J = 7.2 Hz, 12H,8), 1.80 – 1.71 (m, 6H,9), 1.40 (t, J = 7.3 Hz, 3H,8'), 1.31 (d, J = 7.2 Hz, 18H,3), 0.79 (d, J = 6.6 Hz, 36H,10).

¹H NMR (400 MHz, DMSO): δ/ppm = 9.13 (s, 1H,2'), 7.78 (s, 1H,5'), 7.70 (s, 1H,4'), 7.18 (d, J = 7.8 Hz, 12H,6), 7.07 (d, J = 7.9 Hz, 12H,5), 4.19 (q, J = 7.3 Hz, 2H,7'), 3.85 (s, 3H,6'), 3.57 (q, J = 7.1 Hz, 6H,2), 2.41 (d, J = 7.1 Hz, 12H,8), 1.81 (dp, J = 13.4, 6.7 Hz, 6H,9), 1.42 (t, J = 7.3 Hz, 3H,8'), 1.31 (d, J = 7.1 Hz, 18H,3), 0.86 (d, J = 6.6 Hz, 35H,10).

[C₂(OH)C₁Im][Ibu]-based systems**1:1**

¹H NMR (400 MHz, D₂O): δ/ppm = 8.67 (s, 1H,2'), 7.43 (s, 1H,5'), 7.37 (s, 1H,4'), 7.19 (d, J = 7.9 Hz, 4H,6), 7.14 (d, J = 7.9 Hz, 4H,5), 4.23 (t, J = 5.1 Hz, 2H,7'), 3.83 (d, J = 9.1 Hz, 5H,6',8'), 3.64 – 3.54 (m, 2H,2), 2.40 (d, J = 7.1 Hz, 4H,8), 1.82 – 1.70 (m, 2H,9), 1.32 (d, J = 7.2 Hz, 6H,3), 0.79 (d, J = 6.6 Hz, 12H,10).

¹H NMR (400 MHz, DMSO): δ/ppm = 9.17 (s, 1H,2'), 7.73 (s, 1H,5'), 7.69 (s, 1H,4'), 7.16 (d, J = 7.8 Hz, 4H,6), 7.02 (d, J = 7.8 Hz, 4H,5), 4.21 (t, J = 5.0 Hz, 2H,7'), 3.86 (s, 3H,6'), 3.71 (d, J = 5.0 Hz, 2H,8'), 2.39 (d, J = 7.1 Hz, 4H,8), 1.80 (dt, J = 13.5, 6.7 Hz, 2H,9), 1.26 (d, J = 7.1 Hz, 6H,3), 0.86 (d, J = 6.6 Hz, 12H,10).

1:2

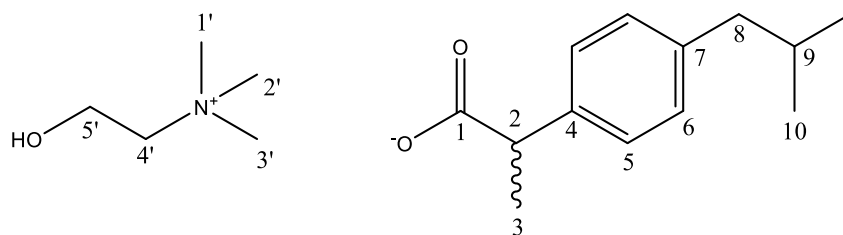
¹H NMR (400 MHz, D₂O): δ/ppm = 8.67 (s, 1H,2'), 7.43 (s, 1H,5'), 7.37 (s, 1H,4'), 7.19 (d, J = 7.8 Hz, 6H,6), 7.14 (d, J = 7.9 Hz, 6H,5), 4.23 (t, J = 5.0 Hz, 2H,7'), 3.83 (d, J = 9.3 Hz, 5H,6',8'), 3.57 (q, J = 7.2 Hz, 3H,2), 2.40 (d, J = 7.2 Hz, 6H,8), 1.79 – 1.71 (m, 3H,9), 1.32 (d, J = 7.2 Hz, 9H,3), 0.79 (d, J = 6.6 Hz, 18H,10).

¹H NMR (400 MHz, DMSO): δ/ppm = 9.16 (s, 1H,2'), 7.73 (d, J = 2.0 Hz, 1H,5'), 7.69 (s, 1H,4'), 7.17 (d, J = 7.8 Hz, 6H,6), 7.04 (d, J = 7.8 Hz, 6H,5), 4.21 (t, J = 5.1 Hz, 2H,7'), 3.86 (s, 3H,6'), 3.72 (t, J = 5.1 Hz, 2H,8'), 3.49 (q, J = 7.1 Hz, 3H,2), 2.40 (d, J = 7.1 Hz, 6H,8), 1.80 (dt, J = 13.5, 6.7 Hz, 3H,9), 1.28 (d, J = 7.1 Hz, 9H,3), 0.86 (d, J = 6.6 Hz, 18H,10).

1:5

¹H NMR (400 MHz, D₂O): δ/ppm = 8.67 (s, 1H,2'), 7.43 (s, 1H,5'), 7.37 (s, 1H,4'), 7.20 (d, J = 7.8 Hz, 12H,6), 7.15 (d, J = 7.8 Hz, 12H,5), 4.23 (s, 2H,7'), 3.83 (d, J = 9.1 Hz, 5H,6',8'), 3.61 (d, J = 7.4 Hz, 6H,2), 2.40 (d, J = 7.2 Hz, 12H,8), 1.80 – 1.69 (m, 6H,9), 1.33 (d, J = 7.2 Hz, 18H,3), 0.79 (d, J = 6.7 Hz, 36H,10).

¹H NMR (400 MHz, DMSO): δ/ppm = 9.13 (s, 1H,2'), 7.73 (s, 1H,5'), 7.69 (s, 1H,4'), 7.18 (d, J = 7.9 Hz, 12H,6), 7.07 (d, J = 7.9 Hz, 12H,5), 4.21 (t, J = 5.1 Hz, 2H,7'), 3.86 (s, 3H,6'), 3.72 (t, J = 5.0 Hz, 2H,8'), 3.57 (q, J = 7.1 Hz, 6H,2), 2.41 (d, J = 7.2 Hz, 12H,8), 1.81 (hept, J = 6.7 Hz, 6H,9), 1.31 (d, J = 7.1 Hz, 18H,3), 0.86 (d, J = 6.6 Hz, 36H,10).

[N_{1112(OH)}][Ibu]-based systems**2:1**

¹H NMR (400 MHz, D₂O): δ/ppm = 7.19 (d, J = 8.0 Hz, 6H,6), 7.13 (d, J = 7.9 Hz, 6H,5), 3.97 (d, J = 4.9 Hz, 4H,5'), 3.55 (q, J = 7.2 Hz, 3H,2), 3.43 (t, J = 5.0 Hz, 4H,4'), 3.11 (s, 18H,1',2',3'), 2.40 (d, J = 7.1 Hz, 6H,8), 1.75 (dt, J = 13.5, 6.7 Hz, 3H,9), 1.31 (d, J = 7.2 Hz, 9H,3), 0.79 (d, J = 6.6 Hz, 18H,10).

¹H NMR (400 MHz, DMSO): δ/ppm = 7.15 (d, J = 7.8 Hz, 6H,6), 7.00 (d, J = 7.8 Hz, 6H,5), 3.83 (dd, J = 6.4, 3.7 Hz, 2H,5'), 3.40 (t, J = 5.1 Hz, 3H,2), 3.34 (q, J = 7.1 Hz, 2H, 4'), 3.10 (s, 9H,1',2',3'), 2.38 (d, J = 7.1 Hz, 6H,8), 1.78 (dq, J = 13.6, 6.8 Hz, 3H,9), 1.23 (d, J = 7.1 Hz, 9H,3), 0.86 (d, J = 6.6 Hz, 18H,10).

1:1

¹H NMR (400 MHz, D₂O): δ/ppm = 7.19 (d, J = 7.9 Hz, 4H,6), 7.13 (d, J = 7.9 Hz, 4H,5), 3.97 (d, J = 5.2 Hz, 2H,5'), 3.54 (q, J = 7.2 Hz, 2H,2), 3.42 (m, 2H,4'), 3.11 (s, 9H, 1',2',3'), 2.40 (d, J = 7.1 Hz, 4H,8), 1.75 (dt, J = 13.6, 6.9 Hz, 2H,9), 1.31 (d, J = 7.2 Hz, 6H,3), 0.79 (d, J = 6.6 Hz, 12H,6).

¹H NMR (400 MHz, DMSO): δ/ppm = 7.16 (d, J = 7.8 Hz, 4H,6), 7.02 (d, J = 7.8 Hz, 4H,5), 3.82 (m, 2H,5'), 3.10 (s, 9H,1',2',3'), 2.39 (d, J = 7.1 Hz, 4H,8), 1.80 (dp, J = 13.4, 6.6 Hz, 2H,9), 1.26 (d, J = 7.1 Hz, 6H,3), 0.86 (d, J = 6.5 Hz, 12H,10).

1:2

¹H NMR (400 MHz, D₂O): δ/ppm = 7.19 (d, J = 8.0 Hz, 6H,6), 7.14 (d, J = 7.9 Hz, 6H,5), 3.97 (s, 2H,5'), 3.59 (d, J = 7.0 Hz, 3H,2), 3.46 – 3.40 (m, 2H,4'), 3.11 (s, 9H,1',2',3'), 2.40 (d, J = 7.1 Hz, 6H,8), 1.84 – 1.67 (m, 3H,9), 1.32 (d, J = 7.2 Hz, 9H,3), 0.79 (d, J = 6.7 Hz, 18H,10).

¹H NMR (400 MHz, DMSO): δ/ppm = 7.17 (d, J = 7.8 Hz, 6H, 6), 7.04 (d, J = 7.8 Hz, 6H, 5), 3.83 (d, J = 5.5 Hz, 2H,5'), 3.51 (q, J = 7.1 Hz, 3H, 2), 3.39 (t, J = 5.1 Hz, 2H,4'), 3.10 (s, 9H, 1',2',3'), 2.40 (d, J = 7.1 Hz, 6H, 8), 1.80 (dt, J = 13.5, 6.7 Hz, 3H,9), 1.28 (d, J = 7.1 Hz, 9H,3), 0.86 (d, J = 6.6 Hz, 18H, 10).

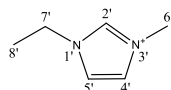
1:5

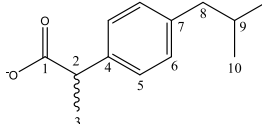
^1H NMR (400 MHz, D_2O): δ/ppm = 7.19 (d, J = 7.9 Hz, 12H,6), 7.14 (d, J = 8.0 Hz, 12H,5), 3.97 (s, 2H,5'), 3.59 (d, J = 7.0 Hz, 6H,2), 3.43 (s, 2H,4'), 3.11 (s, 9H,1',2',3'), 2.40 (d, J = 7.1 Hz, 12H,8), 1.80 – 1.71 (m, 6H,9), 1.32 (d, J = 7.2 Hz, 18H,3), 0.79 (d, J = 6.8 Hz, 36H,10).

^1H NMR (400 MHz, DMSO): δ/ppm = 7.18 (d, J = 7.8 Hz, 12H,6), 7.07 (d, J = 7.8 Hz, 12H,5), 3.83 (s, 2H,5'), 3.57 (q, J = 7.1 Hz, 6H,2), 3.39 (t, J = 5.2 Hz, 2H,4'), 3.10 (s, 9H,1',2',3'), 2.41 (d, J = 7.1 Hz, 12H,8), 1.81 (dp, J = 13.6, 6.8 Hz, 6H,9), 1.31 (d, J = 7.0 Hz, 18H,3), 0.86 (d, J = 6.5 Hz, 36H,10).

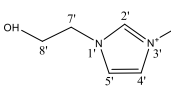
Table 4.S9. ^1H NMR chemical shifts for the position H2' according to the chemical structure of $[\text{C}_2\text{C}_1\text{Im}][\text{Ibu}]$ and $[\text{C}_{2(\text{OH})}\text{C}_1\text{Im}][\text{Ibu}]$ (right) for the neat ionic liquid and its eutectic systems in DMSO.

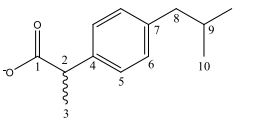
Compounds	H2'
$[\text{C}_2\text{C}_1\text{Im}][\text{Ibu}]$	9.48
$[\text{C}_2\text{C}_1\text{Im}][\text{Ibu}]:\text{Ibu}$ 2:1	9.24
$[\text{C}_2\text{C}_1\text{Im}][\text{Ibu}]:\text{Ibu}$ 1:1	9.19
$[\text{C}_2\text{C}_1\text{Im}][\text{Ibu}]:\text{Ibu}$ 1:2	9.16
$[\text{C}_2\text{C}_1\text{Im}][\text{Ibu}]:\text{Ibu}$ 1:5	9.13
$[\text{C}_{2(\text{OH})}\text{C}_1\text{Im}][\text{Ibu}]$	9.31
$[\text{C}_{2(\text{OH})}\text{C}_1\text{Im}][\text{Ibu}]:\text{Ibu}$ 1:1	9.17
$[\text{C}_{2(\text{OH})}\text{C}_1\text{Im}][\text{Ibu}]:\text{Ibu}$ 1:2	9.16
$[\text{C}_{2(\text{OH})}\text{C}_1\text{Im}][\text{Ibu}]:\text{Ibu}$ 1:5	9.13





$[\text{C}_2\text{C}_1\text{Im}][\text{Ibu}]$





$[\text{C}_{2(\text{OH})}\text{C}_1\text{Im}][\text{Ibu}]$

Table S10. Inhibition of BSA denaturation in PBS pH 7.4 at different concentrations for ibuprofen-based eutectic systems. The presented value is the average of at least two independent measures \pm standard deviation.

Concentration (mM)	Inhibition of BSA denaturation (%)	Concentration (mM)	Inhibition of BSA denaturation (%)
[C₂C₁Im][Ibu]:Ibu 2:1		[C₂C₁Im][Ibu]:Ibu 1:1	
0.536	10.18 \pm 1.31	0.574	22.28 \pm 1.74
1.251	24.04 \pm 1.38	1.339	41.40 \pm 1.94
1.788	53.16 \pm 2.68	1.913	54.21 \pm 1.29
2.681	56.84 \pm 0.86	2.870	68.60 \pm 0.25
[C₂C₁Im][Ibu]:Ibu 1:2		[C₂C₁Im][Ibu]:Ibu 1:5	
0.617	23.33 \pm 1.24	0.668	24.16 \pm 2.28
1.440	40.88 \pm 1.51	1.558	43.41 \pm 0.96
2.058	69.82 \pm 0.99	2.226	65.20 \pm 1.45
3.087	69.65 \pm 1.38	3.339	61.49 \pm 3.31
[C_{2(OH)}C₁Im][Ibu]:Ibu 1:1		[C_{2(OH)}C₁Im][Ibu]:Ibu 1:2	
0.557	31.05 \pm 1.87	0.604	46.84 \pm 1.14
1.299	47.72 \pm 2.37	1.409	52.98 \pm 1.79
1.856	60.18 \pm 2.16	2.014	68.42 \pm 1.49
2.784	67.72 \pm 2.03	3.020	69.30 \pm 3.23
[C_{2(OH)}C₁Im][Ibu]:Ibu 1:5		[N_{1112(OH)}][Ibu]:Ibu 2:1	
0.660	55.56 \pm 2.65	0.545	6.49 \pm 0.50
1.540	55.86 \pm 1.75	1.273	20.88 \pm 1.63
2.200	67.90 \pm 1.15	1.818	70.53 \pm 0.74
3.300	75.15 \pm 2.15	2.727	68.42 \pm 1.14
[N_{1112(OH)}][Ibu]:Ibu 1:1		[N_{1112(OH)}][Ibu]:Ibu 1:2	
0.582	14.01 \pm 2.79	0.623	0.19 \pm 0.00
1.357	45.14 \pm 2.18	1.454	11.67 \pm 2.45
1.939	57.78 \pm 1.93	2.078	33.85 \pm 2.62
2.909	69.07 \pm 0.83	3.117	72.96 \pm 1.20
[N_{1112(OH)}][Ibu]:Ibu 1:5			
0.671	1.36 \pm 0.58		
1.566	15.08 \pm 0.88		
2.238	47.47 \pm 1.91		
3.356	81.13 \pm 3.45		

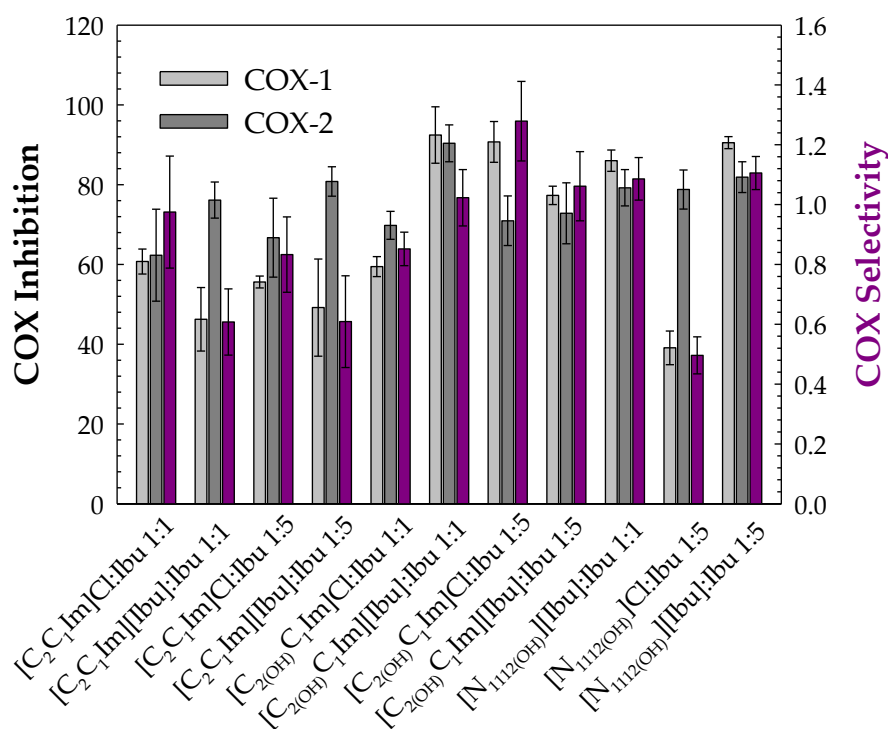


Figure 4.S9. Selective inhibition of COX-1 (ovine) and COX-2 (human) and COX-1/COX-2 selectivity at 3mM for the eutectic systems based on ILs ([C₂C₁Im]Cl, [C_{2(OH)}C₁Im]Cl and [N_{1112(OH)}]Cl) [S1] and for the eutectic systems based on API-ILs ([C₂C₁Im][Ibu], [C_{2(OH)}C₁Im][Ibu] and [N_{1112(OH)}][Ibu]).

References

- S1. Bastos, J.C.; Gaspar, M.M.; Pereiro, A.B.; Araújo, J.M.M. Role of Ionic Liquids in Ibuprofen-Based Eutectic Systems: Aqueous Solubility, Permeability, Human Cytotoxicity, Hemolytic Activity and Anti-Inflammatory Activity. *Nanomaterials* 2023 (*in press*).

**ENHANCED MEMBRANE PERMEABILITY OF
IBUPROFEN: INTERPLAY OF IONIC LIQUIDS AND
EUTECTICS ON IONICITY AND SKIN-PAMPA
PERMEABILITY**

5.1 Abstract

Ibuprofen is a non-steroidal anti-inflammatory drug (NSAID) generally used to treat inflammation, fever, and mild-to-moderate pain. The oral delivery route has been the most widely used, however there are major gastrointestinal side effects associated with their long-term use. Thus, transdermal dosage forms are desirable for the chronic use of this drug. The efficacy of transdermal formulations depends greatly on its capacity to facilitate the drug penetration through the skin. Ionic liquids are currently defined as organic salts with melting points below 100 °C, and as salts they may stay as ion pairs or clusters with increasing lipophilicity promoting a rapidly crossover in biological membranes. Eutectic systems were introduced as an alternative to ionic liquids and are defined as a mixture of two or more components which interact through hydrogen bonding and lead to an overall decrease in the melting temperature of the system. In the present work, the use pharmacologically active ionic liquids based on ibuprofen (API-ILs) and eutectic systems with API-ILs and ibuprofen as counterparts were evaluated to increase skin permeation of the acidic ibuprofen. The assessment of ionicity, through measurements of density, viscosity, and conductivity, was carried out to confirm the formation of ion-pairs or clusters, namely for the molar ratio 1:5 of the Ibuprofen-based eutectic formulations. Besides, an *in vitro* skin permeation testing was carried out through Skin Parallel Artificial Membrane Permeability Assays (Skin PAMPA) and results showed that the ibuprofen-based formulations (API-ILs or eutectic systems) presented similar permeation profile than ibuprofen and higher permeation than the commercially used sodium ibuprofen salt.

Keywords: Ibuprofen, Ionic liquids, Eutectic Systems, Density, Viscosity, Conductivity, Walden-plot, Effective Permeability Coefficient, Skin PAMPA

To be published in: Joana C. Bastos, Ana B. Pereiro, João M. M. Araújo Enhanced Membrane Permeability of Ibuprofen: Interplay of Ionic Liquids and Eutectics on Ionicity and Skin-PAMPA Permeability. Journal of Molecular Liquids 2023 (**Submitted**)

Own experimental contribution: Sample preparation; viscosity, density and conductivity measurements, Skin PAMPA assay

Own written contribution: Viscosity, density and conductivity analysis, Walden plot interpretation and Skin PAMPA analysis.

Other contributions: Experimental design and data analysis.

5.2 Introduction

Ibuprofen (Ibu) is a non-steroidal anti-inflammatory drug (NSAID) with anti-inflammatory, analgesic, and antipyretic properties commonly indicated for the treatment of fever and mild-to-moderate pain. The anti-inflammatory properties of ibuprofen arise from the non-selective inhibition of the enzymes cyclooxygenase-1 (COX-1) and cyclooxygenase-2 (COX-2), which is required for the synthesis of prostaglandins via the arachidonic acid pathway. COXs are needed to convert arachidonic acid to prostaglandin H₂ (PGH₂) in the body. PGH₂ is then converted to prostaglandins. The inhibition of COXs by ibuprofen, therefore, lowers the level of prostaglandins and ultimately reducing inflammation [1]. The oral route of administration is the most common and preferred route of ibuprofen delivery due to easy patient adherence and administration. However, the oral drug bioavailability depends on several factors such as aqueous solubility, dissolution rate, gastrointestinal permeability, first-pass and pre-systemic metabolism which can limit an efficient mode of delivery influencing drug absorption and as consequence the pharmacological effects [2]. When administered orally, ibuprofen can cause well documented and serious gastrointestinal side effects which include gastroduodenal haemorrhage, gastric outlet obstruction, gastroduodenal small or large bowel perforation, large or small bowel haemorrhage, acute gastrointestinal haemorrhage, symptomatic gastric or duodenal ulcer or anaemia [3]. Thus, a transdermal drug delivery system is considered a possible solution to overcome the side effects of ibuprofen oral delivery route, particularly the avoidance of direct gastrointestinal adverse events, since the transdermal route can provide a direct *site* delivery of a drug yet enhance therapeutic efficacy and a rapid onset [2]. Gaur et al. [4] investigated the transdermal application of a liposomal ibuprofen gel formulation containing Carbopol 934. The liposomal drug nanoparticles showed maximum skin permeation with excellent maximum plasma concentration (C_{max}). The formulation containing 7:3:1 molar ratio of phosphatidylcholine, cholesterol, and dicetyl phosphate was found to be optimal for nanoliposome preparations for controlled delivery of ibuprofen. The potential use of surfactants and/or phospholipids vesicles in the transdermal delivery of ibuprofen as drug encapsulated vesicles has been studied.

Several vesicles designed with various ratios of soy lecithin, span 80 and tween 80 were stable and considered a promising prolonged delivery system [5].

Ionic liquids (IL) are salts composed by cations and anions with a melting point below the conventional temperature of 100 °C. Their key physicochemical properties, such as thermal stability, density, viscosity, melting point, surface tension, solubility, hygroscopicity, and even toxicity and biodegradability [6], can be tailored, making ILs task-specific designer materials suitable for the biotechnology and pharmaceutical fields. Several research studies were conducted to show that ILs can enhance permeation of drugs through the skin [7,8] and the best documented case is the activity of 1-octyl-3-methylimidazolium-based ILs which act by disrupting structural integrity by inserting into the membrane [9]. It was also established that ILs possess the ability to fluidize cell membranes, particularly seen with hydrophilic imidazolium-based ILs [10], sustained promising information for the use of ILs as membrane permeation enhancers.

Converting an active pharmaceutical ingredient (API) into a salt (i.e. a ionic liquid) as shown great potential for drug delivery by eliminating polymorphism, tailoring solubility, improving thermal stability, increasing dissolution, controlling drug release, modulating the surfactant properties, enhancing permeability of APIs and modulating cytotoxicity [7,11,12]. The development of ILs-based on active pharmaceutical ingredients (API-ILs) has arisen as a possible solution to some of the problems that crystalline solid APIs present leading to lower melting temperatures and attend to improve bioavailability [13]. To explore the feasibility of transforming NSAIDs into ILs to improve transdermal delivery Hao Wu and co-workers studied the conversion of ibuprofen into ILs with nine structurally diverse cationic counterions, five of which were aromatic counterions and the other four were alkyl counterions [12]. The imidazolium counterions appeared to offer high aqueous solubility, with low values of partition coefficients, while counterions with long alkyl chains resulted in lower aqueous solubility and high values of partition coefficients. The ammonium-based ionic liquids, didecyltrimethylammonium ibuprofenate, $[N_{1,1,10,10}][Ibu]$, and tetrahexylammonium ibuprofenate, $[N_{6,6,6,6}][Ibu]$, were significantly more permeable than the neutral free form of ibuprofen. Furthermore, they correlated the higher transdermal permeability with

higher degree of ionic association were hydrophobic molecular interaction between ibuprofen and alkyl counterions favoured the ionic association and ion pair formation, and ultimately the transdermal permeation [12]. Recently, our group reported on the synthesis of three pharmacology active ionic liquids conjugating the ibuprofenate anion with imidazolium cations (i.e., [C₂C₁Im][Ibu] and [C_{2(OH)}C₁Im][Ibu]) and a cholinium cation (i.e., [N_{1112(OH)}][Ibu]). An upgrade to the aqueous solubility (water and biological simulated fluids) for the ibuprofen-based ILs relative to the ibuprofen neutral and commercial ibuprofen salt form (i.e., sodium ibuprofen) was verified. Cytotoxicity tests in two immortalized human cell lines (Caco-2, colon carcinoma cells and HepG2, hepatocellular carcinoma cells) and hemocompatibility assays substantiated the biocompatibility of the ibuprofen-based ILs. Their pharmacological action was assessed through the inhibition of bovine serum albumin (BSA) denaturation and inhibition of cyclooxygenases (i.e., COX-1 and COX-2), showing that all prepared API-ILs, [C₂C₁Im][Ibu], [C_{2(OH)}C₁Im][Ibu] and [N_{1112(OH)}][Ibu], maintained the anti-inflammatory response of ibuprofen with improved selectivity towards COX-2, allowing for the development of safer NSAIDs [13]. Although the API-ILs proven to be useful for transdermal delivery, they often appear to be solid at room temperature which is a main through back to a transdermal formulation [2,13].

Eutectic systems have been explored as alternative pharmaceutical solvents and permeation enhancers due to their strong deviations from the ideal solid-liquid phase behaviour. Eutectic systems are a mixture of at least two compounds, a salt (hydrogen bond acceptor, HBA) and a hydrogen bond donor (HBD), which can self-associate and it is characterized by a depression in the melting temperature in comparison to each individual components [14]. Sarraguça et al. [15] synthesized two eutectic combinations using chlorpropamide (CLP) and tolbutamide (TLB) with tromethamine (TRIS) and water, CLP:TRIS:H₂O 1:2:6 and TLB:TRIS:H₂O 1:2:8, respectively, and proven to be stable for at least one week at room temperature [15]. The neat parent drugs (CLP and TLB) presented low solubility in water and high permeability, however with a of a eutectic combination the drugs solubility was increased by 188-fold for CLP and by 120-fold for TLB and both maintaining a similar high permeability profile to the parent drugs. Regarding the cytotoxic studies, both, CLP:TRIS:H₂O 1:2:6 and TLB:TRIS:H₂O 1:2:8

proven to be considered safe for human consumption and can be further used in pharmaceutical formulations to improve aqueous solubility [15]. Also, Pedro and coworkers [16] developed an alginate-based hydrogel loaded with ibuprofen solubilized in a eutectic solvent composed of arginine and glycerol (Arg:Gly) at the molar fraction 1:4, respectively. Although the solubility of ibuprofen was slightly improved in an aqueous solution of Arg:Gly (60% w/w), the prepared formulation could be stable for at least 15 days, it has a cytotoxic profile similar to ibuprofen and provides a small decrease in the anti-inflammatory activity of the parent drug. By incorporating the ibuprofen solution in an alginate gel, the amount of ibuprofen permeated achieved using this is 8.5-fold higher than the amount obtained for commercial formulations. Silva et al. [17] constructed hydrophobic eutectics based on menthol and saturated fatty acids with different chain lengths, including stearic acid, myristic acid and lauric acid, and evaluated their toxicity and antibacterial activity in human immortal keratinocyte line (HaCaT) cells. The results revealed that the synergistic effect of menthol and stearic acid on enhancing antibacterial activity and promoting wound healing, whereas the whole mixture exhibited no cytotoxicity, demonstrating the promising application of menthol:stearic acid based eutectics in wound healing. Three other eutectic systems were prepared by complexation of APIs (i.e., ibuprofen, benzoic acid and phenylacetic acid) with menthol, possessed the characteristics of high solubility and high permeability, improving the bioavailability of the APIs [18]. In another study, seven terpenoids, including L-menthol, LD-menthol, D-limonene, L-menthone, 1,8-cineole, thymol and cymene were selected to be mixed with ibuprofen to prepare the eutectic systems [19]. Among them, the combination of ibuprofen and thymol maximizes permeability and produces a synergistic effect in penetration experiments. An ibuprofen-based eutectic conjugated with limonene at a molar ratio 1:4 also effectively inhibits the proliferation of human colon cancer cell line (i.e., HT29) without affecting the viability of healthy cells, providing an anti-cancer pharmacological response [20]. The eutectic system not only retains the therapeutic effects of limonene and ibuprofen, but also increases the solubility of the two components and reduces the side effect of limonene on the viability of normal cell lines. The specific mechanism may be related to the synergistic or additive effects

caused by the hydrogen-bonded supramolecular arrangements between the two components.

Recently, our group developed pharmacologically active eutectic systems conjugating ibuprofen (HBD) with 1-ethyl-3-methylimidazolium chloride ($[\text{C}_2\text{C}_1\text{Im}]\text{Cl}$), 1-(2-hydroxyethyl)-3-methylimidazolium chloride ($[\text{C}_{2(\text{OH})}\text{C}_1\text{Im}]\text{Cl}$), 1-ethyl-3-methylimidazolium acetate, ($[\text{C}_2\text{C}_1\text{Im}][\text{C}_1\text{CO}_2]$) or cholinium chloride ($[\text{N}_{1112(\text{OH})}]\text{Cl}$) in different molar ratios (viz. 2:1, 1:1, 1:2 and 1:5) [14]. An upgrade of the aqueous solubility in water and biological simulated fluids was obtained when compared to the neat ibuprofen and its salt form (i.e., sodium ibuprofen). Moreover, the Ibu-based eutectics and ibuprofen displayed similar cytotoxic profiles in colon carcinoma cells (Caco-2) and hepatocellular carcinoma cells (HepG2) and all forms were hemocompatible. The pharmacological action of the prepared Ibu-based eutectic formulations was evaluated through the inhibition of BSA denaturation and inhibition of COX-1 and COX-2 enzymes and all the eutectics maintain the anti-inflammatory response of ibuprofen with the opportunity to improve the selectivity towards COX-2 in some formulations. Additionally, the permeation potential of the Ibu-based eutectics was evaluated via Walden plot confirming the formation of large charged or non-charged aggregates, or the existence of ionic networks, that increase the potential for these liquids to penetrate membranes more efficiently than ibuprofen. Also, by combining the API-ILs properties with the eutectic systems fundamentals, ten API-IL-based eutectic systems were successfully synthesized with 1-ethyl-3-methylimidazolium ibuprofenate ($[\text{C}_2\text{C}_1\text{Im}][\text{Ibu}]$), 1-(2-hydroxyethyl)-3-methylimidazolium ibuprofenate ($[\text{C}_{2(\text{OH})}\text{C}_1\text{Im}][\text{Ibu}]$) and cholinium ibuprofenate ($[\text{N}_{1112(\text{OH})}][\text{Ibu}]$) as HBA and ibuprofen at the molar ratios 2:1, 1:1, 1:2 and 1:5 [21]. The eutectic systems showed the ability to maintain stable and liquid at room temperature. Likewise, in colon carcinoma cells (Caco-2) and hepatocellular carcinoma cells (HepG2) the API-ILs-based eutectics played similar cytocompatibility and all forms were hemocompatible. The pharmacological activity was evaluated by the inhibition of cyclooxygenases (COX-1 and COX-2) enzymes and inhibition of BSA denaturation and all the eutectics preserve the NSAID anti-inflammatory response, were in some cases the COX-2 selectivity was improved.

The prediction of skin permeability is of greatly importance prior to any drug formulation mainly due to the capacity of the skin to limit the body's accumulation of substances by percutaneous transport. The epidermal skin barrier is the major factor in this process and can reduce overall rates of accumulation by several orders of magnitude [22]. Thus, Skin Parallel Artificial Membrane Permeability Assays (Skin PAMPA) was developed for a quick, reliable, and cost-effective permeability model for the prediction of transdermal penetration of compounds. To match the permeability of the rate-limiting barrier in human skin, synthetic ceramides, which are analogs of the ceramides present in the stratum corneum, were selected for the Skin PAMPA model. Thus, the final Skin PAMPA membrane lipid mixture contains ceramide, free fatty acid, and cholesterol to better predict transdermal permeability. The PAMPA sandwich consists of two 96-well plates whereas one plate is formed to sit precisely under the plate that contains the porous lipid-impregnated filter disk (**Figure 5.1**). The wells of the bottom plate are typically filled with donor solution (API), and the wells of the top plate are filled with acceptor solution (buffer or mixtures of organic solvent and buffer). The plates are then piled up as shown at the left of **Figure 5.1** and then incubated. By comparison to data from three different human skin databases, Skin PAMPA demonstrated its high prediction capability [23].

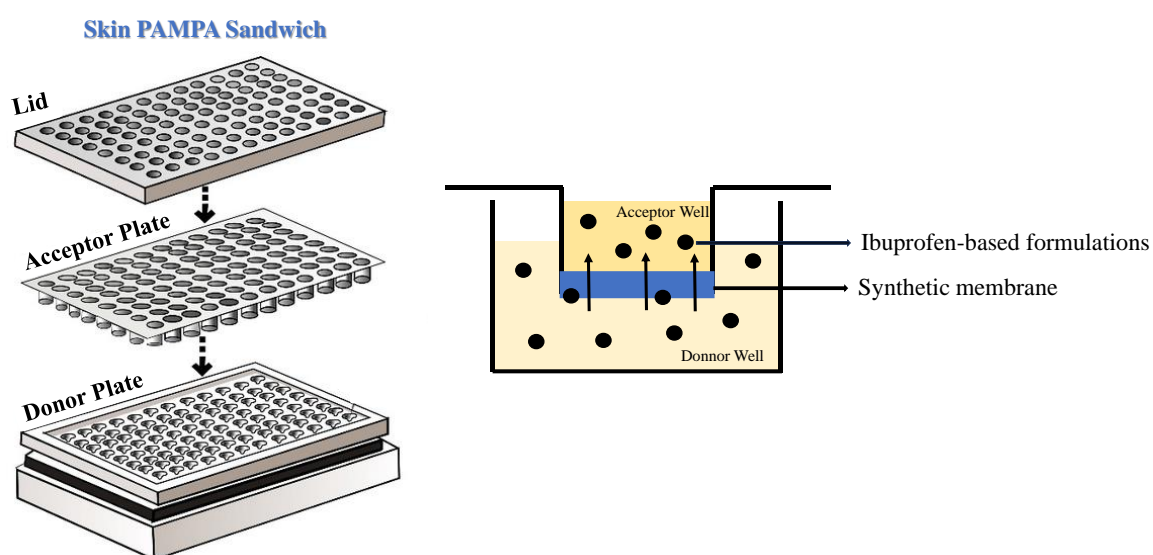


Figure 5.1 Parallel Artificial Membrane Permeability Assay (PAMPA) 96-well setup (left); a single well of PAMPA (right).

Recently, Wu and co-workers [24] explored the feasibility of transdermal delivery of ibuprofen using ionic liquid technology. To evaluate transdermal potential, *in vitro* skin permeation testing was carried out via Skin Parallel Artificial Membrane Permeability Assays (Skin PAMPA) for the ibuprofen, sodium ibuprofen salt ([Na][Ibu]) and the API-ILs 1-butyl-3-methylimidazolium ibuprofenate ([C₄C₁Im][Ibu]), 1-1-(2-hydroxyethyl)-3-methylimidazolium ibuprofenate ([C_{2(OH)}C₁Im][Ibu]), lidocaine Ibuprofenate ([Lid][Ibu]), procainium Ibuprofenate ([Pro][Ibu]), ranitidine Ibuprofenate ([Ran][Ibu]), Didecyldimethylammonium ibuprofenate ([N_{1,1,10,10}][Ibu]), tetrahexylammonium ibuprofenate ([N_{6,6,6,6}][Ibu]), tetrabutylphosphonium ibuprofenate ([P_{4,4,4,4}][Ibu]) and tributyl(tetradecyl)phosphonium ibuprofenate ([P_{6,6,6,14}][Ibu]). The overall aqueous solubility and octanol-water partition coefficients (LogP) values were correlated with lower aqueous solubility obtained at higher LogP values. It was concluded that imidazolium counterions appeared to offer high aqueous solubility, with low values of partition coefficients, while counterions with long alkyl chains resulted in lower aqueous solubility and high values of partition coefficients. Also, the percentage of drug permeated at the end of 12 h study through the Skin PAMPA was in the following order: [N_{6,6,6,6}][Ibu] (52.67%) > [N_{1,1,10,10}][Ibu] (41.12%) > [P_{6,6,6,14}][Ibu] (9.98%) > [Ibu] (9.93%) > [Lid][Ibu] (6.85%) > [Pro][Ibu] (6.67%) > [P_{4,4,4,4}][Ibu] (6.65%) > [Ran][Ibu] (6.32%) > [C₄C₁Im][Ibu] (6.21%) > [C_{2(OH)}C₁Im][Ibu] (4.50%) > [Na][Ibu] (1.66%). The permeation of [N_{1,1,10,10}][Ibu] and [N_{6,6,6,6}][Ibu] through the membrane was much higher than ibuprofen. The rest ILs showed similar or slightly lower permeation than ibuprofen, but all the ILs showed higher permeation than the commercially available sodium ibuprofen ([Na][Ibu]). Further, the authors correlated the higher transdermal permeability with higher degree of ionic association calculated through the ionic conductivity where they acknowledged the hydrophobic molecular interaction between ibuprofen and alkyl counterions which favoured the ionic association and ion pair formation, and ultimately the transdermal permeation.

In the present work, we have further investigated the benefits of using ILs as active pharmaceutical ingredients (API-ILs) and eutectic systems to modulate the permeability

of ibuprofen. The characterized in terms of viscosity, conductivity, density and ionicity (via Walden plot) was achieved for the eutectics systems based on 1-ethyl-3-methylimidazolium ibuprofenate ($[\text{C}_2\text{C}_1\text{Im}][\text{Ibu}]$), 1-(2-hydroxyethyl)-3-methylimidazolium ibuprofenate ($[\text{C}_{2(\text{OH})}\text{C}_1\text{Im}][\text{Ibu}]$) and cholinium ibuprofenate ($[\text{N}_{1112(\text{OH})}][\text{Ibu}]$) as HBA and ibuprofen as HBD at different molar ratio (i.e, 2:1, 1:1, 1:2, and 1:5), to probe the formation of larger charged or non-charged aggregates, or the existence of ionic networks, that increase the possibility for these liquids to penetrate membranes more efficiently. However, the Walden plot analysis it is only used as a qualitative and semiquantitative measurement. The Skin Parallel Artificial Membrane Permeability Assay (Skin PAMPA) was further used to accurately predict transdermal absorption. The ibuprofen-based API-ILs ($[\text{C}_2\text{C}_1\text{Im}][\text{Ibu}]$, $[\text{C}_{2(\text{OH})}\text{C}_1\text{Im}][\text{Ibu}]$ and $[\text{N}_{1112(\text{OH})}][\text{Ibu}]$) were also characterized through the Skin PAMPA assay along with the $[\text{C}_2\text{C}_1\text{Im}][\text{Ibu}]:\text{Ibu}$, $[\text{C}_{2(\text{OH})}\text{C}_1\text{Im}][\text{Ibu}]:\text{Ibu}$ and $[\text{N}_{1112(\text{OH})}][\text{Ibu}]$ at molar ratios 2:1, 1:1, 1:2 and 1:5. The ibuprofen-based eutectics based on 1-ethyl-3-methylimidazolium chloride ($[\text{C}_2\text{C}_1\text{Im}]\text{Cl}$), 1-(2-hydroxyethyl)-3-methylimidazolium chloride ($[\text{C}_{2(\text{OH})}\text{C}_1\text{Im}]\text{Cl}$), 1-ethyl-3-methylimidazolium acetate ($[\text{C}_2\text{C}_1\text{Im}][\text{C}_1\text{CO}_2]$) and cholinium chloride ($[\text{N}_{1112(\text{OH})}]\text{Cl}$) as HBA and ibuprofen as HBD at different molar ratio (i.e, 2:1, 1:1, 1:2, and 1:5) was also evaluated through the Skin-PAMPA assay. The relationship between the formation of ion-pairs or clusters obtained in previous works along with the current data and skin permeability was explored.

5.3 Materials and Methods

5.3.1 Materials

Ibuprofen (>98% mass fraction purity) was acquired from TCI and ibuprofen sodium salt ($\geq 98\%$ mass fraction purity) from Sigma-Aldrich. Both pharmaceuticals were used without further purification. The ionic liquids 1-ethyl-3-methylimidazolium chloride ($[\text{C}_2\text{C}_1\text{Im}]\text{Cl}$; >98% mass fraction purity); 1-(2-hydroxyethyl)-3-methylimidazolium chloride ($[\text{C}_{2(\text{OH})}\text{C}_1\text{Im}]\text{Cl}$; >99% mass fraction purity); 1-ethyl-3-methylimidazolium acetate ($[\text{C}_2\text{C}_1\text{Im}][\text{C}_1\text{CO}_2]$; > 95 % mass fraction purity) were acquired at IoLiTec and cholinium chloride ($[\text{N}_{1112(\text{OH})}]\text{Cl}$; $\geq 98\%$ mass fraction purity) at Sigma-Aldrich. The

pharmacologically active ionic liquids 1-ethyl-3-methylimidazolium ibuprofenate ($[\text{C}_2\text{C}_1\text{Im}][\text{Ibu}]$), 1-(2-hydroxyethyl)-3-methylimidazolium ibuprofenate ($[\text{C}_{2(\text{OH})}\text{C}_1\text{Im}][\text{Ibu}]$) and cholinium ibuprofenate ($[\text{N}_{1112(\text{OH})}][\text{Ibu}]$) were prepared through two-step anion exchange reaction methodology and fully characterized as described in our previous work [13]. To avoid volatile impurities all the ionic liquids and cholinium chloride were dried under a $3 \cdot 10^{-2}$ Torr vacuum for at least 48 hours prior to any use and the water content, determined by Karl Fischer titration, was less than 0.05 wt%. The pharmacologically active ionic liquids (API-ILs), conventional ionic liquids (ILs), and the salt cholinium chloride were used as HBA to formulate eutectic systems with ibuprofen as HBD at the molar ratios 2:1; 1:1; 1:2 and 1:5. Milli-Q water (Milli-Q Integral Water Purification System) was used in all experiments throughout the work. The chemical structure and molecular weight of the ibuprofen, cholinium chloride salt and the six ionic liquids used along the work can be found in **Table 5.1**.

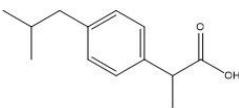
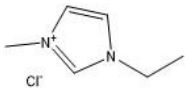
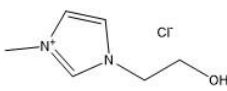
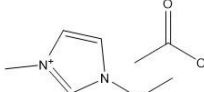
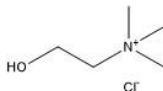
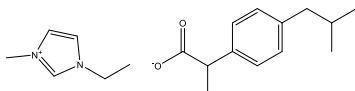
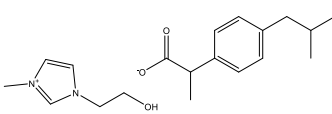
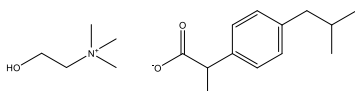
5.3.2 Preparation of Ibuprofen-based eutectic systems

For the preparation of the eutectic systems we have used a similar procedure to the one recently implemented by us [14,21,25], mixing a salt (the ILs $[\text{C}_2\text{C}_1\text{Im}]\text{Cl}$, $[\text{C}_{2(\text{OH})}\text{C}_1\text{Im}]\text{Cl}$ and $[\text{C}_2\text{C}_1\text{Im}][\text{C}_1\text{CO}_2]$, the salt $[\text{N}_{1112(\text{OH})}]\text{Cl}$ or the API-ILs $[\text{C}_2\text{C}_1\text{Im}][\text{Ibu}]$, $[\text{C}_{2(\text{OH})}\text{C}_1\text{Im}][\text{Ibu}]$ and $[\text{N}_{1112(\text{OH})}][\text{Ibu}]$) with ibuprofen as hydrogen-bond donor (HBD) at different molar ratios, namely 2:1, 1:1, 1:2 and 1:5. The ibuprofen-based systems were prepared in crimped seal glass vials using an analytical high precision balance with 0.01 mg resolution (Sartorius, Germany) at atmospheric pressure and under control of moisture content (i.e. sealed under nitrogen atmosphere). To ensure that all components were blended, three heating (up to $85^\circ\text{C} \pm 2^\circ\text{C}$) / cooling (down to $5^\circ\text{C} \pm 2^\circ\text{C}$) cycles were performed under constant stirring. Samples were kept in well-sealed glass vials after preparation and fresh samples were always used for analysis to avoid structural change or environmental effects on their physical properties.

A dynamic visual method implemented by us [14,21,25] (lab benchtop procedure) was attained, after the three heating/cooling cycles, to determine the solid-liquid transitions of the prepared mixtures. Firstly, the mixtures were cooled down to -40°C , for at least 30 min, and examined. If the mixture remained in the liquid state, the melting

temperature was considered below -40°C . If crystals were detected, the mixtures were heated up to achieve a complete liquid phase. For this last case, a second run was attained to confirm the solid-liquid transition. This procedure was carried out with successive increment of 5°C in the heating/cooling runs until the solid-liquid transition was determined, and the prepared mixtures pre-validated as eutectic mixtures.

Table 5.1. Designation, chemical structure, and molecular weight (M_w) of ibuprofen, cholinium salt and all the ionic liquids used along in this work.

Structure	Designation and acronym	M_w (g/mol)
	2-(4-Isobutylphenyl) propionic acid Ibuprofen (Ibu)	206.29
	1-Ethyl-3-methylimidazolium chloride [C ₂ C ₁ Im]Cl	146.62
	1-(2-hydroxyethyl)-3-methylimidazolium chloride [C ₂ (OH)C ₁ Im]Cl	162.62
	1-Ethyl-3-methylimidazolium acetate [C ₂ C ₁ Im][C ₁ CO ₂]	170.21
	Cholinium chloride [N ₁₁₁₂ (OH)]Cl	139.62
	1-Ethyl-3-methylimidazolium ibuprofenate [C ₂ C ₁ Im][Ibu]	316.44
	1-(2-hydroxyethyl)-3-methylimidazolium ibuprofenate [C ₂ (OH)C ₁ Im][Ibu]	332.44
	Cholinium ibuprofenate [N ₁₁₁₂ (OH)][Ibu]	309.44

The ibuprofen-based eutectic systems were previously characterized by ^1H NMR technique to verify that the HBA (ILs, cholinium chloride or API-ILs) and ibuprofen (HBD) have not reacted, and to check the molar ratio [14,21]. Also, the DSC traces of all prepared mixtures and their counterparts were obtained in our previous works to determine the different phase transitions and guarantee the eutectic formulation [14,21]. In **Table 5.S1** are summarized the glass transition temperature (T_g) and melting

temperature (T_m) of the ibuprofen-based eutectic and non-eutectic systems, ibuprofen, and all hydrogen-bond acceptors.

5.3.3 Density, Viscosity and Conductivity measurements

The measurements of density and viscosity were achieved using an automated SVM 3000 Anton Paar rotational Stabinger (Viscosimeter and Densimeter) between the temperature range of 15°C to 50°C at atmospheric pressure. The SVM 3000 uses a Peltier with an error on temperature of ± 0.02 C°. The reproducibility of the dynamic viscosity is $\pm 1\%$ and the density is ± 0.0002 g·cm⁻³. Samples were measured in duplicates and the reported result is the average value. The expanded uncertainty with 0.95 level of confidence of the measurements is estimated to be 2% for the viscosity and 0.1% for the density.

The conductivities measurements were obtained at the temperature range 15 to 50°C ± 0.3 °C with a METTLER TOLEDO fiveeasy plus Model FP30. The conductivimeter was calibrated at each temperature with certified 0.01 D and 0.1 D KCl (D = demal) standard solutions supplied by Radiometer Analytical. This conductivimeter uses an alternating current of 9 to 12 V and a frequency of 1 W in the range of conductivities measured in this work. The eutectic systems were exclusively prepared prior to the experiment and then kept in a glass cell containing a magnetic stirrer during all measurements. Furthermore, the conductivity outcomes are the average of at least two conductivity measurements. The apparatus gives conductivity values with an estimated expanded uncertainty with 0.95 level of confidence of $\pm 2\%$.

5.3.4 Skin Parallel Artificial Membrane Permeability Assay (Skin PAMPA)

The skin permeation tests were performed using Skin Parallel Artificial Membrane Permeability Assays (Skin PAMPA) that was purchased from Pion Inc. (Billerica, MA). Standard Prima buffers (P/N 110151) were prepared at pH 6.5 and 7.4 to serve as the acceptor and donor solutions according to the manufacturing guidelines. Both Prima buffers pH 6.5 and 7.4 were carefully chosen since they mimic the pH environment of the skin and the blood, respectively [26]. Prior to the experiment, the Skin PAMPA sandwiches were overnight submersed in hydration solution (P/N 110255). The sample

solutions of ibuprofen were prepared at 250 mM, 125 mM and 50 mM in DMSO. Due to the low solubility of sodium ibuprofen in DMSO, it was measured only at 20 mM. The sample solutions of ionic liquids and eutectic systems were prepared at 125 mM and 250 mM. To start the Skin PAMPA assay, the sample solutions were prepared in the Deep-Well plate where 5 mL of each sample solution was further added into 1 mL of Prima buffer (cf. pH 6.5 and 7.4). A sample of each solution prepared in the Deep-Well plate was primarily measured using a micro-plate reader (Multiskan GO from ThermoFisher Scientific) to obtain the initial concentration prior to the experiment. The micro-plate measurements were performed in a wavelength interval between 200 and 500 nm and at 25°C.

After the solutions were diluted in the Prisma Buffers according to the manufacturer's guidelines, 180 mL were transferred from the Deep-Well plate to the Donor plate. The acceptor plate was filled with 200 mL of Prima buffer at pH 7.4 and then slowly and gently placed on top of the Donor plate to form the Skin PAMPA sandwich according to the scheme in **Figure 5.1**. To avoid drying out of the membranes, the sandwich apparatus was formed within 4 to 5 minutes. The Skin PAMPA sandwich was incubated at 25 °C for 5 hours and a wet filter paper was placed under the lid to maintain a high relative humidity in order to minimize evaporation. After incubation, the samples in the Donor and Acceptor plates were measured using a micro-plate reader (Multiskan GO from ThermoFisher Scientific) in a wavelength interval between 200 and 500 nm and at 25°C.

The effective permeability coefficient (P_e , cm/s) was calculated according to Chen et al. [27] for the acceptor and donor plates for the ibuprofen, sodium ibuprofen and each ibuprofen formulation at the pH 6.5 and pH 7.4 according to **Equation 5.1** and **Equation 5.2**:

$$P_e = \frac{-\ln \left[1 - \frac{C_{\text{Acceptor}}}{C_{\text{equilibrium}}} \right]}{A \times \left(\frac{1}{V_{\text{Donor}}} + \frac{1}{V_{\text{Acceptor}}} \right) \times t} \quad (\text{Eq. 5.1})$$

$$C_{\text{equilibrium}} = \frac{C_{\text{Donor}} \times V_{\text{Donor}} + C_{\text{Acceptor}} \times V_{\text{Acceptor}}}{V_{\text{Donor}} + V_{\text{Acceptor}}} \quad (\text{Eq. 5.2})$$

where A is the effective filter area ($=f \times 0.3 \text{ cm}^2$, where f is 0,76 and is the apparent porosity of the filter), V_{Donor} is the donor well volume (0.18 mL), V_{Acceptor} is the acceptor well volume (0.2 mL), t is the incubation time in seconds, the C_{Acceptor} is the compound concentration in the acceptor well, and $C_{\text{equilibrium}}$ is the concentration at equilibrium.

5.4 Results and Discussion

5.4.1 Ionicity of ibuprofen-based eutectic systems and their membrane transport potential

The drug transport through biological membranes is among other factors mainly driven by the physico-chemical properties of the API (i.e., molecular weight, melting temperature, density, fluidity, ionicity) [28]. A design strategy for the improvement of membrane transport of an API can aim for modulating their overall chemical structure to increase the chances of trans-epithelial transport. The approach to increase the membrane transport potential by counterion mediated charge shielding of the API, resulting in neutral aggregates has been reported before for ampicillin ILs with ammonium and imidazolium counterions [29]. The resulting ion pairing was reported to increase membrane transport while also improving ampicillin aqueous solubility (water and simulated biological fluids). Likewise, ion pairing was stated for three salicylate API-ILs using the surface active molecules cetylpyridinium, benzalkonium and 1-ethyl-3-methyl-imidazolium as counterions, respectively, as demonstrate improved partitioning and membrane transport [30].

The ideal eutectic system consists of non-associated ions that may not diffuse independently of each other in the liquid, and to some extent the occurrence of aggregates or clusters due to the relative high concentration of salts [31]. In this context, the concept of ionicity, as the effective fraction of ions available to participate in conduction, is of utmost relevance. Ionic interactions could significantly affect other physical properties, such as mobility, which is one of the factors that influences the efficiency of permeation of pharmaceutical formulations for transmembrane transport. The ionicity is a correlation between the molar ionic conductivity and fluidity (inverse viscosity) which gives information about the mobility and the possible formation of

aggregates. Thus, this property is mainly a measure of the formation of aggregates due to the decrease of fluidity and conductivity, yet the high capacity of an IL to create aggregates can facilitate the transport of several molecules. A Walden plot is a common method for ionicity study which is based on Walden rule and relates the molar conductivity to its fluidity (i.e. inverse of viscosity) [32]. Furthermore, the validity of applying the Walden plot to address the ionicity of eutectics was proven by comparing these values with the ionicity calculated by using the self-diffusion coefficients using the PFG-NMR method [33].

The transport properties (i.e. viscosity (η) and conductivity (k) and density (ρ) were obtained for the for the eutectic systems composed of an API-IL ([C₂C₁Im][Ibu]; [C_{2(OH)}C₁Im][Ibu] and [N_{1112(OH)}][Ibu]) as hydrogen-bond acceptor (HBA) and ibuprofen as hydrogen-bond donor (HBD) at different molar ratios, namely 2:1, 1:1, 1:2 and 1:5 (cf. **Section 5.3.2** and **Table 5.S1** in Supporting Information). The density of the ibuprofen-based systems was measured in a range of temperatures from 15°C to 50°C (cf. **Section 5.3.3**) and the results are reported in **Table 5.S2** and plotted in **Figure 5.S1-5.S4** on Supporting Information.

Density is one of the fundamental physical properties of liquids. Most of the reported hydrophilic eutectic solvents present higher densities than water with values ranging between 1.0 and 1.3 g.cm⁻³ at 25 °C, while eutectic solvents based on metal salts have densities in the 1.3–1.6 g.cm⁻³ range [34]. Contrarily, lower densities than water are obtained for more hydrophobic eutectics [35]. Moreover, the density depends on the choice of the hydrogen bond donor [14,35]. The density of the ibuprofen-based eutectic systems (i.e. [C₂C₁Im][Ibu]:Ibu, [C_{2(OH)}C₁Im][Ibu]:Ibu and [N_{1112(OH)}][Ibu]:Ibu; cf. **Table 5.S1** on Supporting Information) showed densities higher than water at 25 °C, in the 1.0137–1.05787 g.cm⁻³ range (c.f. **Table 5.S2** and plotted in **Figure 5.S1-S4** on Supporting Information) imposing that they would represent also a hydrophilic behaviour. The same trend was obtained for the IL-based eutectic systems (i.e. [C₂C₁Im]Cl:Ibu, [C₂C₁Im][C₁CO₂]:Ibu, [C_{2(OH)}C₁Im][Ibu]:Ibu and [N_{1112(OH)}][Ibu]:Ibu; cf. **Table 5.S1** on Supporting Information). The densities ranging from 1.0185 to 1.10065 g.cm⁻³ [14] corresponding to the [C₂C_{1(OH)}Im]Cl:Ibu and to [N_{1112(OH)}Cl]:Ibu, respectively. The density for all the investigated eutectics shows a linear dependence on temperature as seen in

Figure 5.S4 on Supporting Information. Also, the density decreases with the increasing temperature (cf. **Figure 5.S4** on Supporting Information) due to thermal expansion which is expected and in agreement with previously reported eutectics [75].

Viscosity is an important parameter that can describe the flow behaviour which can influence the mass transport and the hydrodynamic applications of a compound [36]. Generally, eutectic systems can exhibit a relatively high viscosity, which could be attributed to the extensive hydrogen bond network inside them causing lower mobility of free species [35,37]. The viscosity profiles of the ibuprofen-based eutectic systems (i.e. [C₂C₁Im]Cl:Ibu, [C₂C₁Im][C₁CO₂]:Ibu, [C_{2(OH)}C₁Im][Ibu]:Ibu and [N_{1112(OH)}][Ibu]:Ibu) were measured in a range of temperatures from 15 °C to 50 °C, and the values are reported in **Table 5.S2** and plotted in **Figures 5.S1-5.S4** on Supporting Information. Also, the viscosity was exponentially dependent on the temperature, following the Arrhenius equation (**Equation 5.3**):

$$\ln \eta = \ln \eta_0 + \frac{E_\eta}{RT} \quad (\text{Eq. 5.3})$$

where η_0 is a constant, E_η is the activation energy, R is the universal gas constant (8.314 J/mol), and T represents the absolute temperature (J). The activation energy of viscosity (E_η) and the η_0 for the IL-based eutectic formulations ([C₂C₁Im]Cl:Ibu, [C_{2(OH)}C₁Im]Cl:Ibu, [C₂C₁Im][C₁CO₂]:Ibu) and [N_{1112(OH)}Cl:Ibu [14] and for the API-IL-based eutectic formulations [C₂C₁Im][Ibu]:Ibu, [C_{2(OH)}C₁Im][Ibu]:Ibu and [N_{1112(OH)}][Ibu]:Ibu at different molar ratios (i.e. 2:1, 1:1, 1:2 and 1:5) are reported in **Table 5.2**. Also, **Figure 5.S5** on Supporting Information shows that the viscosities of the eutectic's alloys with different compositions and at different HBAs increase with decreasing temperature according to the Arrhenius-type empirical equation.

Table 5.2. Activation energy of density (E_η) and its constant (η_0) and activation energy of conductivity (E_Λ) and its constant (s_0) according to the Arrhenius equation for the IL-based eutectic formulations ([C₂C₁Im]Cl:Ibu, [C₂(OH)C₁Im]Cl:Ibu, [C₂C₁Im][C₁CO₂]:Ibu) and [N₁₁₁₂(OH)]Cl:Ibu and for the API-IL-based eutectic formulations [C₂C₁Im][Ibu]:Ibu, [C₂(OH)C₁Im][Ibu]:Ibu and [N₁₁₁₂(OH)][Ibu]:Ibu at different molar ratios (2:1, 1:1, 1:2 and 1:5).

Molar Ratio	E_η (KJ·mol ⁻¹)	η_0	E_Λ (KJ·mol ⁻¹)	σ_0
[C ₂ C ₁ Im]Cl:Ibu [14]				
2:1	67.54	5.23x10 ⁻⁹	-77.26	3.00x10 ¹⁵
1:1	63.20	2.11x10 ⁻⁸	-70.98	1.65x10 ¹⁴
1:2	60.88	3.77x10 ⁻⁸	-72.00	1.38x10 ¹⁴
1:5	59.54	3.62x10 ⁻⁸	-79.40	8.19x10 ¹⁴
[C ₂ (OH)C ₁ Im]Cl:Ibu [14]				
1:1	68.57	6.77x10 ⁻⁹	-76.58	6.25x10 ¹⁴
1:2	66.22	9.39x10 ⁻⁹	-80.11	1.41x10 ¹⁵
1:5	61.76	1.88x10 ⁻⁸	-74.86	4.30x10 ¹³
[C ₂ C ₁ Im][C ₁ CO ₂]:Ibu [14]				
2:1	46.51	2.57x10 ⁻⁶	-49.16	2.28x10 ¹¹
1:1	49.31	1.18x10 ⁻⁶	-53.21	5.70x10 ¹¹
1:2	55.00	2.17x10 ⁻⁷	-61.70	4.53x10 ¹²
1:5	58.58	5.57x10 ⁻⁸	-75.80	2.54x10 ¹⁴
[N ₁₁₁₂ (OH)]Cl:Ibu [14]				
1:5	61.02	3.00x10 ⁻⁸	-68.30	2.61x10 ¹²
[C ₂ C ₁ Im][Ibu]:Ibu				
2:1	87.50	4.10x10 ⁻¹²	-80.38	1.88x10 ¹⁵
1:1	68.04	1.99x10 ⁻⁹	-76.29	3.76x10 ¹⁴
1:2	79.17	6.68x10 ⁻¹¹	-77.70	3.16x10 ¹⁴
1:5	74.35	4.92x10 ⁻⁹	-74.25	8.19x10 ¹³
[C ₂ (OH)C ₁ Im][Ibu]:Ibu				
1:1	92.25	2.03x10 ⁻¹²	-91.72	2.91x10 ¹⁶
1:2	85.09	1.60x10 ⁻¹¹	-81.84	6.36x10 ¹⁴
1:5	78.34	7.24x10 ⁻¹¹	-83.04	6.70x10 ¹⁴
[N ₁₁₁₂ (OH)][Ibu]:Ibu				
2:1	84.13	5.01x10 ⁻¹¹	-86.87	3.20x10 ¹⁵
1:1	77.19	3.29x10 ⁻¹⁰	-85.96	2.32x10 ¹⁵
1:2	76.55	2.80x10 ⁻¹⁰	-83.74	9.74x10 ¹⁴
1:5	76.05	1.48 x10 ⁻¹⁰	-79.70	1.50x10 ¹⁴

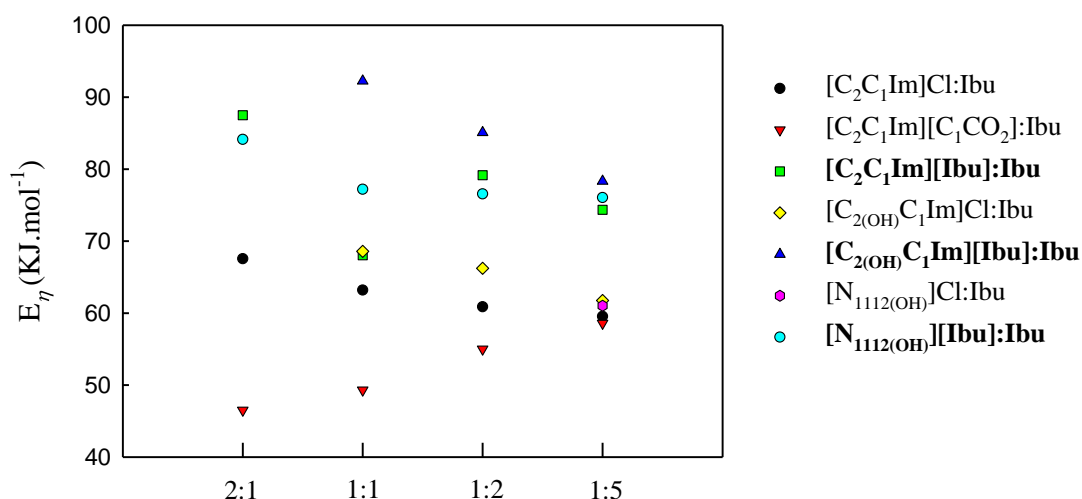


Figure 5.2 Viscosity activation energies (E_{η}) for the eutectic systems calculated from Arrhenius equation (i.e., Eq. 5.1) for the IL-based eutectic systems and API-ILs-based eutectic systems.

As shown in **Figure 5.2**, the values of E_{η} exhibit a general linear relationship with the reversed temperature with the exception of $[\text{C}_2\text{C}_1\text{Im}][\text{Ibu}]:\text{Ibu}$ eutectics where the viscosity activation energies (E_{η}) of $[\text{C}_2\text{C}_1\text{Im}][\text{Ibu}]:\text{Ibu}$ 1:1 show the lowest value ($68.04 \text{ KJ}\cdot\text{mol}^{-1}$, c.f. **Table 5.2**) followed by an increase of the E_{η} at higher concentrations of ibuprofen. Fronduti and co-workers [38] also observed the same trend for the eutectics based on glycolic acid (GA) and betaine (TMG) at different molar ratios, namely GA:TMG 3:1; 2.5:1; 2:1 and 1.5:1. From the analysis of the activation energies of viscosity, it emerges that the eutectic point showed the lowest value in the set at GA:TMG 2:1. This result was further correlated with the solid-liquid phase curves determination for the mixtures of GA:TMG. Thus, it is possible that the $[\text{C}_2\text{C}_1\text{Im}][\text{Ibu}]:\text{Ibu}$ 1:1 corresponds to the “true” eutectic point of the mixtures $[\text{C}_2\text{C}_1\text{Im}][\text{Ibu}]:\text{Ibu}$. Besides, the activation energies of viscosity (i.e. E_{η}) decreases with the increase of the ibuprofen molar ratio with the exception of the $[\text{C}_2\text{C}_1\text{Im}][\text{C}_1\text{CO}_2]:\text{Ibu}$ mixtures where the E_{η} follows the opposite trend (i.e., $[\text{C}_2\text{C}_1\text{Im}][\text{Ibu}]:\text{Ibu}$ 2:1 < 1:1 < 1:2 < 1:5) since the viscosity of the eutectic combination of 1:5 is higher than the 2:1 [14]. This could be explained by the difficulty of moving ions from one position to another and the intensity of interchain interactions between the ibuprofen and the API-IL with the increase of the ibuprofen molar ratio [38,39].

The molar conductivity of the imidazolium and cholinium-based eutectic systems [C₂C₁Im][Ibu], [C_{2(OH)}C₁Im][Ibu] and [N_{1112(OH)}][Ibu] as hydrogen-bond donors and ibuprofen as HBA at the molar ratios 2:1, 1:1, 1:2 and 1:5) was measured in the range of temperatures from 15 °C to 50 °C and the results are given in **Table 5.S2** and plotted in **Figures 5.S1-5.S4** on Supporting Information. The conductivity generally increases as the temperature increases due to a decrease in the viscosity since ions obtain more kinetic energy to overcome the intermolecular force and move easily [35,36]. The values of molar conductivity were fitted by the linearized Arrhenius equation (**Equation 5.4**):

$$\ln \sigma = \ln \sigma_0 + \frac{E_A}{RT} \quad (\text{Eq. 5.4})$$

where σ_0 is a constant, E_A is the activation energy, R is the universal gas constant (8.314 J/mol) , and T represents the absolute temperature. The activation energies of ionic conductivity (E_A) for the IL-based eutectic formulations (i.e., [C₂C₁Im]Cl:Ibu, [C_{2(OH)}C₁Im]Cl:Ibu, [C₂C₁Im][C₁CO₂]:Ibu) and [N_{1112(OH)}Cl:Ibu [14] and for the API-IL-based eutectic formulations (i.e., C₂C₁Im][Ibu]:Ibu, [C_{2(OH)}C₁Im][Ibu]:Ibu and [N_{1112(OH)}][Ibu]:Ibu) at different molar ratios, namely 2:1, 1:1, 1:2 and 1:5, are reported in **Table 5.2** and plotted in **Figure 5.3**. The ionic conductivity is affected by the hydrogen bond acceptor/hydrogen bond donor molar ratio, the nature of both the organic salt and the hydrogen bond donor as well as the salt's anion and water addition [38].

As shown in **Figure 5.3**, the values of the conductivity activation energies (E_A) exhibit a general linear relationship with the increase of molar ratio of ibuprofen since the differences observed are not so significant as observed for the viscosity energies values (i.e. E_A is -80.30 KJ·mol⁻¹ , -76.29 KJ·mol⁻¹ and -77.70 KJ·mol⁻¹ for the [C₂C₁Im][Ibu]:Ibu at 2:1, 1:1 and 1:2, respectively; cf. **Table 5.2**).

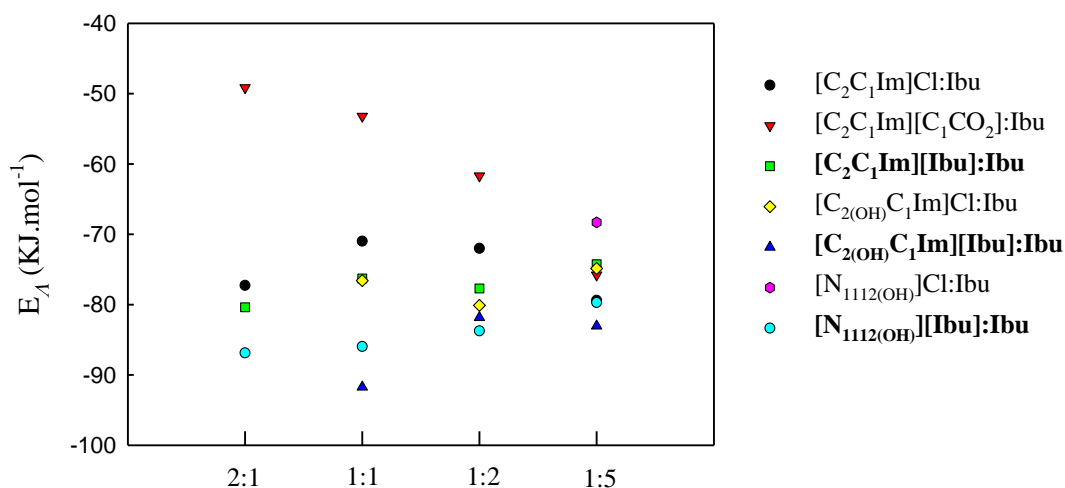


Figure 5.3 Conductivity activation energies (E_A) for the eutectic systems calculated from Arrhenius equation (i.e., Eq. 5.2) for the IL-based eutectic systems and API-ILs-based eutectic systems.

The Walden plot is a convenient and versatile tool for ionicity studies, mainly used as a qualitative and semi-quantitative measurement, that can be implemented in this field to evaluate the ionicity of eutectics [40,41]. **Figure 5.4** is a plot based on the classical concept of the Walden plot for the eleven ibuprofen-based eutectics (**Section 5.3.2** and **Table 5.S1** in Supporting Information). Angel and coworkers [42,43] introduced the ΔW value, the vertical deviation to the reference (ideal) line of slope 1 (black line in **Figure 5.4**) that indicates the region of fully dissociated ions like a dilute solution of 0.01 M KCl, to characterize the medium according to this value. In this framework, “good ionic” liquids are fully dissociated and show a $\Delta W < 1$. ILs with $\Delta W = 1$ exhibit only 10% of the ionic conductivity as would have been expected at the ideal line of 0.01 M KCl (blue line in **Figure 5.4**).

One of the most attractive advantages of API-based eutectics when compared to the API-ILs technology is that that the properties of the parent API could be fine-tuned by simply changing the components and/or the molar ratio of HBA to HBD with no losses during synthesis process, no need for subsequent purification steps and normally approaching yields with a 100% pure product [14,21]. Also, eutectics systems show IL-like behaviour, but they cannot be purely ionic because eutectics form across a range of stoichiometries. Duarte et al. [18] synthesized menthol-based eutectic systems with APIs as HBD, namely menthol:ibuprofen (3:1); menthol:benzoic acid (3:1) and menthol:phenylacetic acid (2:1

and 3:1). The solubility of the APIs when in the eutectic formulation was improved up to 12-fold, namely for the system containing ibuprofen. Furthermore, permeability measurements were conducted using the Franz-type diffusion method and different diffusion profiles were obtained for the systems studied. While the diffusion is much higher in the case of the eutectic systems containing ibuprofen and benzoic acid, the diffusion of phenylacetic acid is only slightly enhanced when the API is in the eutectic form. Also, for the menthol: phenylacetic acid 3:1, the equilibrium is reached at a lower concentration than for the pure API highlighting the interest in eutectic systems as new formulations for improved membrane transport properties. Additionally, melting point depression has been linked with enhanced transdermal delivery [44,45]. The authors proposed the existence of an inverse relationship between the melting point of drug and its lipophilicity where the depression of melting point can increase transdermal drug delivery rate due to an increase in the transdermal drug flux [44,45]. Moreover, Kasting and co-workers suggested that melting point depression is associated with an increase in the solubility of drug in a lipidic solution. According to these authors, the ILs-based eutectics can subsequently speed drug input rate into the skin with subsequent increase in the transdermal concentration gradient [45,46].

The existence of protic pharmaceutically active ILs that rapidly transported through a model membrane, most likely as hydrogen bonded complexes has been shown by MacFarlane et al [47]. The authors hypothesize that those ILs behave more like “neutral” species and hence cross the membrane faster than the more “ionic” drugs. Also, it was verified that the enhanced permeation and the formation of associated species is related to the position of these ILs, sitting well below, relative to ideal line on the Walden plot. In **Figure 5.4** is represented the Walden plot and all the ibuprofen-based mixtures are visible low the ideal line of the Walden plot (i.e. $\Delta W \approx 0.5$, black line in **Figure 5.4**). The $[\text{C}_2\text{C}_1\text{Im}][\text{Ibu}]:\text{Ibu}$ 2:1 is the eutectic more close to the ideal line meaning that in this formulation is fully dissociated and behave like a “good ionic” liquid, and none or only a few ion pairs are expected to exist. However, the remaining eutectics at the molar ratios HBA:Ibu 2:1, 1:1 and 1:2 stand near the second representative line in the Walden plot corresponding to a $\Delta W \approx 1.0$, meaning this group behave like “poor ionic” liquids, where hydrogen-bonds and other specific interactions are more pronounced. For the eutectics

HBA:Ibu 1:5 the vertical deviation is greater than 1.0 ($\Delta W > 1.0$) and are described as liquid ions pairs or “subionic liquids”. In these liquids, ion conductivity is substantially less, based on ion pairs, the formation of larger charged or non-charged aggregates, or the existence of ionic networks. Thus, the possibility of much stronger correlations that are not presented in the ideal cases, such ion pairing, or even large aggregates or networks of ions need to be considered for this group of eutectics. Although the $[C_2C_1Im][Ibu]$ 1:5 was earlier classified as non-eutectic combination, it falls into the same “HBA:IBU 1:5” category.

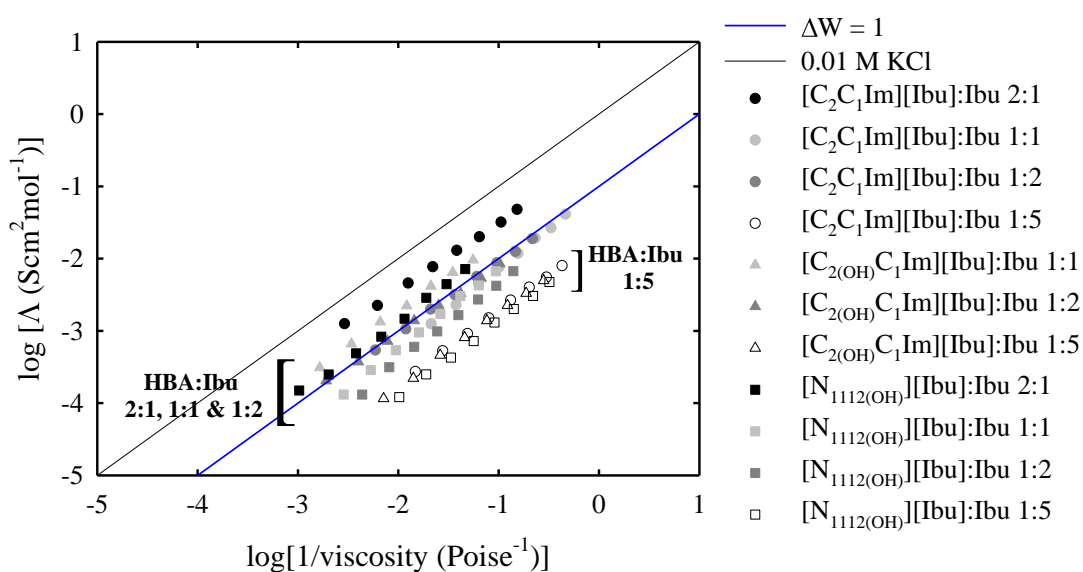


Figure 5.4 Walden plot representation for the eutectic systems $[C_2C_1Im][Ibu]:Ibu$, $[C_{2(OH)}C_1Im][Ibu]$ and $[N_{1112(OH)}][Ibu]$ at the different molar ratios. The straight black line symbolizes the ideal electrode composed of a solution of KCl.

5.4.2 Skin permeation prediction (Skin PAMPA)

The application of ILs in drug delivery is still in its early stages, but the potential consequences are significant given the excellent initial results for transdermal delivery [48]. The conversion of a API into a IL (API-IL) or a eutectic formulation (HBA:Ibu) provide a versatile platform to adjust properties of ionizable APIs (e.g. thermal stability, solubility, toxicity, pharmacologic response) [13,14]. Numerous investigations have been carried out to evaluate the benefit of API-ILs and eutectics for the API’s permeability, however the permeation analysis through the Skin PAMPA assay is not yet very explored. In most cases, animal skins or artificial permeation models (i.e. Franz diffusion cell) are used to test API-IL skin permeability. Shamshina and co-workers [49] developed

a several API-ILs based on different APIs and they found that the ILs formulations penetrated more quickly than free APIs. For instance, the lidocaine ibuprofenate ([Lid][Ibu]) was tested in a topical *in vivo* pharmacokinetic investigation using rats, and the [Lid][Ibu] was transported and faster absorbed than the lidocaine chloride and lidocaine docusate salts. Janus et al. [50] performed permeation experiments in a Franz diffusion cell and reported that L-valine propyl and isopropyl ester carrying ibuprofenate had a greater rate of delivery than free ibuprofen through the skin in an investigation of ibuprofen ILs with L-valine alkyl esters.

To compare the skin permeability of ibuprofen-based formulations (i.e. ILs and eutectics) with ibuprofen and ibuprofen sodium salt, *in vitro* permeation tests with Skin PAMPA were carried out. The effective permeability coefficient (P_e , cm/s) was calculated according to Chen et al. [26] (cf. **Equations 5.1 and 5.2, Section 5.3.4**) for both the ibuprofen and ibuprofen-based formulations. **Table 5.3** summarize the effective permeability coefficient (P_e) at 250 mM obtained from Skin PAMPA and **Figure 5.5** illustrates the permeability profile for the ibuprofen-based formulations at pH 6.5 and pH 7.4. Both samples were also tested and analysed at 125 mM however, all the ibuprofen-based formulations were bellowing the detection limit at pH 6.5 not being possible to calculate the effective permeability coefficient (P_e) at this range of concentration and pH with the exception of the neat ibuprofen (cf. **Table 5.3**).

Measuring the permeability *in vitro* is a way to overcome the variations in the carrier-mediated transport *in vivo*. This *in vitro* permeability is not constrained by active transport processes and therefore is a concentration-independent and less variable measurement [51]. The P_e of ibuprofen at 250 and 125 for both pHs presented the same order of magnitude (t-test, 1 tailed, confidence level 90%, $p < 0.1$) reinforcing that in the Skin PAMPA method the permeability is concentration-independent for the tested ibuprofen-based formulations at the same pH range.

Table 5.3. Effective permeability coefficient (Pe) and LogPe values from the Skin-PAMPA at pH 6.5 and pH 7.4 for ibuprofen at 250mM and 125 mM and ibuprofen-based API-ILs and ibuprofen-based eutectics at 250mM, at 25°C.

Compounds	pH 6.5		pH 7.4	
	Pe (cm/s)	LogPe (cm/s)	Pe (cm/s)	LogPe (cm/s)
Ibuprofen	$1.41 \times 10^{-5} \pm 1.94 \times 10^{-8}$	-4.851	$1.22 \times 10^{-5} \pm 7.14 \times 10^{-7}$	-4.913
Ibuprofen (125mM)	$2.09 \times 10^{-5} \pm 3.41 \times 10^{-5}$	-4.681	$2.16 \times 10^{-5} \pm 3.96 \times 10^{-5}$	-4.666
[C ₂ C ₁ Im][Ibu]	$1.09 \times 10^{-5} \pm 4.84 \times 10^{-7}$	-4.962	$9.85 \times 10^{-6} \pm 7.72 \times 10^{-7}$	-5.007
[C _{2(OH)} C ₁ Im][Ibu]	$1.15 \times 10^{-5} \pm 4.25 \times 10^{-7}$	-4.941	$9.55 \times 10^{-6} \pm 8.99 \times 10^{-7}$	-5.020
[N _{1112(OH)}][Ibu]	$1.10 \times 10^{-5} \pm 2.63 \times 10^{-7}$	-4.959	$1.40 \times 10^{-5} \pm 3.84 \times 10^{-7}$	-4.855
[C ₂ C ₁ Im]Cl:Ibu 2:1	$1.56 \times 10^{-5} \pm 3.03 \times 10^{-7}$	-4.807	$1.00 \times 10^{-5} \pm 5.62 \times 10^{-7}$	-4.998
[C ₂ C ₁ Im]Cl:Ibu 1:1	$1.79 \times 10^{-5} \pm 2.19 \times 10^{-6}$	-4.748	$1.74 \times 10^{-5} \pm 2.39 \times 10^{-6}$	-4.759
[C ₂ C ₁ Im]Cl:Ibu 1:2	$1.26 \times 10^{-5} \pm 7.74 \times 10^{-7}$	-4.900	$8.62 \times 10^{-6} \pm 3.05 \times 10^{-8}$	-5.065
[C ₂ C ₁ Im]Cl:Ibu 1:5	$1.22 \times 10^{-5} \pm 1.69 \times 10^{-6}$	-4.913	$1.04 \times 10^{-5} \pm 6.47 \times 10^{-7}$	-4.985
[C _{2(OH)} C ₁ Im]Cl:Ibu 1:1	$1.67 \times 10^{-5} \pm 6.03 \times 10^{-7}$	-4.777	$1.46 \times 10^{-5} \pm 7.18 \times 10^{-7}$	-4.837
[C _{2(OH)} C ₁ Im]Cl:Ibu 1:2	$1.38 \times 10^{-5} \pm 4.06 \times 10^{-7}$	-4.862	$1.37 \times 10^{-5} \pm 1.44 \times 10^{-6}$	-4.863
[C _{2(OH)} C ₁ Im]Cl:Ibu 1:5	$1.96 \times 10^{-5} \pm 9.48 \times 10^{-7}$	-4.708	$1.18 \times 10^{-5} \pm 1.92 \times 10^{-6}$	-4.929
[N _{1112(OH)} Cl:Ibu 1:5	$1.88 \times 10^{-5} \pm 1.60 \times 10^{-6}$	-4.726	$1.18 \times 10^{-5} \pm 1.07 \times 10^{-6}$	-4.928
[C ₂ C ₁ Im][C ₁ CO ₂]:Ibu 2:1	$2.21 \times 10^{-5} \pm 1.28 \times 10^{-6}$	-4.656	$1.95 \times 10^{-5} \pm 2.17 \times 10^{-6}$	-4.710
[C ₂ C ₁ Im][C ₁ CO ₂]:Ibu 1:1	$1.38 \times 10^{-5} \pm 2.75 \times 10^{-6}$	-4.860	$1.36 \times 10^{-5} \pm 3.89 \times 10^{-6}$	-4.867
[C ₂ C ₁ Im][C ₁ CO ₂]:Ibu 1:2	$1.40 \times 10^{-5} \pm 2.78 \times 10^{-6}$	-4.853	$1.11 \times 10^{-5} \pm 9.24 \times 10^{-7}$	-4.954
[C ₂ C ₁ Im][C ₁ CO ₂]:Ibu 1:5	$1.46 \times 10^{-5} \pm 1.61 \times 10^{-6}$	-4.837	$1.15 \times 10^{-5} \pm 5.47 \times 10^{-7}$	-4.941
[C ₂ C ₁ Im][Ibu]:Ibu 2:1	$1.30 \times 10^{-5} \pm 2.15 \times 10^{-6}$	-4.887	$1.05 \times 10^{-5} \pm 6.17 \times 10^{-7}$	-4.978
[C ₂ C ₁ Im][Ibu]:Ibu 1:1	$1.14 \times 10^{-5} \pm 8.16 \times 10^{-7}$	-4.943	$8.76 \times 10^{-6} \pm 2.37 \times 10^{-7}$	-5.057
[C ₂ C ₁ Im][Ibu]:Ibu 1:2	$1.03 \times 10^{-5} \pm 1.15 \times 10^{-6}$	-4.986	$8.93 \times 10^{-6} \pm 5.18 \times 10^{-7}$	-5.049
[C ₂ C ₁ Im][Ibu]:Ibu 1:5	$1.14 \times 10^{-5} \pm 8.80 \times 10^{-7}$	-4.944	$7.56 \times 10^{-6} \pm 1.39 \times 10^{-6}$	-5.121
[C _{2(OH)} C ₁ Im][Ibu]:Ibu 1:1	$1.02 \times 10^{-5} \pm 2.95 \times 10^{-6}$	-4.991	$9.73 \times 10^{-6} \pm 7.30 \times 10^{-7}$	-5.012
[C _{2(OH)} C ₁ Im][Ibu]:Ibu 1:2	$1.01 \times 10^{-5} \pm 2.41 \times 10^{-6}$	-4.994	$9.06 \times 10^{-6} \pm 7.07 \times 10^{-7}$	-5.043
[C _{2(OH)} C ₁ Im][Ibu]:Ibu 1:5	$1.07 \times 10^{-5} \pm 2.24 \times 10^{-6}$	-4.971	$9.00 \times 10^{-6} \pm 3.02 \times 10^{-7}$	-5.046
[N _{1112(OH)}][Ibu]:Ibu 2:1	$1.32 \times 10^{-5} \pm 1.06 \times 10^{-6}$	-4.880	$1.22 \times 10^{-5} \pm 5.21 \times 10^{-6}$	-4.913
[N _{1112(OH)}][Ibu]:Ibu 1:1	$1.65 \times 10^{-5} \pm 2.24 \times 10^{-6}$	-4.783	$7.32 \times 10^{-6} \pm 1.17 \times 10^{-6}$	-5.136
[N _{1112(OH)}][Ibu]:Ibu 1:2	$1.49 \times 10^{-5} \pm 2.00 \times 10^{-6}$	-4.828	$1.14 \times 10^{-5} \pm 1.21 \times 10^{-6}$	-4.943
[N _{1112(OH)}][Ibu]:Ibu 1:5	$1.34 \times 10^{-5} \pm 8.77 \times 10^{-7}$	-4.872	$1.45 \times 10^{-5} \pm 5.73 \times 10^{-6}$	-4.840

In **Figure 5.5** (cf. **Table 5.3**) it is clearly demonstrated that the ibuprofen-based formulations showed similar or slightly higher permeation in both pH 6.4 and pH 7.5,

than ibuprofen in their ionized status ($pK_a=4.4$ [52]). However, the main advantage of using the ILs and eutectics platform to modulate the permeability of NSAIDs is that ibuprofen remain solid at room temperature while all the eutectic systems are liquid at room temperature with the exception of $[N_{1112(OH)}][Ibu]:Ibu$ 2:1 and $[N_{1112(OH)}][Ibu]:Ibu$ 1:1 ($T_m=36.55$ °C and $T_m=44.83$ °C, respectively) [14,21]. Also, the API-IL $[C_{2(OH)}C_1Im][Ibu]$ is easily handle liquid at room temperature ($T_m=-13.97$ °C) [13].

The ibuprofen-based eutectics $[C_2C_1Im]Cl:Ibu$ 2:1, $[C_{2(OH)}C_1Im]Cl:Ibu$ 1:1, $[C_{2(OH)}C_1Im]Cl:Ibu$ 1:5, $[N_{1112(OH)}]Cl:Ibu$ 1:5 and $[C_2C_1Im][C_1CO_2]:Ibu$ 2:1 at pH 6.4 increased the effective permeability coefficient (P_e) when compared to the neat ibuprofen (t-test, 1 tailed, confidence level 90%, $p<0.1$). The P_e was also higher for the $[C_{2(OH)}C_1Im]Cl:Ibu$ 1:1, $[C_{2(OH)}C_1Im]Cl:Ibu$ 1:5 and $[C_2C_1Im][C_1CO_2]:Ibu$ 2:1 when compared to ibuprofen at pH 7.4 (t-test, 1 tailed, confidence level 90%, $p<0.1$). The rest of the ibuprofen-based formulations showed a similar permeation than ibuprofen (cf. **Table 5.3** and **Figure 5.5**).

The major impact in ibuprofen permeability is clearly attained by the eutectic's formulations attributed to the extensive hydrogen bond network causing a higher permeability through Skin PAMPA membrane. With the ibuprofen-based eutectics, the permeability profile of ibuprofen is increased or at least maintained (t-test, 1 tailed, confidence level 90%, $p<0.1$). For the imidazolium-based formulations, both $[C_2C_1Im]Cl:Ibu$ 2:1 ($1.56\times 10^{-5} \pm 3.03\times 10^{-7}$) and $[C_2C_1Im]Cl:Ibu$ 1:1 ($1.79\times 10^{-5} \pm 2.19\times 10^{-6}$) are higher than the $[C_2C_1Im][Ibu]$ ($1.09\times 10^{-5} \pm 4.84\times 10^{-7}$). Also, the $[C_2C_1Im][C_1CO_2]:Ibu$ 2:1 and 1:5 ($2.21\times 10^{-5} \pm 1.28\times 10^{-6}$ and $1.46\times 10^{-5} \pm 1.61\times 10^{-6}$, respectively) has higher P_e values when compared to the $[C_2C_1Im][Ibu]$. Regarding the $[C_{2(OH)}C_1Im]Cl:Ibu$ eutectics, all the molar ratios in this study (i.e. 1:1, 1:2 and 1:5) presented higher P_e then the $[C_{2(OH)}C_1Im][Ibu]$ (cf. **Table 5.3**). The $[N_{1112(OH)}]Cl:Ibu$ 1:5 ($1.88\times 10^{-5} \pm 1.60\times 10^{-6}$) also improved the permeability of ibuprofen when compared to $[N_{1112(OH)}][Ibu]$ ($1.10\times 10^{-5} \pm 2.63\times 10^{-7}$). In case of the eutectics with API-ILs as HBA, the $[N_{1112(OH)}][Ibu]:Ibu$ (i.e. 2:1, 1:1, 1:2 and 1:5) was the only one with higher permeability (t-test, 1 tailed, confidence level 90%, $p<0.1$) then the corresponding $[N_{1112(OH)}][Ibu]$ (cf. **Table 5.3**). All the rest of

eutectic formulations showed a similar permeation than the corresponding HBA (i.e. API-IL).

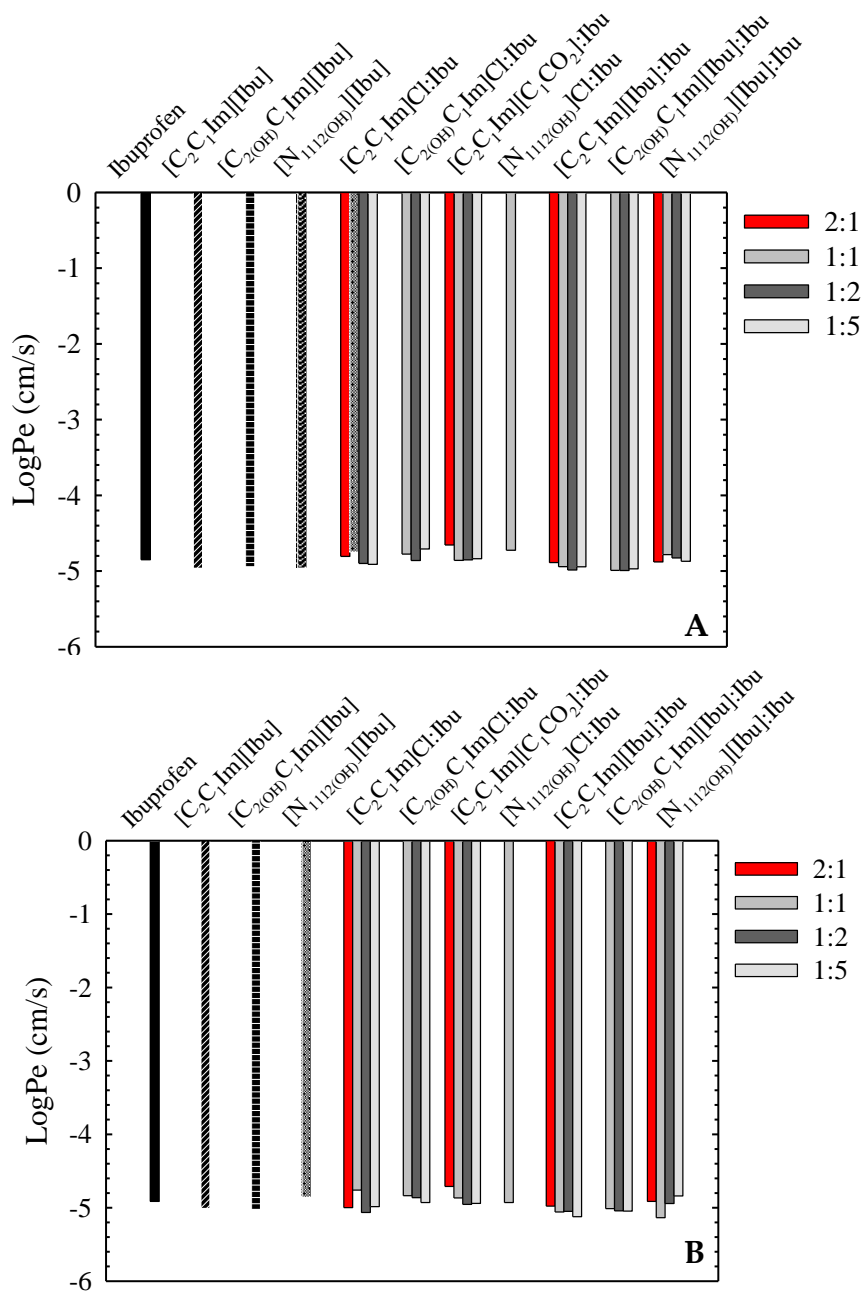


Figure 5.5 Effective permeability (LogPe) obtained from Skin PAMPA of ibuprofen, ibuprofen-based API-ILs and ibuprofen-based eutectics at 250 mM for pH 6.5 (A) and pH 7.4 (B), at 25°C.

For the pH 7.4, the $[C_2C_1Im]Cl:Ibu$ 1:1 ($1.74 \times 10^{-5} \pm 2.39 \times 10^{-6}$) and $[C_2C_1Im][C_1CO_2]:Ibu$ 2:1 ($1.95 \times 10^{-5} \pm 2.17 \times 10^{-6}$) promote a statistically higher effective permeability (t-test, 1 tailed, confidence level 90%, $p < 0.1$) than the $[C_2C_1Im][Ibu]$ ($9.85 \times 10^{-6} \pm 7.72 \times 10^{-7}$). Also, the $[C_{2(OH)}C_1Im]Cl:Ibu$ 1:1 and $[C_{2(OH)}C_1Im]Cl:Ibu$ 1:2 and the $[N_{112(OH)}]Cl:Ibu$ 1:5

presented a higher Pe than the $[C_{2(OH)}C_1Im][Ibu]$ and $[N_{1112(OH)}][Ibu]$, respectively (cf. Table 3). Regarding to the API-ILs-based eutectics, only the $[N_{1112(OH)}][Ibu]:Ibu$ 1:1 and 1:2 presented better permeability than the $[N_{1112(OH)}][Ibu]$ (t-test, 1 tailed, confidence level 90%, $p < 0.1$) at pH 7.4. Besides, all the rest of API-ILs-based eutectic formulations showed a similar permeation than the corresponding API-IL (i.e. eutectic's HBA).

5.5 Conclusion

The benefits of transdermal drug delivery are apparent. However, the absorption of most drug molecules is still elusive due to the skin and its barrier properties. The possibility of using or eutectics formulations as transdermal delivery systems was evaluated in this work. We previously developed three API-ILs ($[C_2C_1Im][Ibu]$, $[C_{2(OH)}C_1Im][Ibu]$ and $[N_{1112(OH)}][Ibu]$) and several NSAID-based eutectic formulations, conjugating ibuprofen (HBD) with three imidazolium-based ILs ($[C_2C_1Im]Cl$, $[C_{2(OH)}C_1Im]Cl$ and $[C_2C_1Im][C_1CO_2]$) and cholinium salt ($[N_{1112(OH)}]Cl$) and three API-ILs ($[C_2C_1Im][Ibu]$, $[C_{2(OH)}C_1Im][Ibu]$ and $[N_{1112(OH)}][Ibu]$). Firstly, the characterization in terms of viscosity, conductivity, density and ionicity (via Walden plot) was attained, confirming the formation of large charged or non-charged aggregates, or the existence of ionic networks, that could increase the potential for these liquids to penetrate membranes more efficiently than ibuprofen (parent solid API). Also, the effective permeability coefficient (Pe) was also evaluated for the ibuprofen-based ILs (API-ILs) and all the ibuprofen-based eutectics (IL-based and API-IL-based eutectic), where the designed formulations showed a similar or higher permeation profile when compared to ibuprofen (parent API). The $C_2C_1Im]Cl:Ibu$ 2:1, $[C_{2(OH)}C_1Im]Cl:Ibu$ 1:1, $[C_{2(OH)}C_1Im]Cl:Ibu$ 1:1, $[N_{1112(OH)}]Cl:Ibu$ 1:5 and $[C_2C_1Im][C_1CO_2]:Ibu$ 2:1 at pH 6.4 significantly increased the effective permeability coefficient when compared to neat ibuprofen. At pH 7.4 the $[C_{2(OH)}C_1Im]Cl:Ibu$ 1:1, $[C_{2(OH)}C_1Im]Cl:Ibu$ 1:1 and $[C_2C_1Im][C_1CO_2]:Ibu$ 2:1 were the only Ibu-based eutectics that increased the permeability of ibuprofen. However, in the Skin PAMPA assay all room temperature solid formulations are solubilized and in optimal conditions for the testing. A way of fully understand the advantages of using room temperature liquid formulations instead of solid formulations is to develop a method to measure the effective permeability

coefficient without need to solubilize the test compounds to fully access the permeability coefficients (that will be the efforts of a future work). Nevertheless, with this work it was possible to understand some of the advantages of using the interplay between ionic liquids and eutectics to improve the membrane permeability of ibuprofen (one of the most used NSAID).

Funding

Authors would like to acknowledge the financial support FCT/MCTES (Portugal), through grants PD/BD/135078/2017 and COVID/BD/151824/2021 (J.C.B.), the Individual Call to Scientific Employment Stimulus 2020.00835.CEECIND (J.M.M.A.) and 2021.01432.CEECIND (A.B.P.), and the project PTDC/EQU-EQU/2223/2021. This work was also supported by the Associate Laboratory for Green Chemistry—LAQV which was financed by national funds from FCT/MCTES (UIDB/50006/2020 and UIDP/50006/2020).

5.6 References

- [1] B.J. Orlando, M.J. Lucido, M.G. Malkowski, The structure of ibuprofen bound to cyclooxygenase-2, *J Struct Biol.* 189 (2015) 62–66. <https://doi.org/10.1016/J.JSB.2014.11.005>.
- [2] J. Irvine, A. Afrose, N. Islam, Formulation and delivery strategies of ibuprofen: challenges and opportunities, *Drug Dev Ind Pharm.* 44 (2018) 173–183. <https://doi.org/10.1080/03639045.2017.1391838>.
- [3] D.H. Solomon, M.E. Husni, P.A. Libby, N.D. Yeomans, A.M. Lincoff, T.F. Lüscher, V. Menon, D.M. Brennan, L.M. Wisniewski, S.E. Nissen, J.S. Borer, The Risk of Major NSAID Toxicity with Celecoxib, Ibuprofen, or Naproxen: A Secondary Analysis of the PRECISION Trial, *American Journal of Medicine.* 130 (2017) 1415-1422.e4. <https://doi.org/10.1016/j.amjmed.2017.06.028>.
- [4] P.K. Gaur, M. Bajpai, S. Mishra, A. Verma, Development of ibuprofen nanoliposome for transdermal delivery: Physical characterization, in vitro/in vivo studies, and anti-inflammatory activity, *Artif Cells Nanomed Biotechnol.* 44 (2016) 370–375. <https://doi.org/10.3109/21691401.2014.953631>.
- [5] S.A.T. Opatha, V. Titapiwatanakun, R. Chutoprapat, Transfersomes: A Promising Nanoencapsulation Technique for Transdermal Drug Delivery, *Pharmaceutics.* 12 (2020). <https://doi.org/10.3390/pharmaceutics12090855>.

- [6] R. Ferraz, L.C. Branco, I.M. Marrucho, J.M.M. Araújo, L.P.N. Rebelo, M.N. da Ponte, C. Prudêncio, J.P. Noronha, Ž. Petrovski, Development of novel ionic liquids based on ampicillin, *Med. Chem. Commun.* 3 (2012) 494–497. <https://doi.org/10.1039/C2MD00269H>.
- [7] N.S.M. Vieira, J.C. Bastos, L.P.N. Rebelo, A. Matias, J.M.M. Araújo, A.B. Pereiro, Human cytotoxicity and octanol/water partition coefficients of fluorinated ionic liquids, *Chemosphere.* 216 (2019) 576–586. <https://doi.org/10.1016/J.CHEMOSPHERE.2018.10.159>.
- [8] Z. Sidat, T. Marimuthu, P. Kumar, L.C. du Toit, P.P.D. Kondiah, Y.E. Choonara, V. Pillay, Ionic liquids as potential and synergistic permeation enhancers for transdermal drug delivery, *Pharmaceutics.* 11 (2019). <https://doi.org/10.3390/pharmaceutics11020096>.
- [9] G.S. Lim, S. Jaenicke, M. Klähn, How the spontaneous insertion of amphiphilic imidazolium-based cations changes biological membranes: a molecular simulation study, *Physical Chemistry Chemical Physics.* 17 (2015) 29171–29183. <https://doi.org/10.1039/C5CP04806K>.
- [10] N. Kundu, S. Roy, D. Mukherjee, T.K. Maiti, N. Sarkar, Unveiling the Interaction between Fatty-Acid-Modified Membrane and Hydrophilic Imidazolium-Based Ionic Liquid: Understanding the Mechanism of Ionic Liquid Cytotoxicity, *J Phys Chem B.* 121 (2017) 8162–8170. <https://doi.org/10.1021/acs.jpcc.7b06231>.
- [11] X. Wu, Q. Zhu, Z. Chen, W. Wu, Y. Lu, J. Qi, Ionic liquids as a useful tool for tailoring active pharmaceutical ingredients, *Journal of Controlled Release.* 338 (2021) 268–283. <https://doi.org/10.1016/j.jconrel.2021.08.032>.
- [12] H. Wu, Z. Deng, B. Zhou, M. Qi, M. Hong, G. Ren, Improved transdermal permeability of ibuprofen by ionic liquid technology: Correlation between counterion structure and the physicochemical and biological properties, *J Mol Liq.* 283 (2019) 399–409. <https://doi.org/10.1016/j.molliq.2019.03.046>.
- [13] J.C. Bastos, N.S.M. Vieira, M.M. Gaspar, A.B. Pereiro, J.M.M. Araújo, Human Cytotoxicity, Hemolytic Activity, Anti-Inflammatory Activity and Aqueous Solubility of Ibuprofen-Based Ionic Liquids, *Sustainable Chemistry.* 3 (2022) 358–375. <https://doi.org/10.3390/suschem3030023>.
- [14] J.C. Bastos, M.M. Gaspar, A.B. Pereiro, J.M.M. Araújo, Role of Ionic Liquids in Ibuprofen-based Eutectic Systems: Aqueous Solubility, Permeability, Human Cytotoxicity, Hemolytic Activity and Anti-Inflammatory Activity, *Nanomaterials.* (2023).
- [15] M.C. Sarraguça, P.R.S. Ribeiro, C. Nunes, C.L. Seabra, Solids Turn into Liquids—Liquid Eutectic Systems of Pharmaceutics to Improve Drug Solubility, *Pharmaceutics.* 15 (2022). <https://doi.org/10.3390/ph15030279>.
- [16] S.N. Pedro, M.S.M. Mendes, B.M. Neves, I.F. Almeida, P. Costa, I. Correia-Sá, C. Vilela, M.G. Freire, A.J.D. Silvestre, C.S.R. Freire, Deep Eutectic Solvent Formulations and Alginate-Based Hydrogels as a New Partnership for the Transdermal Administration of

Anti-Inflammatory Drugs, *Pharmaceutics*. 14 (2022).
<https://doi.org/10.3390/pharmaceutics14040827>.

- [17] J.M. Silva, C. V. Pereira, F. Mano, E. Silva, V.I.B. Castro, I. Sá-Nogueira, R.L. Reis, A. Paiva, A.A. Matias, A.R.C. Duarte, Therapeutic Role of Deep Eutectic Solvents Based on Menthol and Saturated Fatty Acids on Wound Healing, *ACS Appl Bio Mater*. 2 (2019) 4346–4355. <https://doi.org/10.1021/acsabm.9b00598>.
- [18] A.R.C. Duarte, A.S.D. Ferreira, S. Barreiros, E. Cabrita, R.L. Reis, A. Paiva, A comparison between pure active pharmaceutical ingredients and therapeutic deep eutectic solvents: Solubility and permeability studies, *European Journal of Pharmaceutics and Biopharmaceutics*. 114 (2017) 296–304. <https://doi.org/10.1016/j.ejpb.2017.02.003>.
- [19] P.W. Stott, A.C. Williams, B.W. Barry, *Transdermal delivery from eutectic systems: enhanced permeation of a model drug, ibuprofen*, 1998.
- [20] C. V. Pereira, J.M. Silva, L. Rodrigues, R.L. Reis, A. Paiva, A.R.C. Duarte, A. Matias, Unveil the Anticancer Potential of Limonene Based Therapeutic Deep Eutectic Solvents, *Sci Rep*. 9 (2019). <https://doi.org/10.1038/s41598-019-51472-7>.
- [21] J. Bastos, A.B. Pereiro, J.M.M. Araújo, Eutectic Systems with Pharmaceutically Active Ionic Liquids: Human Cytotoxicity, Hemolytic Activity and Anti-Inflammatory Activity, *Pharmaceutics*. (2023).
- [22] P. Fabrice, K. Yogeshvar N., S. Audra L., K. Garrett, B. Annette, G. Richard H., Characterization of the permeability barrier of human skin in vivo, *Proceedings of the National Academy of Sciences*. 94 (1997) 1562–1567. <https://doi.org/10.1073/pnas.94.4.1562>.
- [23] B. Sinkó, T.M. Garrigues, G.T. Balogh, Z.K. Nagy, O. Tsinman, A. Avdeef, K. Takács-Novák, Skin-PAMPA: a new method for fast prediction of skin penetration., *Eur J Pharm Sci*. 45 (2012) 698–707. <https://doi.org/10.1016/j.ejps.2012.01.011>.
- [24] H. Wu, Z. Deng, B. Zhou, M. Qi, M. Hong, G. Ren, Improved transdermal permeability of ibuprofen by ionic liquid technology: Correlation between counterion structure and the physicochemical and biological properties, *J Mol Liq*. 283 (2019) 399–409. <https://doi.org/10.1016/j.molliq.2019.03.046>.
- [25] P.J. Castro, A.E. Redondo, J.E. Sosa, M.E. Zakrzewska, A.V.M. Nunes, J.M.M. Araújo, A.B. Pereiro, Absorption of Fluorinated Greenhouse Gases in Deep Eutectic Solvents, *Ind Eng Chem Res*. 59 (2020) 13246–13259. <https://doi.org/10.1021/acs.iecr.0c01893>.
- [26] E. Proksch, pH in nature, humans and skin, *J Dermatol*. 45 (2018) 1044–1052. <https://doi.org/10.1111/1346-8138.14489>.
- [27] X. Chen, A. Murawski, K. Patel, C.L. Crespi, P. V. Balimane, A Novel Design of Artificial Membrane for Improving the PAMPA Model, *Pharm Res*. 25 (2008) 1511–1520. <https://doi.org/10.1007/s11095-007-9517-8>.

- [28] A. Naik, Y.N. Kalia, R.H. Guy, Transdermal drug delivery: overcoming the skin's barrier function, *Pharm Sci Technol Today*. 3 (2000) 318–326. [https://doi.org/10.1016/S1461-5347\(00\)00295-9](https://doi.org/10.1016/S1461-5347(00)00295-9).
- [29] C. Florindo, J.M.M. Araújo, F. Alves, C. Matos, R. Ferraz, C. Prudêncio, J.P. Noronha, Ž. Petrovski, L. Branco, L.P.N. Rebelo, I.M. Marrucho, Evaluation of solubility and partition properties of ampicillin-based ionic liquids, *Int J Pharm*. 456 (2013) 553–559. <https://doi.org/10.1016/j.ijpharm.2013.08.010>.
- [30] P.C.A.G. Pinto, D.M.G.P. Ribeiro, A.M.O. Azevedo, V. Dela Justina, E. Cunha, K. Bica, M. Vasiliou, S. Reis, M.L.M.F.S. Saraiva, Active pharmaceutical ingredients based on salicylate ionic liquids: insights into the evaluation of pharmaceutical profiles, *New Journal of Chemistry*. 37 (2013) 4095. <https://doi.org/10.1039/c3nj00731f>.
- [31] C. D'Agostino, R.C. Harris, A.P. Abbott, L.F. Gladden, M.D. Mantle, Molecular motion and ion diffusion in choline chloride based deep eutectic solvents studied by ¹H pulsed field gradient NMR spectroscopy, *Physical Chemistry Chemical Physics*. 13 (2011) 21383–21391. <https://doi.org/10.1039/c1cp22554e>.
- [32] A.B. Pereira, J.M.M. Araújo, S. Martinho, F. Alves, S. Nunes, A. Matias, C.M.M. Duarte, L.P.N. Rebelo, I.M. Marrucho, Fluorinated Ionic Liquids: Properties and Applications, *ACS Sustain Chem Eng*. 1 (2013) 427–439. <https://doi.org/10.1021/sc300163n>.
- [33] Y. Wang, W. Chen, Q. Zhao, G. Jin, Z. Xue, Y. Wang, T. Mu, Ionicity of deep eutectic solvents by Walden plot and pulsed field gradient nuclear magnetic resonance (PFG-NMR), *Physical Chemistry Chemical Physics*. 22 (2020) 25760–25768. <https://doi.org/10.1039/D0CP01431A>.
- [34] B. Tang, K.H. Row, Recent developments in deep eutectic solvents in chemical sciences, *Monatshefte Für Chemie - Chemical Monthly*. 144 (2013) 1427–1454. <https://doi.org/10.1007/s00706-013-1050-3>.
- [35] C. Florindo, L.C. Branco, I.M. Marrucho, Quest for Green-Solvent Design: From Hydrophilic to Hydrophobic (Deep) Eutectic Solvents, *ChemSusChem*. 12 (2019) 1549–1559. <https://doi.org/10.1002/cssc.201900147>.
- [36] C. Austen Angell, Y. Ansari, Z. Zhao, Ionic Liquids: Past, present and future, *Faraday Discuss*. 154 (2012) 9–27. <https://doi.org/10.1039/c1fd00112d>.
- [37] A. Roda, A. Paiva, A.R.C. Duarte, Therapeutic liquid formulations based on low transition temperature mixtures for the incorporation of anti-inflammatory drugs, *Pharmaceutics*. 13 (2021). <https://doi.org/10.3390/pharmaceutics13101620>.
- [38] M. Fronduti, T. Del Giacco, E. Rossi, M. Tiecco, R. Germani, Insights into the structural features of deep eutectic solvents: the eutectic point as an unicum in their physical properties and the surface tension as a method for its determination, *J Mol Liq*. 379 (2023) 121679. <https://doi.org/10.1016/j.molliq.2023.121679>.

- [39] S. Ning, X. Bian, Z. Ren, Correlation between viscous-flow activation energy and phase diagram in four systems of Cu-based alloys, *Physica B Condens Matter*. 405 (2010) 3633–3637. <https://doi.org/10.1016/j.physb.2010.05.055>.
- [40] W. Xu, E.I. Cooper, C.A. Angell, Ionic liquids: Ion mobilities, glass temperatures, and fragilities, *Journal of Physical Chemistry B*. 107 (2003) 6170–6178. <https://doi.org/10.1021/jp0275894>.
- [41] C. Schreiner, S. Zugmann, R. Hartl, H.J. Gores, Fractional Walden Rule for Ionic Liquids: Examples from Recent Measurements and a Critique of the So-Called Ideal KCl Line for the Walden Plot, *J Chem Eng Data*. 55 (2010) 1784–1788. <https://doi.org/10.1021/je900878j>.
- [42] C.A. Angell, N. Byrne, J.-P. Belieres, Parallel developments in aprotic and protic ionic liquids: physical chemistry and applications, *Acc Chem Res*. 40 (2007) 1228–1236.
- [43] A.B. Pereiro, J.M.M. Araújo, F.S. Oliveira, C.E.S. Bernardes, J.M.S.S. Esperança, J.N. Canongia Lopes, I.M. Marrucho, L.P.N. Rebelo, Inorganic salts in purely ionic liquid media: the development of high ionicity ionic liquids (HIILs), *Chemical Communications*. 48 (2012) 3656. <https://doi.org/10.1039/c2cc30374d>.
- [44] G.B. Kasting, R.L. Smith, E.R. Cooper, Effects of lipid solubility and molecular size on percutaneous absorption, *Skin Pharmacol*. 1 (1987) 138–153.
- [45] A.C. Calpena, C. Blanes, J. Moreno, R. Obach, J. Domenech, A Comparative in Vitro Study of Transdermal Absorption of Antiemetics, *J Pharm Sci*. 83 (1994) 29–33. <https://doi.org/10.1002/jps.2600830108>.
- [46] P. Stott, Transdermal delivery from eutectic systems: enhanced permeation of a model drug, ibuprofen, *Journal of Controlled Release*. 50 (1998) 297–308. [https://doi.org/10.1016/S0168-3659\(97\)00153-3](https://doi.org/10.1016/S0168-3659(97)00153-3).
- [47] J. Stoimenovski, D.R. MacFarlane, Enhanced membrane transport of pharmaceutically active protic ionic liquids, *Chemical Communications*. 47 (2011) 11429. <https://doi.org/10.1039/c1cc14314j>.
- [48] Md.K. Ali, R.M. Moshikur, M. Goto, M. Moniruzzaman, Recent Developments in Ionic Liquid-Assisted Topical and Transdermal Drug Delivery, *Pharm Res*. 39 (2022) 2335–2351. <https://doi.org/10.1007/s11095-022-03322-x>.
- [49] J.L. Shamshina, P. Berton, H. Wang, X. Zhou, G. Gurau, R.D. Rogers, Ionic Liquids in Pharmaceutical Industry, in: *Green Techniques for Organic Synthesis and Medicinal Chemistry*, Wiley, 2018: pp. 539–577. <https://doi.org/10.1002/9781119288152.ch20>.
- [50] E. Janus, P. Ossowicz, J. Kleboko, A. Nowak, W. Duchnik, Ł. Kucharski, A. Klimowicz, Enhancement of ibuprofen solubility and skin permeation by conjugation with α -valine alkyl esters, *RSC Adv*. 10 (2020) 7570–7584. <https://doi.org/10.1039/D0RA00100G>.

- [51] L. Fredlund, S. Winiwarter, C. Hilgendorf, In Vitro Intrinsic Permeability: A Transporter-Independent Measure of Caco-2 Cell Permeability in Drug Design and Development, *Mol Pharm.* 14 (2017) 1601–1609. <https://doi.org/10.1021/acs.molpharmaceut.6b01059>.
- [52] D. Shin, S.J. Lee, Y.-M. Ha, Y.S. Choi, J.W. Kim, S. Park, M.K. Park, Pharmacokinetic and pharmacodynamic evaluation according to absorption differences in three formulations of ibuprofen, *Drug Des Devel Ther.* Volume11 (2017) 135–141. <https://doi.org/10.2147/DDDT.S121633>.

5.7 Supporting Information

Table 5.S1. Thermal properties (T_g and T_m) of the ibuprofen and ibuprofen-based formulations determined by DSC at a heating rate of 1°C/min.

	T_g (C°)	T_m (C°)
Ibuprofen [S1]	-43.57	74.89
[C ₂ (OH)C ₁ Im]Cl [S2]	-	77.48
[C ₂ C ₁ Im]Cl [S2]	-	71.39
[C ₂ C ₁ Im][C ₁ CO ₂] [S2]	-	-76.16
[N ₁₁₁₂ (OH)]Cl [S2]	-	302
[C ₂ C ₁ Im][Ibu] [S1]	-30.55	72.44
[C ₂ (OH)C ₁ Im][Ibu] [S1]	-	-13.87
[N ₁₁₁₂ (OH)][Ibu] [S1]	-	70.89
[C ₂ (OH)C ₁ Im]Cl:Ibu 1:1 [S2]	-48.27	-
[C ₂ (OH)C ₁ Im]Cl:Ibu 1:2 [S2]	-46.96	-
[C ₂ (OH)C ₁ Im]Cl:Ibu 1:5 [S2]	-48.33	-
[C ₂ C ₁ Im]Cl:Ibu 2:1 [S2]	-54.35	-
[C ₂ C ₁ Im]Cl:Ibu 1:1 [S2]	-56.27	-
[C ₂ C ₁ Im]Cl:Ibu 1:2 [S2]	-48.80	-
[C ₂ C ₁ Im]Cl:Ibu 1:5 [S2]	-54.14	-
[C ₂ C ₁ Im][C ₁ CO ₂]:Ibu 2:1 [S2]	-66.76	-
[C ₂ C ₁ Im][C ₁ CO ₂]:Ibu 1:1 [S2]	-69.50	-
[C ₂ C ₁ Im][C ₁ CO ₂]:Ibu 1:2 [S2]	-52.74	-
[C ₂ C ₁ Im][C ₁ CO ₂]:Ibu 1:5 [S2]	-50.61	-
[N ₁₁₁₂ (OH)]Cl:Ibu 1:5 [S2]	-50.11	13.87
[C ₂ C ₁ Im][Ibu]:Ibu 2:1	-37.95	-
[C ₂ C ₁ Im][Ibu]:Ibu 1:1	-35.64	-
[C ₂ C ₁ Im][Ibu]:Ibu 1:2	-37.96	-
[C ₂ C ₁ Im][Ibu]:Ibu 1:5	-46.41	72.00
[C ₂ (OH)C ₁ Im][Ibu]:Ibu 1:1	-32.27	-
[C ₂ (OH)C ₁ Im][Ibu]:Ibu 1:2	-34.53	-
[C ₂ (OH)C ₁ Im][Ibu]:Ibu 1:5	-43.45	-
[N ₁₁₁₂ (OH)][Ibu]:Ibu 2:1	-32.50	36.55
[N ₁₁₁₂ (OH)][Ibu]:Ibu 1:1	-33.79	44.83
[N ₁₁₁₂ (OH)][Ibu]:Ibu 1:2	-37.88	-
[N ₁₁₁₂ (OH)][Ibu]:Ibu 1:5	-41.61	-

Table 5.S2. Density, ρ , dynamic viscosity, η , and ionic conductivity, k , as a function of temperature of ibuprofen-based systems with [C₂C₁Im][Ibu], [C₂(OH)C₁Im][Ibu] and [N₁₁₁₂(OH)][Ibu] as hydrogen bond acceptor at the molecular ratios 2:1, 1:1, 1:2 and 1:5.

T/C°	$\rho/g\cdot cm^{-3}$	$\eta/m\cdot Pa\cdot s$	$k/mS\cdot cm^{-1}$	T/C°	$\rho/g\cdot cm^{-3}$	$\eta/m\cdot Pa\cdot s$	$k/mS\cdot cm^{-1}$
[C ₂ C ₁ Im][Ibu]:Ibu 2:1				[C ₂ C ₁ Im][Ibu]:Ibu 1:1			
15	1.04233	34255	0.005	15	1.03763	4697.1	0.005
20	1.03927	16137	0.008	20	1.03447	2660.3	0.009
25	1.03630	7962.1	0.017	25	1.03137	1586.3	0.018
30	1.03390	4528.3	0.028	30	1.02833	989.31	0.030
35	1.03173	2614.3	0.048	35	1.02527	642.26	0.046
40	1.03007	1556.4	0.074	40	1.02220	432.27	0.075
45	1.02833	945.74	0.117	45	1.01913	300.68	0.104
50	1.02607	654.97	0.176	50	1.01597	215.20	0.160
[C ₂ C ₁ Im][Ibu]:Ibu 1:2				[C ₂ C ₁ Im][Ibu]:Ibu 1:5			
15	1.03187	16883	0.002	15	1.02020	6758.9	0.001
20	1.02863	8411.0	0.004	20	1.01687	3606.7	0.002
25	1.02567	4745.8	0.008	25	1.01370	2041.7	0.004
30	1.02297	2727.9	0.013	30	1.01090	1250.8	0.007
35	1.02077	1647.5	0.024	35	1.00850	759.96	0.012
40	1.01873	1039.2	0.037	40	1.00697	494.54	0.018
45	1.01650	681.55	0.052	45	1.00517	333.77	0.025
50	1.01400	460.38	0.079	50	1.00267	232.87	0.036
[C ₂ (OH)C ₁ Im][Ibu]:Ibu 1:1				[C ₂ (OH)C ₁ Im][Ibu]:Ibu 1:2			
15	1.06527		0.001	15	1.04937	52459	0.001
20	1.06133	60630	0.001	20	1.04590	25010	0.002
25	1.05787	29308	0.003	25	1.04263	12811	0.003
30	1.05463	15105	0.005	30	1.03960	6941.5	0.006
35	1.05153	8229.1	0.009	35	1.03680	3972.2	0.009
40	1.04860	4728.9	0.016	40	1.03413	2389.4	0.014
45	1.04567	2863.2	0.025	45	1.03163	1497.1	0.022
50	1.04247	1798.5	0.037	50	1.02903	974.55	0.035

Table 5.S2. cont.

T/C°	$\rho/\text{g}\cdot\text{cm}^{-3}$	$\eta/\text{m}\cdot\text{Pa}\cdot\text{s}$	$k/\text{mS}\cdot\text{cm}^{-1}$	T/C°	$\rho/\text{g}\cdot\text{cm}^{-3}$	$\eta/\text{m}\cdot\text{Pa}\cdot\text{s}$	$k/\text{mS}\cdot\text{cm}^{-1}$
[C ₂ (OH)C ₁ Im][Ibu]:Ibu 1:5				[N ₁₁₁₂ (OH)][Ibu]:Ibu 2:1			
15	1.03253	13996	0.001	15	1.0341	97144	0.001
20	1.02913	7072.6	0.001	20	1.0304	49392	0.001
25	1.02583	3826.8	0.002	25	1.0273	26375	0.002
30	1.02277	2185.3	0.004	30	1.0243	14793	0.003
35	1.01987	1308.7	0.006	35	1.0216	8663.8	0.006
40	1.01710	817.59	0.010	40	1.0191	5259.5	0.011
45	1.01423	531.27	0.015	45	1.0167	3311.9	0.017
50	1.01127	355.87	0.022	50	1.0144	2155.3	0.028
[N ₁₁₁₂ (OH)][Ibu]:Ibu 1:1				[N ₁₁₁₂ (OH)][Ibu]:Ibu 1:2			
15	1.03187	35120	0.001	15	1.02850	22912	0.001
20	1.02867	18830	0.001	20	1.02523	12296	0.001
25	1.02560	10587	0.002	25	1.02210	6941.2	0.002
30	1.02263	6222.3	0.004	30	1.01907	4096.3	0.004
35	1.01977	3806.5	0.007	35	1.01610	2516.9	0.007
40	1.01693	2412.3	0.012	40	1.01313	1602.4	0.011
45	1.01403	1579.8	0.017	45	1.01020	1054.7	0.017
50	1.01097	1065.8	0.026	50	1.00703	714.85	0.026
[N ₁₁₁₂ (OH)][Ibu]:Ibu 1:5							
15	1.02205	9778.8	0.000				
20	1.01950	5268.4	0.001				
25	1.01670	2987.6	0.002				
30	1.01360	1774.0	0.003				
35	1.01035	1099.3	0.005				
40	1.00705	706.90	0.008				
45	1.00373	454.92	0.012				
50	1.00040	311.83	0.018				

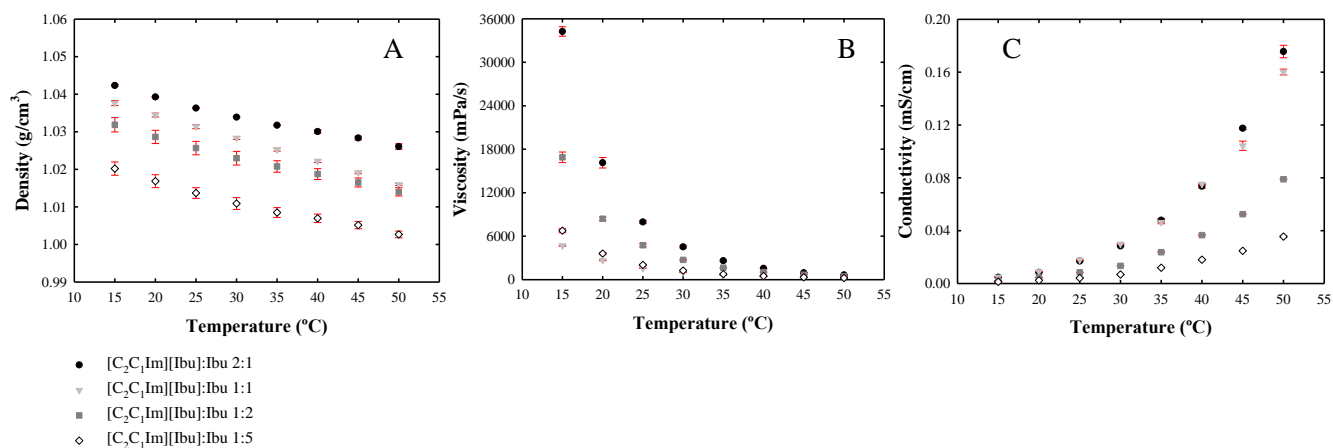


Figure 5.S1. Density (A), Viscosity (B) and Conductivity (C) measurements for the formulations $[C_2C_1Im][Ibu]:Ibu$ 2:1, $[C_2C_1Im][Ibu]:Ibu$ 1:1, $[C_2C_1Im][Ibu]:Ibu$ 1:2 and $[C_2C_1Im][Ibu]:Ibu$ 1:5.

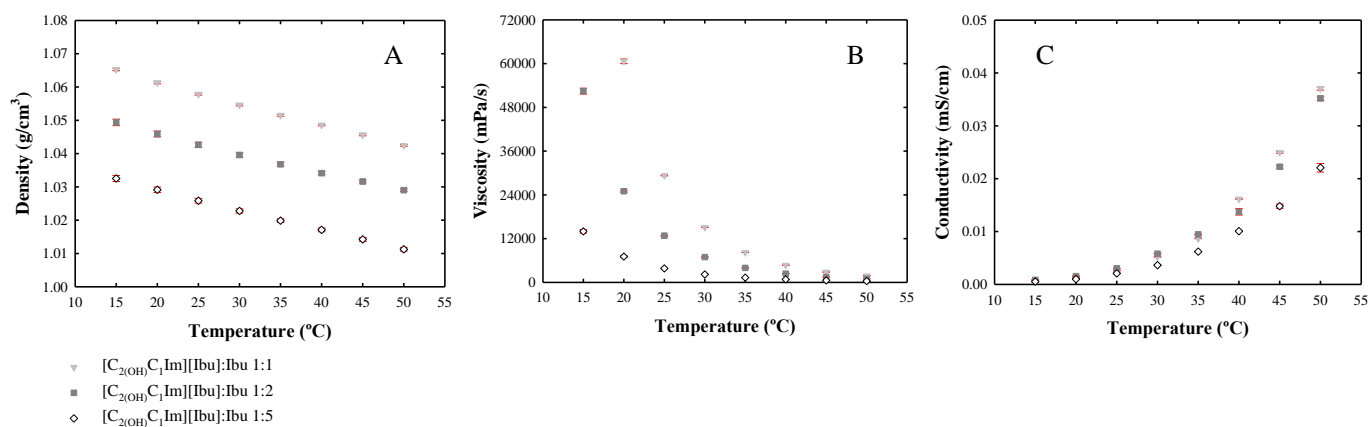


Figure 5.S2. Density (A), Viscosity (B) and Conductivity (C) measurements for the formulations $[C_{2(OH)}C_1Im][Ibu]:Ibu$ 1:1, $[C_{2(OH)}C_1Im][Ibu]:Ibu$ 1:2 and $[C_{2(OH)}C_1Im][Ibu]:Ibu$ 1:5.

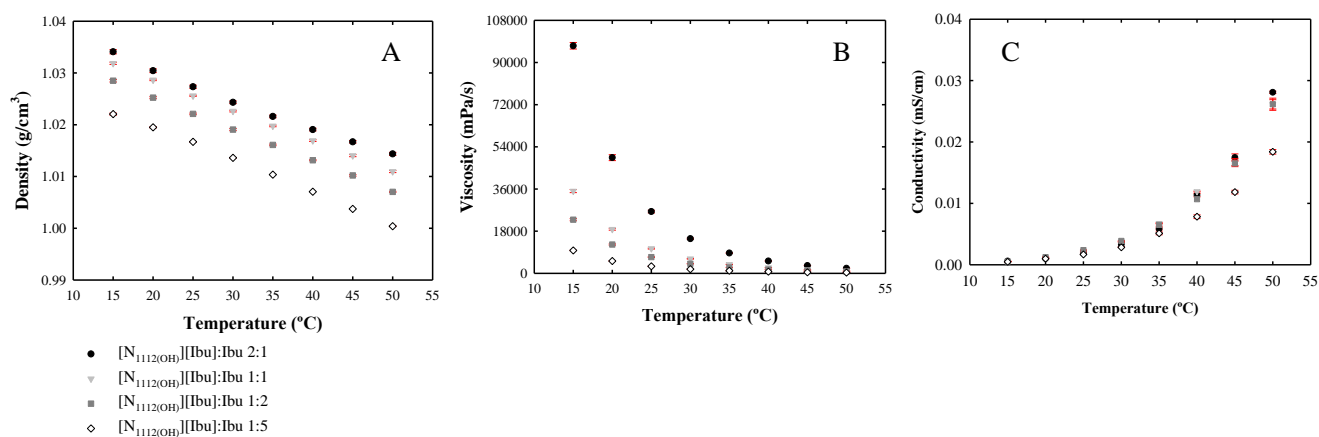


Figure 5.S3 Density (A), Viscosity (B) and Conductivity (C) measurements for the eutectic formulations $[N_{112(OH)}][Ibu]:Ibu$ 2:1, $[N_{112(OH)}][Ibu]:Ibu$ 1:1, $[N_{112(OH)}][Ibu]:Ibu$ 1:2 and $[N_{112(OH)}][Ibu]:Ibu$ 1:5.

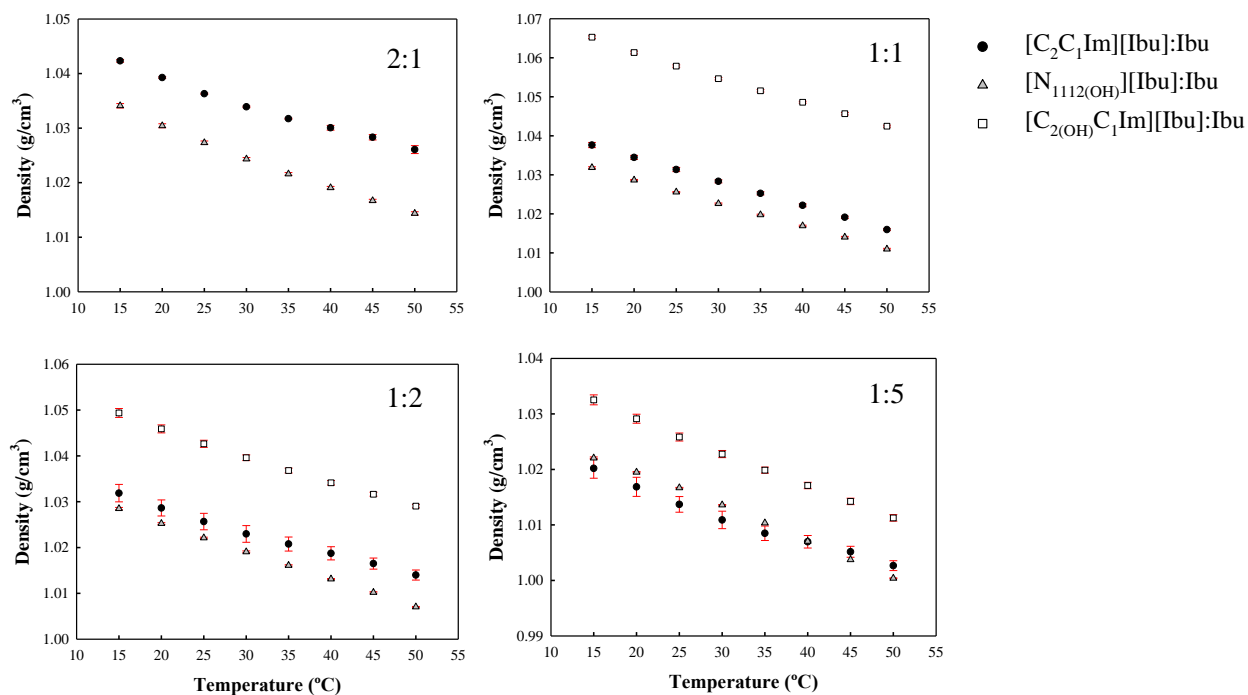


Figure 5.S4 Density of the Ibuprofen-based eutectic systems at different molar ratio, namely 2:1, 1:1, 1:2 and 1:5.

Table 5.S3. Activation energy of density (E_η) and its constant (η_0) and activation energy of conductivity (E_Λ) and its constant (s_0) according to the Arrhenius equation for the IL-based eutectic formulations ($[\text{C}_2\text{C}_1\text{Im}]\text{Cl}:\text{Ibu}$, $[\text{C}_{2(\text{OH})}\text{C}_1\text{Im}]\text{Cl}:\text{Ibu}$, $[\text{C}_2\text{C}_1\text{Im}][\text{C}_1\text{CO}_2]:\text{Ibu}$) and $[\text{N}_{1112(\text{OH})}]\text{Cl}:\text{Ibu}$ [2] and for the API-IL-based eutectic formulations $[\text{C}_2\text{C}_1\text{Im}][\text{Ibu}]:\text{Ibu}$, $[\text{C}_{2(\text{OH})}\text{C}_1\text{Im}][\text{Ibu}]:\text{Ibu}$ and $[\text{N}_{1112(\text{OH})}][\text{Ibu}]:\text{Ibu}$ at different molar ratios (2:1, 1:1, 1:2 and 1:5).

Molar Ratio	$E_\eta(\text{KJ}\cdot\text{mol}^{-1})$	η_0	$E_\Lambda(\text{KJ}\cdot\text{mol}^{-1})$	s_0
$[\text{C}_2\text{C}_1\text{Im}]\text{Cl}:\text{Ibu}$				
2:1	67.54	5.23×10^{-9}	-77.26	3.00×10^{15}
1:1	63.20	2.11×10^{-8}	-70.98	1.65×10^{14}
1:2	60.88	3.77×10^{-8}	-72.00	1.38×10^{14}
1:5	59.54	3.62×10^{-8}	-79.40	8.19×10^{14}
$[\text{C}_{2(\text{OH})}\text{C}_1\text{Im}]\text{Cl}:\text{Ibu}$				
1:1	68.57	6.77×10^{-9}	-76.58	6.25×10^{14}
1:2	66.22	9.39×10^{-9}	-80.11	1.41×10^{15}
1:5	61.76	1.88×10^{-8}	-74.86	4.30×10^{13}
$[\text{C}_2\text{C}_1\text{Im}][\text{C}_1\text{CO}_2]:\text{Ibu}$				
2:1	46.51	2.57×10^{-6}	-49.16	2.28×10^{11}
1:1	49.31	1.18×10^{-6}	-53.21	5.70×10^{11}
1:2	55.00	2.17×10^{-7}	-61.70	4.53×10^{12}
1:5	58.58	5.57×10^{-8}	-75.80	2.54×10^{14}
$[\text{N}_{1112(\text{OH})}]\text{Cl}:\text{Ibu}$				
1:5	61.02	3.00×10^{-8}	-68.30	2.61×10^{12}
$[\text{C}_2\text{C}_1\text{Im}][\text{Ibu}]:\text{Ibu}$				
2:1	87.50	4.10×10^{-12}	-80.38	1.88×10^{15}
1:1	68.04	1.99×10^{-9}	-76.29	3.76×10^{14}
1:2	79.17	6.68×10^{-11}	-77.70	3.16×10^{14}
1:5	74.35	4.92×10^{-9}	-74.25	8.19×10^{13}
$[\text{C}_{2(\text{OH})}\text{C}_1\text{Im}][\text{Ibu}]:\text{Ibu}$				
1:1	92.25	2.03×10^{-12}	-91.72	2.91×10^{16}
1:2	85.09	1.60×10^{-11}	-81.84	6.36×10^{14}
1:5	78.34	7.24×10^{-11}	-83.04	6.70×10^{14}
$[\text{N}_{1112(\text{OH})}][\text{Ibu}]:\text{Ibu}$				
2:1	84.13	5.01×10^{-11}	-86.87	3.20×10^{15}
1:1	77.19	3.29×10^{-10}	-85.96	2.32×10^{15}
1:2	76.55	2.80×10^{-10}	-83.74	9.74×10^{14}
1:5	76.05	1.48×10^{-10}	-79.70	1.50×10^{14}

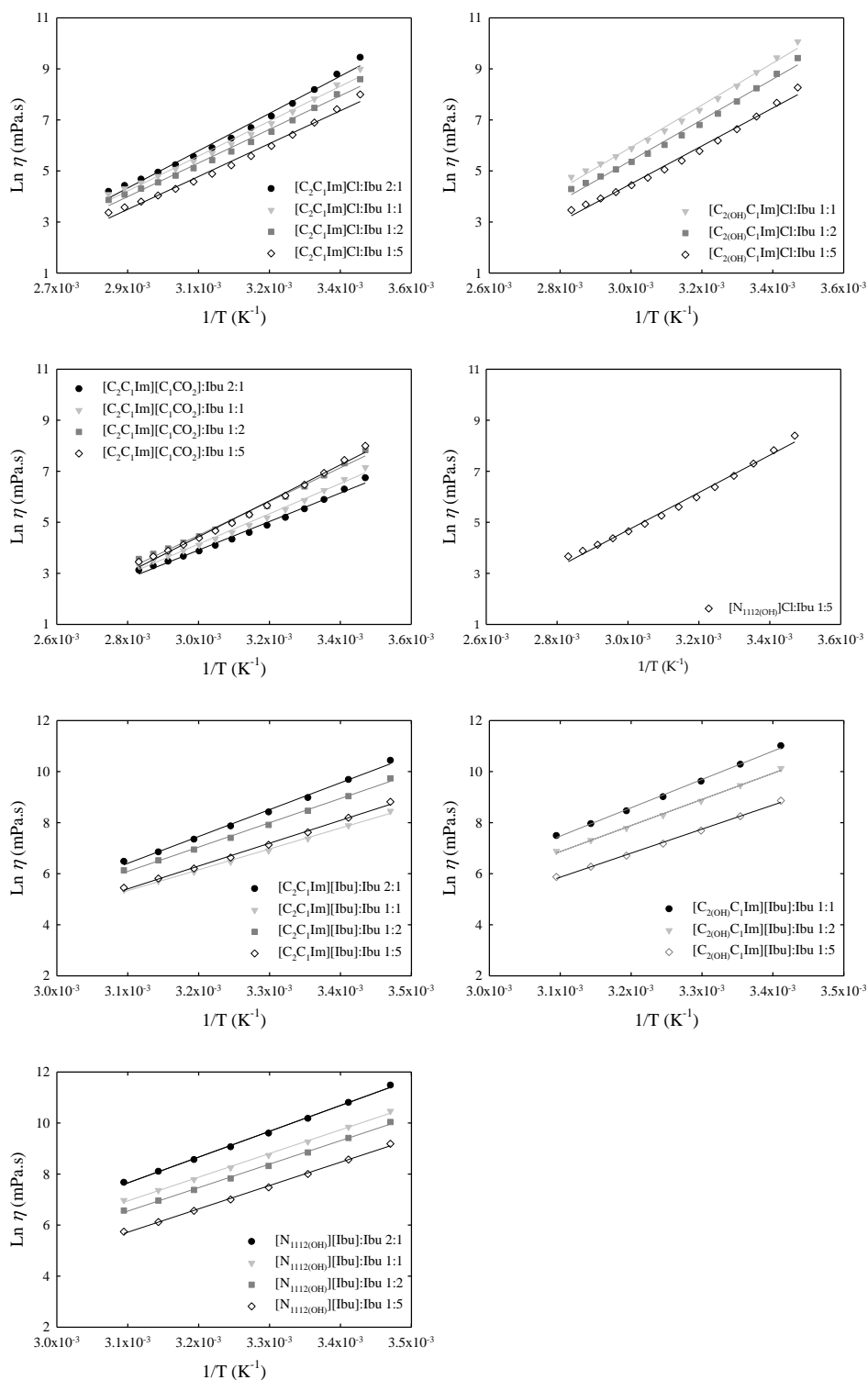


Figure 5.S5 Plot of the natural logarithm of the viscosity $\ln \eta$ versus the reciprocal temperature for the IL-based eutectic formulations ($[\text{C}_2\text{C}_1\text{Im}]\text{Cl}:\text{Ibu}$, $[\text{C}_{2(\text{OH})}\text{C}_1\text{Im}]\text{Cl}:\text{Ibu}$, $[\text{C}_2\text{C}_1\text{Im}][\text{C}_1\text{CO}_2]:\text{Ibu}$ and $[\text{N}_{1112(\text{OH})}]\text{Cl}:\text{Ibu}$ at the molar ratios 2:1, 1:1, 1:2 and 1:5[2]) and for the API-IL-based eutectic formulations ($[\text{C}_2\text{C}_1\text{Im}][\text{Ibu}]:\text{Ibu}$, $[\text{C}_{2(\text{OH})}\text{C}_1\text{Im}][\text{Ibu}]:\text{Ibu}$ and $[\text{N}_{1112(\text{OH})}][\text{Ibu}]:\text{Ibu}$ at the molar ratios 2:1, 1:1, 1:2 and 1:5)

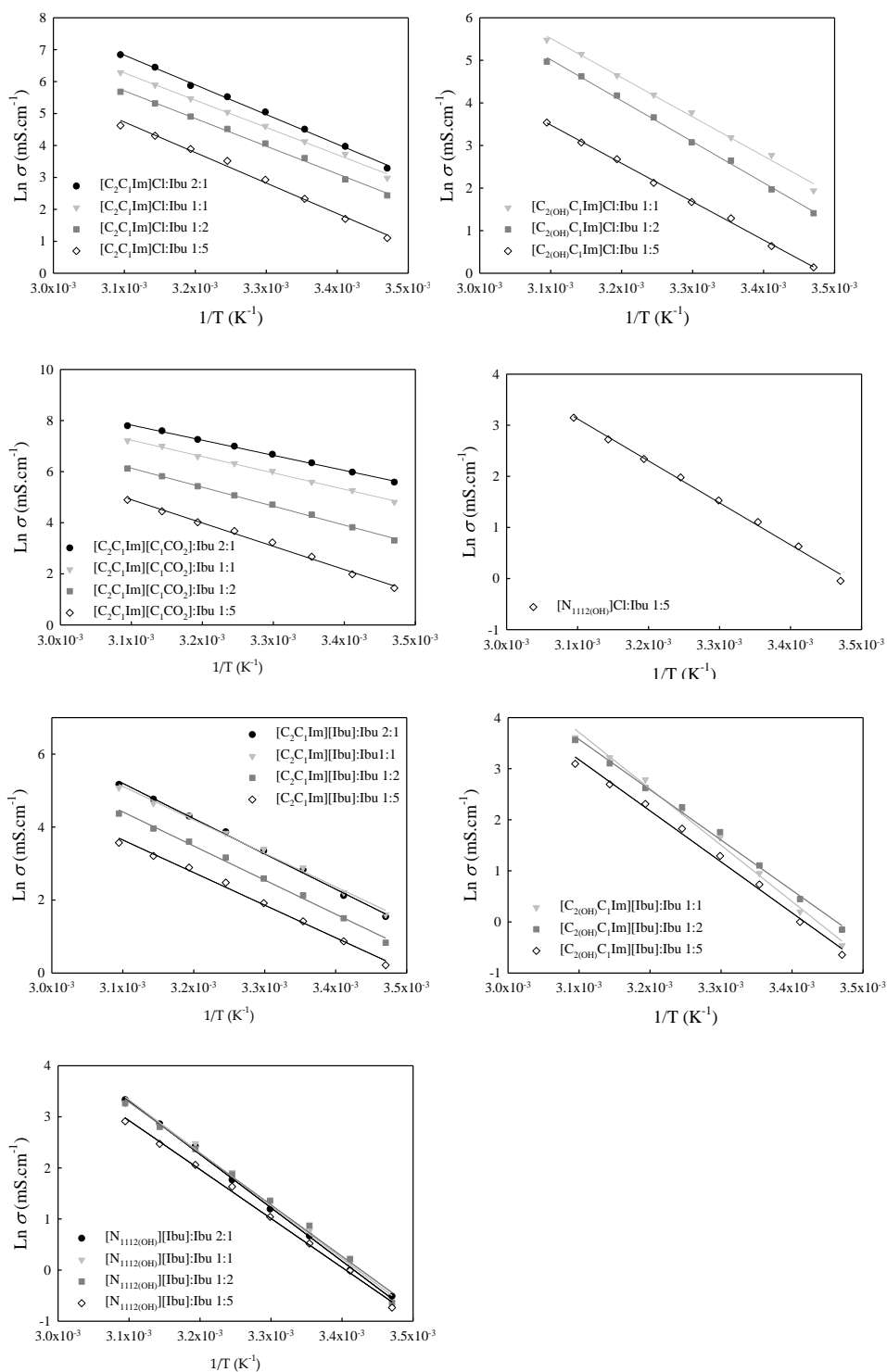


Figure 5.S6 Plot of the natural logarithm of the viscosity $\text{Ln } \sigma$ versus the reciprocal temperature for the IL-based eutectic formulations ($[\text{C}_2\text{C}_1\text{Im}]\text{Cl}:\text{Ibu}$, $[\text{C}_2(\text{OH})\text{C}_1\text{Im}]\text{Cl}:\text{Ibu}$, $[\text{C}_2\text{C}_1\text{Im}][\text{C}_1\text{CO}_2]:\text{Ibu}$ and $[\text{N}_{1112}(\text{OH})]\text{Cl}:\text{Ibu}$ at the molar ratios 2:1, 1:1, 1:2 and 1:5 [2]) and for the API-IL-based eutectic formulations ($[\text{C}_2\text{C}_1\text{Im}][\text{Ibu}]:\text{Ibu}$, $[\text{C}_2(\text{OH})\text{C}_1\text{Im}][\text{Ibu}]:\text{Ibu}$ and $[\text{N}_{1112}(\text{OH})][\text{Ibu}]:\text{Ibu}$ at the molar ratios 2:1, 1:1, 1:2 and 1:5).

GENERAL CONCLUSIONS

The main goal of this thesis was to demonstrate the feasibility of using the ionic liquids (ILs) platform to boost “old” drugs efficiency, namely non-steroidal anti-inflammatory drugs (NSAIDs). Ibuprofen (Ibu), one of the more common over-the-counter NSAIDs, which is used for pain and inflammation relief through the inhibition of cyclooxygenase (COX), was selected as the model NSAID. Most NSAIDs are poorly water-soluble, a major drawback for their bioavailability, and their oral administration is currently the most used route, with gastrointestinal and renal toxicity as possible side effects.

Most biological applications involve aqueous solutions (water and biological fluids), accordingly insights into task-specific fluorinated ionic liquids (FILs) that reduce the impact of the addition of water upon the IL's H-bond acceptance ability, a key factor to obtain functionalized materials to be used in the dissolution of drugs or biomolecules, were attained. The hydrogen-bonding ability and dipolarity/ polarizability was evaluated using Kamlet-Taft parameters for neat and aqueous solutions of FILs and conventional ILs. Comparing the hydrogen bond acceptance and the hydrogen bond donation abilities it was possible to see that the fluorination of the anion restricts the impact of the addition of water to the ILs. Additionally, the choice of the fluorinated alkyl chain length (at least four carbon atoms in the IL anion) can make constant the hydrogen bond acceptance ability. By examining the ILs structures in aqueous solutions with molecular dynamics simulations it was possible to evaluate the rich-aggregation behavior of these ILs and their networking with water aggregates.

The synthesis of three pharmaceutically active ILs (API-ILs), conjugating the ibuprofenate anion with imidazolium cations ([C₂C₁Im][Ibu] and [C₂(OH)C₁Im][Ibu]) and a cholinium cation ([N₁₁₂(OH)][Ibu]) was successfully accomplished. The aqueous solubility of these API-ILs in water and biological simulated fluids was achieved, where the solubility was much higher relative to the ibuprofen neutral and commercial ibuprofen salt form (i.e., sodium ibuprofen). Also, cytotoxicity tests on human cell lines (i.e., Caco-2 colon carcinoma cells and HepG2 hepatocellular carcinoma cells) and hemocompatibility assays substantiated the biocompatibility of the ibuprofen-based ILs. Additionally, the pharmacological action of the prepared API-ILs were tested through the inhibition of BSA denaturation and inhibition of cyclooxygenases (COX-1 and COX-

2). Results showed that anti-inflammatory response of ibuprofen was maintained with an improved selectivity towards COX-2, allowing the development of safer NSAIDs and the recognition of new avenues for selective COX-2 inhibitors.

Imidazolium-based ILs ($[\text{C}_2\text{C}_1\text{Im}]\text{Cl}$, $[\text{C}_{2(\text{OH})}\text{C}_1\text{Im}]\text{Cl}$, $[\text{C}_2\text{C}_1\text{Im}][\text{C}_1\text{CO}_2]$), cholinium salt ($[\text{N}_{1112(\text{OH})}]\text{Cl}$) and API-ILs ($[\text{C}_2\text{C}_1\text{Im}][\text{Ibu}]$, $[\text{C}_{2(\text{OH})}\text{C}_1\text{Im}][\text{Ibu}]$, $[\text{N}_{1112(\text{OH})}][\text{Ibu}]$) were used to formulate eutectic systems with ibuprofen as parent active pharmaceutical ingredient (API) in different molar ratio, namely 2:1, 1:1, 1:2 and 1:5. All eutectic systems were characterized by DSC and NMR to confirm their molar ratio and the eutectic formation. The polarity was assessed by the Kamlet-Taft approach (β and π^* values) for the ILs-based eutectics formulations. The Kamlet-Taft results confirmed that the developed Ibu-based eutectics have high ability to establish hydrogen bonds (specific interactions) and high polarity and ability to establish dipole-dipole and dipole-induced dipole interactions (non-specific interactions). Also, the aqueous solubility (water and biological simulated fluids) was assessed for the IL-based eutectic mixtures and all of them achieved an upgrade in solubility.

All the ibuprofen-based eutectics (eutectics formed between conventional ILs and ibuprofen, and eutectics formed between ibuprofen-ILs and ibuprofen) and ibuprofen displayed similar cytotoxic response (Caco-2 and HepG2 human cell lines) and all forms proven to be hemocompatible. The pharmacological action for all the prepared eutectic formulations was validated through the inhibition of BSA denaturation and inhibition of cyclooxygenases (COX-1 and COX-2). All the IL- and API-IL-based systems improve or at least maintain the anti-inflammatory response of ibuprofen (parent API). Additionally, the ibuprofen-based eutectics were characterized in terms of viscosity, conductivity, density and ionicity (via Walden plot), confirming the formation of large charged or non-charged aggregates, or the existence of ionic networks, that increase the potential for these liquids to penetrate membranes more efficiently than ibuprofen (parent solid API). At last, the ability of the developed ibuprofen API-ILs and ibuprofen-based eutectics (both IL- and API-IL-based eutectics) to permeate skin was accessed through the Skin-PAMPA (Skin Parallel Artificial Membrane Permeability Assays) model. The obtained effective permeability coefficient (P_e) showed a similar or slightly

higher permeation profile when compared to ibuprofen, more significant for the liquid eutectic formulations.

The development of API-ILs and ionic liquid-based eutectics represents a paradigm that poses diverse opportunities to drug development and delivery, which may play a relevant role in the future of healthcare, taking ILs from the benchtop to the bedside. This work presents strong evidence that the ionic liquids and eutectics platforms are of fundamental importance for the improvement of solubility of poor water-soluble drugs maintaining their pharmacologic action. The data presented in this work clearly indicates the beneficial effects of the interplay of ionic liquids and eutectics to improve the efficiency of ibuprofen, a EMA- and FDA-approved drug, with all the undisputable advantages and profits in improving an already approved drug.



2023

Joana Campainhas Bastos

THE DIFFERENT FACES OF IBUPROFEN-BASED IONIC LIQUIDS AND EUTECTIC SYSTEMS:
PROMISING INNOVATIVE IONIC-LIQUID-BASED FORMULATIONS OF AN OVER-THE-COUNTER
ANTI-INFLAMMATORY DRUG

